PHYTOCHEMICAL STUDIES OF *Cryptocarya* SPECIES AND THEIR BIOACTIVITIES

WAN NURUL NAZNEEM BINTI WAN OTHMAN

FACULTY OF SCIENCE
UNIVERSITY OF MALAYA
KUALA LUMPUR

2017

PHYTOCHEMICAL STUDIES OF *Cryptocarya* SPECIES AND THEIR BIOACTIVITIES

WAN NURUL NAZNEEM BINTI WAN OTHMAN

THESIS SUBMITTED IN FULFILMENT OF THE REQUIREMENTS FOR THE DEGREE OF DOCTOR OF PHILOSOPHY

DEPARTMENT OF CHEMISTRY
FACULTY OF SCIENCE
UNIVERSITY OF MALAYA
KUALA LUMPUR

2017

UNIVERSITY OF MALAYA

ORIGINAL LITERARY WORK DECLARATION

Name of Candidate: **WAN NURUL NAZNEEM BINTI WAN OTHMAN**

I.C/Passport No:

Registration/Matric No: **SHC 100100**

Name of Degree: **DOCTOR OF PHILOSOPHY**

Title of Project Paper/Research Report/Dissertation/Thesis ("this Work"):

PHYTOCHEMICAL STUDIES OF *Cryptocarya* SPECIES AND THEIR BIOACTIVITIES

Field of Study: **CHEMISTRY (NATURAL PRODUCTS)**

I do solemnly and sincerely declare that:

(1) I am the sole author/writer of this Work;
(2) This Work is original;
(3) Any use of any work in which copyright exists was done by way of fair dealing and for permitted purposes and any excerpt or extract from, or reference to or reproduction of any copyright work has been disclosed expressly and sufficiently and the title of the Work and its authorship have been acknowledged in this Work;
(4) I do not have any actual knowledge nor do I ought reasonably to know that the making of this work constitutes an infringement of any copyright work;
(5) I hereby assign all and every rights in the copyright to this Work to the University of Malaya ("UM"), who henceforth shall be owner of the copyright in this Work and that any reproduction or use in any form or by any means whatsoever is prohibited without the written consent of UM having been first had and obtained;
(6) I am fully aware that if in the course of making this Work I have infringed any copyright whether intentionally or otherwise, I may be subject to legal action or any other action as may be determined by UM.

Candidate's Signature Date: 13th July 2017

Subscribed and solemnly declared before,

Witness's Signature Date: 13th July 2017

Name: Dr. Khalijah Awang

Designation: Professor

ABSTRACT

Phytochemical analysis and bioactivity studies on three species of Lauraceae, *Cryptocarya densiflora* Blume, *Cryptocarya infectoria* Miq. and *Cryptocarya griffithiana* Wight have been conducted. A total of twenty alkaloids were successfully isolated and purified using several chromatographic techniques such as column chromatography (CC), thin layer chromatography (TLC) and preparative thin layer chromatography (PTLC). The structural elucidations were established through several spectroscopic methods; notably 1D NMR (^{1}H, ^{13}C and DEPT), 2D NMR (COSY, NOESY, HSQC and HMBC), MS, UV, IR, as well as by comparison with those reported in the literature. Investigation of the leaves of *C. densiflora* yielded fourteen alkaloids in which four of them are new. The new alkaloids were named as prodensiflorin A **126**, prodensiflorin B **127**, (-)-densiindolizidine **128** and (-)-desmethylsecoantofine-*N*-oxide **131**, while the known alkaloids were characterized as (-)-antofine **6**, (-)-isocaryachine **61**, (+)-reticuline **76**, (+)-laurotetanine **86**, (+)-*N*-methyllaurotetanine **87**, (+)-nornantenine **123**, dicentrinone **124**, (+)-oridine **125**, (-)-desmethylsecoantofine **130** and crychine **134**. Isolation works on the bark of *C. infectoria* has resulted six known alkaloids; (+)-*N*-methylisococlaurine **14**, atherosperminine **15**, (+)-reticuline **76**, (+)-laurotetanine **86**, (+)-*N*-methyllaurotetanine **87** and argentinine **135**, meanwhile the leaves afforded two compounds, argentinine **135** and liriodenine **136**. Extensive chromatographic purification on the bark of *C. griffithiana* has led to the isolation of six known alkaloids; 2-hydroxyatherosperminine **13**, 2-methoxyatherosperminine **72**, (+)-reticuline **76**, (+)-*N*-methyllaurotetanine **87**, (+)-nornantenine **123** and argentinine **135**. DPPH inhibitory activity of the four alkaloids from the leaves of *C. densiflora* was evaluated and compared to ascorbic acid **137**, as the positive control. Alkaloid (-)-desmethylsecoantofine **130** exhibited more effective free radical scavenging with an IC_{50} value of 62.40 ± 0.05 µg/mL followed by (+)-*N*-methyllaurotetanine **87** with an IC_{50} value of 130.00 ± 0.07 µg/mL.

Twelve isolated alkaloids in sufficient amount, (+)-laurotetanine **86**, (+)-nornantenine **123**, (+)-oridine **125**, prodensiflorin A **126**, prodensiflorin B **127**, (-)-desmethylsecoantofine **130** and (-)-desmethylsecoantofine-*N*-oxide **131** from the leaves of *C. densiflora*, (+)-*N*-methylisococlaurine **14**, atherosperminine **15** and (+)-*N*-methyllaurotetanine **87** from the bark of *C. infectoria*, 2-methoxyatherosperminine **72** and (+)-reticuline **76** from the bark of *C. griffithiana* were evaluated for their acetylcholinesterase and butyrylcholinesterase inhibitory activity. As a result, phenanthrene type alkaloid, 2-methoxyatherosperminine **72** showed strong activity with IC_{50} values of 3.95 μM against BChE and was the most potent inhibitor among all the tested compounds. Enzyme kinetic studies suggested that the most potent alkaloid, 2-methoxyatherosperminine **72** possesses mixed inhibition mode with an inhibition constant (*Ki*) of 6.72 μM.

ABSTRAK

Analisis dan bioaktiviti fitokimia kajian mengenai tiga spesies Lauraceae, *Cryptocarya densiflora* Blume, *Cryptocarya infectoria* Miq. dan *Cryptocarya griffithiana* Wight telah dijalankan. Sebanyak dua puluh alkaloid telah berjaya diasingkan dan ditulenkan dengan menggunakan pelbagai teknik kromatografi seperti kromatografi turus, kromatografi lapisan nipis dan kromatografi lapisan nipis persediaan. Struktur bagi sebatian yang diasingkan telah dikenalpasti dengan menggunakan beberapa kaedah spektroskopi; terutamanya 1D NMR (^{1}H, ^{13}C dan DEPT), 2D NMR (COSY, NOESY, HSQC dan HMBC), MS, UV, IR dan perbandingan dengan kajian-kajian lepas. Penyiasatan terhadap daun *C. densiflora* telah menghasilkan empat belas alkaloid di mana empat daripadanya adalah baru. Alkaloid baru ini telah dinamakan sebagai prodensiflorin A **126**, prodensiflorin B **127**, (-)-densiindolizidina **128** dan (-)-desmetilsekoantofina-*N*-oksida **131**, manakala alkaloid-alkaloid yang telah pun dikenalpasti sebelum ini adalah (-)-antofina **6**, (-)-isocaryacin **61**, (+)-retikulina **76**, (+)-laurotetanina **86**, (+)-*N*-metillaurotetanina **87**, (+)-nornantenina **123**, disentrinon **124**, (+)-oridina **125**, (-)-desmetilsekoantofina **130** dan crycin **134**. Kerja pengasingan terhadap kulit kayu *C. infectoria* telah menghasilkan enam alkaloid dikenali sebagai; (+)-*N*-metilisokoklaurina **14**, atherosperminina **15**, (+)-retikulina **76**, (+)-laurotetanina **86**, (+)-*N*-metillaurotetanina **87** dan argentinina **135**, manakala dua sebatian daripada daun, argentinina **135** dan liriodenina **136**. Penulenan meluas kromatografi pada kulit kayu *C. griffithiana* telah membawa kepada pengasingan enam alkaloid yang telah dikenali; 2-hidroksiatherosperminina **13**, 2-metoksiatherosperminina **72**, (+)-retikulina **76**, (+)-*N*-metillaurotetanina **87**, (+)-nornantenina **123** dan argentinina **135**. Aktiviti DPPH empat alkaloid daripada daun *C. densiflora* telah dinilai dan dibandingkan dengan asid askorbik **137**, sebagai kawalan positif. Alkaloid (-)-desmetilsekoantofina **130** lebih berkesan penghapus radikal bebas dengan nilai IC_{50} 62.40 ± 0.05 μg/mL diikuti oleh (+)-*N*-

metillaurotetanina **87** dengan nilai IC_{50} 130.00 ± 0.07 μg/mL. Dua belas alkaloid yang telah diasingkan dalam jumlah yang mencukupi; (+)-laurotetanina **86**, (+)-nornantenina **123**, (+)-oridina **125**, prodensiflorin A **126**, prodensiflorin B **127**, (-)-desmetilsekoantofina **130** dan (-)-desmetilsekoantofina-*N*-oksida **131** daripada daun *C. densiflora*, (+)-*N*-metilisokoklaurina **14**, atherosperminina **15** dan (+)-*N*-metillaurotetanina **87** daripada kulit kayu *C. infectoria*, 2-metoksiatherosperminina **72** dan (+)-retikulina **76** daripada kulit kayu *C. griffithiana* telah dinilai untuk aktiviti perencatan asetilkolinesterase, dan butirilkolinesterase. Keputusannya, alkaloid jenis phenanthrena; 2-metoksiatherosperminina **72** menunjukkan aktiviti kukuh dengan nilai IC_{50} 3.95 μM terhadap BChE dan merupakan perencat yang paling berpotensi di kalangan semua sebatian yang diuji. Kajian kinetik enzim mencadangkan bahawa alkaloid yang paling berpotensi, 2-metoksiatherosperminina **72**, mempunyai mod jenis perencatan campuran dengan nilai pemalar perencatan (*Ki*), 6.72 μM.

ACKNOWLEDGEMENTS

In the name of Allah the Most Gracious and the Most Merciful. Alhamdulillah, all praises to Allah for the strengths and His blessing in completing this thesis. First and foremost, I offer my most sincere gratitude to my supervisor, Prof. Dr. Khalijah Awang, who has supported me throughout the course of this study with her kind supervision, motivation, constant support, enthusiasm and immense knowledge. I am very indebted to her patience and invaluable advices that inspired me to see things positively and honored with her confidence on my ability. Not forgotten, a special gratitude to my late supervisors, Allahyarham Assoc. Prof. Dr. Mat Ropi Mukhtar and Prof. Datuk Dr. A. Hamid A. Hadi for their supervision throughout this study during their presence. May Allah SWT grant them the highest of Jannah.

I would like to acknowledge the Institute of Postgraduate Studies (IPS) for giving me an opportunity to pursue my postgraduate studies in UM. I would also like to thank the Ministry of Higher Education for awarding me with the Mybrain15 scholarship which covered my tuition fees.

Next, I thank all the people who create such a good atmosphere in the lab, Dr. Azeana, Dr. Yasodha, Dr. Fadzli, Dr. Chan Gomathi, Dr. Kee, Dr. Azmi, Dr. Liew Sook Yie, Dr. Chong Soon Lim, Dr. Omer, Dr. Ahmad Kalem, Mrs. Shelly, Mrs. Faezah, Mrs. Nadia, Ms. Mariam, Mr. Aqmal, Mrs. Julia, Ms. Devi Rosmy, Mrs. Norsita, Mr. Azrul, Mr. Hafiz, Ms. Hazrina, Ms. Aimi, Mr. Arshia, Mr. Hisyam, Mrs. Mahfuzah, Ms. Haslinda, Ms. Rosalind and Ms. Tein.

I would also like to thank Herbarium staffs, Mr. Din, Mr. Teo and Mr. Rafly for their help in sample collection, the NMR and LCMS staffs, Mr. Nordin, Mr. Zakaria, Ms. Norzalida, Mr. Fateh, Mrs. Fiona and Mr. Siew. Without their support, this research would not have been possible to be completed.

I warmly thank and appreciate my parents for always been there for me no matter where I am, for all unconditional supports and patience. I thank my brothers for providing assistance in numerous ways. I want to express my gratitude and deepest appreciation to my lovely sweet daughter, Hayra Camelia and sons, Muhammad Harris Caliph and Muhammad Hadiff Cashfy for their great patience and understandings and for being a good Muslim. Finally, I would like to express my eternal appreciation towards my beloved husband, Iskandar Ismail for always sticking by my side, even when I was irritable and depressed; without his supports and encouragements, I could not have finished this work. I can just say thanks for everything and may Allah SWT give you all the best in return.

TABLE OF CONTENTS

LIST OF SCHEMES

LIST OF FIGURES

LIST OF TABLES

LIST OF ABBREVIATIONS, SYMBOLS AND UNITS

ABBREVIATIONS

A	
ACh	Acetylcholine
AChE	Acetylcholinesterase
AD	Alzheimer Disease
ATCI	Acetylthiocholine Iodide
B	
BChE	Butyrylcholinesterase
C	
Calcd.	Calculated
CC	Column Chromatography
$CDCl_3$	Deuterated Chloroform
C_5D_5N	Deuterated Pyridine
CH_2Cl_2	Dichloromethane
CH_3	Methyl Group
CH_3OH	Methanol
COSY	^1H-^1H Correlation Spectroscopy
^{13}C NMR	13-Carbon NMR
D	
DCM	Dichloromethane
DTNB	5,5′-dithiobis (2-nitrobenzoic acid)
1D NMR	One Dimensional Nuclear Magnetic Resonance
2D NMR	Two Dimensional Nuclear Magnetic Resonance
DEPT	Distortionless Enhancement by Polarisation Transfer

DPPH	2,2-diphenylpicrylhydrazyl
d	Doublet
dd	Doublet of Doublets
dt	Doublet Triplet
E	
EtOH	Ethanol
F	
FT-NMR	Fourier Transform Nuclear Magnetic Resonance
H	
^{1}H NMR	Proton NMR
HMBC	Heteronuclear Multiple Bond Coherence
HSQC	Heteronuclear Single Quantum Coherence
I	
IC_{50}	Concentration Required to Inhibit 50% of Activity
IR	Infrared
K	
Ki	Inhibition Constant
L	
LB plot	Lineweaver-Burk plot
LCMS-IT-TOF	Liquid Chromatography Mass Spectroscopy-Ion Trap-Time of Flight
M	
MS	Mass Spectroscopy
MeOH	Methanol
m	Multiplet
m/z	Mass to Charge Ratio

N

NaCl	Natrium/Sodium Chloride
NH_3	Ammonia
NMR	Nuclear Magnetic Resonance
NOESY	Nuclear Overhauser Enhancement Spectroscopy

O

OCH_2O	Methylenedioxy Group
OMe/OCH_3	Methoxyl Group
OH	Hydroxyl Group

P

PTLC	Preparative Thin Layer Chromatography

R

ROS	Reactive Oxygen Species
R_f	Retention Factor

S

SAM	*S*-adenosylmethionine
SAH	*S*-adenosylhomocysteine
SD	Standard Deviation
s	Singlet

T

TLC	Thin Layer Chromatography
t	Triplet
td	Triplet Doublet

U

UV	Ultraviolet

SYMBOLS

α	Alpha
β	Beta
δ	Chemical Shift
δ_C	Chemical Shift Carbon
δ_H	Chemical Shift Proton
λ_{max}	Lambda (maximum wavelength in nanometer)
ν_{max}	Maximum Absorption

UNITS

Å	Angstrom
cm	Centimeter
cm^{-1}	Per Centimeter
^oC	Degree Celsius
g	Gram
Hz	Hertz
J	Coupling Constant (Hz)
Kg	Kilogram
Kg/m^3	Kilogram per Cubic Meter
L	Liter
M	Molar Concentration
MHz	Mega Hertz
m	Meter
mg	Milligram
min	Minute

mM	Millimolar
mL	Milliliter
mg/mL	Milligram per Milliliter
nm	Nanometer
nM	Nanomolar
ppm	Parts per Million
µg/mL	Microgram per Milliliter
µL	Microliter
µM	Micromolar

CHAPTER 1: INTRODUCTION

1.1 General

Fossil records date human use of plants as medicines at least to the Middle Paleolithic age some 60,000 years ago (Fabricant & Farnsworth, 2001). Information on the ancient uses of plant materials as medicines can be found in archeological artifacts, old literature, history books and pharmacopoeias. In fact in the Quran and the Bible, about 20 and 125 plants are mentioned, respectively, as being used as medicinal agents to treat various ailments (Jantan, 2004). From that point the development of traditional medical systems incorporating plants as a means of therapy can be traced back only as far as recorded documents of their likeness (Fabricant & Farnsworth, 2001). Later, as different civilizations developed, man was able to communicate his knowledge and ideas, with the results that his knowledge became known to the coming generations.

Recently, the development of new technologies has revolutionized the screening of natural products. Applying these technologies compensates for the inherent limitations of natural products and offers a unique opportunity to re-establish natural products as a major source for drug discovery (Lam, 2007). Natural products chemistry actually began with the work of Sertürner a young German pharmacist who first isolated and described morphine **1** from opium in 1804 and was introduced in medicine in 1818. This, in turn, was obtained from opium poppy (*Papaver somniferum*) by processes that have been used for over 5000 years (Huxtable & Schwarz, 2001). Many such similar developments followed such as quinine **2** from cinchona tree, nicotine **3** (tobacco), reserpine **4** (*Rauwolfia serpentina*) and strychnine **5** (*Strychnos nux-vomica*) (Patwardhan, 2009). It is of interest that most of the drugs derived or originally isolated from higher plants were discovered in an ethnobotanical context (Cox, 2008).

The World Health Organization also has recognized the importance of traditional medicine and has been active in creating strategies, guidelines and standards for botanical medicines. Commercially, these plant-derived medicines are worth about US$ 14 billion a year in the United States and US$ 40 billion worldwide. Americans paid an estimated US$ 21.2 billion for services provided by alternative medicine practitioners (Patwardhan, Vaidya, & Chorghade, 2004). In recent times, focus on plant research has increased all over the world and a large body of evidence has collected to show immense potential of medicinal plants used in various traditional systems.

The number of higher plant species (angiosperms and gymnosperms) on this planet is estimated at 250,000, with a lower level at 215,000 and an upper level as high as 500,000. Of these, only about 6% have been screened for biological activity, and a reported 15% have been evaluated phytochemically. With high throughput screening methods becoming more advanced and available, these numbers will change, but the primary discriminator in evaluating one plant species versus another is the matter of approach to finding leads (Fabricant & Farnsworth, 2001).

The Lauraceae family is by far the largest and important families of trees and shrubs throughout the Malaysian reserve forest. About 2500-3000 species in 67 genera estimated worldwide with over 16 genera distributed across over 213 species in Malaysia (K Thakur, Anthwal, Singh Rawat, Rawat, & Rawat, 2012; Kochummen, 1997). Among the 16 genera, *Cryptocarya* has been studied in this investigation. This genus is well known as rich in isoquinoline derived alkaloids that exhibit various interesting biological activities such as cytotoxic, anti-inflammatory and anti-oxidant activities (Chou et al., 2010; Nasrullah, Zahari, Mohamad, & Awang, 2013). However, until recently very few studies on phytochemical and biological activity have been performed. Hence, the investigation of the alkaloids from *Cryptocarya densiflora*,

Cryptocarya infectoria and *Cryptocarya griffithiana* as well as their biological activities, antioxidant and anticholinesterase study were attempted.

Thomas Jefferson wrote that "The greatest service which can be rendered any country is to add a useful plant to its culture." Plants have forever been a catalyst for our healing. In order to halt the trend of increased emerging and resistant infectious disease, it will require a multi-pronged approach that includes the development of new drugs. Using plants as the inspiration for new drugs provides an infusion of novel compounds or substances for healing disease (Iwu, Duncan, & Okunji, 1999).

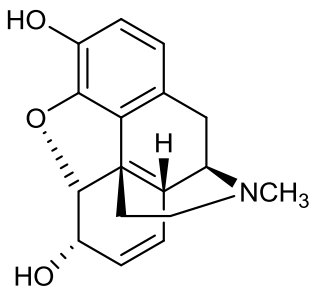

1

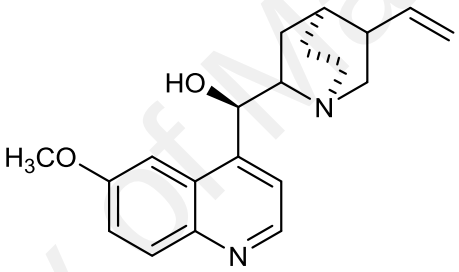

2

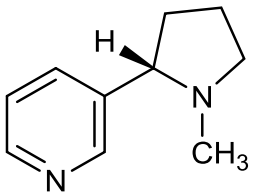

3

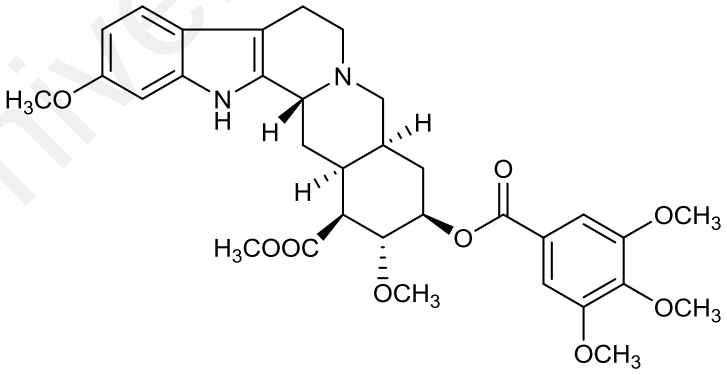

4

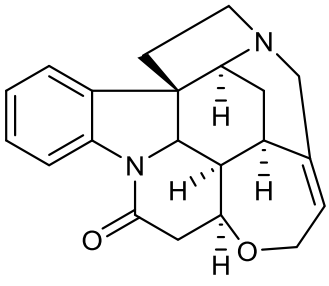

5

1.2 Lauraceae: Distribution and Habitat

The family Lauraceae, which derives its name from the prominent member, the Grecian laurel, *Laurus nobilis*, is characterized by plants which have prominent oil cells in the leaves, wood and fruits. These oils are mostly aromatic hence provide a number of flavouring materials and spices (K Thakur et al., 2012). The taxon comprises 67 genera and about 2,500-3,000 species which are widely distributed in all over the world (K Thakur et al., 2012). Trees of the Laurel family predominate in the world's Laurel forests, which occur in a few humid subtropical and mild temperate regions of the northern and southern hemispheres, including the Macaronesian islands, southern Japan, Madagascar, and central Chile.

In Malaysia, this family popularly known as '*Medang*' or '*Tejur*' and contribute about 213 species, from 16 genera. They are scattered from lowland forest up to montane forest (Khamis & Nizam, 2013). In the lowland of Malaysia, members of Lauraceae are typically small trees of the canopy except for a few species which may reach 30 m tall. In the highland, the Lauraceae becoming more abundant reaching the top layer of the forest canopy and thus the term "oak-laurel forest'' is given to this vegetation which lies at altitude 1200-1600 m.

1.3 Lauraceae: General Appearance and Morphology

The tree of Lauraceae are usually evergreen, shrubs, and without buttresses. The bark is usually smooth, rarely fissured, scaly or dippled, often covered with large lenticels, grey-brown to reddish-brown while the inner bark is very thick, granular, mottled or laminated, often with strong aromatic smell, yellow, orange-brown, pinkish or reddish. The sapwood is pale yellow to pale brown with satiny luster when freshly cut. The terminal bud is naked or covered with bud scales which sometimes appear like small leaves.

The leaves of this family are simple, without stipules, and usually alternate, spiral, opposite, subopposite, or whorled (*Actinodaphne*), entire and leathery. The secondary veins pinnate have only one pair as in *Cinnamommum*. The colours of the new leaves is vary from nearly white to pink, purple or brown (Corner, 1988; Keng, 1978).

The flowers are bisexual or unisexual. There are two whorls of three tepals; the whorls are usually equal in size and shape, but in some cases the whorls are unequal. If the whorls are unequal, the outer whorl is usually smaller than the inner one, although the reverse can also be the case. The flowers contain four whorls of three stamens, but in most genera, one, two, or three whorls are reduced to staminodia (Corner, 1988; van der Werff & Richter, 1996).

The fruit of this family are small to large (one seed berry), sometimes enveloped by the accrescent perianth tube or persiting and clasping the base of fruit. In some genera perianth lobes are dropping but the tube developing into a shallow or deep cup at base of fruit. The fruits stalk enlarging and becoming highly coloured in some species of *Dehaasia* and *Alseodaphne*. The seed is without albumen, with thin testa while the cotyledons are large, flat, convex, pressed against each other (Keng, 1978).

Wood of Lauraceae is soft to moderately hard, light to moderately heavy to varying from 350-880 kg/m^3 air dry. Grain straight or slightly interlocked, texture moderately fine and even. Sapwood usually is a distinctly lighter shade than the heartwood. The heartwood is yellow-white (*Beilschmiedia*), yellow brown or red-brown in most species of *Cinnamomum*, *Cryptocarya* and *Endiandra*, olive green in species of *Litsea, Actinodaphne, Alseodaphne, Notaphoebe, Phoebe,* and dark olive green-brown in *Dehaasia*.

Lauraceae plants provide a wide selection of valuable economic products. A great number of them are important resource in the construction timber, spice, essential oil, and medicinal plants for example, *Ocotea porosa*, the popular '*Imbuia*' and *Ocotea*

odorifera, known as '*Sassafras*'. *Persea maericana* or known as '*avocado*' have been reported that the skin of the avocado fruit is active against parasitic intestinal worms and also been occasionally used in treatment of cancer and tumours. Additional, natural products found in species such as *Aniba rosaeodora*, with an essential oil rich in linalool, an excellent perfume fixative, possess high economic value in international markets (Custodio & da Veiga Junior, 2014).

1.4 Classification of Tribe

There are many primitive and archaic features, which characterize the Lauraceae family. The determination is dependent on a combination of characters (Scheme 1.1). Sixty seven plant genera including *Cryptocarya* have been reported under the family Lauraceae, within "The Plant List" which have been enlisted below (K Thakur et al., 2012; Keng, 1978).

Kingdom : Plantae

Division : Magnoliophyta

Class : Magnoliopsida

Order : Laurales

Family : Lauraceae

Genera: :

1. *Actinodaphne*
2. *Aiouea*
3. *Alseodaphne*
4. *Aniba*
5. *Apollonias*
35. *Misanteca*
36. *Mocinnodaphne*
37. *Mutisiopersea*
38. *Nectandra*
39. *Neocinnamomum*

6. *Aspidostemon*
7. *Beilschmiedia*
8. *Benzoin*
9. *Camphora*
10. *Caryodaphnopsis*
11. *Cassytha*
12. *Chlorocardium*
13. *Cinnadenia*
14. *Cinnamomum*
15. *Cinnamonum*
16. ***Cryptocarya***
17. *Dehaasia*
18. *Dicypellium*
19. *Dodecadenia*
20. *Endiandra*
21. *Endlicheria*
22. *Eusideroxylon*
23. *Gamanthera*
24. *Hufelandia*
25. *Hypodaphnis*
26. *Iteadaphne*
27. *Kubitzkia*
28. *Laurus*
29. *Licaria*
30. *Lindera*
31. *Litsea*
40. *Neolitsea*
41. *Notaphoebe*
42. *Nothaphoebe*
43. *Ocotea*
44. *Oreodaphne*
45. *Parasassafras*
46. *Parthenoxylon*
47. *Persea*
48. *Phoebe*
49. *Phyllostemonodaphe*
50. *Pleurothyrium*
51. *Polyadenia*
52. *Potameia*
53. *Potoxylon*
54. *Povedadaphne*
55. *Ravensara*
56. *Rhodostemonodaphe*
57. *Sassafras*
58. *Schauera.*
59. *Sextonia*
60. *Sinopora*
61. *Sinosassafras*
62. *Syndiclis*
63. *Tetranthera*
64. *Tylostemon*
65. *Umbellularia*

32. *Machilus*

33. *Malapoenna*

34. *Mezilaurus*

66. *Urbanodendron*

67. *Williamodendron*

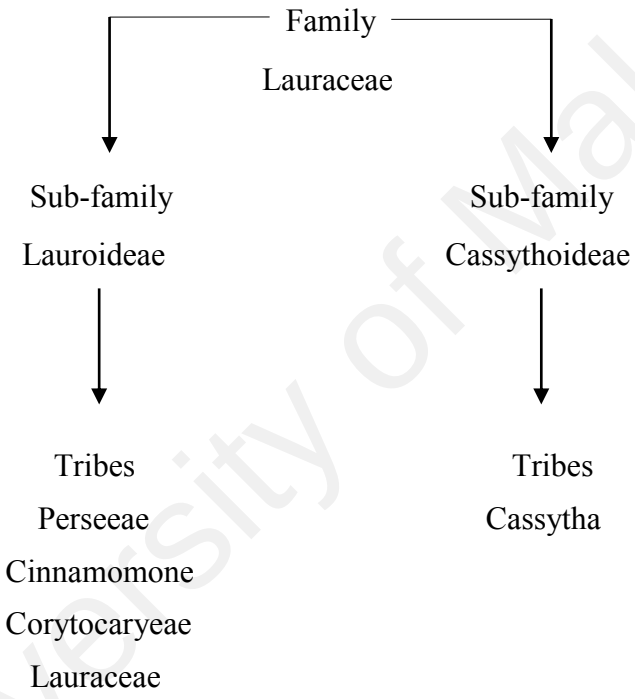

Scheme 1.1: Classification of family Lauraceae

1.5 The Genus of *Cryptocarya*

The genus *Cryptocarya* was first described by Robert Brown, based upon material he collected from the Australian subcontinent (Brown, 1810) in which he described three distinct species (*C. glaucescens* R. Br., *C. triplinervis* R. Br. and *C. obovata* R. Br.). The genus has subsequently been typified based upon the first species; *C. glaucescens* (Kostermans, 1939). Currently, between 200 and 250 distinct species are recognised, with the epicenter of species diversity being located within the *Flora Malesiana* region, although the genus ranges from South China and India to North Australia, Madagascar and South America (De Kok, 2016).

In Malaysia, about 17 species were recorded in a recent taxonomic study; *C. amygdalina*, *C. bracteolata, C. costata, C. densiflora, C. diversifolia*, *C. enervis, C. ferrea, C. griffithiana, C. impressa, C. kurzii, C. laevigata, C. malayana, C. nitens, C. rugulosa, C. teysmanniana, C. wrayi and C. zollingeriana* (De Kok, 2016).

1.6 General Morphology of *Cryptocarya*

Cryptocarya twigs are smooth to longitudinally ridged. The young twigs of most species are sparsely to densely hairy. Twigs lose their hairs when maturing, so that mature twigs are usually completely glabrous. The shape, size and texture of *Cryptocarya* leaves can vary considerably with leaf age and position relative to the inflorescence/infructescense. Older leaves tend to be bigger and thicker than younger ones, while leaves placed closely to the inflorescence/infructescence are usually smaller, thinner and sometimes slightly different in their length/with ratio compared to those placed further from the inflorescence/infructescence. The fruits are entirely included in the enlarged perianth tube leaving only a minute opening at apex (Ng, 1989).

1.7 *Cryptocarya densiflora* Blume

Cryptocarya densiflora is a medium sized tree, up to 20 m in height and 135 cm in girth. The bark is smooth and grayish in colour with large scattered lenticels (Figure 1.3). The inner bark is reddish brown and granular while their sapwood is pale yellow. The leaves blades (Figure 1.1) are leathery and elliptic to oblong, apex acuminate, base cuneate to rounded, secondary nerves up to 3 pairs, trinerved at base, tertiary nerves scalariform; reticulations circular, distinctly visible below, faint or inconspicuous above. The flower of this plant (Figure 1.2) are in axillary panicles, pale yellow, sessile, perianth funnel shaped, densely hairy; perianth lobes oblong, as long as perianth tube. The fruits are green ripening blue, globose, 2 cm across when dry; surface shallow ridged and warty.

This species is distributed throughout hills and mountain forests up to 1500 m in Malaysia (Kelantan, Perak, Pahang, Selangor) and Indonesia (Ng, 1989).

Figure 1.1: Leaves of *Cryptocarya densiflora*

Figure 1.2: Flowers of *Cryptocarya densiflora*

Figure 1.3: Bark of *Cryptocarya densiflora*

1.8 *Cryptocarya infectoria* Miq.

Cryptocarya infectoria is a medium sized tree, up to 21 m in height and 100 cm in girth. The bole is short buttresses up to 1 m high. The bark (Figure 1.4) is reddish brown and smooth while their inner bark is brown with radial wedges. The sapwood is pale yellow and fragrant. The twigs are velvety hairy. The leaves stalk (Figure 1.5) is about 1.0-1.5 cm long, velvety hairy; blade leathery, elliptic to oblong or narrowly obovate, (6.5 x 2.5) 12-26 x 4-9 cm; apex pointed with distinct 1 cm long trip; base cuneate; upper surface glabrous except midrib; lower surface glaucous and tomentose; secondary nerves 7-11 pairs, strongly raised below, sunken above; tertiary nerves and reticulations

strongly raised below, sunken above. The flowers are in axillary and terminal hairy panicles. The fruits are velvety reddish hairy when young, becoming glabrous and shiny and blue when ripe, ovate, 1.2 x 1 cm.

Scattered occurrence in lowlands, hills and upper hills up to 600 m: Kedah, Perak, Kelantan, Pahang, Selangor, Negeri Sembilan, Johore, Java. This species is very close to *C. griffithiana* from which it differs in the smaller, less pubescent leaves and in the short bracts (Ng, 1989).

Figure 1.4: Bark of *Cryptocarya infectoria*

Figure 1.5: Leaves of *Cryptocarya infectoria*

1.9 *Cryptocarya griffithiana* Wight

Cryptocarya griffithiana is a medium sized tree, growing up to 20 m tall, rarely to 30 m tall and 125 cm in girth. The bole is brownish and scaly. The inner bark (Figure 1.6) is reddish brown and granular while their sapwood is pale yellow. The leaves of this plants are narrow with distinct long tips. It has very long bracts and the non-chanelled midrib below. The flowers are pale yellow to creamy, hairs reddish; perianth tube 1 – 2 mm long, velutinous; perianth lobes elliptic, 2.5 – 4 × 1.2 – 1.5 mm, apex round to acute, velutinous.

The species commonly found in primary and secondary forests, often recorded as dry forest, at 120 – 1000 m altitude in Malaysia (Perak, Negeri Sembilan, Pahang, Johor, Kedah, Selangor, Kelantan, Sarawak) and Singapore (De Kok, 2016).

Figure 1.6: Bark of *Cryptocarya griffithiana*

Figure 1.7: Fruits of *Cryptocarya griffithiana*

Table 1.1: Species of *Cryptocarya* and their distribution (Ng, 1989)

Species	**Distribution**
C. bracteolata Gamb.	Widely distributed from lowland including swamps, to medium forest in Kedah, Kelantan, Terengganu, Pahang, Selangor and Java.
C. caesia Bl.	Rare; in lowland forest; Malacca, Singapore, Andaman Island, Java.
C. costata Bl.	Lowland forests by streams; locally abundant; Kedah, Pahang, Johore, Java.
C. crassinervia Miq.	The species occurrence from lowlands to hill forest up to 900 m and distributed in Kedah, Perak, Terengganu, Pahang, Johore and Java.
C. enervis Hk. f.	Very rare; Selangor (peat swamp); Malacca, Borneo.

C. ferrea Bl.	Widely distributed from lowlands including swamps, to mountain forests Kedah, Kelantan, Terengganu, Pahang, Selangor, Java.
C. griffithiana Wight	Uncommon; Perak, Pahang, Selangor, Negeri Sembilan, Malacca, Johore, Singapore in lowland forests, Burma, Thailand, Indonesia, Borneo, the Philippines.
C. impressa Miq.	Rare; known only from lowland forests, including swamps, from Negeri Sembilan, Malacca and Johore, Indo-China, Sumatra, Java.
C. infectoria Miq.	Scattered occurrence in lowlands, hills and upper hills up to 600 m; Kedah, Perak, Kelantan, Pahang, Selangor, Negeri Sembilan, Johore, Java.
C. kurzii Hk. f.	Scattered in lowland forests; Kedah, Perak, Terengganu, Pahang, Malacca, Johore, Java, Borneo.
C. laevigata Bl.	Rare, known only from a single collection, SFN 28958 from swamp forest in Johore, Borneo, the Philippines, Madagascar.
C. nitens (BI.) K. et V. (Lat.,shiny)	Uncommon tree of riversides in lowland forests including limestone in Kedah, Perak, Terengganu, Pahang and Selangor, Java.
C. rugulosa Hk. f.	Lowlands and hill forest in Kedah, Penang, Perak, Terengganu, Malacca, Johore, Singapore, Indonesia and Sarawak.

C. teysmanniana Miq.	Rare; Selangor, Johore; in hill forests, Sumatra.
C. tomentosa Bl.	Rare, lowland to upper hill forests up to 1000 m; by streams, Kedah, Perak, Indonesia, Borneo.
C. wrayi Gamb.	Common; mountain forests between 900-1200 m; Perak, Kelantan, Pahang, Johore.

1.10 Ethnic Medical Usage of *Cryptocarya* Species

It is known that several thousands of plants have been used as medicines, by some people or other at some time or other. Folk medicine represents an important tool to spot plants of pharmacological interest, since it can predict sources of bioactive compounds (Norscia & Borgognini-Tarli, 2006).

The ethnopharmacological history of *Cryptocarya* indicates that some species have been used in local medicine to treat a broad range of ailments and conditions. For example, *C. massoy* is a native of New Guinea. Known as '*massoi*' throughout the archipelago and by various local Papuan name, their aromatic bark is employed to treat fever, and often it is used by the natives to treat bad cases of tuberculosis of the lungs. A small plug of the bark is placed so as to close a fresh wound. It is chewed and the saliva rubbed over the limbs to ease muscular pains. In small quantities, mostly in combination with other vegetable drugs, it is ingested for violent headache, pain in the joints, puerperal infection, distention of the stomach, vomiting and chronic constipation; it is also mixed with cloves and sandalwood and used by the natives as rubefacient (Lemmens, Soerianegara, & Wong, 1995).

In Peninsular Malaysia, the bark of this species is used by the women after childbirth, and also is added to tonics and cigarettes, while, in Indonesia, it is used against diarrhea and spasmodic bowel trouble, usually in combination with a *Cinnamon*.

Furthermore, it is an ingredient of various native medicines and has a characteristic odor (Perry & Metzger, 1980).

The leaves and bark of the South African plant *C. latifolia*, have been long sought after for their legendary magical and medicinal properties. These properties range from the treatment of headaches and morning sickness to that of cancer, pulmonary diseases, and various bacterial and fungal infections (Hunter & O'Doherty, 2001).

C. mandioccana Meisner, the Brazilian-nutmeg (noz-moscada-do-brasil), is also known to have many medicinal uses. Its fruits are distinct by their aroma and pungent flavor, being carminative, and with stomachical properties. Its bark, bitter and scented, is also considered to be stomachical and helpful in fighting colics and diarrhea. The tea from its seeds is used against stomachache, and its crushed leaves, against aches and colics (de Moraes, Nehme, Alves, Derbyshire, & Cavalheiro, 2007).

1.11 Pharmacological Importance of *Cryptocarya* Species

Cryptocarya has been known to possess interesting pharmacological properties. Its crude extracts have been demonstrated to have an antiproliferative ability against cancer. For example, methanolic extracts of the leaves of *C. griffithiana* and the roots of *C. concinna* can inhibit cell proliferation of human HL60 promyelocytic leukemia cells and oral cancer cells, respectively (Huang et al., 2014). Furthermore, the ethanolic extracts of the fruit and trunk bark of *C. obovata* have been reported to have an antiproliferative effect against human KB cells (Dumontet et al., 2004).

Alkaloids from *C. chinensis* were tested *in vitro* for their cytotoxic activities against four cancer cell lines, human leukemia (L-1210), murine lymphocytic leukimia (P-388), human pulmonary cancer (A-549) and human colon cancer (HCT-8), with antofine **6** being the most potent against A-549 and HCT-8 with EC_{50} values of 0.002 and 0.001 µg/mL, respectively. In addition, an *in vitro* anti-HIV assay resulted

dehydroantofine **7**, suppressed HIV-infected H-9 cell growth significantly, with an EC_{50} value of 1.88 µg/mL. This promising finding is the first example of a dehydrophenanthroindolizidine alkaloid exhibiting anti-HIV activity. Thus, this compound type might provide a useful lead for anti-AIDS drug development (Wu, Su, & Lee, 2012).

The bioactivity of the *C. oubatchensis* was evaluated on human KB carcinoma cells. As a results, phenanthroindolizidine analogues; antofine **6**, hydroxyantofine **8** and desmethylantofine **9** exhibited very pronounced cytotoxicity toward the KB cancer cell line, with IC_{50} values ranging from 1.0 to 6.4 nM. Conversely, compounds ficuseptine C **10**, antofine-*N*-oxide **11** and oubatchensine **12** displayed low to null activity (Toribio et al., 2006).

The compounds isolated from the bark of *C. nigra* were evaluated for antiplasmodial activity based on the promising screening results of the dichloromethane extract (IC_{50} = 2.82 µg/mL). The *in vitro* antiplasmodial activity of compounds isolated from *C. nigra* against a chloroquine resistant strain of *P. falciparum* (K1 strain) resulted 2-hydroxyatherosperminine **13** displayed the strongest inhibition activity, with an IC_{50} value of 0.75 µM, followed by *N*-methylisococlaurine **14** and atherosperminine **15** with IC_{50} values of 5.40 µM and 5.80 µM respectively. Meanwhile, the same group has performed a study on the isolated compounds, which found *N*-methylisococlaurine **14** showed high scavenging activity towards the free radical DPPH at IC_{50} = 29.56 µg/mL (Nasrullah et al., 2013).

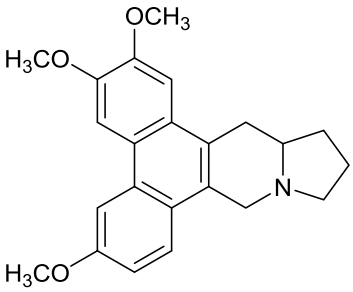

6

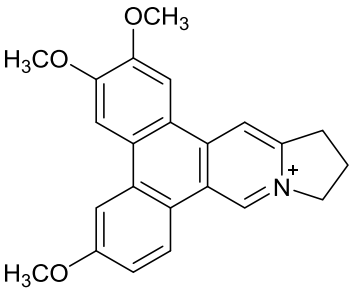

7

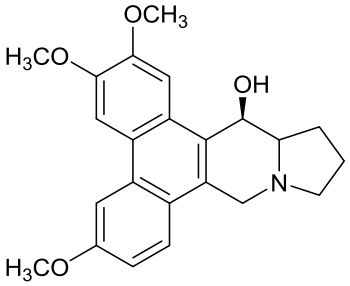

8

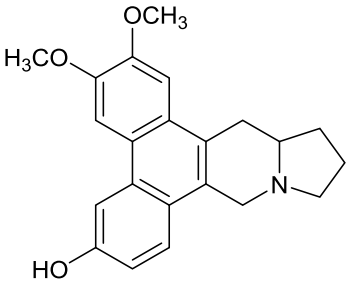

9

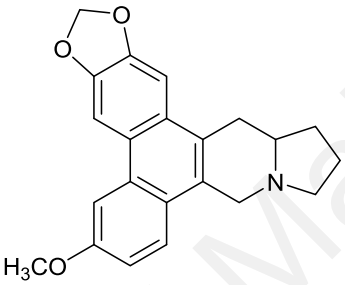

10

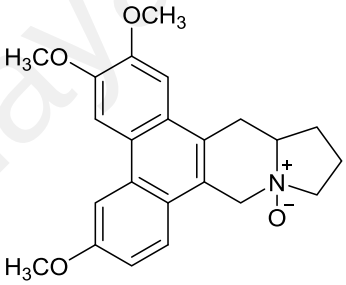

11

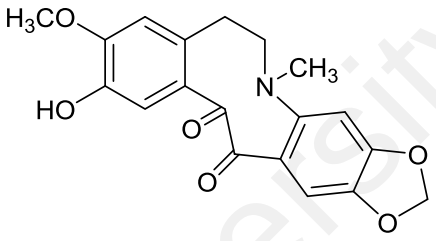

12

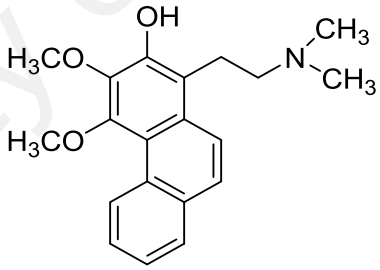

13

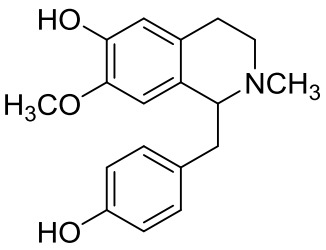

14

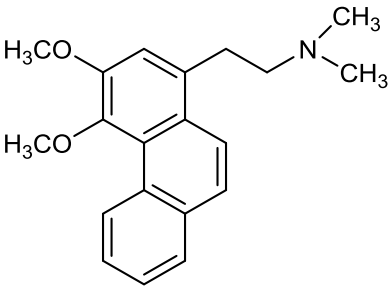

15

1.12 Objectives of the Study

The objectives of the study are as follows:

1. To isolate the compounds mainly alkaloids from *C. densiflora*, *C. infectoria* and *C. griffithiana* by using chromatographic techniques such as column chromatography (CC), thin layer chromatography (TLC) and preparative thin layer chromatography (PTLC).
2. To characterize the chemical structures of the isolated alkaloids by using various spectroscopic methods such as 1D NMR (^{1}H, ^{13}C and DEPT), 2D NMR (COSY, NOESY, HSQC and HMBC), UV, IR and LCMS-IT-TOF analysis.
3. To evaluate the antioxidant (DPPH) and cholinesterase inhibitory activities of selected alkaloids isolated from these three species.

CHAPTER 2: GENERAL CHEMICAL ASPECTS

2.1 General

Plants provide a plethora of natural products that are essential for human survival. For much of the world populations, the botanical kingdom supplies most medicines, resins, latex, gums, dyes, poison and fragrance. These compounds belong to a group collectively known as secondary metabolites (Mulabagal & Tsay, 2004). The molecules are known to play a major role in the adaptation of plants to their environment, but also represent an important source of pharmaceuticals (Rao & Ravishankar, 2002). The uptake of many secondary plant metabolites is an active process, because the compounds are often polar and have a large molecular weight, making active transport the only route to sequestration (Wink, 1998a).

During the last 20 to 30 years, the analysis of secondary plant products has progressed a lot. The use of modern analytical techniques like chromatography, electrophoresis, isotope techniques and enzymology have succeeded in the elucidation of exact structural formulas and the most important biosynthetic pathways (Kabera, Semana, Mussa, & He, 2014). Among the secondary metabolites that are produced by plants, alkaloids figure as a very prominent class of defence compound. Over 21, 000 alkaloids have been identified, which thus constitute the largest group among the nitrogen-containing secondary metabolites (Aiello et al., 2008).

Due to the high interest in this valuable compound, researchers from all over the world have tried to find new and better techniques for the extraction and the estimation of alkaloids. Like all the other secondary metabolites, the extraction of alkaloids was also started with the paper chromatography (Tso & Jeffrey, 1953). It was the easiest method for extraction, which was rapid and cheap. With the advancements in the field of science

and technology, alkaloids are being exploited for various purposes especially in the field of pharmaceutical (Kaur & Arora, 2015).

2.2 Alkaloids

The earliest evidence that humans used alkaloids-producing plants is derived from Assyrian clay tablets, written in cuneiform characters. On these 4,000-year-old plates, about 250 different plants are mentioned, including number of alkaloid-containing plants such as *Papaver somniferum*, *Atropa belladonna*, and *Mandragora officinarum* (Wink, 1998b).

Applications of such alkaloids included empirical medicines for animals and humans as well as sources of poison for hunting expeditions or executions (Wink, 1998b). All throughout the centuries these plants and associated isolated compounds were increasingly and continuously used for, as one scholar encapsulates it, 'Murder, Magic and Medicine' (Mann, 2000).

The nature of alkaloids was not understood until the early part of the nineteenth century, and the term itself was not coined until 1821. Attempts to define the term 'alkaloid' originated at the time of the discovery of these compounds. Friedrich Sertürner, an apothecary's assistant from Westphalia, first isolated morphine **1**, one of the most important alkaloids in the applied sense, thus proved a significant step forward in chemistry and pharmacology. The term "alkaloid" was first mentioned in 1819 by Carl F. W. Meissner, an apothecary from Halle as observed that these compounds appeared "like alkali", and so named them alkaloids (Tadeusz, 2007).

To man, alkaloids represent one of the largest and most interesting groups of plants metabolite. One reason for the continuing attention towards them is pharmaceutical and therapeutical values (García et al., 2006).

2.3 Occurrence and Distribution of Alkaloids

At least 25% of higher plants contain alkaloids. In effect this means that on average, at least one in fourth plants contains some alkaloid (Tadeusz, 2007). Alkaloids may occur in any plant part, but they are usually accumulated in plant parts involved in biological interactions, for example, in the plant epidermis (Seigler, 2012). Alkaloid distribution in the angiosperms is uneven. The dicotyledon orders Salicales, Fagales, Cucurbitales and Oleales at present appear to be alkaloid-free. However, alkaloids are commonly found in the orders Centrospermae (Chenopodiaceae), Magnoliales (Lauraceae, Magnoliaceae), Ranunculales (Berberidaceae, Menispermaceae, Ranunculaceae), Papaverales (Papaveraceae, Fumariaceae), Rosales (Leguminosae, subfamily Papilionaceae), Rutales (Rutaceae), Gentiales (Apocynaceae, Loganiaceae, Rubiaceae), Tubiflorae (Boraginaceae, Convolvulaceae, Solanaceae) and Campanulales (Campanulaceae, sub-family Lobelioideae; Compositae, subfamily Senecioneae) (Trease & Evans, 2001).

2.4 Classification of Alkaloids

Alkaloids are a group of chemical compounds which are characterized by carbon rings that usually contain nitrogen and by the fact that they are usually basic on the pH scale. Several approaches to the classification of alkaloids are available, including, chemical, taxonomic, biological, and biosynthetic to construct the molecule and also to categorize different alkaloid (Funayama & Cordell, 2014). From a structural point of view, alkaloids are divided according to their shapes and origins (Wang & Liang, 2009). Alkaloids could thus be further classified into three groups according to their biosynthesis origin:

1. 'True alkaloids', which contain nitrogen in the heterocycle and originate from amino acids (Plemenkov, 2001). Their characteristic examples are nicotine **3**, morphine **1** and hygrine **16**.

2. ‘Protoalkaloids’ are compounds in which the nitrogen atom derived from an amino acid is not a part of the heterocyclic bond. Such alkaloids include compounds derived from L-tyrosine **17** and L-tryptophan **18**. Mescaline **19**, hordenine **20** and serotonine **21** are good examples of these kinds of alkaloids (Tadeusz, 2007).
3. ‘Pseudoalkaloids’ are compounds, the basic carbon skeletons of which are not originated from amino acids. This group includes terpene-like and steroid-like alkaloids, as well as purine-like alkaloids such as caffeine **22**, theobromine **23**, theacrine **24**, theophylline **25** (Plemenkov, 2001; Tadeusz, 2007).

The true alkaloids can be further classified into different types of basic skeletons. This is the most popular methods/ factors of alkaloids classification. Classification also can be done based on other factors such as, biogenesis, structural relationships, botanical origin and spectroscopic criteria. Several examples of common alkaloid ring skeletons are shown in Scheme 2.1.

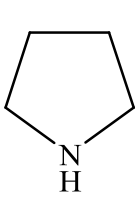

Pyrrolidine

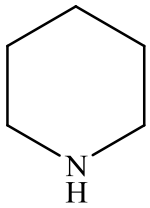

Piperidine

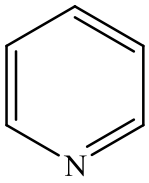

Pyridine

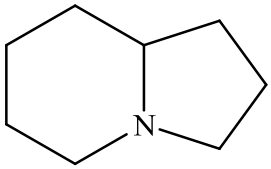

Indolizidine

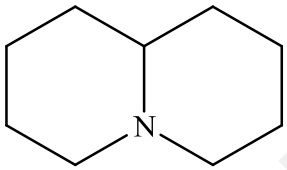

Quinolizidine

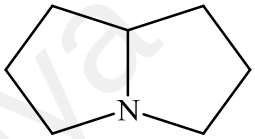

Pyrrolizidine

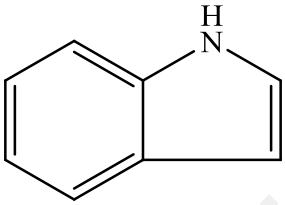

Indole

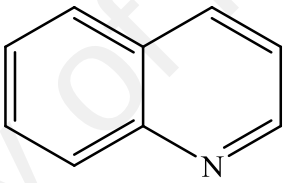

Quinoline

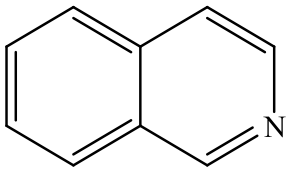

Isoquinoline

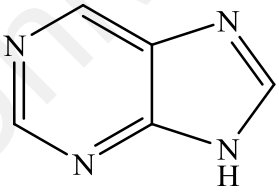

Purine

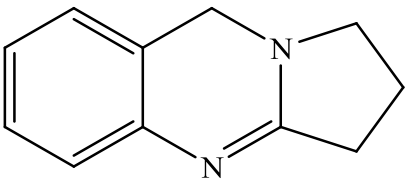

Quinazoline

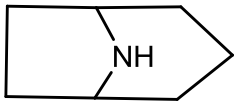

Tropane

Scheme 2.1: Examples of alkaloid ring skeletons

Applications in medical use of alkaloid-containing plants has a long history, and thus, when the first alkaloids were isolated in the 19th century, they immediately found application in clinical practice. Many alkaloids are still used in medicine, including the following (Table 2.1) which listed the pharmacological activities of some alkaloids of different skeletal types.

Table 2.1: Some alkaloids and their pharmacological activities

Groups	**Alkaloids**	**Pharmacological activities**	**Source**
Pyrrolidine	Odorine **26**	Exhibited potent anti-carcinogenic effects and anti-tumor promoting activity. (Inada et al., 2001)	*Aglaia odorata* (Meliaceae)
Piperidine	(-)-Lobeline **27**	Respiratory stimulant, Treatment for Central Nervous System (CNS) disorder, drug deterrent, potent AChE inhibitory. (Felpin & Lebreton, 2004)	*Lobelia inflata* (Campanulaceae)
Pyridine	Malloapeltine **28**	Anti-HIV (Cheng, Meng, & Chen, 1998)	*Mallotus apelta* (Euphorbiaceae)
Indolizidine	Tylophorinidine **29**	Showed significant activity in murine leukimia. (I. R. C. Bick & Sinchai, 1982)	*Tylophora asthmatica* (Apocynaceae)
Quinolizidine	Matrine **30**	Strong antitumor activities *in vitro* and *in vivo*. (Ma et al., 2008)	*Sophora flavescens* (Fabaceae)
Pyrrolizidine	Clivorine **31**	Antiproliferative activity in human normal liver L-02 cells, by induce apoptosis.	*Ligularia hodgsonii* (Compositae)

		(Ji, Zhang, Sheng, & Wang, 2005)	
Indole	Cryptolepine **32**	Displayed potent cytotoxic, present antibacterial and antiparasitic properties. (Dassonneville et al., 2000)	*Cryptolepis sanguinolenta* (Apocynaceae)
Quinoline	Veprisine **33**	Exhibited moderate to higher antimycobacterial activity. (Erasto, Omolo, & Hamilton, 2013)	*Teclea amaniensis* (Rutaceae)
Isoquinoline	Berberine **34**	Antiinflammatory, antibacterial, antidiabetes, antiulcer, sedation, protection of myocardial ischemia-reperfusion injury, expansion of blood vessels, inhibition of platelet aggregation, hepatoprotective, and neuroprotective effects. (J.-J. Lu, Bao, Chen, Huang, & Wang, 2012) Antidiarrheal (Rabbani, Butler, Knight, Sanyal, & Alam, 1987)	*Rhizoma coptidis* (Ranunculaceae) *Berberis aristata* (Berberidaceae)
Purine	Caffeine **22**	Central Nervous System (CNS) stimulant. (McCarthy, Candelario, & Liu, 2014)	*Camellia sinensis* (Theaceae) *Coffea robusta*/*Arabica* (Rubiaceae) *Theobroma cacao* (Malvaceae)
Quinazoline	(±)-Vasicine **35**	Significant antitussive, expectorant, and bronchodilating activities. (Liu et al., 2015)	*Peganum harmala* (Nitrariaceae)

Tropane	Hyoscyamine **36**	Potent anticonvulsant, antinociceptive, motor incoordination, and antioxidant activities. (Al-Ashaal, Aboutabl, Maklad, & El-Beih, 2013)	*Atropa belladonna* (Solanaceae)

2.5 Alkaloids of Lauraceae

Interest in Lauraceae, a pantropical family with 67 genera and 2500-3500 species, is of considerable interest to both taxonomists and natural product chemists (Drewes, Horn, & Mavi, 1997). This family have been known for a long time to contain rich source of secondary metabolites with interesting biological activities. Most of the alkaloids isolated from this family have been found in stem bark as well as in leaves and roots. The Lauraceae alkaloids represent a large number with over 300 different alkaloids have been isolated, and still expanding group of biogenetically related isoquinoline alkaloids that are found exclusively in plants belonging to this family. About 287 structures of alkaloids distributed among all the genera within this family have been reported. Subsequently, these isoquinolines were divided into subclasses inclusive of 148 aporphines, 47 benzylisoquinolines, 23 pavines, 21 bisbenzylisoquinolines, 21 proaporphines, 18 morphinandienones, 4 phenanthrenes and 5 simple isoquinolines. The most frequently detected alkaloids in the Lauraceae are those with the aporphine skeleton. (Custodio & da Veiga Junior, 2014).

2.6 Alkaloids of *Cryptocarya*

Cryptocarya is one of the main genera of Lauraceae comprising at least 200-250 species and it is distributed mainly in the tropical region of the world (De Kok, 2016). Previous studies have revealed *Cryptocarya* genus is a rich source of secondary metabolites, such as flavonoids, pyrones, lignans, terpenoids and alkaloids (Juliawaty,

Kitajima, Takayama, Achmad, & Aimi, 2000b). Extensive works on the isolation and identification of chemical compounds from the *Cryptocarya* species, as well as their biological activities have been reported by numerous scientists, as many of the plants from this genus are known for their medicinal values (I. Bick, N. Preston, & P. Potier, 1972; Cave et al., 1989).

Cryptocarya species are known to furnish various types of alkaloids in which the majority are from isoquinoilne type such as aporphine, benzylisoquinoline, phenanthroindolizidine, pavine and many more. Some of the alkaloids isolated from the *Cryptocarya* species are listed in Table 2.2.

Table 2.2: Some alkaloids isolated from the *Cryptocarya* species

Plant	Plant part	Extract	Alkaloids isolated	Skeletal type
C. amygdalina Nees (Borthakur, Mahanta, & Rastogi, 1981)	Bark	MeOH	(+)-Orientaline **37** Laudanidine **38**	Benzylisoquinoline Benzylisoquinoline
C. angulata C. T. White (Cooke & Haynes, 1954)	Bark	MeOH	Roemerine **39** Atherosperminine **15** Isocorydine **40**	Aporphine Phenanthrene Aporphine
C. archboldiana C. K. Allen (Johns, Lamberton, & Tweeddale, 1969)	Leaves	None reported	Armepavine **41**	Benzylisoquinoline
C. bowiei Hook. Druce (Ewing, Hughes, Ritchie, & Taylor, 1953)	Bark	MeOH	Cryptaustoline **42** Cryptowoline **43**	Dibenzopyrrocoline Dibenzopyrrocoline
C. chinensis Hemsl. (T.-S. Wu & Lin, 2001)	Wood	EtOH	(+)-Eschscholtzidine-*N*-oxide **44** (-)-12-hydroxycrychine **45** (-)-12-hydroxy-*O*-methylcaryachine **46** (-)-*N*-demethylcrychine **47** Isocryprochine **48** Prooxocryptochine **49** Isoamuronine **50** (+)-8,9-dihydrostepharine **51**	Pavine Pavine Pavine Pavine Proaporphine Proaporphine Proaporphine Proaporphine

(T.-S. Wu, Su, & Lee, 2012)			(-)-(*R*)-13aα-antofine **6**	Phenanthroindolizidine
			Dehydroantofine **7**	Phenanthroindolizidine
			(-)-6-hydroxycrychine **52**	Pavine
			(-)-12-hydroxyeschscholtzidine **46**	Pavine
			(+)-Eschscholtzidine **53**	Pavine
			(-)-Argemonine **54**	Pavine
			Cryprochine **55**	Proaporphine
			Doryanine **56**	Isoquinoline
			(-)-*N*-demethylphyllocryptine **57**	Benzylisoquinoline
(Lin, Wu, & Wu, 2001)	Leaves	EtOH	(-)-Isocaryachine-*N*-oxide **58**	Pavine
			Isoboldine-β-*N*-oxide **59**	Aporphine
			1-hydroxycryprochine **60**	Proaporphine
			(±)-Isocaryachine **61**	Pavine
			(±)-Caryachine **62**	Pavine
			Isoboldine **63**	Aporphine
			(-)-Munitagine **64**	Pavine
			Bisnorargemonine **65**	Pavine
(S.-S. Lee, Chen, & Liu, 1993)			(±)-Romneine **66**	Benzylisoquinoline

(Lin, Wang, & Wu, 2002) (S.-S. Lee, Liu, & Chen, 1990) (S.-S. Lee, Chen, et al., 1993)	Stem bark	EtOH	(±)-Isocaryachine-*N*-oxide **58** (-)-Caryachine-*N*-oxide **67** 6,7-methylenedioxy-*N*-methylisoquinoline **68** (-)-Neocaryachine **69** (±)-Caryachine **62** (-)-Isocaryachine **61** (+)-Cinnamolaurine **70** 1-hydroxycryprochine **60** (-)-Eschscholtzidine **53** Cryprochine **55**	Pavine Pavine Isoquinoline Pavine Pavine Pavine Benzylisoquinoline Proaporphine Pavine Proaporphine
C. crassinervia Miq. (Awang et al., 2008; Saidi, 2011)	Bark	DCM	2-hydroxyatherosperminine **13** *N*-demethyl-2-methoxyatherosperminine **71** 2-methoxyatherosperminine **72** 2-methoxyatherosperminine-*N*-oxide **73** (+)-Lirinine **74** (+)-Lirioferine **75** (+)-Reticuline **76** (-)-*N*-methylisococlaurine **14**	Phenanthrene Phenanthrene Phenanthrene Phenanthrene Aporphine Aporphine Benzylisoquinoline Benzylisoquinoline
C. ferrea (Saidi, Hadi, Awang, & Mukhtar, 2010)	Bark	DCM	(-)-*O*-methylisopiline **77** (+)-Norlirioferine **78** (+)-Lirioferine **75**	Aporphine Aporphine Aporphine
C. foveolata White & Francis (Lamberton & Vashist, 1972)	Bark	None reported	(+)-Reticuline **76**	Benzylisoquinoline
C. konishii Hayata ex Kawakami	Stem bark	EtOH	(+)-(1*R*, 1a*R*)-1*a*-hydroxymagnocurarine **79**	Benzylisoquinoline

(S.-S. Lee, Lin, Chen, Liu, & Chen, 1993) (S.-T. Lu, 1967)			Crykonisine **80**	Benzylisoquinoline
C. longifolia Kosterm. (I. Bick, Sevenet, Sinchai, Skelton, & White, 1981)	Leaves, stems, roots	MeOH	Thalifoline **81** Longifolonine **82** (-)-Longifolidine **83** (+)-Reticuline **76** (-)-*N*-methylcoclaurine **84** (+)-Coclaurine **85** (+)-Laurotetanine **86** (+)-*N*-methyllaurotetanine **87** (+)-Laurolitsine **88** (+)-Isoboldine **63** (+)-Norisocorydine **89** (-)-Norargemonine **90** (-)-Bisnorargemonine **65** (-)-Scoulerine **91**	Isoquinoline Benzylisoquinoline Benzylisoquinoline Benzylisoquinoline Benzylisoquinoline Benzylisoquinoline Aporphine Aporphine Aporphine Aporphine Aporphine Pavine Pavine Protoberberine
C. nigra Kosterm. (Nasrullah, Zahari, Mohamad, & Awang, 2013)	Bark	DCM	(+)-*N*-methylisococlaurine **14** Atherosperminine **15** 2-hydroxyatherosperminine **13** Noratherosperminine **92**	Benzylisoquinoline Phenanthrene Phenanthrene Phenanthrene
C. odorata Guillaumin (I. Bick, N. W. Preston, & P. Potier, 1972)	Stem bark		Laurotetanine **86** *N*-methyllaurotetanine **87** Reticuline **76** Isocorydine **40** Cryptodorine **93**	Aporphine Aporphine Benzylisoquinoline Aporphine Aporphine

C. oubatchensis Schltr. (Toribio et al., 2006)	Bark Leaves	None reported	Oubatchensine **12** (-)-13aα-antofine **6** (-)-14β-hydroxy-13aα-antofine **8** (-)-13aα-6-*O*-desmethyl-antofine **9** Ficuseptine C **10** (-)-10β, 13aα-antofine-*N*-oxide **11**	*Seco*-dibenzopyrrocoline Phenanthroindolizidine Phenanthroindolizidine Phenanthroindolizidine Phenanthroindolizidine Phenanthroindolizidine
C. phyllostemon Kosterm. (Cave et al., 1989)	Stem bark Leaves, twigs, roots and fruit Stem bark Stem bark	EtOH MeOH	(-)-Antofine **6** Dehydroantofine **7** (-)-Cryptowoline **43** (-)-Cryptowolidine **94** (-)-Cryptowolinol **95** (-)-Phyllostemine **96** (-)-Phyllosteminine **97** (-)-Phyllostone **98** (+)-Phyllocryptine **99** (+)-Phyllocryptonine **100**	Phenanthroindolizidine Phenanthroindolizidine Dibenzopyrrocoline Dibenzopyrrocoline Dibenzopyrrocoline *Seco*-phenanthroindolizidine *Seco*-phenanthroindolizidine Pyrrolidinylacetophenone Benzyltetrahydroisoquinoline Benzyltetrahydroisoquinoline
C. pleurosperma C. T. White & W. D. Francis (De la Lande, 1948)	Bark	MeOH (hot)	Cryptopleurine **101**	Phenanthroquinolizidine
C. rugulosa Hook. f. (Saidi et al., 2011)	Bark	DCM	Papraline **102** (+)-Norcinnamolaurine **103** (+)-Codamine **104** (+)-6-methoxy-1-(3'-methoxybenzyl)-*N*-methyl-7-isoquinolinol **105** (+)-Reticuline **76**	Isoquinoline Benzylisoquinoline Benzylisoquinoline Benzylisoquinoline Benzylisoquinoline

			(+)-Reticuline-*N*-oxide **106** (-)-*N*-methylisococlaurine **14**	Benzylisoquinoline Benzylisoquinoline
C. strictifolia Kosterm. (Juliawaty, Kitajima, Takayama, Achmad, & Aimi, 2000a)	Stem bark	MeOH	Lysicamine **107**	Oxoaporphine
C. velutinosa Kosterm. (Lebœuf, Ranaivo, Cavé, & Moskowitz, 1989)	Leaves	DCM	Velucryptine **108** Atheroline **109**	Isoquinoline Oxoaporphine

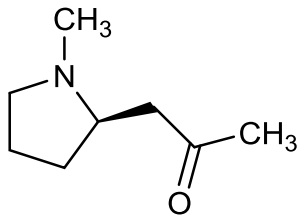

16

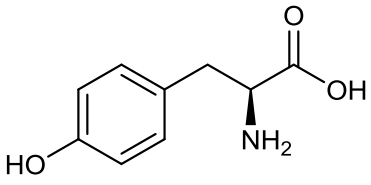

17

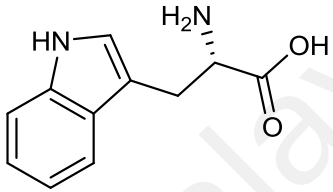

18

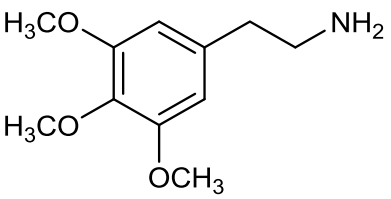

19

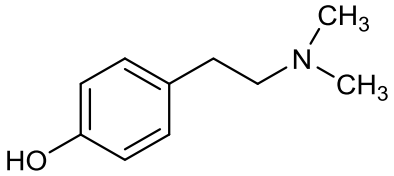

20

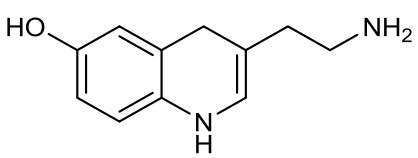

21

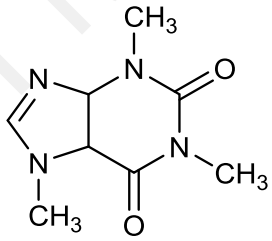

22

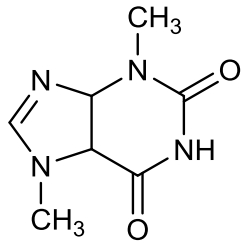

23

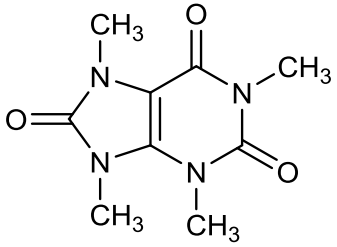

24

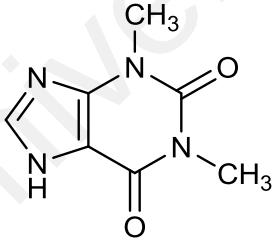

25

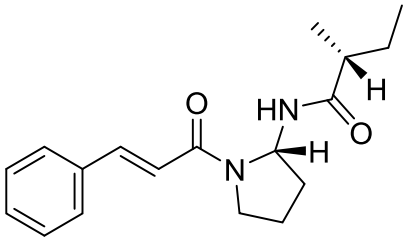

26

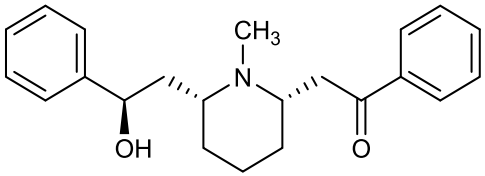

27

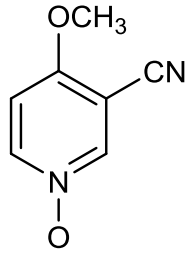

28

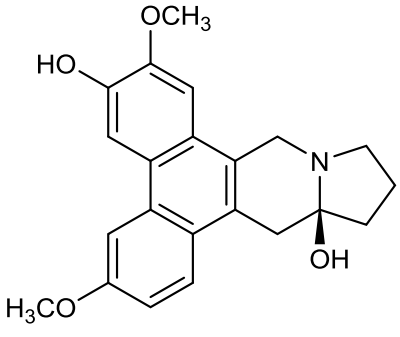

29

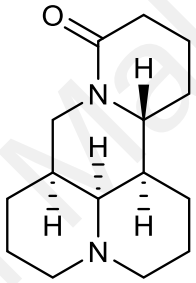

30

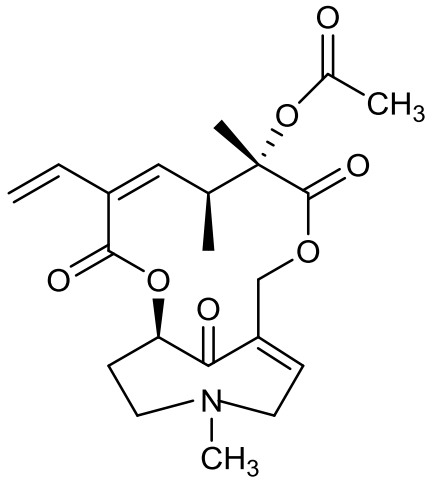

31

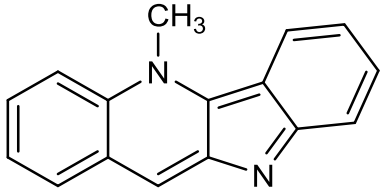

32

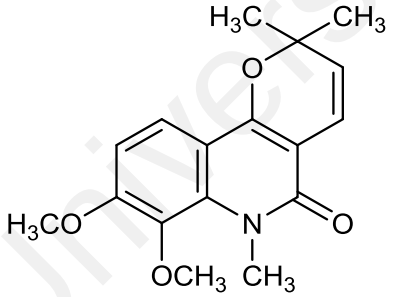

33

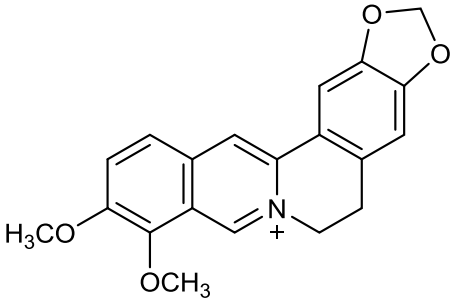

34

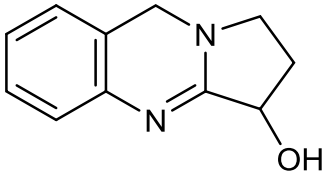

35

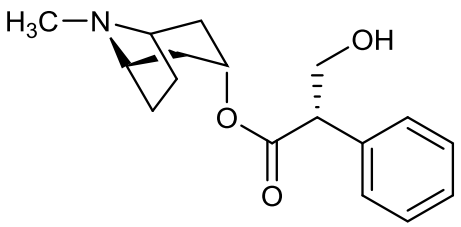

36

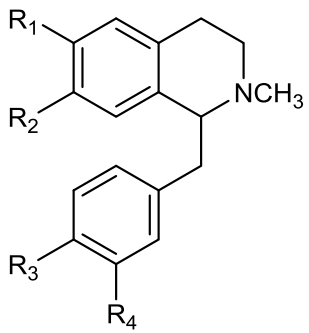

R_1=R_4=OCH_3, R_2=R_3=OH **37**
R_1+R_2=OCH_2O, R_3=OCH_3, R_4=OH **57**

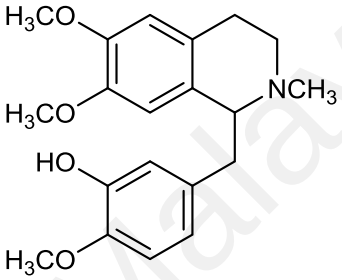

38

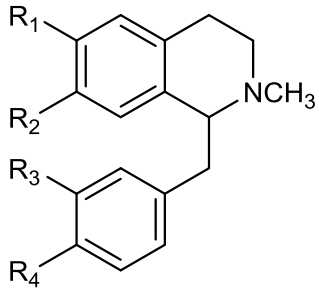

R_1=R_2=OCH_3, R_4=OH **41**
R_1+R_2=OCH_2O, R_3=R_4=OCH_3 **66**
R_1+R_2=OCH_2O, R_4=OH **70**

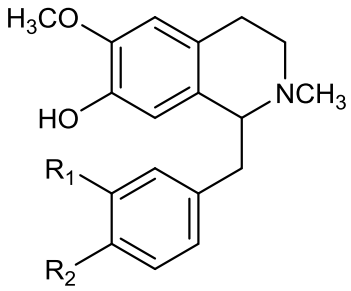

R_1=OH, R_2=OCH_3 **76**
R_1=H, R_2=OH **84**
R_1=OCH_3, R_3=OCH_3 **104**
R_1=OCH_3, R_2=H **105**

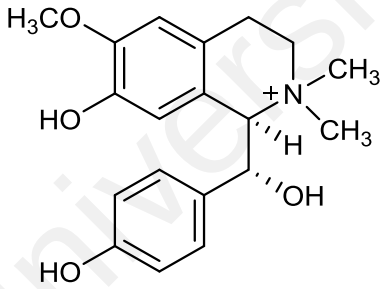

79

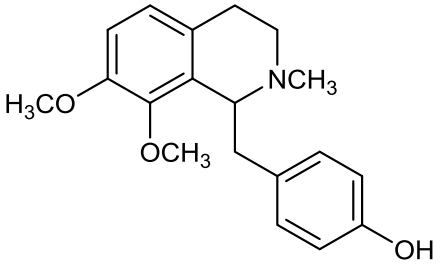

83

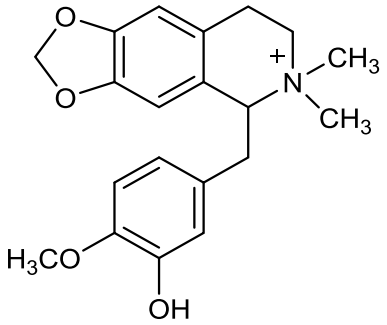

99

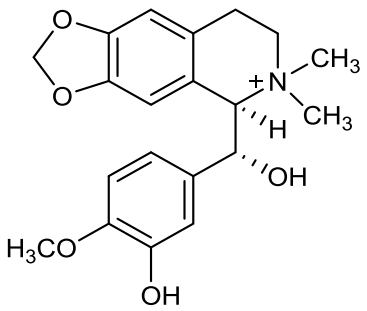

100

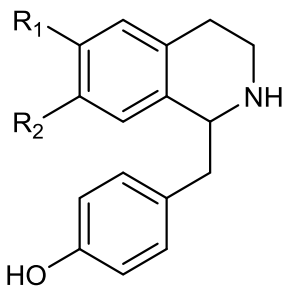

R_1=OCH_3, R_2=OH **85**
R_1+R_2=OCH_2O **103**

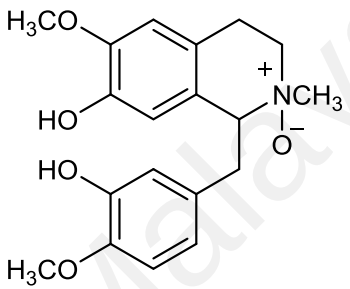

106

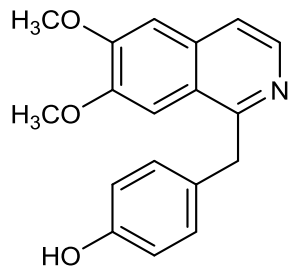

80

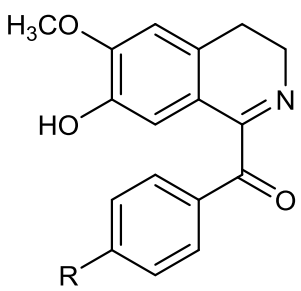

R=OH **82**
R=OCH_3 **108**

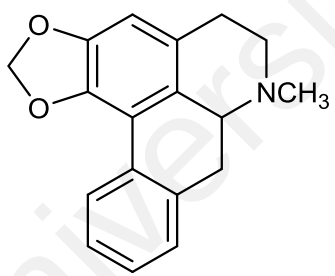

39

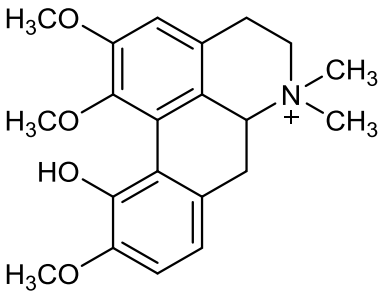

40

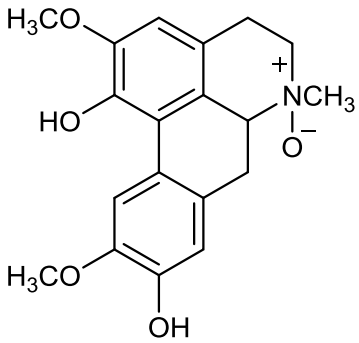

59

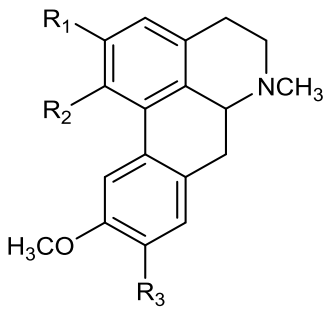

R_1=OCH_3, R_2=OH, R_3=OH **63**
R_1+R_2=OCH_2O, R_3=OCH_3 **66**

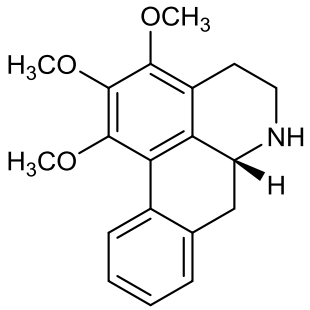

77

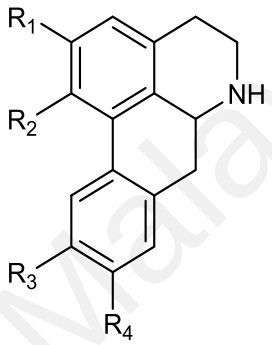

R_1=R_2=R_4=OCH_3, R_3=OH **78**
R_1=R_2=R_3=OCH_3, R_4=OH **86**
R_1=R_4=OH, R_2=R_3=OCH_3 **88**
R_1+R_2=OCH_2O, R_3+R_4=OCH_2O **93**

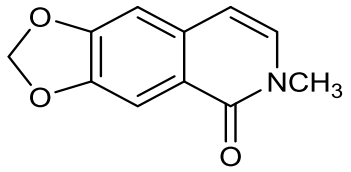

56

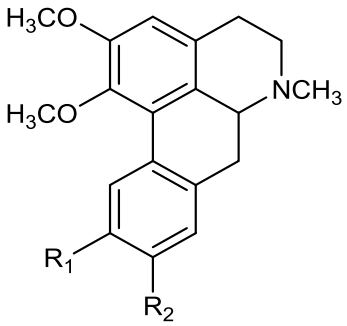

R_1=OH, R_2=OCH_3 **75**
R_1=OCH_3, R_2=OH **87**

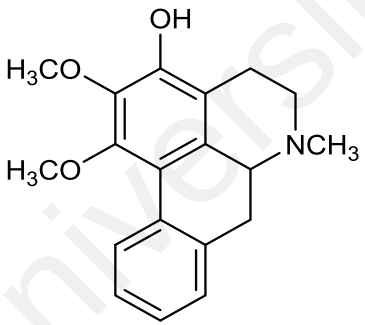

74

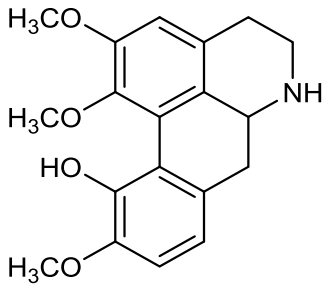

89

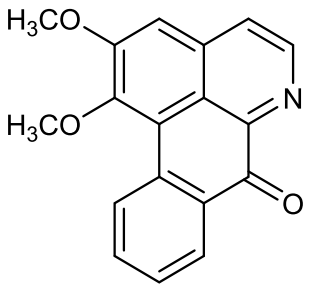

107

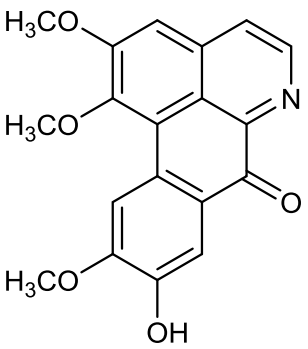

109

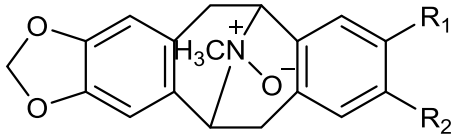

R_1=OCH_3, R_2=OCH_3 **44**
R_1=OCH_3, R_2=OH **58**
R_1=OH, R_2=OCH_3 **67**

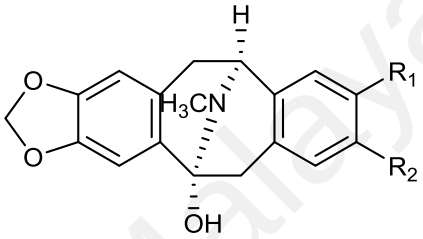

R_1+R_2=OCH_2O **45**
R_1=R_2=OCH_3 **46**

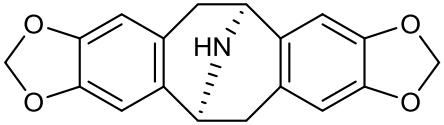

47

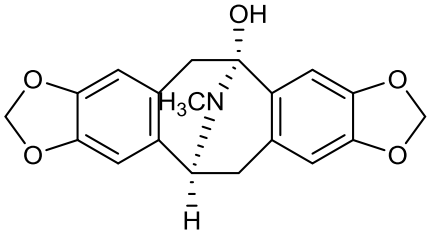

52

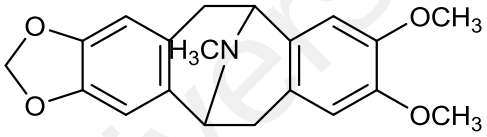

53

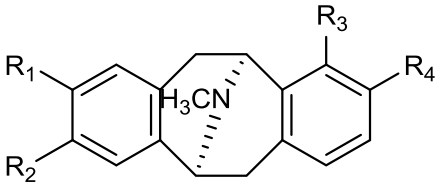

R_1=OCH_3, R_2=OH, R_3=OH, R_4=OCH_3 **64**
R_1+R_2=OCH_2O, R_3=OH, R_4=OCH_3 **69**

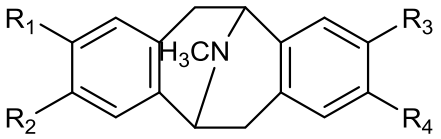

$R_1=R_2=R_3=R_4=OCH_3$ **54**
$R_1+R_2=OCH_2O$ $R_3=OCH_3$, $R_4=OH$ **61**
$R_1+R_2=OCH_2O$, $R_3=OH$, $R_4=OCH_3$ **62**
$R_1=OCH_3$, $R_2=OH$, $R_3=OCH_3$,
$R_4=OH$ **65**
$R_1=OCH_3$, $R_2=OH$, $R_3=OCH_3$,
$R_4=OCH_3$ **90**

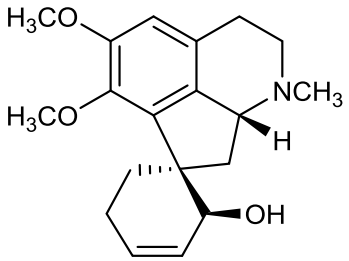

48

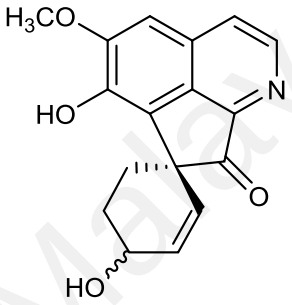

49

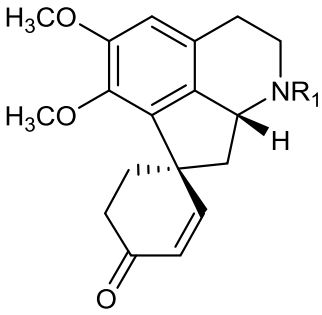

$R_1=CH_3$ **50**
$R_1=H$ **51**

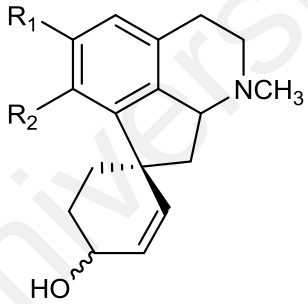

$R_1=R_2=OCH_3$ **55**
$R_1=OCH_3$, $R_2=OH$ **60**

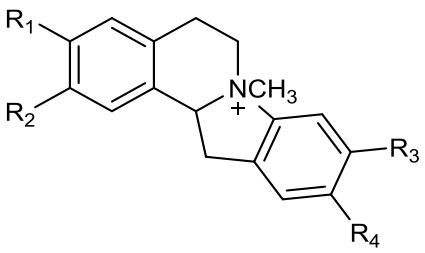

R_1=OCH_3, R_2=OH, R_3=OCH_3, R_4=OCH_3 **42**
R_1=OCH_3, R_2=OH, R_3+R_4=OCH_2O **43**
R_1=OH, R_2=OCH_3, R_3+R_4=OCH_2O **94**

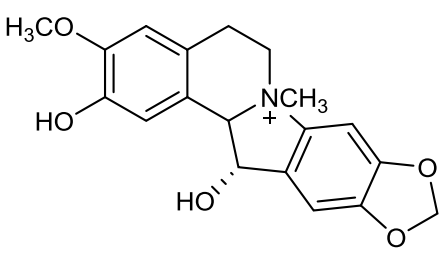

95

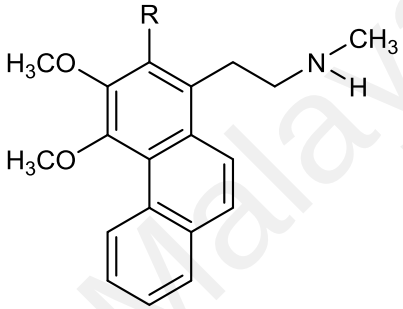

R=OCH_3 **71**
R=H **92**

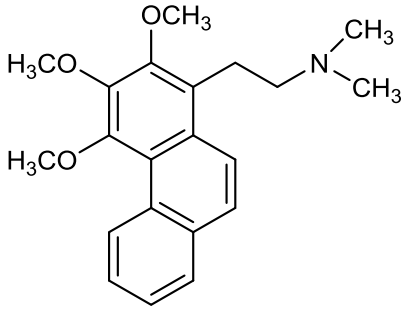

72

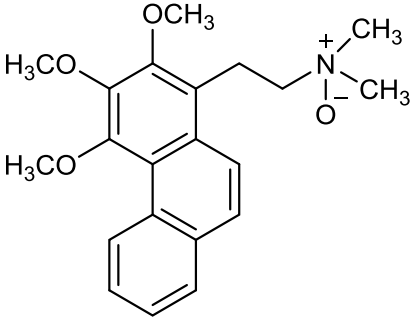

73

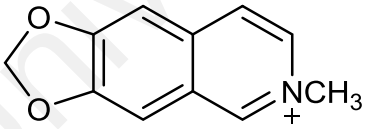

68

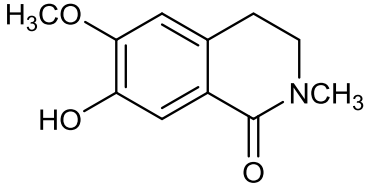

81

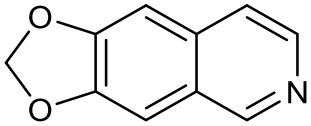

102

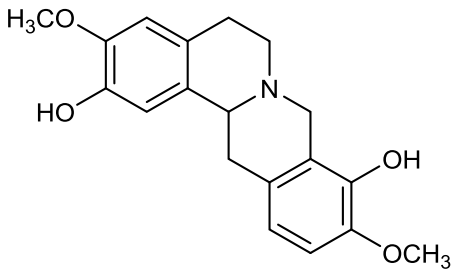

91

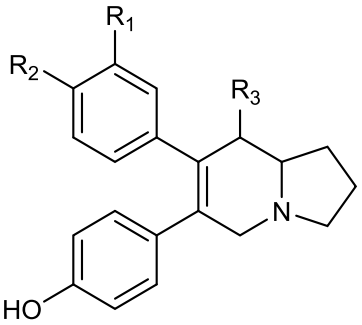

R_1=OCH_3, R_2=OH, R_3=H **96**
R_1+R_2=OCH_2O, R_3=OH **97**

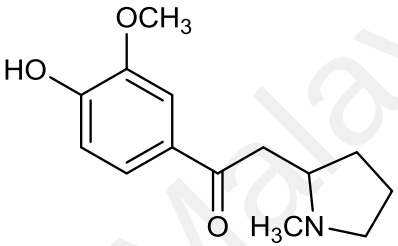

98

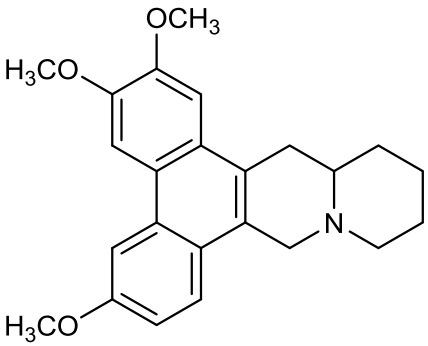

101

2.7 Biosynthesis of Isoquinoline Alkaloids

Lauraceae is one of the most represented botanical families, presenting 67 genera, with over 2500 species and more than 300 different alkaloids reported, mainly isoquinolines (Custodio & da Veiga Junior, 2014). The biosynthetic pathway for isoquinoline alkaloids starts with L-tyrosine **17** which is hydroxylated and decarboxylated to yield the substrate of dopamine **110**. The second substrate, *p*-hydroxyphenylacetaldehyde **111** is synthesized by transamination and decarboxylation of L-tyrosine **17**. Dopamine **110** and *p*-hydroxyphenylacetaldehyde **111** further coupled by the enzyme norcoclaurine synthase to form (*S*)-norcoclaurine **112** (Mander & Liu, 2010). Among isoquinoline alkaloids, the biosynthesis of benzylisoquinoline alkaloid from norcoclaurine **112** has been the most investigated to date (Giglioli-Guivarc'h, 2013) and was accepted as the central precursor to all benzylisoquinoline alkaloids produced in plants (Stadler, Kutchan, & Zenk, 1989). Feeding experiments with (*S*)-[1-^{13}C]-norcoclaurine **112** demonstrate that this trihydroxylated precursor is specifically incorporated into protoberberine, aporphine and benzophenanthridine alkaloids in cell suspension cultures, as well as into pavine and benzophenanthridine alkaloids in whole plants (Scheme 2.2) (Stadler et al., 1989).

(*S*)-norcoclaurine **112** next undergoes two methylations and a hydroxylation to give (*S*)-3-hydroxy-*N*-methylcoclaurine **113**, which is methylated a third time to produce (*S*)-reticuline **76a** (Scheme 2.3). Epimerization of (*S*)-reticuline **76a** then yields (*R*)-reticuline **76b**. (*S*)-reticuline **76a** is a branch-point intermediate in the biosynthesis of many benzylisoquinoline alkaloids including those in pharmaceutical usage such as morphine **1** and berberine **34** (Hawkins & Smolke, 2008). Isoquinoline can be categorised into several classes base on the skeletal of the structure (Table 2.3).

Table 2.3: Categories of isoquinoline alkaloids

Simple isoquinoline	Dibenzazonines
Benzylisoquinoline	Protoberberines and retroprotoberberines
Isoquinolones	Secoberberines
Pavines and isopavines	Benzophenantridhines
Bisbenzylisoquinolines	Arylisoquinolines
Baluchistanamines	Protopines
Cularines	Phthalideisoquinolines
Dibenzopyrrocolines	Rhoeadines
Proaporphines	Emetines
Aporphines	Phenethylisoquinolines
Proaporphine-benzylisoquinoline	Homoaporphines and homoproaporphines
Dimers	1-Phenylisoquinolines
Aporphine-pavine dimmers	*N*-Benzyltetrahydroisoquinolines
Oxoaporphines	4-Arylisoquinolines
Aristolochic acid and aristolactams	Azafluoranthenes and tropolosoquinolines
1, 6-Diazafluoanthenes	

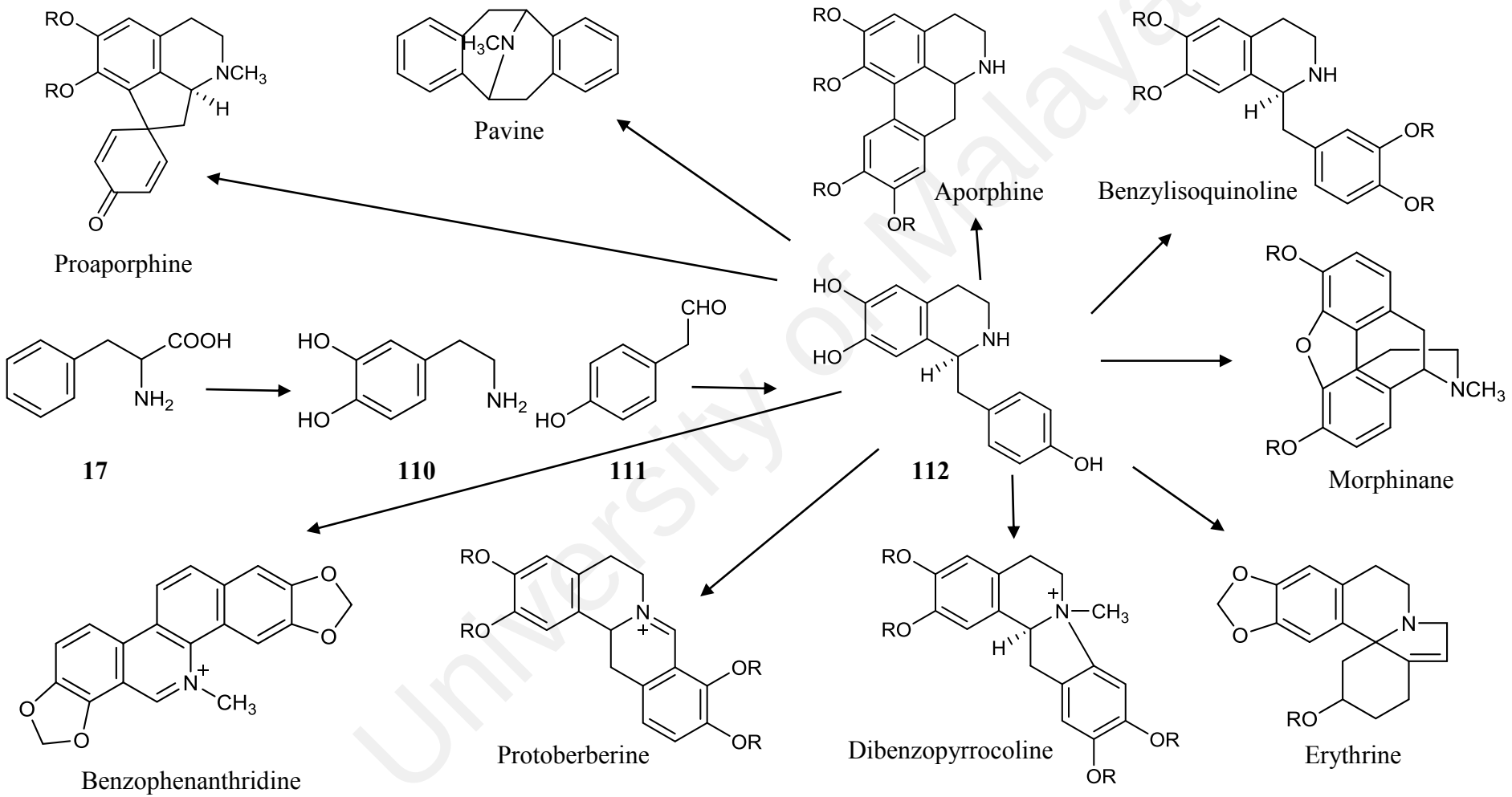

Scheme 2.2: Biosynthesis of various isoquinoline alkaloids from (*S*)-norcoclaurine **112**

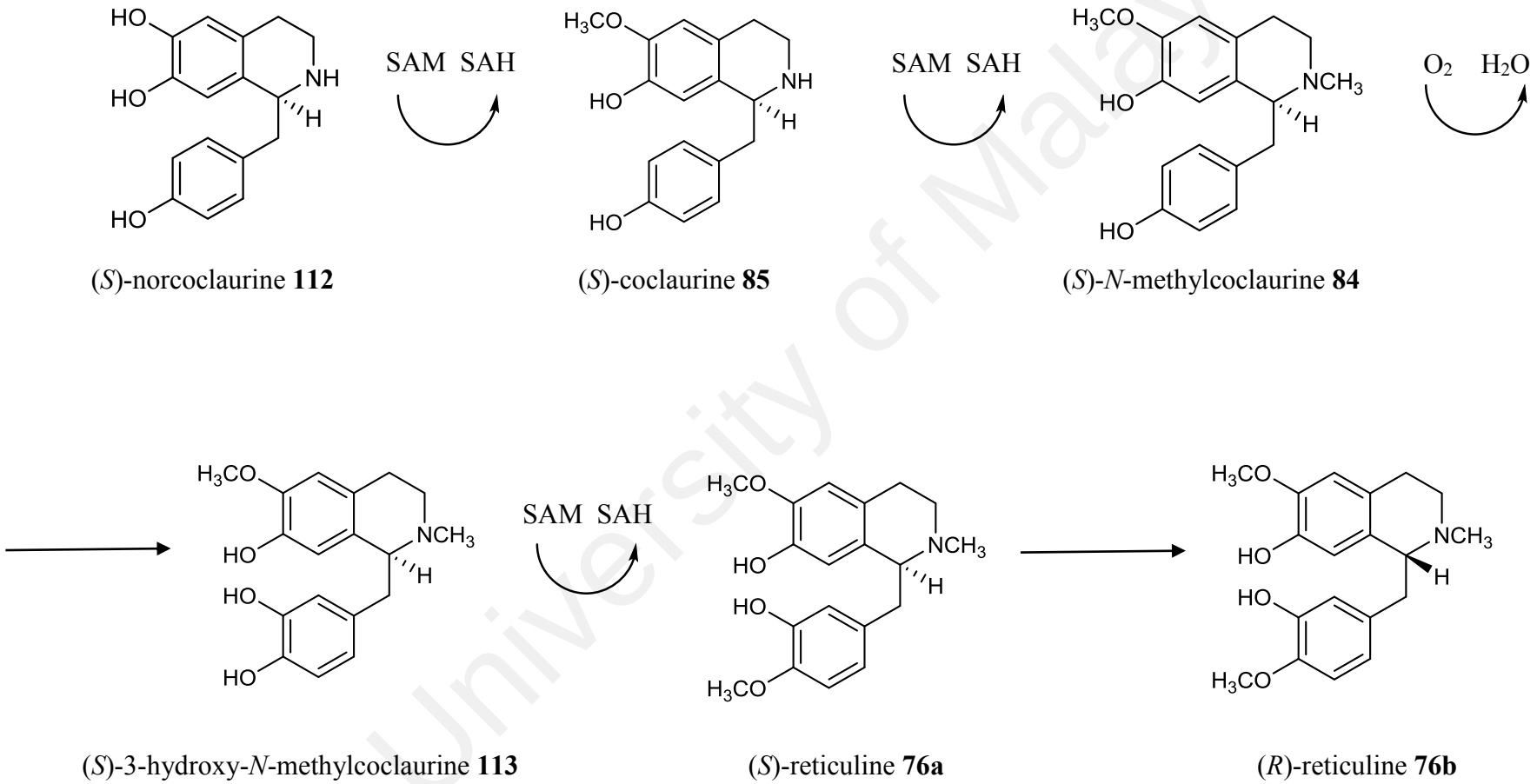

(*S*)-norcoclaurine **112** (*S*)-coclaurine **85** (*S*)-*N*-methylcoclaurine **84**

(*S*)-3-hydroxy-*N*-methylcoclaurine **113** (*S*)-reticuline **76a** (*R*)-reticuline **76b**

Scheme 2.3: Biosynthetic origin of the benzyltetrahydroisoquinoline

2.8 General Chemical Aspects of Isoquinoline Alkaloids

Cryptocarya plants are known producers of various compounds, notably isoquinoline derived alkaloids. Therefore, the following sub-chapters will discuss briefly on the biosynthesis and charactersistics of the isoquinoline derived alkaloids.

2.8.1 Aporphine

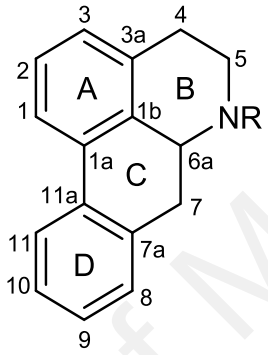

The aporphine alkaloids are one of the largest and most widely distributed subgroup of benzylisoquinolines (Ríos, Máñez, Giner, & Recio, 1999). A range of interesting biological activities has been documented, including serotonergic (Linnanen, Brisander, Mohell, & Johansson, 2001), antiplatelet (Chia, Chen, Chang, Teng, & Wu, 1999), anticancer (Likhitwitayawuid et al., 1993), antimalarial (Munoz et al., 1999) and vasorelaxing activity (Y. C. Wu, Chang, Chao, & Teng, 1998). The aporphine alkaloids contain a twisted biphenyl systems and consists with four rings, A, B, C and D. The nitrogen atom is usually tertiary in the base form but may also be quaternary, less frequently acetylated or formylated. *N*-oxide compounds have also been described. If the nitrogen is secondary, the alkaloid is called a noraporphine. In natural aporphines, positions 1 and 2 are always substituted, the substituents being hydroxyl, methoxyl, or methylenedioxy groups. The tetracyclic core can be substituted in different places, at position 9, 10, 11, and less frequently at position 3 and 8. In a few cases, a hydroxyl

function is located at the position C-7, while steporphine is the only aporphine alkaloid known to be oxygenated at C-4. Aporphines are optically active, possessing either the *R*-(-) or *S*-(+) absolute configuration, depending on the stereochemistry of C-6a (Stevigny, Bailly, & Quetin-Leclercq, 2005).

2.8.1.1 Biosynthesis of Aporphines

Aporphine alkaloids are known to be derived from the corresponding phenolic tetrahydrobenzylisoquinolines by direct oxidative coupling or by the formation of dienone derivatives (proaporphines or proerythrinadienones), which then rearrange into aporphine through dienone-phenol or dienol-benzene rearrangements. The feeding experiment of labeled reticuline **76** has showed that isoboldine **63** was derived from reticuline **76** by direct *ortho-para* oxidative coupling while bulbocapnine **114** has been shown to be derived directly by *ortho-ortho* phenolic oxidative coupling (Scheme 2.4). Another possible biogenetic route for aporphine involve dienone intermediates. This pathway was postulated by the incorporation of orientaline **37** into isothebaine **115** *via* orientalinone **116** and orientalinol **117** (Scheme 2.5). The dienol benzene rearrangement involved in the above biosynthesis resulted in the loss of one oxygen in its D ring (Geissman, 1972).

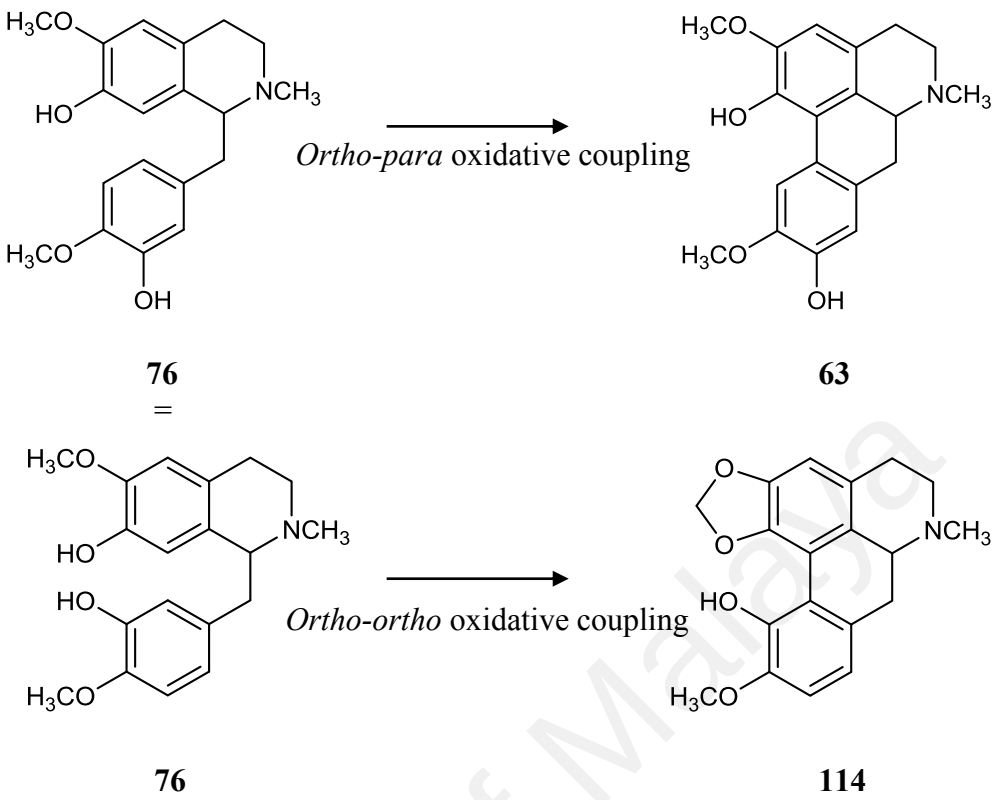

Scheme 2.4: Formation of aporphine alkaloids by the direct coupling of phenolic rings

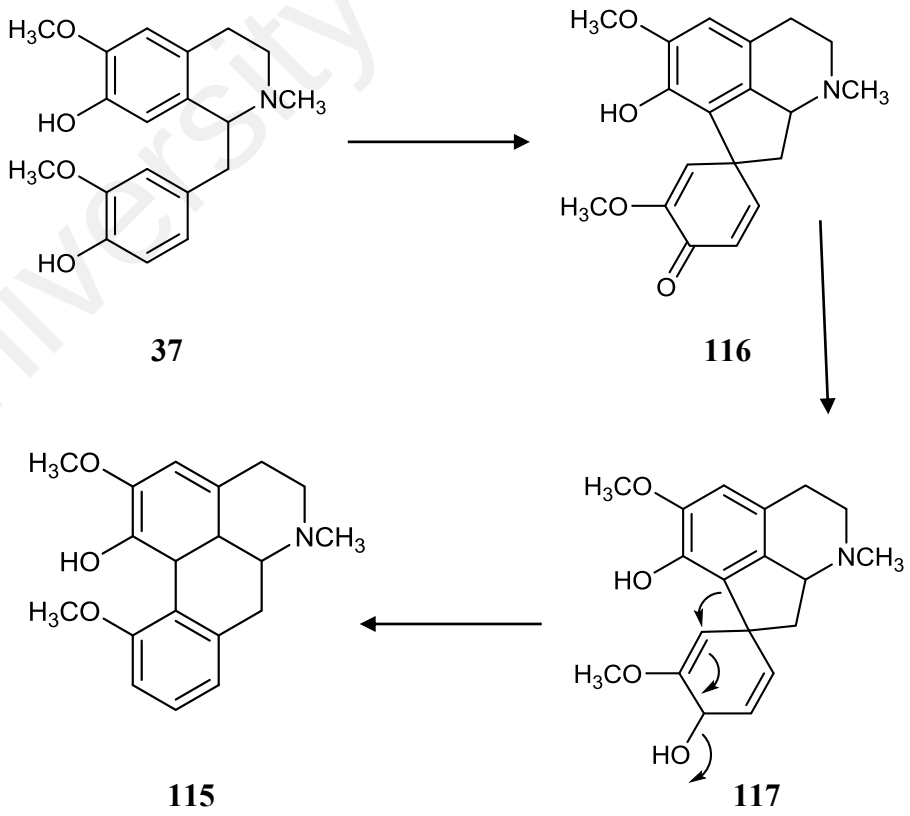

Scheme 2.5: Formation of aporphine alkaloids *via* dienone intermediates

2.8.1.2 ^{1}H NMR

Several general features of the proton shift belonging to the aporphines group had been observed. The proton in different chemical environments have different chemical shift and *vice versa*. The shifts are very dependent on the position of the protons with respect to the aromatic rings.

In the ^{1}H NMR spectra of aporphines, the aromatic protons appeared at δ_H 6.30-8.20. The most downfield aromatic proton, H-11, was observed between δ_H 7.50 and 8.20 (Shamma, 1972b). If the C-1 and C-2 positions have methylenedioxy group, the C-11 proton has a chemical shift between δ_H 7.50 and 7.90 while when C-1 and C-2 position is occupied by hydroxyl or a methoxyl group, the signal of the C-11 proton shifts more downfield. The ^{1}H chemical shift of (-)-stephanine **118** (Bartley, Baker, & Carvalho, 1994) and (-)-nornuciferine **119** (Chang, Chen, Hsieh, Cho, & Wu, 2000) are shown in Figure 2.1.

The C-3 proton was most shielded and typically appeared as a singlet in the range of δ_H 6.50-7.50. The presence of methoxyl group at C-11 causes the proton at C-8 and C-9 to had significantly different chemical shift. If a C-11 bears a hydroxyl group, no observable splitting is usually found and the C-8 and C-9 protons absorptions overlapped as a singlet.

Normally, the methoxyl (-OCH_3) groups were resonated at about δ_H 3.50-4.00. The position of C-2 is always substituted when position of C-1 and C-11 are substituted. This affects the methoxyl groups at C-1 and C-11 would be sterically hindered. As a results, the methoxyl protons were pushed out of the aromatic plane, which is shielded area. In addition, ring A and D was facing each other. Hence the protons of the methoxyl groups can arrange themselves on top of the adjacent ring, which happens to be a shielded zone giving a more up field shift (Blanchfield, Sands, Kennard, Byriel, & Kitching, 2003). The methoxyl group at C-1 will consistently appear further upfield at δ_H 3.40-3.70 than if at

C-2, C-9 or C-10 at δ_H 3.80-3.90 while the methoxyl group at C-11 will have an intermediate chemical shift at δ_H 3.60-3.80.

The methylenedioxy (-OCH_2O-) group shows resonances at range δ_H 5.80-6.10. The four possible location for this group were C-1,2; C-2,3; C-9,10 and C-10,11. The presence of C-1,2 methylenedioxy group is proved by an upfield shift of the C-11 proton which appeared in the range δ_H 7.50-7.90 and caused the twisted biphenyl system induce magnetic non-equivalent between the methylene proton, which then appeared as doublets at δ_H 5.90-6.10 while the methylenedioxy group at C-9 and C-10 will appear as a singlet. The inequivalence arises from the torsion caused by the twisted biphenyl system of ring A and D. The appearance of the torsional effect on the methylenedioxy depends on their positions and at position C-9, 10 the effect appears to be negligible. The *N*-methyl (*N*-CH_3) group was typically observed in the upfield region of δ_H 2.50-2.60 while the aliphatic protons of H-4, H-5, H-6a and H-7 appeared at δ_H 2.40-4.44 as a complex splitting patterns (Baarschers, Arndt, Pachler, Weisbach, & Douglas, 1964).

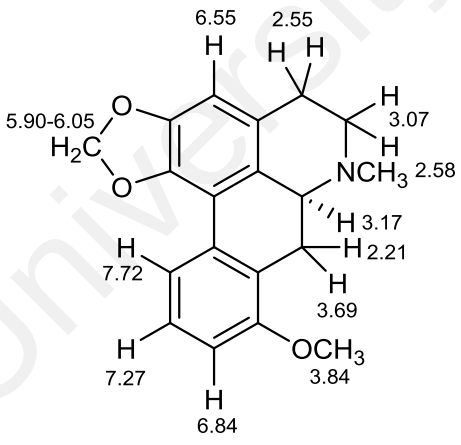

118

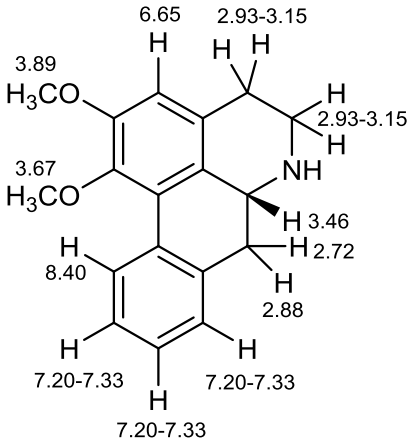

119

Figure 2.1: ^{1}H NMR of (-)-stephanine **118** and (-)-nornuciferine **119**

2.8.1.3 ^{13}C NMR

The general shift regions of the different type carbons of aporphines are; unsubstituted sp^2 carbons usually resonated at δ_C 105.0-112.0. Quaternary carbon 1a, 1b, 3a, 7a and 11a resonated at δ_C 119.0-130.0. The sp^3 carbon; C-4 and C-7 appeared at δ_C 28.0-30.0 and 34.0-36.0 respectively. The chemical shifts of C-5 and C-6a, which are adjacent to nitrogen atom, appeared further downfield at about δ_C 53.0 and 62.0, respectively. Positions C-1, C-2 may be substituted by hydroxyl or methoxyl or methylenedioxy. Substitution at C-1 and C-2 will cause them to resonate further downfield at δ_C 141.0-151.0. In addition, substituted carbons, *N*-methyl, methoxyl and methylenedioxy appeared at δ_C 42.0-44.0, 55.0-62.0 and 100.0-102.0 respectively (Jackman et al., 1979).

2.8.1.4 Mass Spectroscopy

The principle fragmentation that occurs in aporphines involve the loss of the hydrogen atom on C-6a. The $[M-1]^+$ peak always serves as the base peak of the molecule. Additional peak at $[M–15]^+$ and $[M–31]^+$ are mainly due to the loss of methyl or methoxyl from one of the methoxyl substituent, respectively. Also if it is hydroxyl group substituted, a $[M-17]^+$ peak will be observed. Compounds with *N*H or *N*-CH_3 functional groups will display peaks at $[M-29]^+$ and $[M-43]^+$, respectively due to the loss of methylene imine group (-CH_2=NR) which is expelled *via* a retro Diels-Alder mechanism (or by the cyclic process in ring B). The ions formed can further loose another methyl or methoxyl group to produce peaks at $[M-74]^+$, $[M-58]^+$, $[M-60]^+$ and [M-44]. The main fragmentation pathways for the aporphines are outlines in Scheme 2.6 (Ohashi et al., 1963).

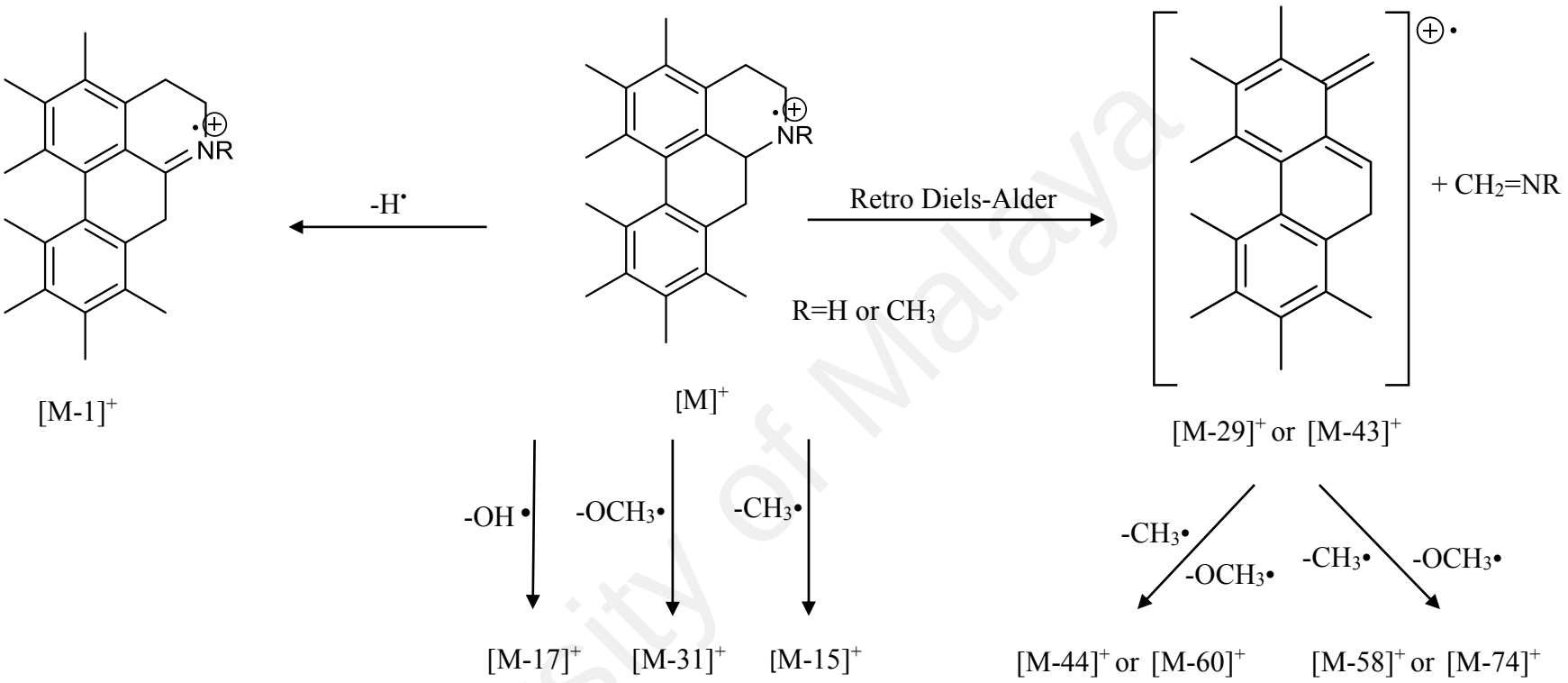

Scheme 2.6: Mass fragmentation of aporphine

2.8.1.5 Ultraviolet Spectroscopy

The position of the maximum absorptions in the ultraviolet spectra of aporphines depends mainly upon the location of the substituents. It is derived from the basic biphenyl system with the added influence of several auxochromes. The approximate absorption for various substitution patterns are listed in Table 2.4 (Pelletier, 1970).

Table 2.4: Ultraviolet spectroscopy of aporphine type alkaloids

Position of Substituents	Absorption Maximums (nm)
1,2	234, 273, 312
1,2,9	233, 280, 305
1,2,10	226, 266, 275, 305
1,2,11	220, 265, 272, 300
1,2,9,10	220, 282, 305
1,2,10,11	220, 270, 305

When substituents are at position 1 and 2, the spectra show one maxima absorption at 220 nm and two in the region 270-310 nm. The shape of the curve and the intensity of the latter two maxima depend on the substitution in ring D.

For instance, aporphine alkaloids with position 11 free show two maxima at 282 and 303-310 nm but when position 11 is substituted the two maxima are observed at 268-272 nm and 303-310 nm. These differences are due to the increase strain present in the conjugated diphenyl system when both 1 and 11 substituents are present. In addition, the monophenolic aporphine at position C-3 and C-9 displays a bathochromic shift at 315 nm and 350 nm in the alkaline environment (Shamma, Yao, Pai, & Charubala, 1971).

2.8.2 Oxoaporphine

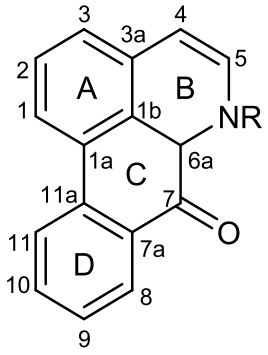

The oxoaporphine represents the most highly oxidized state of aporphine skeleton which consist of carbonyl group at C-7. It arises from the oxidation of aporphines via a dehydroaporphine and subsequent 4, 5, 6a, 7-didehydroaporphine, which is susceptible to oxidation at C-7 (Cordell, 2000). Scheme 2.7 exhibits biogenetic pathway to an oxoaporphine. The oxoaporphine alkaloids are widely distributed and the first reported oxoaporphine was liriodenine **120** which was isolated from *Liriodendron tulipfera* (Barton et al., 1965; Blaschke, 1968).

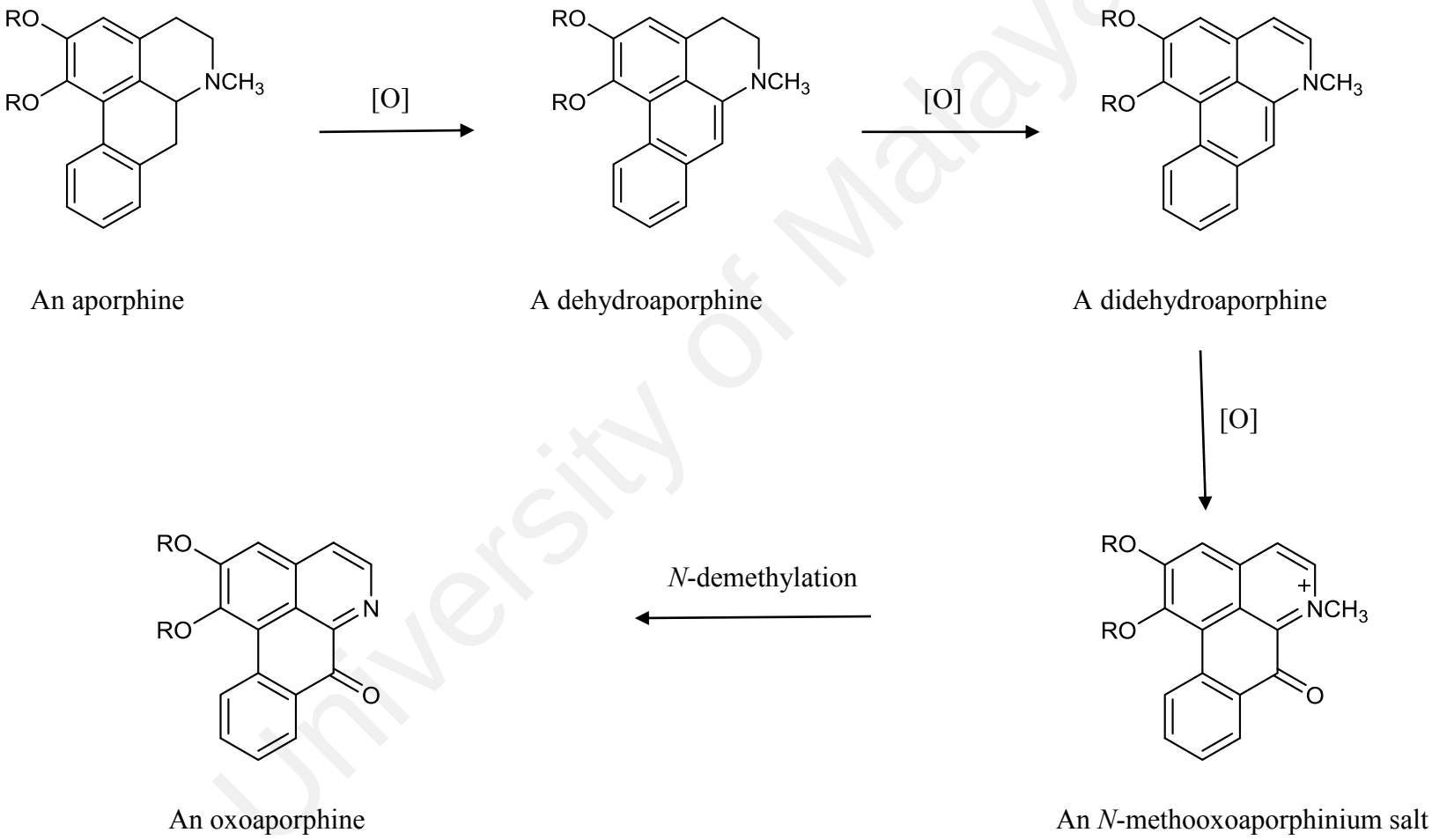

Scheme 2.7: The biogenetic pathway to an oxoaporphine

2.8.2.1 ^{1}H NMR

The most characteristic features of oxoaporphine are the highly deshielded chemical shift values of the aromatic protons and the absence of the aliphatic proton signals (Broadbent & Paul, 1983). The oxoaporphine, having a carbonyl group at C-7 and a double bond between C-4 and C-5, give a characteristic AB doublet of doublets at about δ_H 7.65 and 8.75 (deshielded) with a coupling constant of 5.4 Hz which correspond to H-4 and H-5. The small of *J* value is due to the adjacent of electronegative atom, nitrogen. Besides that, H-8 resonates more downfield at δ_H 8.20-8.60 due to the existence of carbonyl group at C-7 which exerts an inductive effect.

In addition, the methylenedioxy gave a singlet signal at about δ_H 6.10 due to the planarity of the oxoaporphine skeleton. The methoxyl group located at C-1 gave the average shifts of about δ_H 3.55 meanwhile methoxyl groups present at position C-2, C-9 and C-10 reveal peaks at δ_H 3.80. Nevertheless, we found that in the position C-1 and C-11 the methoxyl gave chemical shift at δ_H 3.70. In the latter case, the more upfield shift may be due to the OCH_3 bond sticking out of the plane of the benzene rings which a deshielded effect is expected (Shamma & Castenson, 1973).

2.8.2.2 ^{13}C NMR

The ^{13}C NMR spectral data of oxoaporphine showed much closer to those observed in aporphine. The carbons are all sp^2, indicating that it was unsaturated and fully aromatic. The carbonyl group at C-7 usually appeared at δ_C 175.0-183.0 (Marsaioli, Magalhães, Rúveda, & de AM Reis, 1980).

2.8.2.3 Mass Spectroscopy

The main fragment ions observed in the mass spectrum of oxoaporphine are given in Scheme 2.8. The important fragmentations are the $[M\text{-}CO]^+$, $[M\text{-}CH_2\text{-}O]^+$ and $[M\text{-}CHO]^+$.

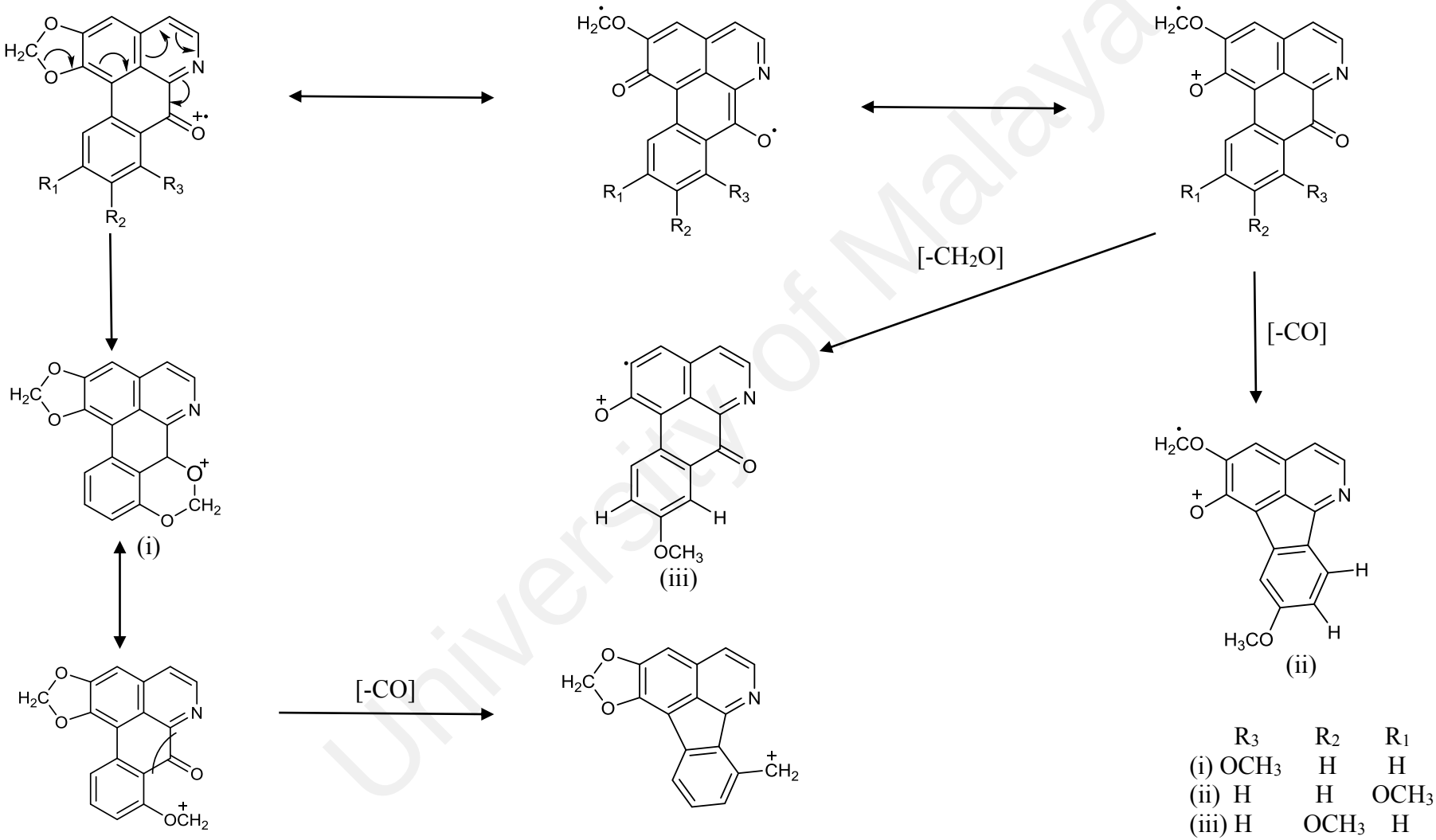

	R_3	R_2	R_1
(i)	OCH_3	H	H
(ii)	H	H	OCH_3
(iii)	H	OCH_3	H

Scheme 2.8: Mass fragmentation of oxoaporphine

2.8.2.4 Ultraviolet Spectroscopy

The UV spectral data for the oxoaporphine are quite characteristic for the skeletal type. These yellowish colored alkaloids possess a highly unsaturated chromophoric system with extended absorption in the ultraviolet and visible. For example, liriodenine **120** shows three main absorption bands at 245-270, 309 and 413 nm. On acidification, the oxoaporphines exhibit bathochromic shift or the spectrum is shifted to longer wavelengths with a series of undulating maxima between 325 and 460 nm (Baarschers et al., 1964).

2.8.3 Proaporphine

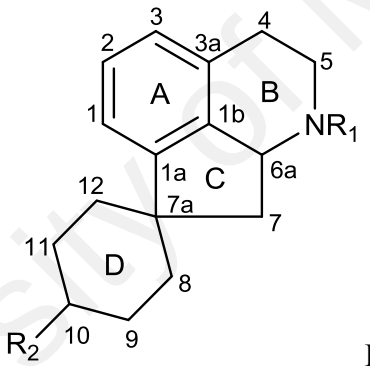

R_1 = H, CH_3

R_2 = H, OH, =O

The proaporphine alkaloids belong according to the reductive stage of their spirane ring to several types (Dolejš, 1974). The majority of these compounds possess a cyclohexadienone system incorporated into the tetrahydroisoquinoline nucleus, which may be partially or fully saturated and yield dihydro or hexahydroproaporphines (Cordell, 2000). This group of alkaloids represents as an intermediate stage in the conversion of the benzylisoquinoline alkaloids by phenol oxidative coupling into the aporphines through acid catalysed (Scheme 2.5). In other words, proaporphine alkaloids can be considered to be the biogenetic precursor of the aporphines.

The proaporphine alkaloids can be found in several species especially from the family of Menispermaceae (Flor, Doorenbos, Svoboda, Knapp, & Schiff, 1974), Papaveraceae (H. Wu, Ding, Shen, Zhu, & Zhang, 2009), Lauraceae (Mukhtar et al., 2008) and Annonaceae (Costa, Sampaio, Salvador, Nepel, & Barison, 2015). Some of the compounds showed interesting bioactivities (Bhakuni, Satish, & Dhar, 1970).

2.8.3.1 ^{1}H NMR

In the ^{1}H NMR spectra of proaporphine, the dienone type C-9 and C-11 vinylic protons appear as a doublet doublet signal between δ_H 6.10 and 6.60. The C-8 and C-12 hydrogens, being in an environment of lesser electron density are situated further downfield between δ_H 6.70 and 7.30 with average values for the coupling constants are $J_{8,9}$=$J_{11,12}$=10.0 Hz, $J_{9,11}$=1.5 Hz, $J_{8,12}$=2.5 Hz. A methoxyl group at C-1 is shielded by the cyclohexadienone system and can be readily detected since it appears relatively upfield near δ_H 3.60 instead of at the more usual site of δ_H 3.80. The *N*-methyl group is found at its expected position near δ_H 2.40 (Stuart & Cava, 1968). An alternate method exists for differentiating between a 1-hydroxy-2-methoxy and the reverse 1-methoxy-2-hydroxy arrangement in ring A of a proaporphine. The C-3 aromatic proton normally occurs as singlet between δ_H 6.50 and 6.70. The presence of this signal shows that C-1 and/or C-2 are substituted. As in the aporphine alkaloids, the aliphatic protons will appear between δ_H 1.80-3.80 (Shamma, 1972b).

2.8.3.2 ^{13}C NMR

Analysis of ^{13}C NMR also shows significant chemical shifts for *syn* and *anti*-isomers of reduced proaporphine. The signal of C-7 in *syn* and *anti* reduced proaporphines bearing an allylic alcohol in ring D is observed around δ_C 50.2 and 45.0 while, in the *syn* and *anti* reduced enone proaporphines the signal for C-7 is observed around δ_C 49.0 and

43.0 respectively. However, the C-7 carbonyl peak was observed at δ_C 204.0. The resonance of the quaternary spiro carbon, C-7a, at δ_C 52.7 implied the proaporphinic nature of compound (Mukhtar et al., 2009).

2.8.3.3 Mass Spectroscopy

The molecular ion peak for proaporphine is usually observed as the base peak. Most of the compounds showed a large $[M-1]^+$ peak by losing one hydrogen atom from the carbon adjacent to the nitrogen atom and form a quaternary ammonium ion $[M-H]^+$. The most interesting fragmentation is the formation of the metastable peak from the retro-Diels Alder at $[M-15]^+$ or $[M-31]^+$ (Scheme 2.9) (Shamma, 1972b).

2.8.3.4 Ultraviolet Spectroscopy

The UV spectra of proaporphine possessing a dienone ring usually show maxima near 230 and 285 nm. The partially reduced proaporphine showed maxima absorptions at 228, 282 and 288 nm, while fully reduced, cyclohexanolic proaporphine at 240 and 291 nm (Stuart & Cava, 1968).

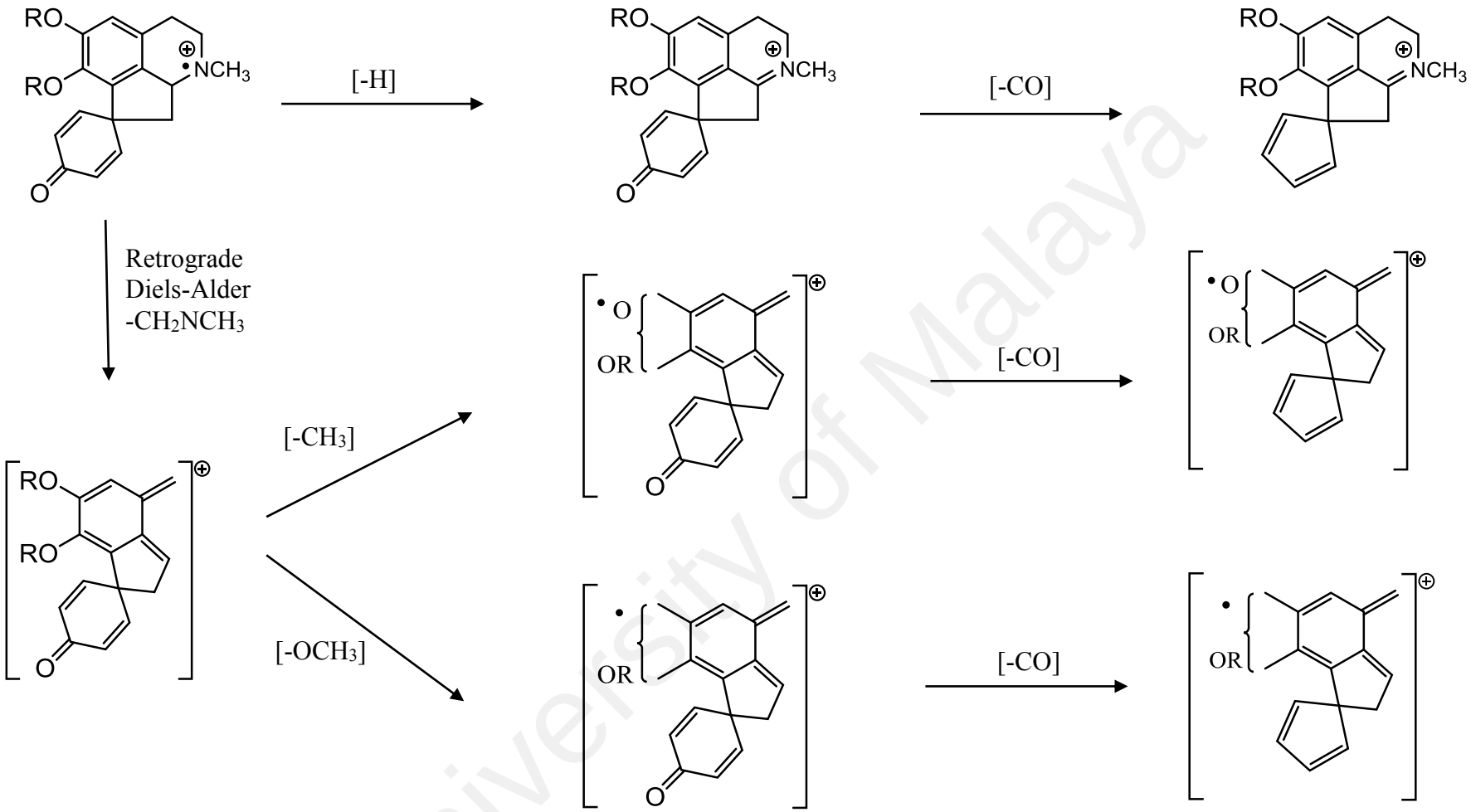

Scheme 2.9: Mass fragmentation of proaporphine

2.8.4 Benzylisoquinoline

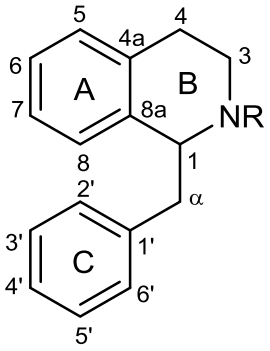

The benzylisoquinoline occupy a paramount position in alkaloid chemistry because they act as *in vivo* precursors to so many of the other naturally occurring isoquinolines (Deulofeu, Comin, & Vernengo, 1968). The benzylisoquinoline alkaloids are either of the 1, 2, 3, 4-tetrahyrdro type or of the completely aromatic type. Ring A in the benzylisoquinoline alkaloids may possess two or three oxygenated substituents, while ring C has only one or two substituents. The benzylisoquinoline alkaloids are widely distributed in the plant kingdom and mostly occur in the Annonaceae, Berberidaceae, Combretaceae, Hernandiaceae, Lauraceae, Magnoliaceae, Menispermaceae, Nymphaceae, Papaveaceae, Ranunculaceae, Rhamnaceae and Rutaceae families (Shamma, 1972b).

2.8.4.1 ^{1}H NMR

The ^{1}H NMR data of benzylisoquinoline shows a number of interesting features due to the one asymmetric center. The H-1 appeared as a triplet or doublet-doublet (J_1=8.0-9.0, J_2=1.5-3.0 Hz) with chemical shift (in $CDCl_3$) between δ_H 3.60-3.70 while the aliphatic proton signals for H-3, H-4 and H-α, normally appeared as multiplet at δ_H 2.50-3.50. The methoxyl, *N*-methyl and methylenedioxy groups of the benzylisoquinoline

generally resonated at δ_H 3.50-4.00, 2.40-2.60 and 5.60-6.00 respectively (Janssen, Lousberg, Wijkens, Kruk, & Theuns, 1989).

2.8.4.2 ^{13}C NMR

In the ^{13}C NMR spectra, C-1 normally resonated at δ_C 52.0-58.0, but it resonated at higher field i.e. δ_C 60.0-67.0 in the presence of *N*-methyl group. Substituted carbons *N*-methyl, methoxyl and methylenedioxy appeared at δ_C 40.0-45.0, 54.0-63.0 and 100.0-103.0, respectively. The quaternary carbon at the position 4a, 8a and 1' resonated at δ_C 115.0-132.0 while quaternary carbons with methoxyl and hydroxyl attached groups appeared at δ_C 140.0-152.0. Unsubstituted sp^2 carbons usually appeared at δ_C 100.0-130.0 and the sp^3 carbons at the position C-α and C-3 resonated at δ_C 38.0-40.0 and 45.0-46.0 respectively. The chemical shift of C-4 with *N*-methyl group in the structure appeared at δ_C 23.0-24.0, but it will appear at δ_C 28.0-29.0 without *N*-methyl group. (Janssen et al., 1989).

2.8.4.3 Mass Spectroscopy

In the mass spectra of benzylisoquinoline, the main cleavage occurs between C-1 and C-α to form an imine ion. The fragmentation at *m/z* 192 appeared as a base peak indicated that the carbons C-6 and C-7 was substituted with methoxyl and hydroxyl groups, respectively and in the structure beared *N*-methyl group (Tomita et al., 1966). If both C-6 and C-7 was substituted with methoxyl groups, peak at *m/z* 206 appeared as a base peak. The fragmentation at *m/z* 176 which appeared as a base peak indicated the carbons C-6 and C-7 attached to methylenedioxy without *N*-methyl in the structure.

The compounds having a methoxyl and hydroxyl groups in the ring C displayed peak at *m/z* 137. Two methoxyl groups attached to C-3' and C-4' showed the fragmentation peak at *m/z* 151 and a hydroxyl group in the ring C showed peak at *m/z* 107

(Al-Amri, Smith, El-Haj, & Juma'a, 2004). The illustration of mass fragmentation pattern of benzylisoquinoline is shown in Scheme 2.10.

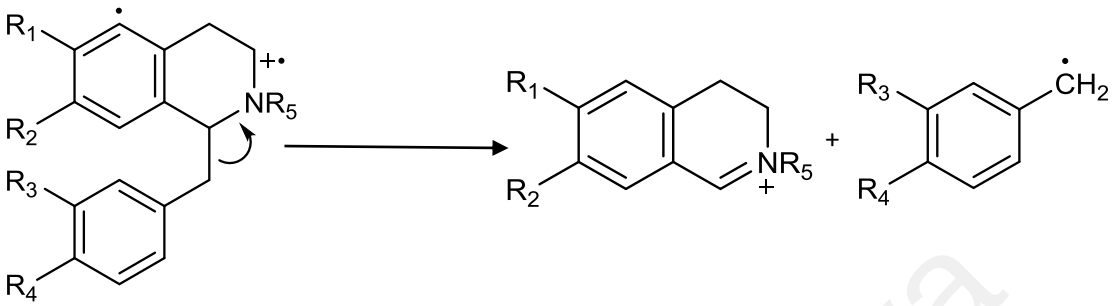

m/z = 192	$R_1 = OCH_3$, $R_2 = OH$, $R_5 = CH_3$	*m/z* = 107	$R_3 = H$, $R_4 = OH$
m/z = 176	$R_1 = R_2 = OCH_2O$, $R_5 = H$	*m/z* = 121	$R_3 = OCH_3$, $R_4 = H$
m/z = 206	$R_1 = R_2 = OCH_3$, $R_5 = CH_3$	*m/z* = 137	$R_3 = OCH_3$, $R_4 = OCH_3$

Scheme 2.10: Mass fragmentation of benzylisoquinoline

2.8.4.4 Ultraviolet Spectroscopy

The ultraviolet spectra of benzylisoquinoline showed maxima between 280 and 296 nm which was little effect by additional aromatic substitution. Compounds having methylenedioxy and fully aromatic show increased and more intensity absorption maximum (Shamma, 1972b).

2.8.5 Phenanthroindolizidine

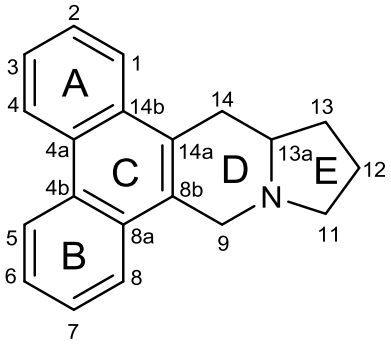

(i)

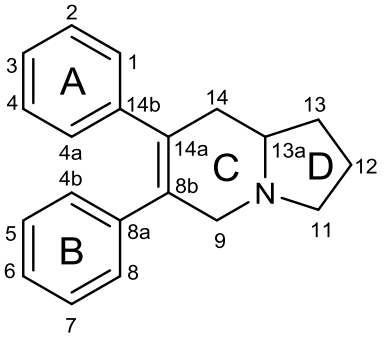

(ii)

Phenanthroindolizidine (i) alkaloids contain a phenanthrene ring fused to a saturated indolizine ring while *seco* phenantroindolizidine (ii) alkaloids derived from *seco* analogs of phenanthroindolizidine. The naturally occuring phenanthroindolizidine alkaloids differ from the synthetic derivatives in containing the alkoxy substituents in the phenanthrene ring, hydroxyl group in the C14 position or existing as an *N*-oxide derivative (Mandhare, Dhulap, Dhulap, & Biradar, 2015). Phenanthroindolizidine alkaloids have been isolated principally from the Asclepiadaceae family, most importantly from the genera *Tylophora*, *Vincetoxicum*, *Pergularia*, and *Cynanchum* and also from *Hypoestes* spp. (Acanthaceae), *Cryptocarya* (Lauraceae) and *Ficus spp*. (Moraceae) (Gellert & Pelletier, 1987). Since the first isolation of tylophorine **121** in 1935 from the perennial climbing plant *Tylophora indica* (Ratnagiriswaran & Venkatachalam, 1935), the number of phenanthroindolizidine alkaloids reported has grown considerably, presently encompassing close to 100 structurally related phenanthroindolizidine together with their *seco*-derivatives, *N*-oxides and phenantroquinolizidine (Li, Jin, & Huang, 2001). These group of alkaloids are well known for their cytotoxic activity, due to the inhibition of protein and nucleic acid synthesis (Mandhare et al., 2015).

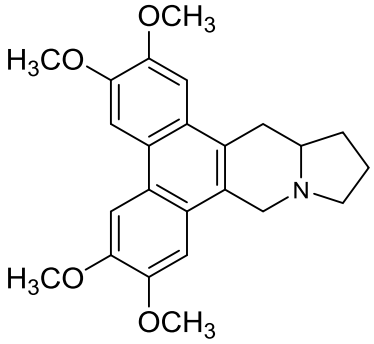

121

2.8.5.1 ^{1}H NMR

In the ^{1}H NMR spectrum of phenanthroindolizidine, the multiplicity of the proton signals due to rings A and B either to be at C-3,4,6,7 or C-2,3,5,6. The aromatic protons of phenanthroindolizidine normally appeared at δ_H 6.20-6.90 in $CDCl_3$ and it resonated more deshielded at δ_H 9.00-9.50 for H-5 due to the presence of substituents group of C-4 (either OCH_3 or OH) in ring A which caused the deshielding effect (Y.-Z. Lee et al., 2011). The average chemical shifts of methoxyl ($-OCH_3$) groups were resonated at δ_H 3.30-4.11 while the aliphatic protons were observed in the range of δ_H 1.50 to 3.98 (Abe et al., 1998).

2.8.5.2 ^{13}C NMR

In the ^{13}C NMR spectra, the chemical shift of the methoxyl group appeared at δ_C 60.0-61.0 and the chemical shift of sp^2 carbon bearing the hydrogen aromatic appeared at δ_C 120.0-128.0. The quaternary carbons with methoxyl and hydroxyl groups appeared at δ_C 140.0-152.0. The chemical shift of C-13a normally resonated at δ_C 60.0-61.0 and indicated a *cis*-fused ring junction of the indolizidine moiety. Moreover, the presence of an *N*-oxide gave a large deshielding effect on C-13a (δc 70.0-71.0), C-9 (δ_C 66.0-68.0) and C-11 (δ_C 67.0-68.0) (Stærk et al., 2000).

2.8.5.3 Mass Spectroscopy

The phenanthroindolizidine give easily recognizable mass spectra owing to the intense ion at M-69, usually the base peak, formed by loss of ring E as a pyrroline unit by a retro-Diels-Alder fission (Scheme 2.11) (Manske, 1981).

2.8.5.4 Ultraviolet Spectroscopy

Phenanthroindolizidine alkaloids may be recognized by their UV spectra which correspond to a substituted phenanthrene chromophore. There is a distinct increase in intensity of the absorption maximum around 260 nm as the number of oxy substituents increases (I. R. C. Bick & Sinchai, 1982).

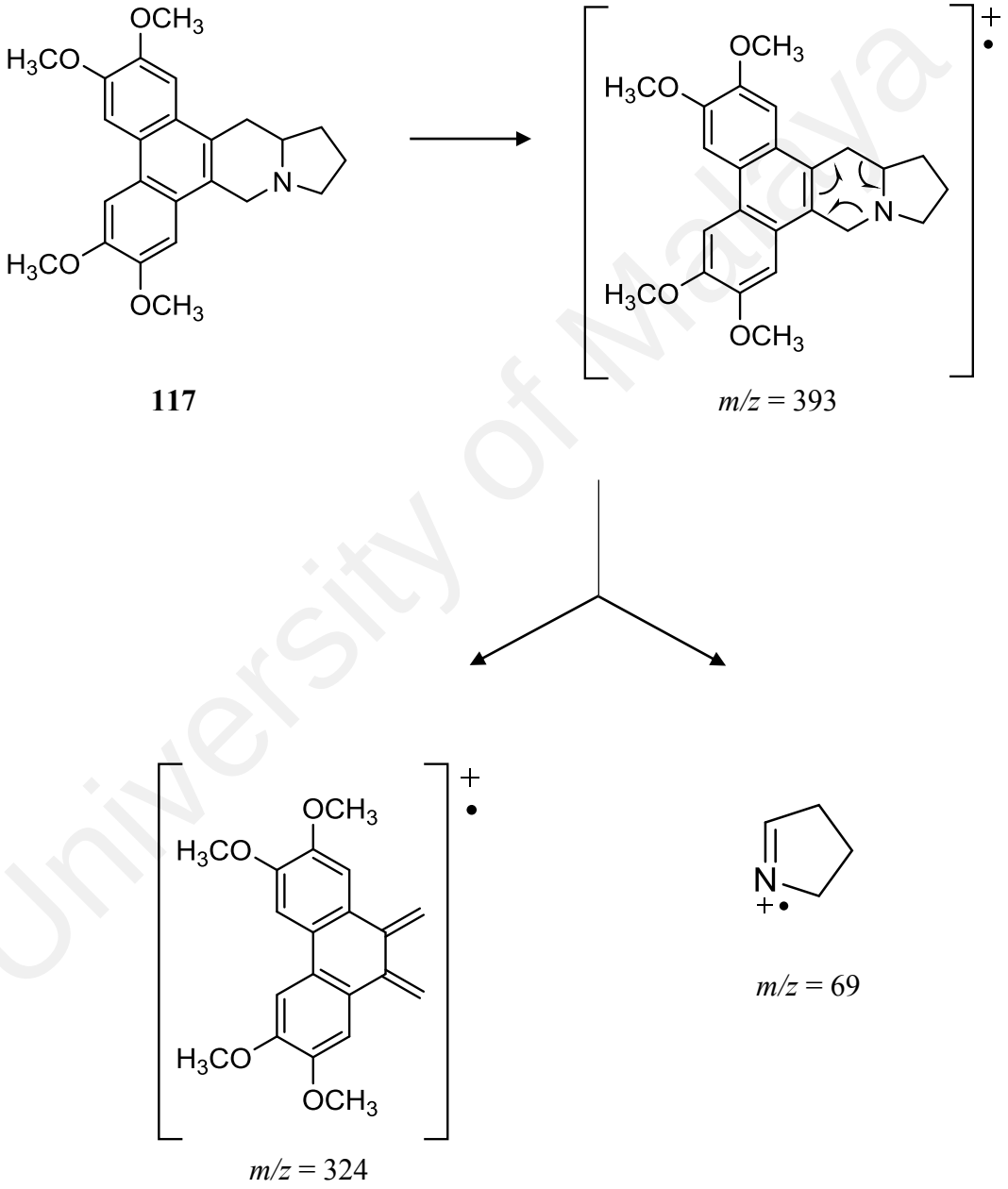

Scheme 2.11: Mass fragmentation of phenanthroindolizidine

2.8.6 Phenanthrene

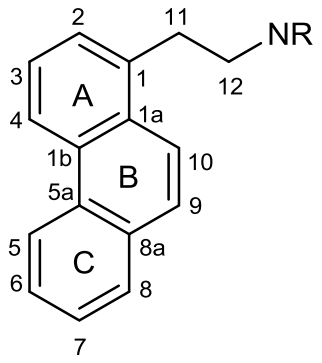

Phenanthrene alkaloids also known as '*seco*-aporphines' are a very rare type, probably formed biogenetically from an aporphine precursor through the opening of ring B. It is also based on a phenathrene nucleus with an ethylamine side chain, where the nitrogen carries one or two methyl substituents (Castedo & Tojo, 1990; Cordell, 2000). The phenanthrene alkaloids are always substituted at C-3, 4 since their precursors, the aporphines, are found with substituents at these two positions corresponding to C-1, 2 of the aporphine skeleton (Shamma, 1972b). This group has been found previously in the following families of the Angiospermae: Annonaceae, Aristolochiae, Berberidaceae, Fumariaceae, Hermandiaceae, Menispermaceae, Lauraceae, Monimiaceae and Ranunculaceae and its normally occur in minor amounts, together with the aporphines from which they originate by oxidative degradation (Castedo & Tojo, 1990).

2.8.6.1 ^{1}H NMR

The ^{1}H NMR spectra of phenanthrene displayed the C-5 proton falls appreciably downfield and apart from the other aromatic hydrogens. The presence of two doublets arising from the protons at C-9 and C-10 is a very characteristic of phenanthrene alkaloid skeleton. They appear close to each other at δ_H 7.30-7.90, with coupling constant of 9.0-10.0 Hz. In some cases, the C-9,10- hydrogens cannot be differentiated easily from the

hydrogens at C-6,7, or 8. The C-2 proton is often found further upfield from the other aromatic hydrogens (Shamma, 1972a). The 2-aminoethyl side chain give rise to two batches of multiplets or doublet-doublet (J=15.0 Hz) at δ_H 3.20-3.60 and 2.60-3.00, each derived from two protons, which were typically of phenanthrene alkaloids for C-11 and C-12 protons (Castedo & Tojo, 1990).

The average chemical shifts of methoxyl groups of phenanthrene alkaloids resonated at δ_H 3.90-4.10. As with the aporphines, a C-4 methoxyl in a phenanthrene alkaloid is found further upfield than the other methoxyl groups. Usually, one sharp peak attributed to the three or six hydrogen group attached to nitrogen was observed at δ_H 2.40-2.80. The methylenedioxy group shows a peak at a region at δ_H 6.00-6.30 (López-Martín, Anam, Boira, Sanz, & Blázquez, 2002).

2.8.6.2 ^{13}C NMR

In the ^{13}C NMR spectra, the chemical shift of the methoxyl group appeared at δ_C 56.0-61.0, whereas the *N*-methyl resonated at δ_C 43.0-44.0 and the chemical shift of sp^2 carbon bearing the hydrogen aromatic appeared at δ_C 120.0-128.0 (López-Martín et al., 2002).

2.8.6.3 Mass Spectroscopy

The mass spectra of phenanthrene alkaloids are very informative regarding the nature of the side chains. The two main fragmentations correspond to the loss of $CH_2NR_1R_2$ and to the $CH_2=N^+R_1R_2$ cation. This cation is usually the base peak and allows the identification of R_1 and R_2. Thus, phenanthrenes with a 2-dimethylaminoethyl side chain present the base peak at *m/z* 58, whereas ones with a 2-monomethylaminoethyl side chain show the base peak at *m/z* 44 (Scheme 2.12) (Castedo & Tojo, 1990).

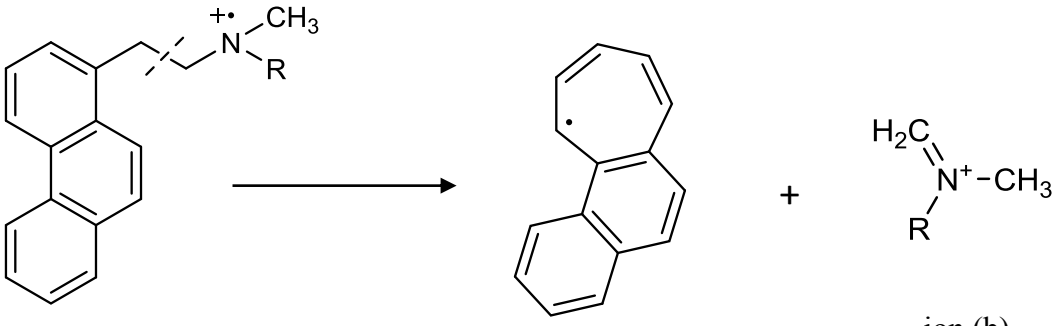

ion (a)

ion (b)

R = H $m/z = 44$

R = CH_2 $m/z = 58$

Scheme 2.12: Mass fragmentation of phenanthrene

2.8.6.4 Ultraviolet Spectroscopy

The phenanthrene alkaloids exhibit at least four peaks in the UV range, the most diagnostic of which falls between 255 and 266 nm (Shamma, 1972a).

2.8.7 Pavine

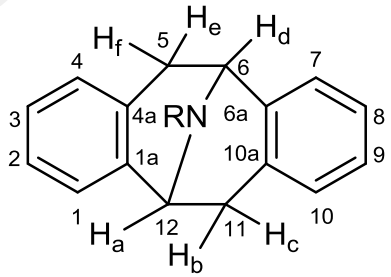

The pavine alkaloids was characterized with bridgehead nitrogen atom to the eight-membered ring. This group of alkaoids are very rare in plant kingdom. Recently, only four plant families were known to elaborate pavine alkaloids, namely Papaveraceae, Berberidaceae, Lauraceae, and Ranunculaceae, with about 50 different alkaloids. Several of the pavines are probably derived biogenetically from the tetrahydrobenzylisoquinoline

(Gözler, Lantz, & Shamma, 1983). Previous investigation on pavine alkaloids were reported to possess biological activities such as immunological and antiarrhythmic activities (T.-S. Wu & Lin, 2001).

2.8.7.1 ^{1}H NMR

In the ^{1}H NMR spectra, the oxygenation pattern of a pavine may be deduced from a careful examination of the methine ($H_{a,d}$) and methylene ($H_{b,c,e,f}$) proton absorptions. In the case of 2,3,8,9 substitution, the abc and def protons furnish two superimposable ABX patterns. A doublet integrating for two protons at the lower field end of the system at approximately δ_H 4.00 represents the bridgehead protons, H_a and H_d. At 60 MHz, it appears as if these protons are coupled to only one of the neighboring protons (J=6.0 Hz). Furthermore, the geminal hydrogens couple to each other with a coupling constant of 17.0 Hz. On the other hand, in the ^{1}H-NMR spectra of pavines bearing 2,3,7,8 substituents, the H_a and H_d, protons are represented by two doublets at about δ_H 4.00 and 4.40, where the latter is assigned to H_d, which is proximal to one of the oxygen functions positioned on ring D. In alkaloids with 2,3,8,9 symmetric substitution, the aromatic protons are paired into two singlets, each integrating for two protons, whereas asymmetric substitution, results in four well-defined singlets. In a 2,3,7-tetrasubstituted pavine, H-9 and H-10 are expected to appear as an AB quartet. The determining factor has been stated to be the inductive effect of the bridgehead C-N bond, causing deshielding and consequently downfield shifting of H-1 and H-7. However, it has been justifiably pointed out that it is rather the anisotropic shielding by the aromatic rings which results in the upfield chemical shift of H-4 and H-10.

In symmetrical pavines, the C-2 and C-8 methoxyls will appear as a singlet of six hydrogens just as the C-3 and C-9 methoxyls. The former pair, which is proximate to the bridgehead, will appear more downfield by about 0.07-0.1 ppm with respect to the latter.

The methylenedioxy protons center around δ_H 5.80-5.90 as an AB quartet (J=1.0-1.5 Hz). The *N*-methyl protons appear almost invariably between δ_H 2.49 and 2.57 in $CDCl_3$, solutions and at δ_H 2.35 in DMSO solutions. The general absorption pattern of quaternary pavines strongly resembles that of the tertiary analogs with the exception of the expected downfield shifts for each of the protons. In particular, the bridgehead protons will move downfield by about 1.0-1.5 ppm. *N*,*N*-Dimethyl protons will be observed as a singlet between δ_H 3.30 and 3.70. The set of empirical rules deduced for aromatic proton chemical shifts in a tertiary system has been shown to apply also to the quaternary system. (Gözler, 1987).

2.8.7.2 ^{13}C NMR

In the ^{13}C NMR spectra, the chemical shift of the methoxyl and methylenedioxy group resonated at δ_C 55.0-56.0 and 100.0-101.0 respectively, whereas *N*-methyl resonated at δ_C 40.0-41.0. The chemical shift of sp^2 carbon at positions 4a, 6a, 10a and 1a and sp^2 carbon bearing a hydrogen resonated at δ_C 120.0-135.0 and δ_C 106.0-112.0 respectively. Carbon C-1a (δ_C 130.9) was located downfield from C-4a (δ_C 126.2), obviously due to the anisotropic effect of the bridgehead substituent. Also notable were the differences between the pairs of carbons, C-1 (δ_C 107.0) vs. C-4 (δ_C 108.7), and C-2 (δ_C 145.8) vs. C-3 (δ_C 146.1), which reflected greater shielding effects for those carbons adjacent to the bridgehead. The sp^3 carbon at position 5, 11 and 6, 12 appeared at δ_C 31.0-35.0 and δ_C 51.0-57.0 respectively (S.-S. Lee, Liu, & Chen, 1989).

2.8.7.3 Mass Spectroscopy

In mass spectra, the principle fragmentation of the pavine alkaloids occurred with the loss of one phenyl ring to give a basic ion as the base peak. For example, alkaloid

amurensinine **122** shows a molecular ion at *m/z* 339, a strong $[M-43]^+$ ion and a base peak at *m/z* 188 (Cordell, 1981). These ions have been proposed as shown in Scheme 2.13.

2.8.7.4 Ultraviolet Spectroscopy

A pavine skeleton may be regarded as two *N*-methyl- 1,2,3,4-tetrahydroisoquinoline nuclei fused together. In accordance with this observation, the UV spectrum of a pavine alkaloid demonstrates close similarity to that of an analogous tetrahydroisoquinoline. 2,3,8,9-tetrasubstituted *N*-methylpavines generally display a broad absorption band between 287 and 295 nm in polar solvents. However, a triplet absorption has also been reported in ethanolic solutions between 280 and 295 nm, where the lowest and highest wavelength absorptions may appear as shoulders. Some generalizations have been made about the effect of various substituents on the absorption maxima and molar absorptivities. The absorption band around 280 nm is displaced to lower wavelengths when two methoxyls are replaced by a methylenedioxy group. The UV spectra of pavines are slightly affected by protonation on nitrogen. Similarly, quaternary species furnish UV spectra which closely resemble those of their tertiary counterparts. In some pavine bases such as norargemonine **90**, the expected bathochromic shift on addition of alkali has not been observed (Gözler, 1987).

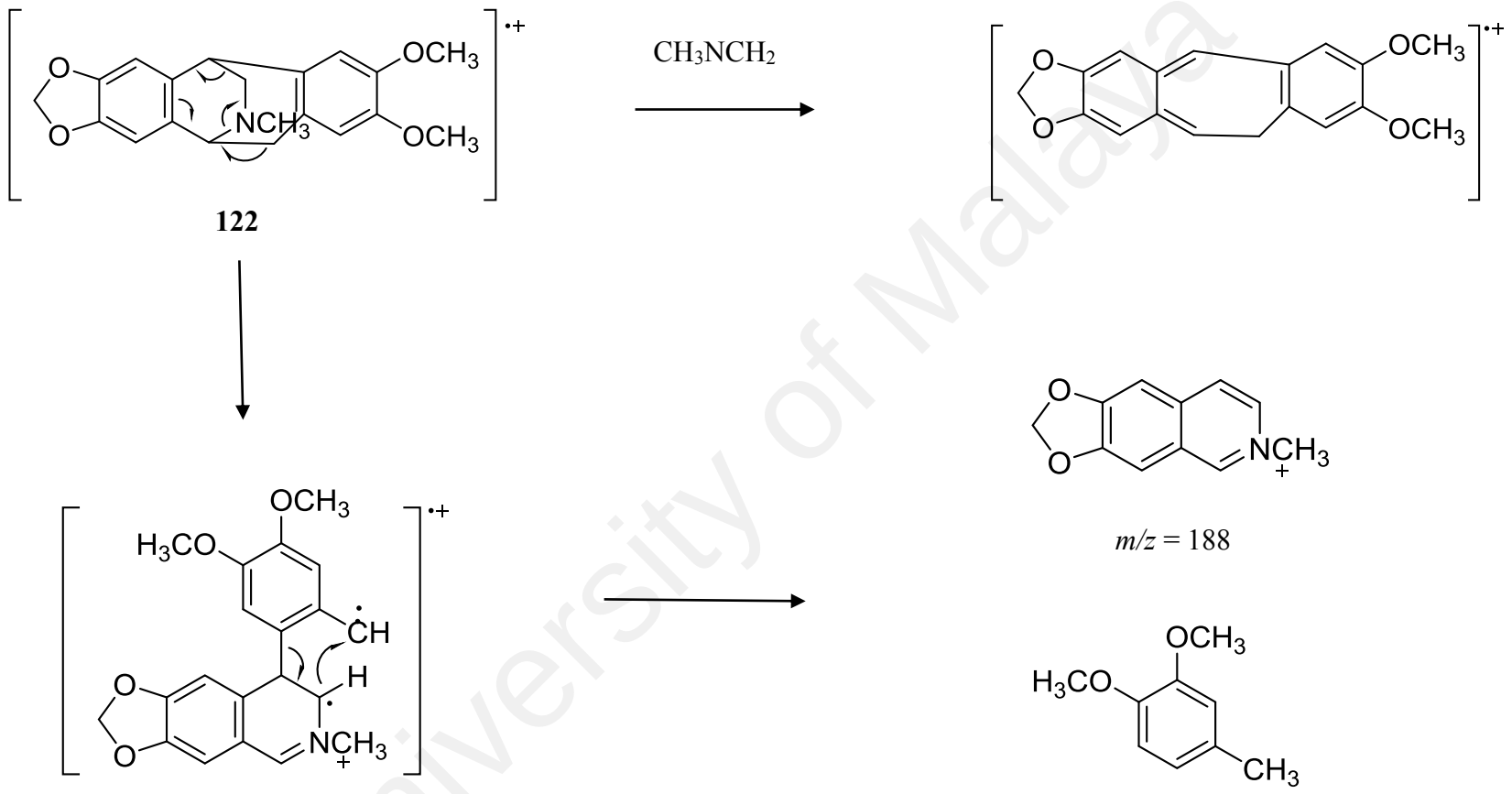

Scheme 2.13: Mass fragmentation of pavine

CHAPTER 3: RESULTS AND DISCUSSION

3.1 General

Three Malaysian plants from the genus *Cryptocarya*; namely *C. densiflora* Blume (KL 5211), *C. infectoria* Miq (KL 5229) and *C. griffithiana* Wight (KL 5469) have been studied for their alkaloids content. The plant parts investigated were the leaves and bark. The extraction and isolation procedures of the alkaloids from these three species have been described in chapter 6. The structures of all isolated alkaloids were performed through several spectroscopic methods notably 1D NMR (^{1}H, ^{13}C and DEPT), 2D NMR (COSY, NOESY, HSQC and HMBC), LCMS-IT-TOF, UV, IR, as well as by comparison with those reported in the literature. The following sub-chapters shall discuss briefly and concisely on the structural elucidation of each compounds isolated.

3.2 Alkaloids from the dichloromethane extracts of *C. densiflora*, *C. infectoria* and *C. griffithiana*.

Phytochemical analysis of dichloromethane extract from the leaves of *C. densiflora* resulted in the isolation of fourteen isoquinoline-derived alkaloids. The alkaloids were characterized as (-)-antofine **6**, (-)-isocaryachine **61**, (+)-reticuline **76**, (+)-laurotetanine **86**, (+)-*N*-methyllaurotetanine **87**, (+)-nornantenine **123**, dicentrinone **124**, (+)-oridine **125**, prodensiflorin A **126**, prodensiflorin B **127**, (-)-densiindolizidine **128**, (-)-desmethylsecoantofine **130**, (-)-desmethylsecoantofine-*N*-oxide **131** and crychine **134**. Among them, four alkaloids were identified as new namely, prodensiflorin A **126**, prodensiflorin B **127**, densiindolizidine **128**, and (-)-desmethylsecoantofine-*N*-oxide **131**.

In addition, six alkaloids were successfully purified from the bark of *C. infectoria*; (+)-*N*-methylisococlaurine **14**, atherosperminine **15**, (+)-reticuline **76**, (+)-laurotetanine

86, (+)-*N*-methyllaurotetanine **87** and argentinine **135**, while two alkaloids were isolated from its leaves; argentinine **135** and liriodenine **136**.

Furthermore, isolation and structural elucidation of the bark of *C. griffithiana* yielded six alkaloids. The alkaloids were characterized as 2-hydroxyatherosperminine **13**, 2-methoxyatherosperminine **72**, (+)-reticuline **76**, (+)-*N*-methyllaurotetanine **87**, (+)-nornantenine **123** and argentinine **135**. The alkaloids isolated from these three samples were summarized in Table 3.1.

Table 3.1: Summary of compounds isolated from the three samples

Alkaloids isolated	**Skeletal type**	**Plant**	**Plant parts**
(-)-Antofine **6**	Phenanthroindolizidine	*C. densiflora*	Leaves
2-Hydroxyatherosperminine **13**	Phenanthrene	*C. griffithiana*	Bark
(+)-*N*-methylisococlaurine **14**	Benzylisoquinoline	*C. infectoria*	Bark
Atherosperminine **15**	Phenanthrene	*C. infectoria*	Bark
(-)-Isocaryachine **61**	Pavine	*C. densiflora*	Leaves
2-Methoxyatherosperminine **72**	Phenanthrene	*C. griffithiana*	Bark
(+)-Reticuline **76**	Benzylisoquinoline	*C. densiflora*	Leaves
		C. Infectoria	Bark
		C. griffithiana	Bark
(+)-Laurotetanine **86**	Aporphine	*C. densiflora*	Leaves
		C. infectoria	Bark
(+)-*N*-methyllaurotetanine **87**	Aporphine	*C. densiflora*	Leaves
		C. infectoria	Bark
		C. griffithiana	Bark
(+)-Nornantenine **123**	Aporphine	*C. densiflora*	Leaves
		C. griffithiana	Bark
Dicentrinone **124**	Oxoaporphine	*C. densiflora*	Leaves
(+)-Oridine **125**	Proaporphine	*C. densiflora*	Leaves
Prodensiflorin A **126**	Proaporphine	*C. densiflora*	Leaves
Prodensiflorin B **127**	Proaporphine	*C. densiflora*	Leaves
(-)-Densiindolizidine **128**	Phenanthroindolizidine	*C. densiflora*	Leaves
(-)-Desmethylsecoantofine **130**	*Seco*-phenanthroindolizidine	*C. densiflora*	Leaves
(-)-Desmethylsecoantofine-*N*-oxide **131**	*Seco*-phenanthroindolizidine	*C. densiflora*	Leaves
Crychine **134**	Pavine	*C. densiflora*	Leaves
Argentinine **135**	Phenanthrene	*C. infectoria*	Bark
		C. infectoria	Leaves
		C. griffithiana	Bark
Liriodenine **136**	Oxoaporphine	*C. infectoria*	Leaves

3.2.1 Alkaloid A: (+)-Laurotetanine 86

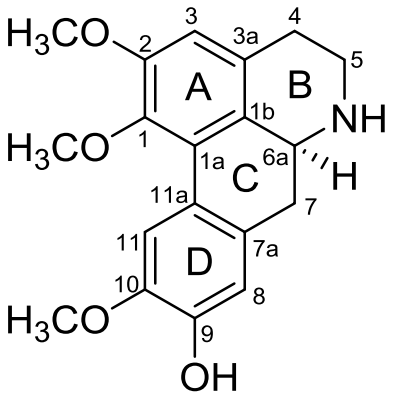

86

Alkaloid **A** was isolated as an optically active dark brownish amorphous with $[\alpha]_D^{25}$ +36° (*c*=0.098, MeOH). The positive LCMS-IT-TOF analysis exhibited a pseudomolecular ion peak, $[M+H]^+$ at *m/z* 328.1521 (calcd. for $C_{19}H_{22}NO_4$, 328.1543), which corresponded to the molecular formula of $C_{19}H_{21}NO_4$. The UV spectrum revealed absorption bands at λ_{max} 220, 281, 302 and 312 nm, which were typical of an aporphine moiety, thus suggesting a 1,2,9,10-tetrasubstituted aporphine skeleton (Shamma, 1972). The IR spectrum revealed strong peak at ν_{max} 3430 cm^{-1} due to the stretching of hydroxyl (OH) group. Other absorption peaks were observed at ν_{max} 2098 and 1654 cm^{-1} indicating the presence of an NH group and C=C aromatic respectively.

The ^1H NMR spectrum of alkaloid **A** (Figure 3.1) showed three distinct methoxyl signals at δ_H 3.66, 3.89 and 3.90 which were most probably attached to C-1, C-2 and C-10, respectively. The former was assigned to the methoxyl at C-1 since the protons were shielded by the anisotropic effect caused by ring D. A singlet appeared at δ_H 6.60, corresponded to aromatic proton at position C-3, thus, suggesting that C-1 and C-2 was substituted. Furthermore, the singlets at δ_H 6.80 and 8.08 could be attributed to H-8 and H-11, respectively. H-11 has the highest chemical shift due to the deshielding effect

caused by ring A. The remaining aliphatic signals, H-4, H-5, H-6a and H-7 can be observed between δ_H 2.67 to 3.84.

The ^{13}C NMR spectrum (Figure 3.2) as well as DEPT experiment (Figure 3.3) revealed a total of nineteen carbon signals which represented three methyls, three methylenes, four methines and nine quaternary carbons in the molecule, consistent with the structure proposed. The downfield signal for the quaternary carbons resonated at δ_C 144.3, 152.2, 145.0 and 145.4 which were assigned to C-1, C-2, C-9 and C-10 respectively, suggested that they were oxygenated. The aliphatic carbons consisting of three methylene resonated at δ_C 29.1, 43.1 and 36.6 were assigned to C-4, C-5 and C-7 respectively, while a methine carbon signal appeared at δ_C 53.8 corresponded to C-6a.

HMBC correlations of H-8 to C-11a, H-7 to C-8 and H-11 to C-7a, indicated that ring C was fused to ring D through C-7a and C-11a junction. Furthermore, the connectivity of ring A with ring B and C was observed via the correlation between H-3 to C-4 and H-3 to C-1b respectively. The HMBC correlations between 1-OC$\underline{H}_3$ and C-1, 2-OC$\underline{H}_3$ and C-2 and between 10-OC$\underline{H}_3$ and C-10 rendered the placements of the methoxyl groups at C-1, C-2 and C-10, respectively. The full assignments of all the cross peaks in order to construct this alkaloid are shown in Figure 3.5.

The complete assignment of proton and carbon were obtained through the aid of the 2D (COSY, NOESY, HSQC and HMBC) experiments and were confirmed by direct comparison with the literature values (Costa, Dutra, Nepel, & Barison, 2013). Thus, the structure of alkaloid **A** was deduced as (+)-laurotetanine **86**, which widely exists among the family of Annonaceae (Pimenta & Mendonça, 2012), Monimiaceae (Johns, Lamberton, & Sioumis, 1967) and Lauraceae (Uprety, Bhakuni, & Dhar, 1972).

Table 3.2: ^{1}H NMR (400 MHz) and ^{13}C NMR (100 MHz) spectroscopic assignments of alkaloid **A** in $CDCl_3$

Position	δ_H (ppm, *J* in Hz)		δ_C (ppm)	
	Alkaloid **A**	Laurotetanine **86** (Costa et al., 2013) ($CDCl_3$ + drops of CD_3OD, 400 MHz)	Alkaloid **A**	Laurotetanine **86** (Costa et al., 2013) ($CDCl_3$ + drops of CD_3OD)
1	-	-	144.3	144.3
1a	-	-	126.8	127.1
1b	-	-	127.4	126.5
2	-	-	152.2	152.2
3	6.60 (1H, *s*)	6.61 (1H, *s*)	110.8	110.7
3a	-	-	129.0	128.4
4	α=2.77 (1H, *m*) β=3.04 (1H, *m*)	α=2.75 (1H, *m*) β=3.04 (1H, *m*)	29.1	28.2
5	α=3.02 (1H, *m*) β=3.40 (1H, *m*)	α=3.02 (1H, *m*) β=3.41 (1H, *m*)	43.1	42.5
6a	3.84 (1H, *dd*, *J*=13.6, 4.4)	3.84 (1H, *dd*, *J*=14.5, 4.9)	53.8	53.5
7	2.67 (2H, *d*, *J*=13.6, 10.0)	α=2.68 (1H, *dd*, *J*=14.5, 13.8) β=2.78 (1H, *dd*, *J*=13.8, 4.9)	36.6	35.7
7a	-	-	129.8	129.1
8	6.80 (1H, *s*)	6.77 (1H, *s*)	114.0	114.4
9	-	-	145.0	145.6
10	-	-	145.4	146.1
11	8.08 (1H, *s*)	8.06 (1H, *s*)	111.4	111.8
11a	-	-	124.0	123.6
1-OCH_3	3.66 (3H, *s*)	3.67 (3H, *s*)	60.3	60.2
2-OCH_3	3.89 (3H, *s*)	3.89 (3H, *s*)	56.1	56.1
10-OCH_3	3.90 (3H, *s*)	3.90 (3H, *s*)	55.9	55.9

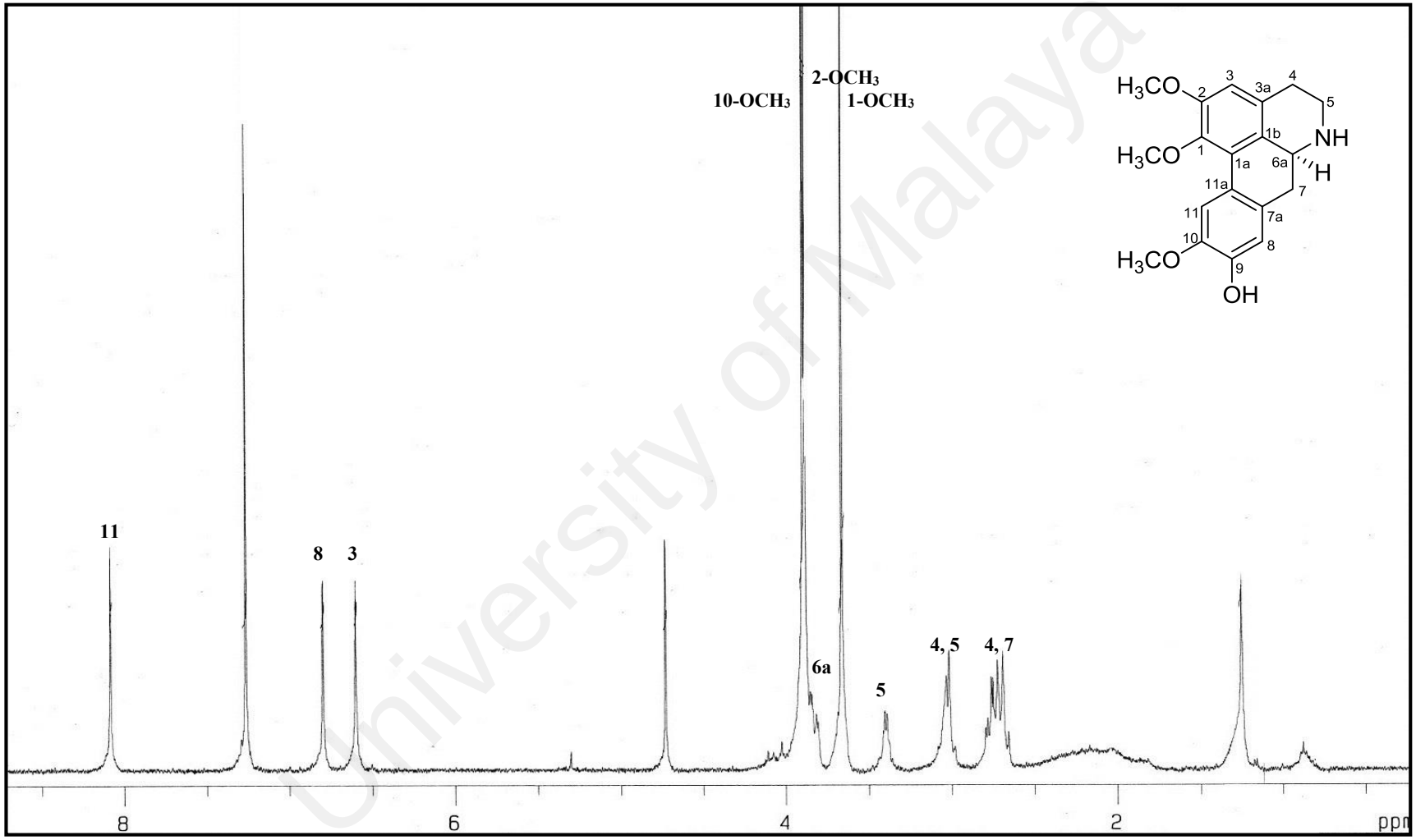

Figure 3.1: ^{1}H NMR spectrum of alkaloid **A**

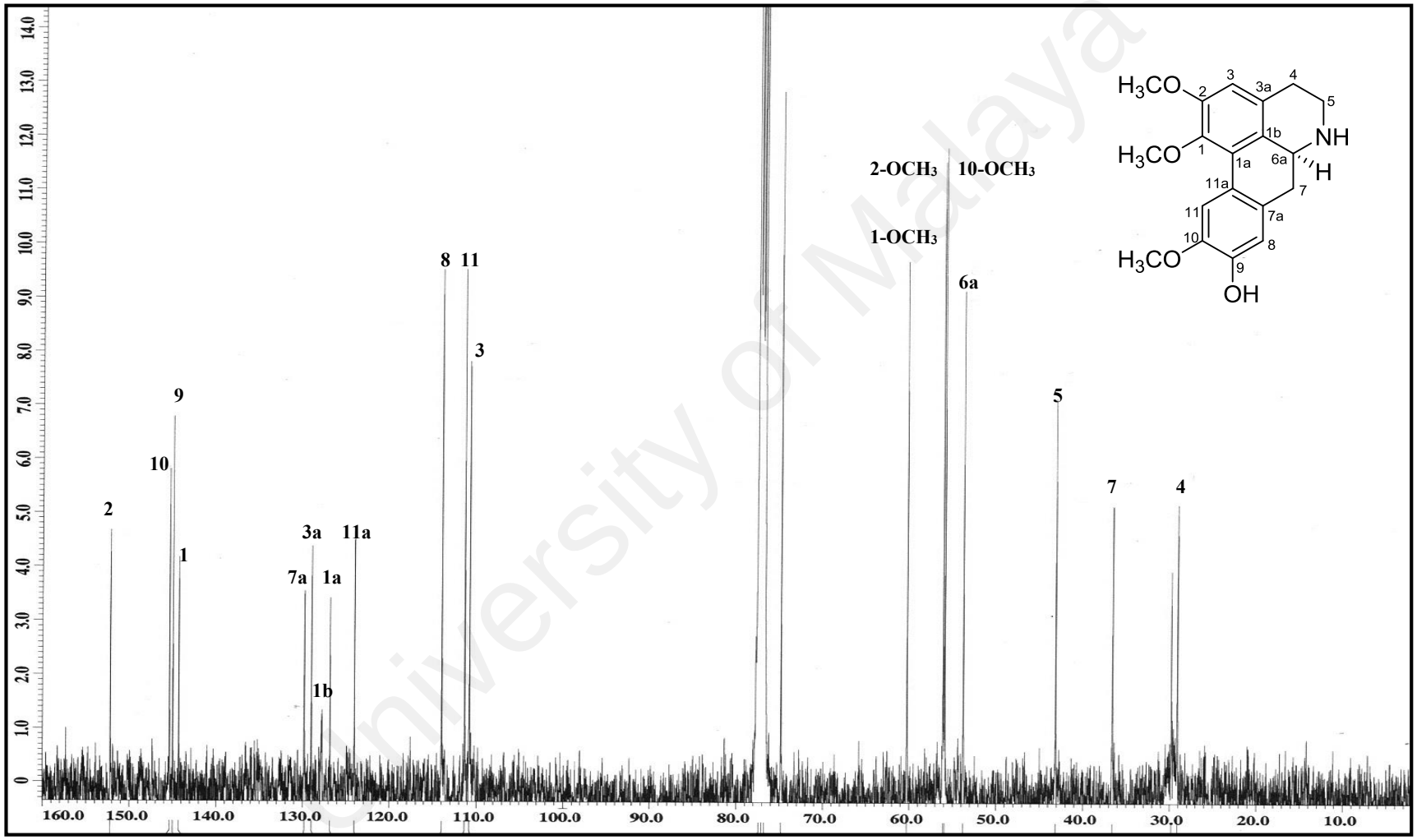

Figure 3.2: ^{13}C NMR spectrum of alkaloid **A**

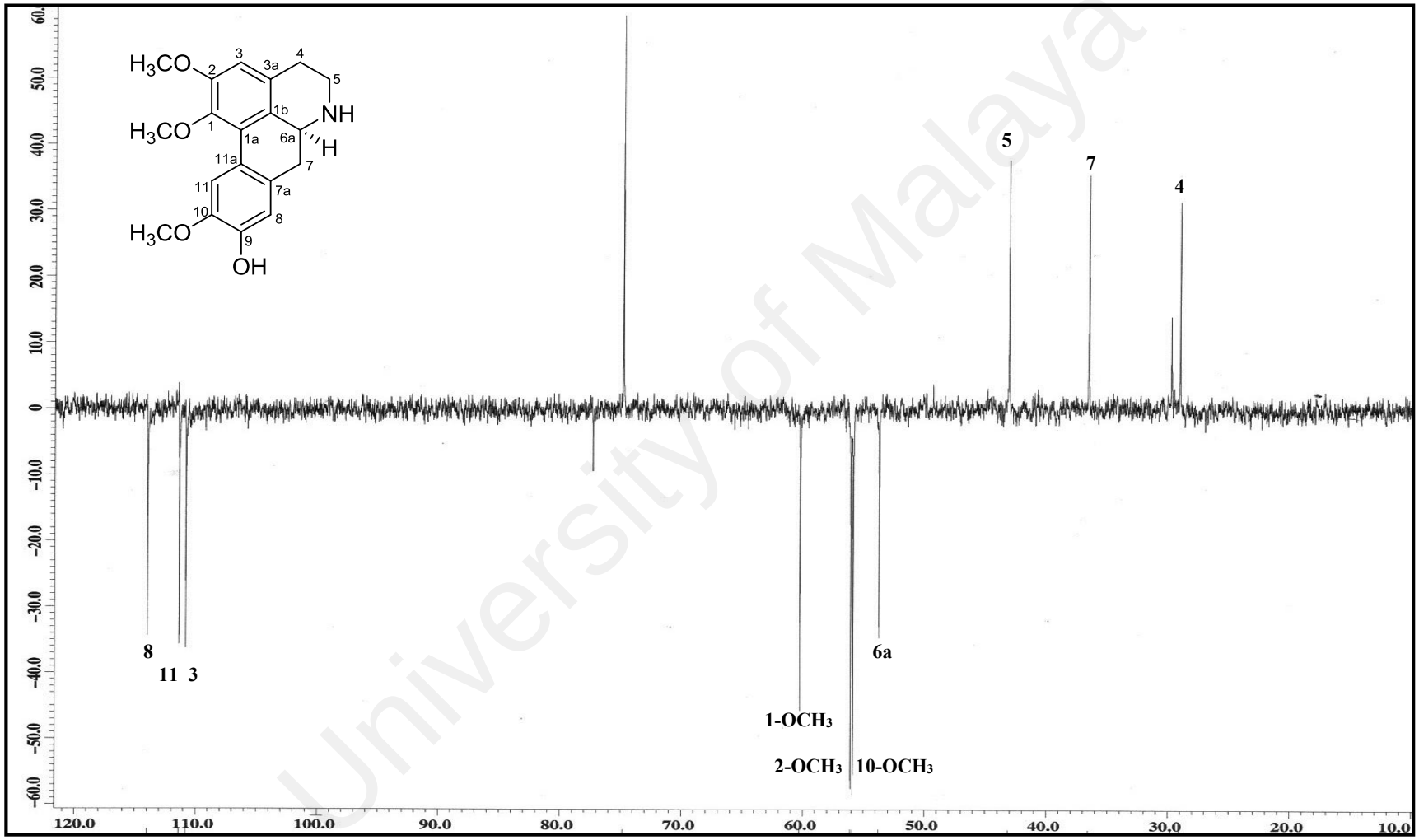

Figure 3.3: DEPT spectrum of alkaloid **A**

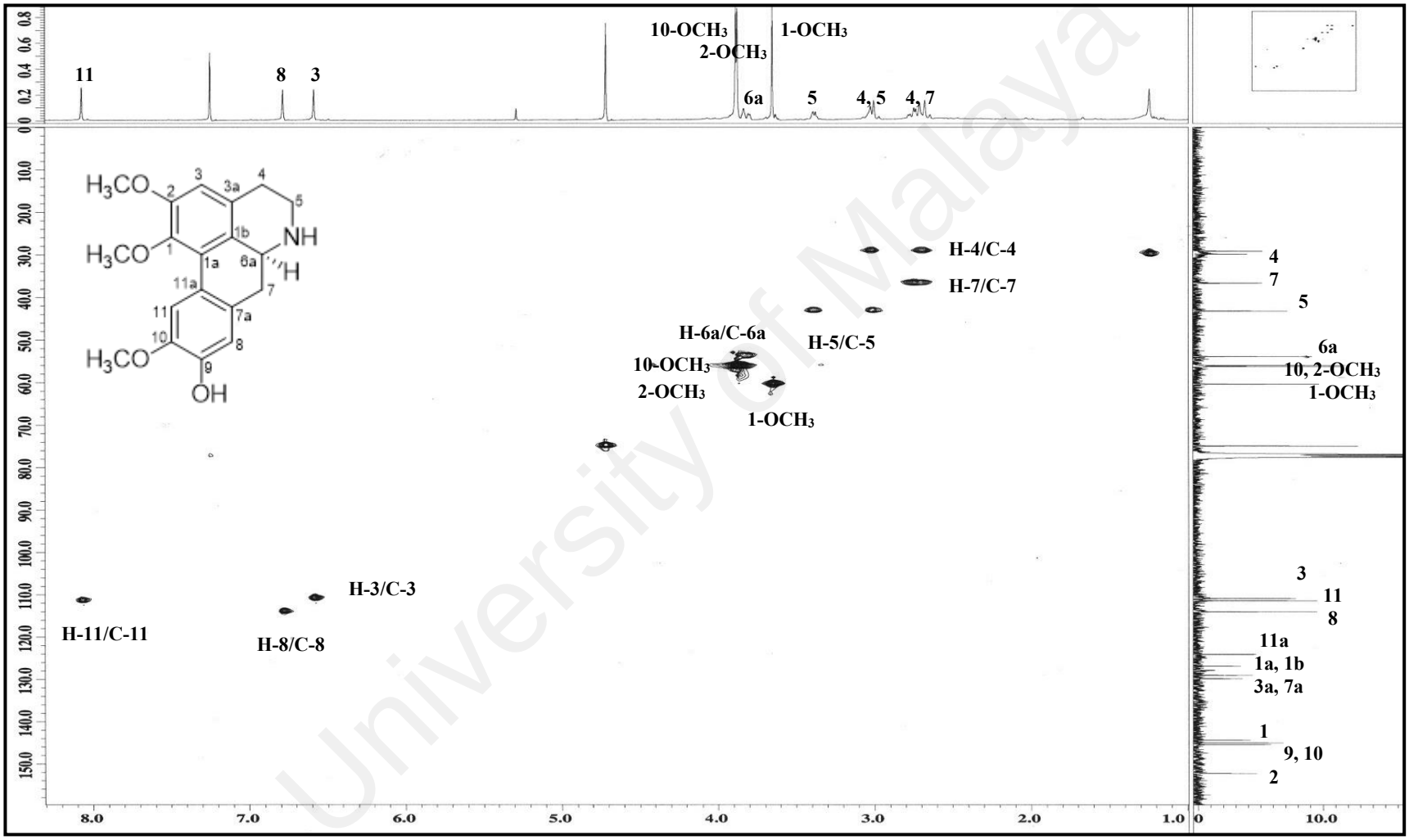

Figure 3.4: HSQC spectrum of alkaloid **A**

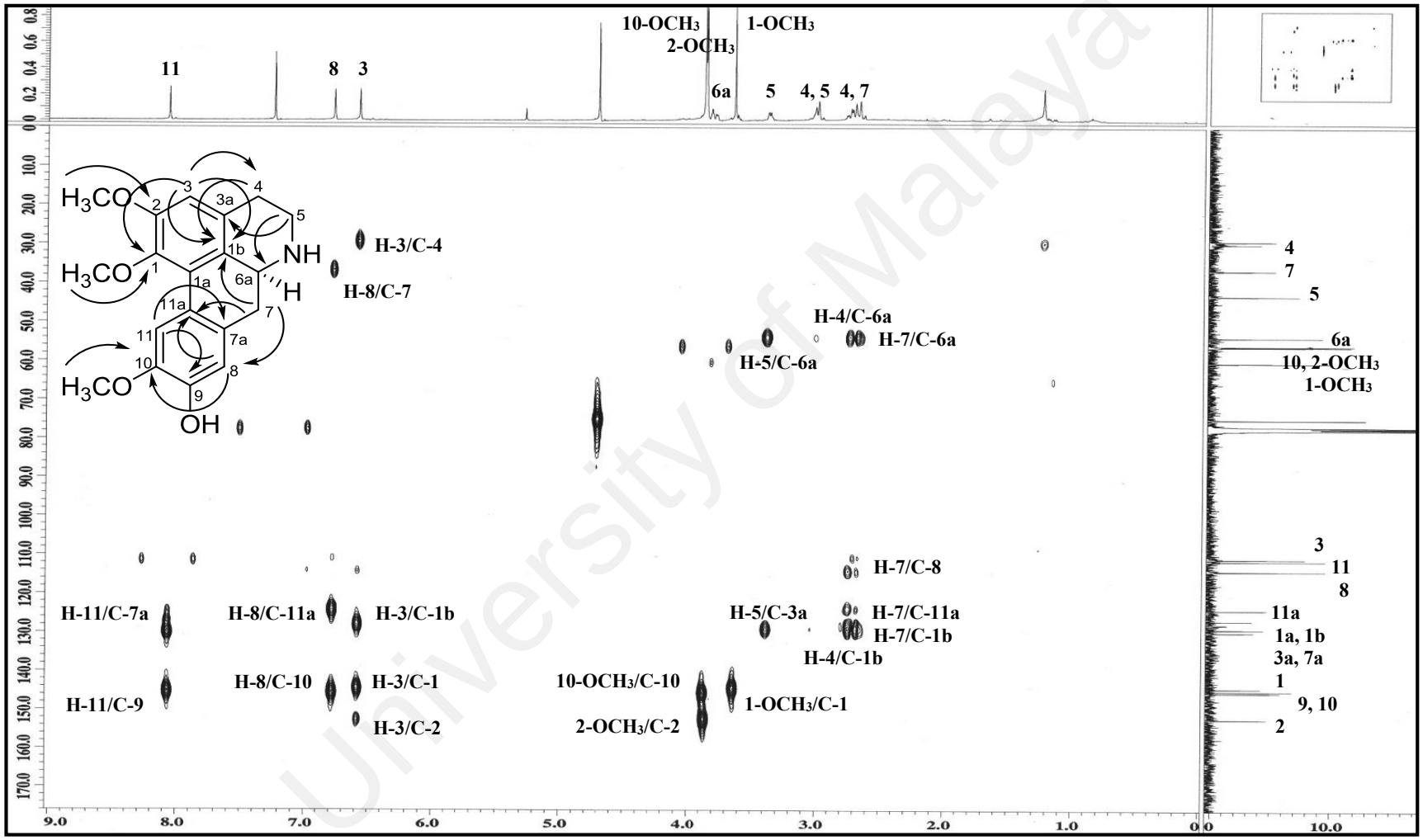

Figure 3.5: HMBC spectrum of alkaloid **A**

3.2.2 Alkaloid B: (+)-*N*-methyllaurotetanine 87

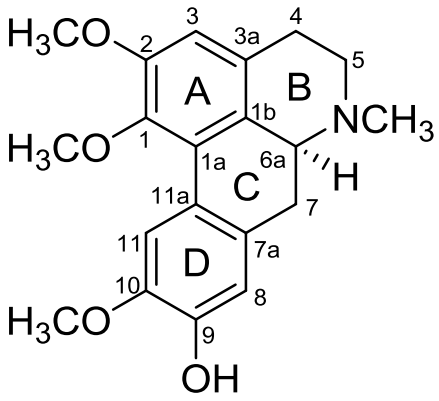

87

Alkaloid **B** was obtained as an optically active dark brownish amorphous with $[\alpha]_D^{25}$ +70° (*c*=0.02, MeOH). The positive LCMS-IT-TOF spectrum exhibited a pseudomolecular ion peak, $[M+H]^+$ at *m/z* 342.1683 (calcd. for $C_{20}H_{24}NO_4$, 342.1700), which was associated with the molecular formula of $C_{20}H_{23}NO_4$, consistent with ten degrees of unsaturation. The UV spectrum exhibited maximum absorptions at λ_{max} 227, 248 and 303 nm which were typical of an aporphine moiety, thus suggesting a 1,2,9,10-tetrasubstituted aporphine skeleton (Shamma, 1972). The IR spectrum showed absorptions at ν_{max} 3465 and 2998 cm^{-1} indicating the presence of a hydroxyl (OH) group and CH aromatic respectively.

The ^1H and ^{13}C NMR spectra (Figure 3.6 and Figure 3.7) of alkaloid **B** was reminiscent with those of alkaloid **A** by exhibiting three aromatic singlets at δ_H 6.58, 6.81 and 8.06 which could be place at C-3, C-8 and C-11, respectively. Three distinct methoxyl group signals were also observed at δ_H 3.64, 3.88 and 3.90 corresponding to C-1, C-2 and C-10, respectively. However, a marked difference between alkaloid **B** and alkaloid **A** was observed with the presence of a sharp singlet peak at δ_H 2.54 in the ^1H NMR spectrum of alkaloid **B**, therefore suggesting that it could be due to the presence of an *N*CH_3 group. The relatively upfield H-6a in alkaloid **B** (δ_H 2.99) as compared to the corresponding atom

in alkaloid **A** (δ_H 3.84) might due to the decreasing inductive effect by the nitrogen atom attached to the methyl group which is an electron donating group (Baarschers, Arndt, Pachler, Weisbach, & Douglas, 1964). The assignment of the proton was also confirmed by the analysis of the COSY data (Figure 3.8) which showed the correlation of H-4/H-5 and H-6a/H-7.

The ^{13}C NMR experiment (Figure 3.7) revealed the presence of twenty carbon signals which validated the molecular formula as proposed above. The *N*CH_3 group was resonated at δc 44.0. The HMBC spectrum (Figure 3.11) showed correlations between H-3 to C-4, 1b and H-7 to C-8, 11a, thus supporting the connectivity of ring A with ring B and C, and also ring C with ring D respectively. Furthermore, HMBC correlations of *N*C$\underline{H}_3$ to C-5 and C-6a further supported the attachment of the *N*CH_3 group in ring B.

Finally, the observed data of alkaloid **B** (Table 3.3) indicated that this compound was (+)-*N*-methyllaurotetanine **87** as reported in the literature, which has previously been isolated from *Xylopia laevigata* (Annonaceae) (Menezes et al., 2016).

Table 3.3: ^{1}H NMR (400 MHz) and ^{13}C NMR (100 MHz) spectroscopic assignments of alkaloid **B** in $CDCl_3$

Position	δ_H (ppm, *J* in Hz)		δ_C (ppm)	
	Alkaloid **B**	(+)-*N*-methyllaurotetanine **87** (Menezes et al., 2016) ($CDCl_3$ + drops of CD_3OD, 400 MHz)	Alkaloid **B**	(+)-*N*-methyl-laurotetanine **87** (Menezes et al., 2016) ($CDCl_3$ + drops of CD_3OD, 100 MHz)
1	-	-	144.2	144.3
1a	-	-	127.1	127.4
1b	-	-	127.2	126.5
2	-	-	152.0	152.3
3	6.58 (1H, *s*)	6.59 (1H, *s*)	110.3	110.5
3a	-	-	128.9	128.7
4	α=2.67 (1H, *dd*, *J*=16.5, 3.6) β=3.16 (1H, *m*)	α=2.70 (1H, *dd*, *J*=16.3, 3.6) β=3.15 (1H, *m*)	29.3	28.7
5	α=2.52 (1H, *d*, *J*=3.6) β=3.05 (1H, *dd*, *J*=11.9, 6.0)	α=2.55 (1H, *m*) β=3.06 (1H, *m*)	53.4	53.3
6a	2.99 (1H, *m*)	3.07 (1H, *d*, *J*=13.6)	62.6	62.6
7	α=2.58 (1H, *m*) β=2.96 (1H, *d*, *J*=4.1)	α=2.54 (1H, *m*) β=2.97 (1H, *dd*, *J*=13.6, 4.0)	34.3	33.8
7a	-	-	130.2	129.6
8	6.81 (1H, *s*)	6.78 (1H, *s*)	113.9	114.5
9	-	-	144.9	145.3
10	-	-	145.3	146.1
11	8.06 (1H, *s*)	8.03 (1H, *s*)	111.2	111.9
11a	-	-	124.0	123.7
NCH_3	2.54 (3H, *s*)	2.54 (3H, *s*)	44.0	43.6
1-OCH_3	3.64 (3H, *s*)	3.64 (3H, *s*)	60.2	60.2
2-OCH_3	3.88 (3H, *s*)	3.88 (3H, *s*)	55.9	56.0
10-OCH_3	3.90 (3H, *s*)	3.89 (3H, *s*)	56.1	56.2

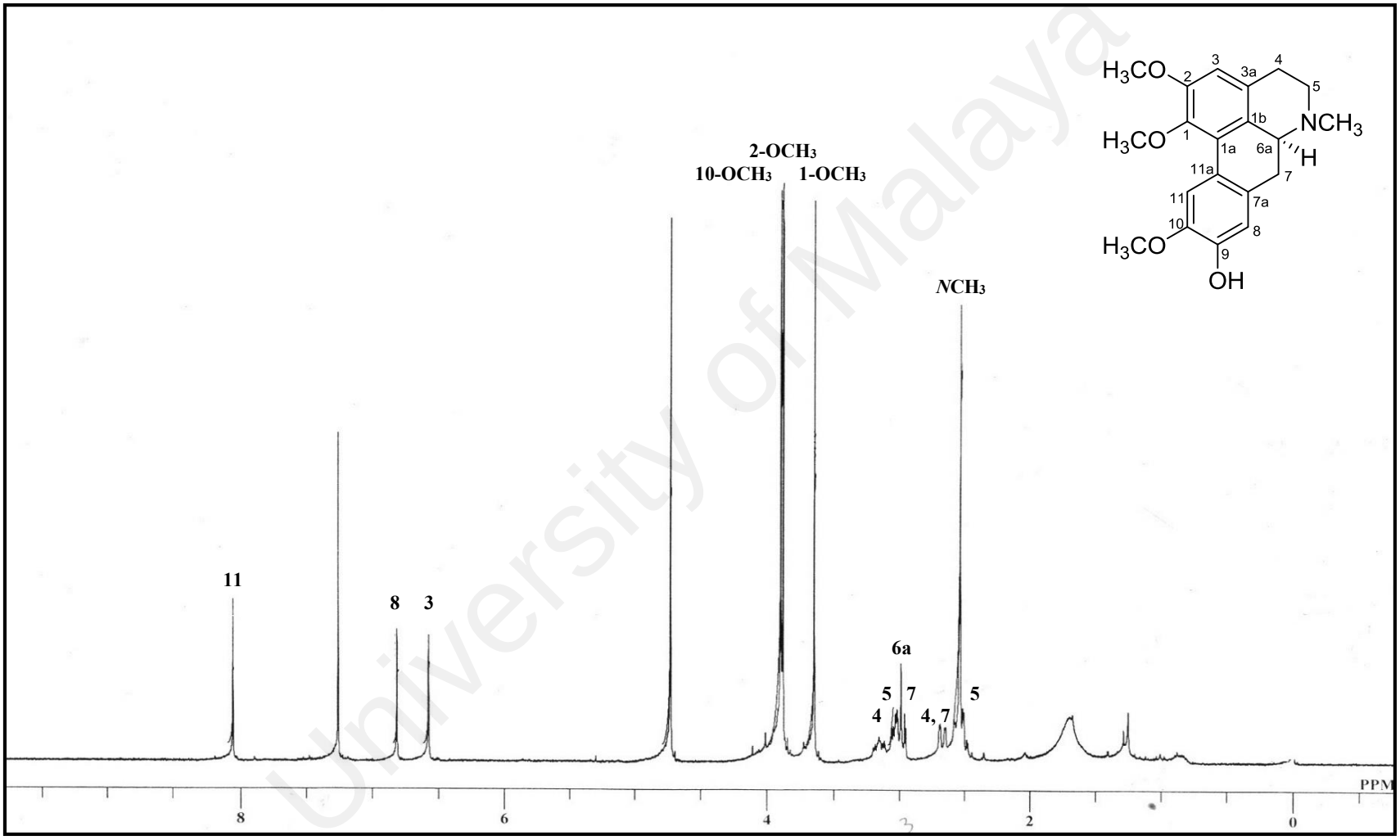

Figure 3.6: ^{1}H NMR spectrum of alkaloid **B**

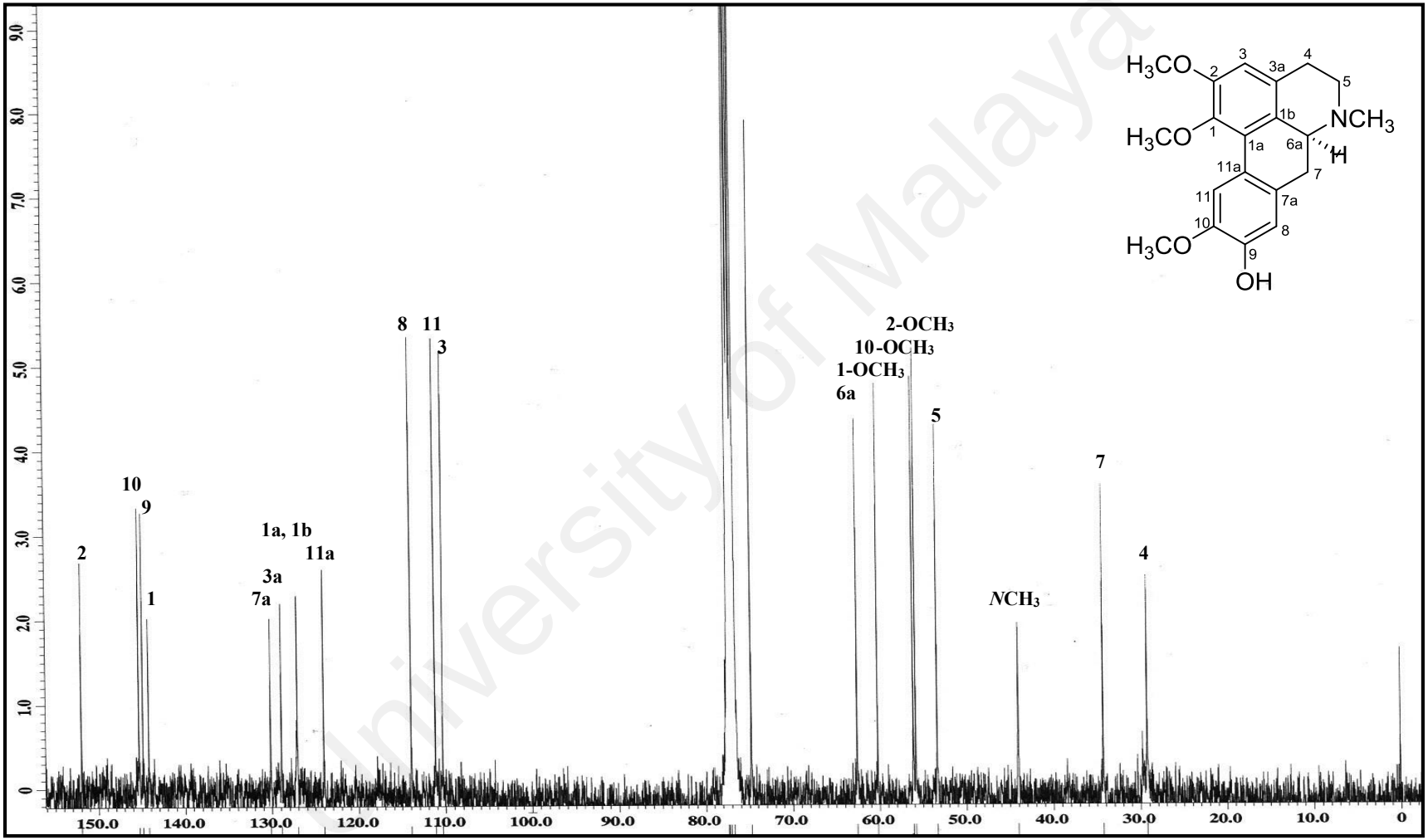

Figure 3.7: ^{13}C NMR spectrum of alkaloid **B**

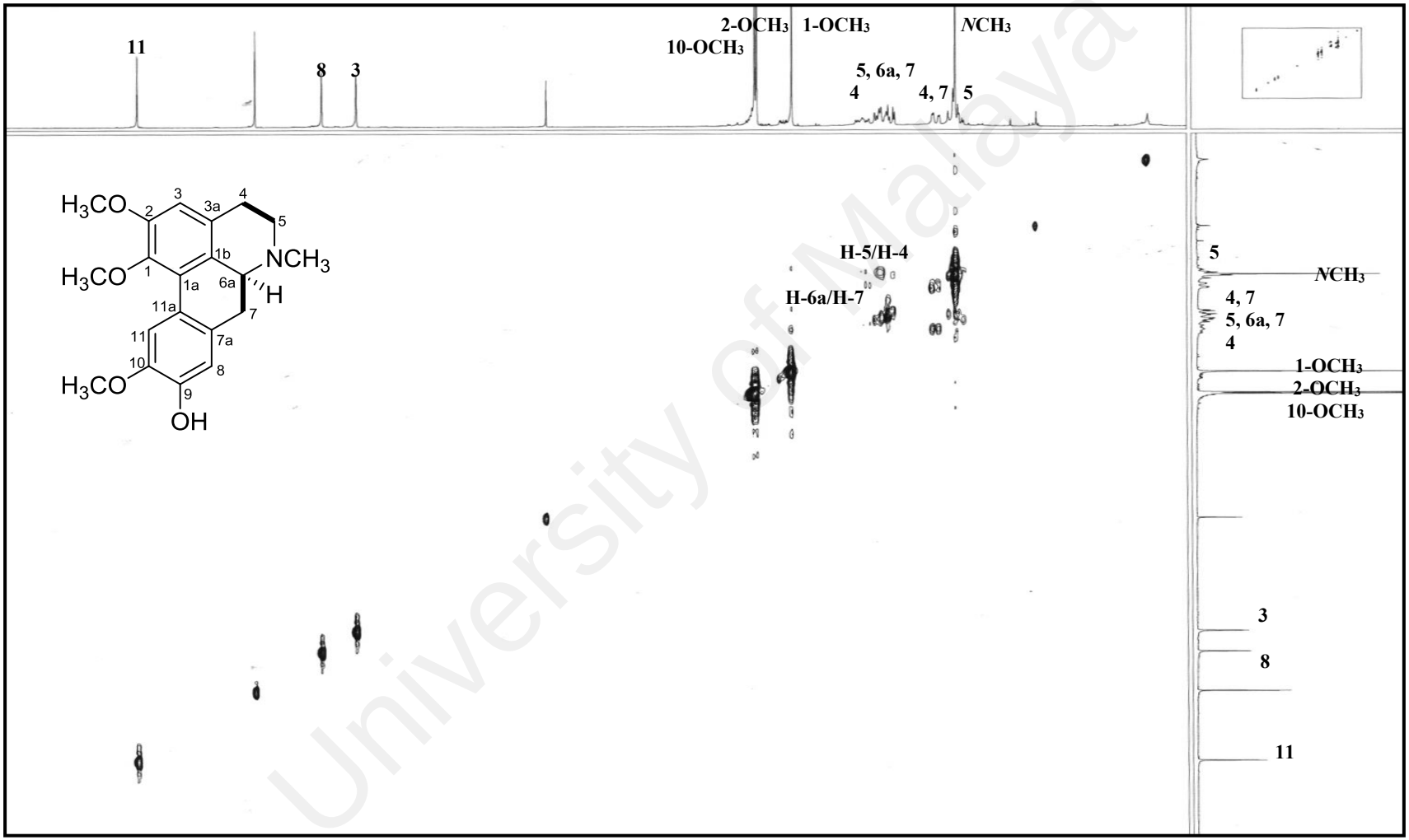

Figure 3.8: COSY spectrum of alkaloid **B**

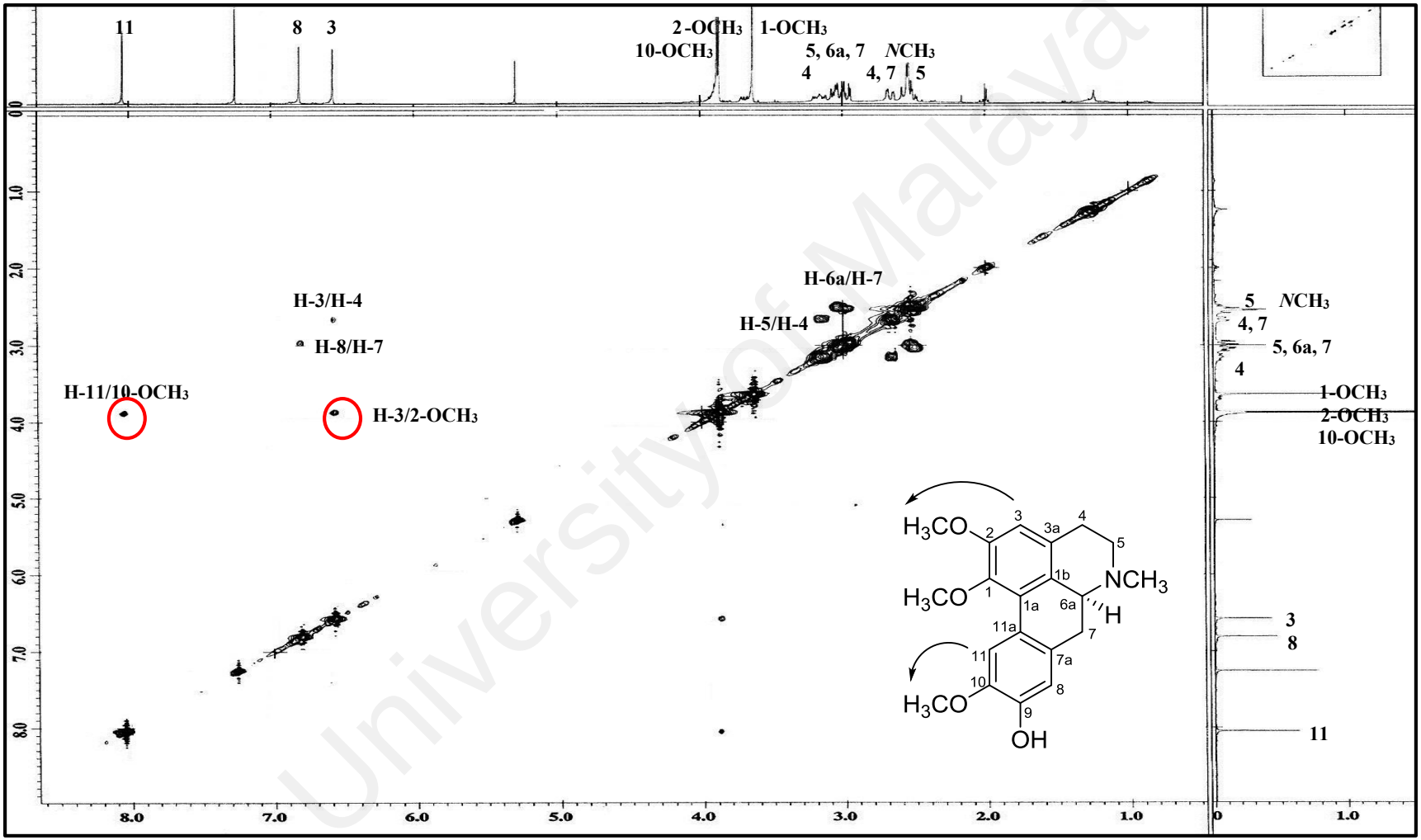

Figure 3.9: NOESY spectrum of alkaloid **B**

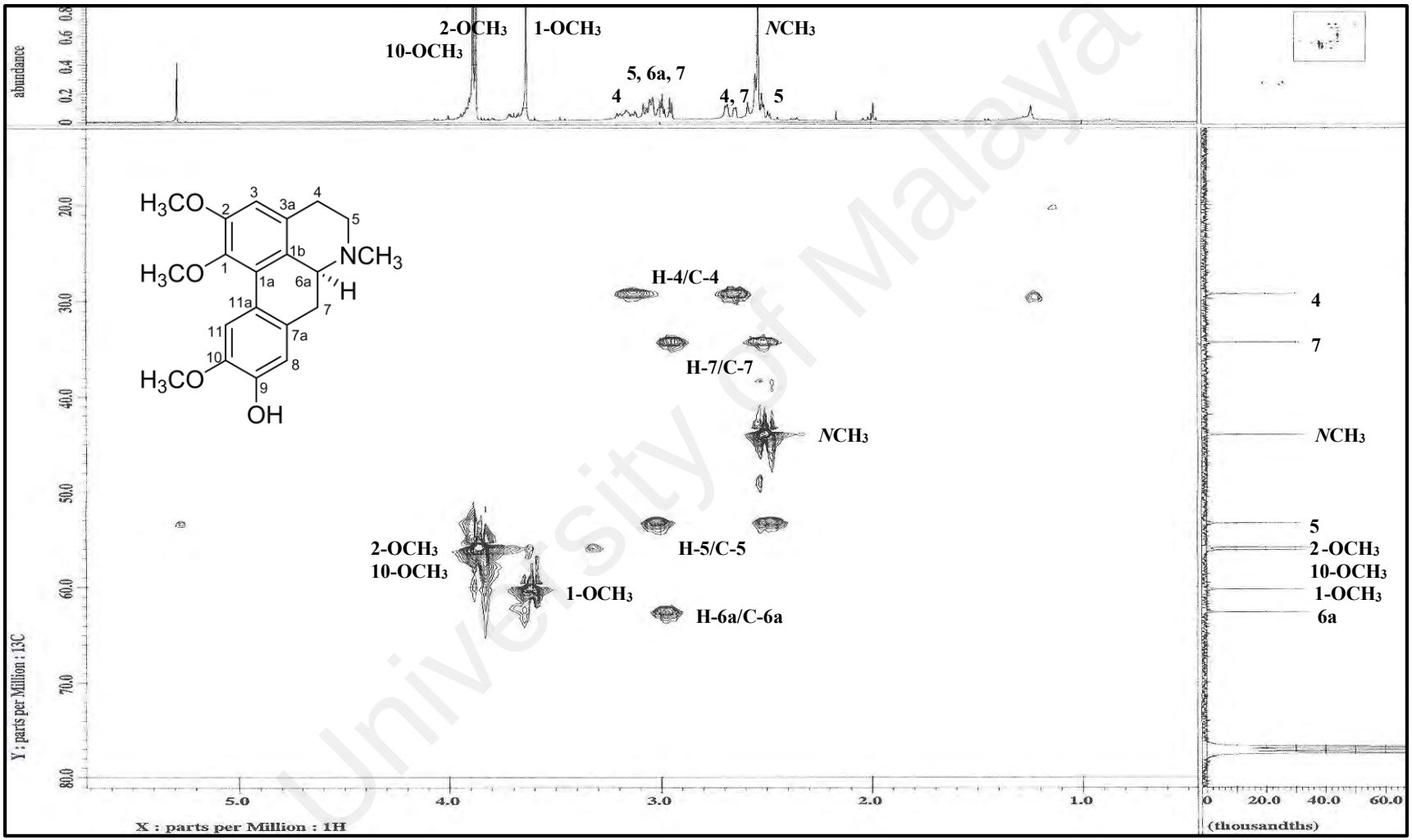

Figure 3.10: HSQC spectrum of alkaloid **B**

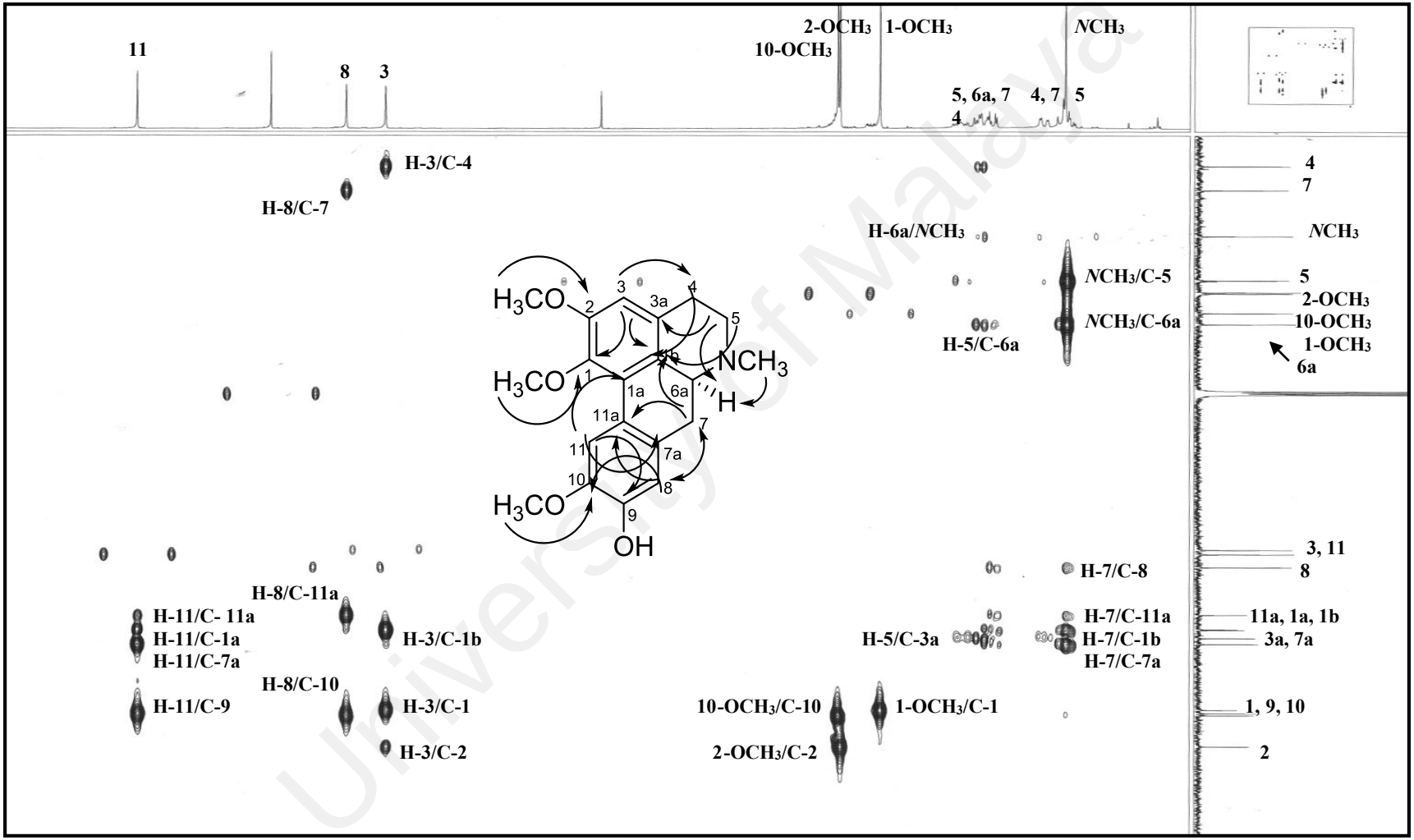

Figure 3.11: HMBC spectrum of alkaloid **B**

3.2.3 Alkaloid C: (+)-Nornantenine 123

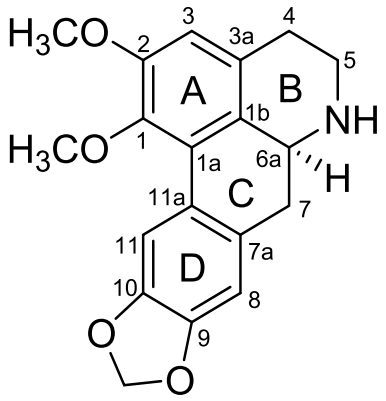

123

Alkaloid **C** was purified as an optically active brownish amorphous with $[\alpha]_D^{25}$ +49° (*c*=0.12, MeOH). The positive LCMS-IT-TOF analysis showed an intense pseudomolecular ion peak, $[M+H]^+$ at *m/z* 326.1389 (calcd. for $C_{19}H_{20}NO_4$, 326.1387), compatible with the molecular formula of $C_{19}H_{19}NO_4$, and suggested the presence of eleven degrees of unsaturation.

The UV, ^{1}H NMR (Figure 3.12) and ^{13}C NMR (Figure 3.13) spectra of alkaloid **C** were closely resembled to those of alkaloid **A**, by replacement of hydroxyl and methoxyl group at C-9 and C-10 with methylenedioxy group, which was observed as a doublet at δ_H 5.97 (2H, *d*, *J*=3.6 Hz) due to the asymmetry of the twisted biphenyl system (Castro, Lopez, & Vegara, 1985). An absorption peaks observed at ν_{max} 1273 and 984 cm^{-1} in the IR spectrum further confirmed the presence of methylenedioxy group in the structure due to the asymmetric O-C-O stretching (Guinaudeau, Lebœuf, & Cavé, 1994). Two singlet signals were observed at δ_H 3.67 and 3.88 in the ^{1}H NMR spectrum, indicating the presence of 1-OC<u>H</u>$_3$ and 2-OC<u>H</u>$_3$, respectively. The 1-OC<u>H</u>$_3$, signal was rather shielded compared to 2-OC<u>H</u>$_3$, since the protons of the former were forced to place themselves on top of ring A where the electron density was high due to anisotropic effect (Baarschers, Arndt, Pachler, Weisbach, & Douglas, 1964).

The ^{13}C NMR spectrum (Figure 3.13) indicated a total of nineteen carbon signals which comprising of two methyls, four methylenes, four methines and nine quaternary carbons consistent with the structure proposed. The methylenedioxy signal was observed at δ_C 101.0 and it was supported by HSQC data (Figure 3.14) which showed the correlation between methylene proton at δ_H 5.97 and methylene carbon at δ_C 101.0. The HMBC spectrum (Figure 3.15) showed the cross peak between O$C\underline{H_2}$O and C-9 thus, confirmed the position of this group attached to ring D.

In depth analyses of 1D and 2D NMR spectra and comparison with the data from literature, alkaloid **C** was identified as (+)-nornantenine **123**, which has been previously isolated from the family of Atherospermataceae (Urzúa & Cassels, 1982) and Annonaceae (Montenegro et al., 2003).

Table 3.4: ^{1}H NMR (400 MHz), ^{13}C NMR (100 MHz) spectroscopic assignments of alkaloid **C** in $CDCl_3$

Position	δ_H (ppm, *J* in Hz)		δ_C (ppm)	
	Alkaloid **C**	Nornantenine **123** (Fienena et al. 2016)	Alkaloid **C**	Nornantenine **123** (CD_3OD, 125 MHz) (Fienena et al. 2016)
1	-	-	144.9	144.9
1a	-	-	126.8	125.6
1b	-	-	128.0	128.4
2	-	-	152.4	152.5
3	6.60 (1H, *s*)	6.60 (1H, *s*)	111.2	111.2
3a	-	-	128.8	126.9
4	α=2.67 (1H, *brd*, *J*=13.7) β=2.99 (1H, *m*)	α=2.71 (1H, *t*) β=3.14 (1H, *t*)	29.1	28.6
5	α=2.99 (1H, *m*) β=3.35 (1H, *d*, *J*=6.9)	α=3.06 (1H, *t*) β=3.40 (1H, *t*)	43.1	42.9
6a	3.81 (1H, *dd*, *J*=13.5, 4.1)	3.85 (1H, *m*)	53.7	53.7
7	2.67 (2H, *dd, J*=13.5, 5.0)	α=2.74 (1H, *d*) β=2.85 (1H, *d*)	37.5	37.1
7a	-	-	130.6	130.1
8	6.73 (1H, *s*)	6.73 (1H, *s*)	108.3	108.4
9	-	-	146.7	146.7
10	-	-	146.7	146.8
11	7.96 (1H, *s*)	7.95 (1H, *s*)	109.1	109.1
11a	-	-	125.7	126.9
1-OCH_3	3.67 (3H, *s*)	3.66 (3H, *s*)	60.3	60.4
2-OCH_3	3.88 (3H, *s*)	3.87 (3H, *s*)	56.0	56.1
9, 10-OCH_2O	5.97 (2H, *d*, *J*=3.6)	5.97 (2H, *s*)	101.0	101.1

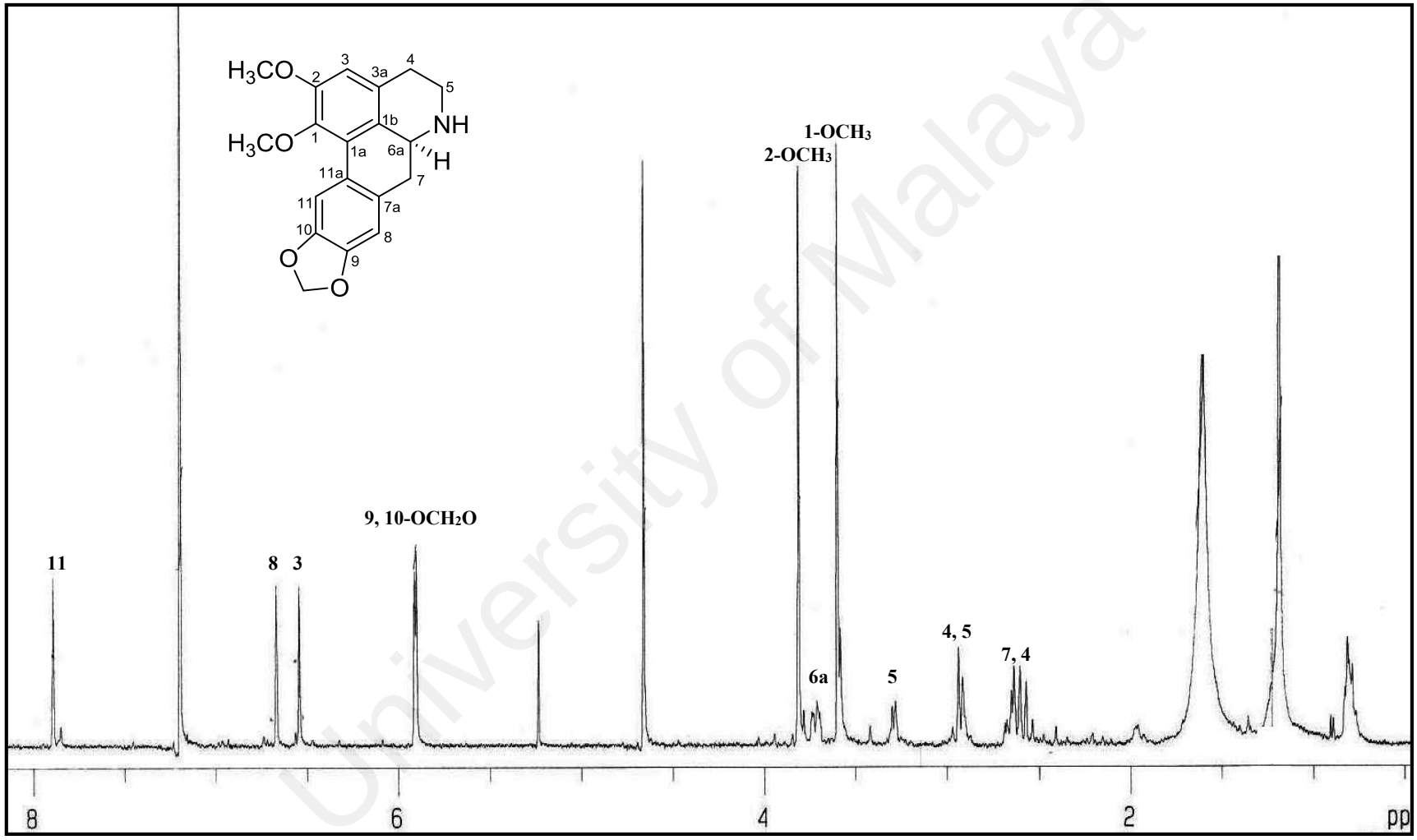

Figure 3.12: ^{1}H NMR spectrum of alkaloid **C**

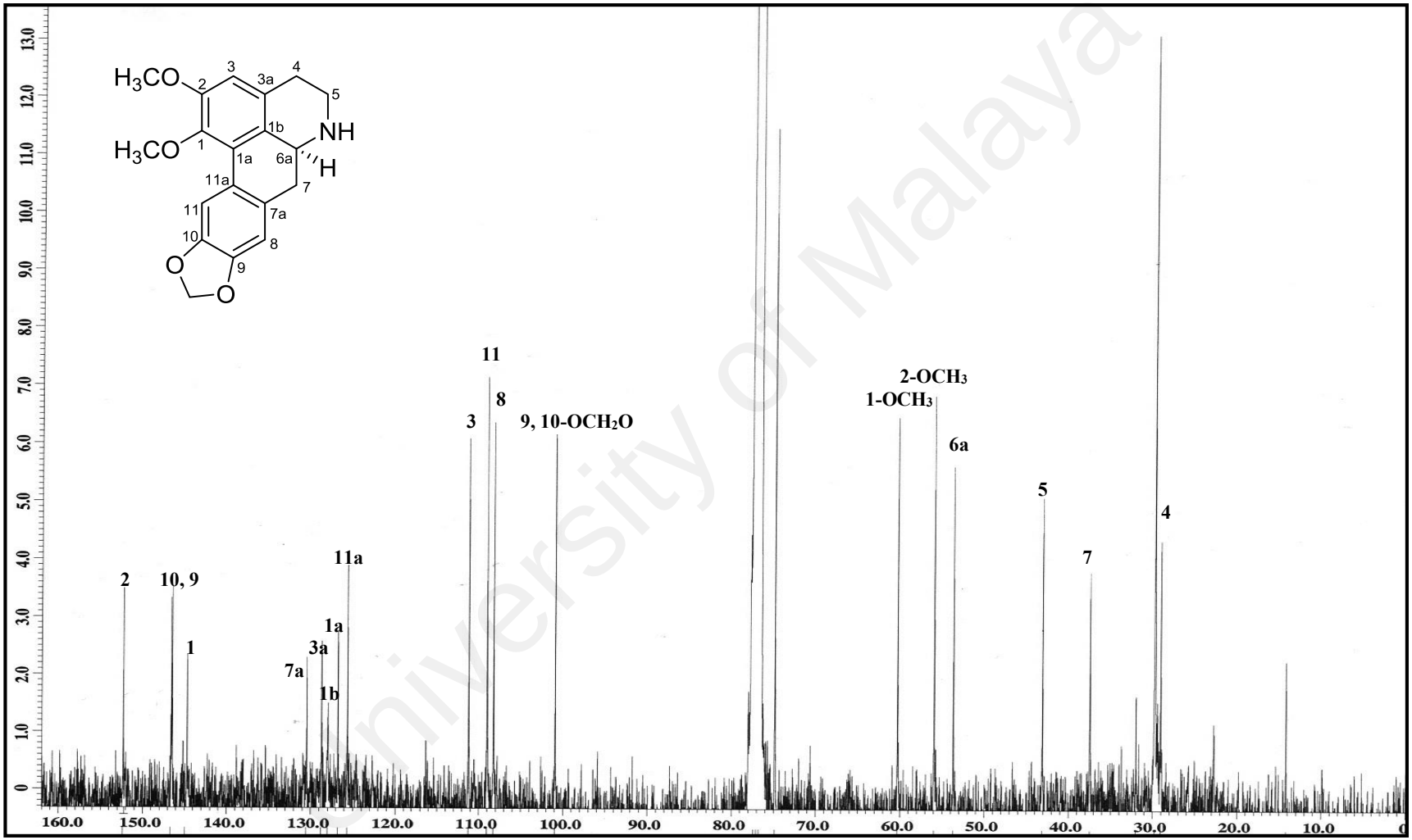

Figure 3.13: ^{13}C NMR spectrum of alkaloid **C**

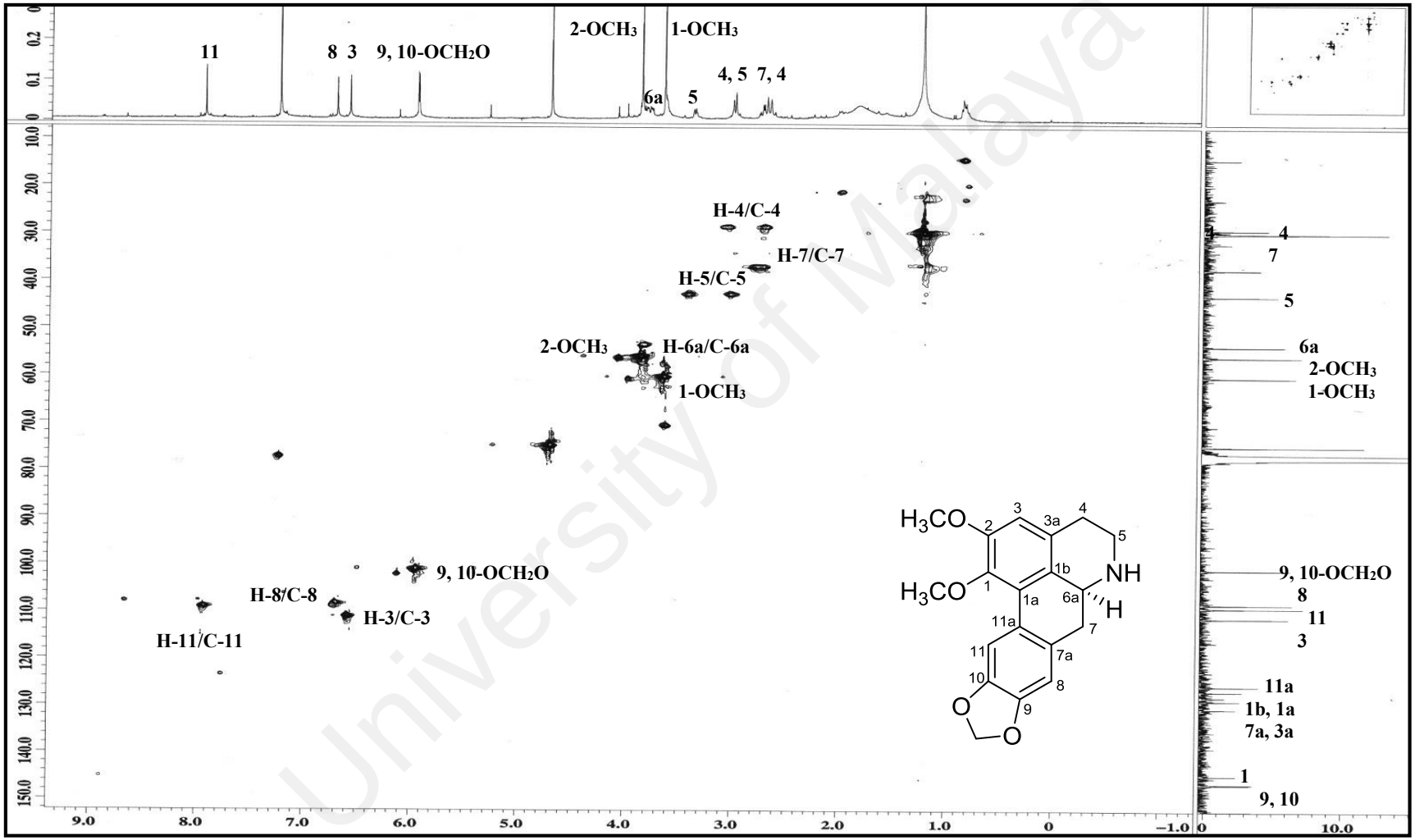

Figure 3.14: HSQC spectrum of alkaloid **C**

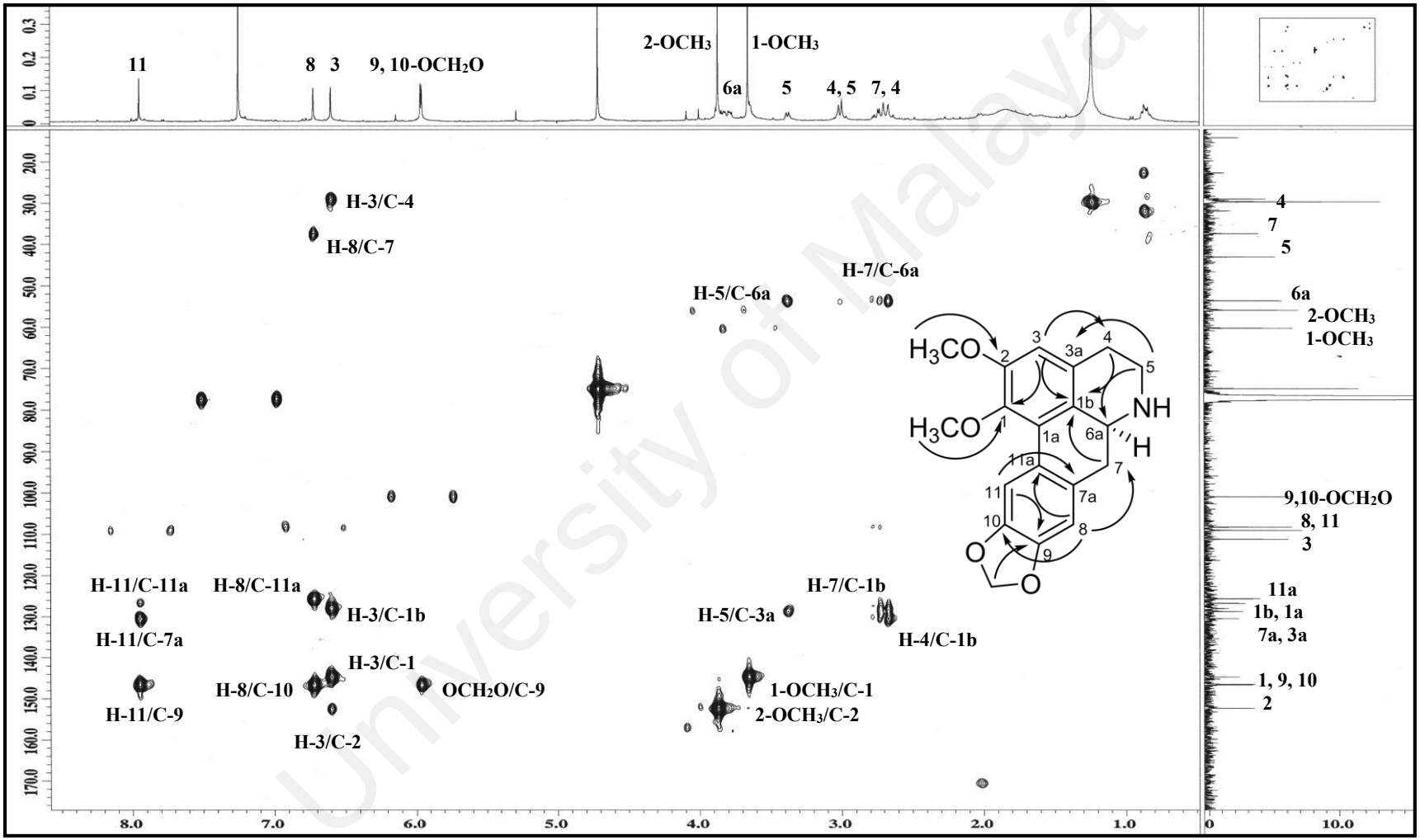

Figure 3.15: HMBC spectrum of alkaloid **C**

3.2.4 Alkaloid D: Dicentrinone 124

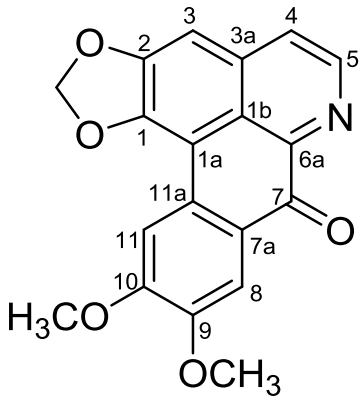

124

Alkaloid **D** was isolated as an optically inactive yellowish amorphous. The positive LCMS IT-TOF analysis revealed a pseudomolecular ion peak $[M+H]^+$ at *m/z* 336.0795 (calcd. for $C_{19}H_{14}NO_5$, 336.0866), appropriate for a molecular formula of $C_{19}H_{13}NO_5$ indicating fourteen degrees of unsaturation. The UV spectrum supported an oxoaporphine type carbon skeleton, with absorptions at λ_{max} 246, 273, 295 and 410 nm (Harrigan, Gunatilaka, Kingston, Chan, & Johnson, 1994). Absorption bands in the IR spectrum at ν_{max} 1598 and 1644 cm^{-1} were typical of an imine and conjugated carbonyl (Sulaiman et al., 2011). The presence of a methylenedioxy group was evident by its characteristic absorption at ν_{max} 1264 and 980 cm^{-1}, which also indicated asymmetric O-C-O stretching (Chang, Chang, Khalil, Hsieh, & Wu, 2003).

Analysis of the ^{1}H-NMR spectrum (Figure 3.16) revealed the characteristic of AB type doublet doublet, typical of an oxoaporphinic H-4 (δ_H 7.76, 1H, *d*, *J*=5.4 Hz) and H-5 (δ_H 8.87, 1H, *d*, *J*=5.4 Hz) coupling pattern (Mukhtar et al., 2009). A coupling constant of 5.4 Hz for H-4 and H-5 was small compared to the normal *cis* pattern coupling. This is due to the fact that H-5 is adjacent to a *N* atom and resonated more downfield at δ_H 8.87. A singlet peak was observed at δ_H 7.18, attributable to H-3 indicating that, C-1 and C-2 could be substituted by methylenedioxy group. This group displayed a characteristic singlet of two proton intensity at δ_H 6.13. Two other aromatic protons were resonated as

singlet at δ_H 8.67 and 7.99 corresponding to H-11 and H-8, respectively. H-11 has the highest chemical shift due to the deshielding effect caused by ring A and most probably forming the hydrogen bonding with the methylenedioxy group. Two distinct methoxyl signals appeared as singlet at δ_H 3.99 and 4.08 which were attached to C-9 and C-10, respectively. Due to the limitation of the sample amount, we were unable to get its ^{13}C NMR and 2D NMR spectrum including HMBC data.

Based on the available spectral data and extensive literature review (Wijeratne, Hatanaka, Kikuchi, Tezuka, & Gunatilaka, 1996), the structure of alkaloid **D** was deduced as dicentrinone **124**, which has previously been reported from *Ocotea macropoda* (Lauraceae) for the first time in 1971 (Cava & Venkateswarlu, 1971).

Table 3.5: ^1H NMR (400 MHz) spectroscopic assignments of alkaloid **D** in $CDCl_3$

Position	**δ_H (ppm, *J* in Hz)**	
	Alkaloid **D**	Dicentrinone **124** (Wijeratne et al., 1996) (400 MHz)
1	-	-
1a	-	-
1b	-	-
2	-	-
3	7.18 (1H, *s*)	7.16 (1H, *s*)
3a	-	-
4	7.76 (1H, *d*, *J*=5.4)	7.74 (1H, *d*, *J*=5.5)
5	8.87 (1H, *d*, *J*=5.4)	8.86 (1H, *d*, *J*=5.5)
6a	-	-
7	-	-
7a	-	-
8	7.99 (1H, *s*)	7.97 (1H, *s*)
9	-	-
10	-	-
11	8.67 (1H, *s*)	8.64 (1H, *s*)
11a	-	-
1, 2-OCH_2O	6.13 (2H, *s*)	6.13 (2H, *s*)
9-OCH_3	3.99 (3H, *s*)	3.99 (3H, *s*)
10-OCH_3	4.08 (3H, *s*)	4.08 (3H, *s*)

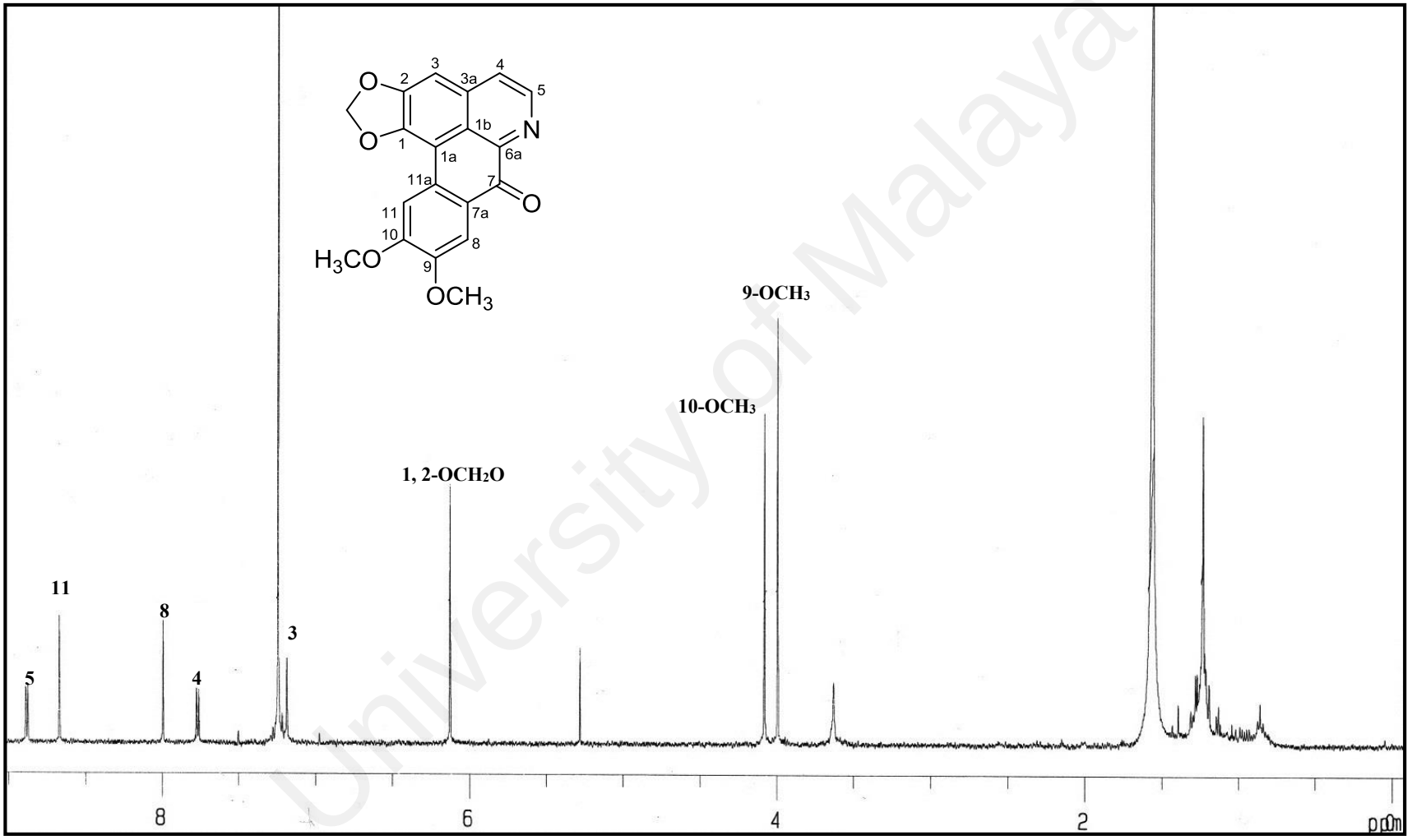

Figure 3.16: ^{1}H NMR spectrum of alkaloid **D**

3.2.5 Alkaloid E: (+)-Oridine 125

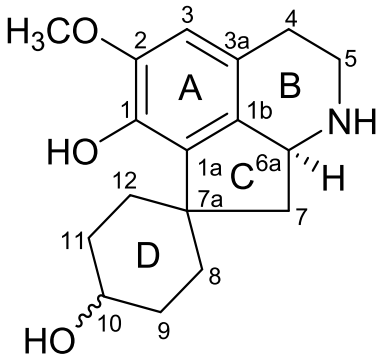

125

Alkaloid **E** was obtained as a brownish amorphous with $[\alpha]_D^{25}$ +30° (*c*=0.045, MeOH). Its empirical formula was determined as $C_{17}H_{23}NO_3$ by LCMS-IT-TOF $[M+H]^+$ *m/z* 290.1762 (calcd. for $C_{17}H_{24}NO_3$, 290.1751), corresponding with seven degrees of unsaturation. The UV spectrum showed absorption bands at λ_{max} 217, 228 and 286 nm while its IR spectrum revealed absorption peaks at ν_{max} 3408 and 3156 cm^{-1} which indicated the presence of hydroxyl (OH) and primary amine (NH) group, respectively.

The ^1H NMR spectrum (Figure 3.17) exhibited signals corresponding to one aromatic proton, one methoxyl group, two methine protons and seven methylene groups. Two singlets observed at δ_H 6.49 (1H) and 3.83 (3H), were assigned to H-3 and 2-O$\underline{CH_3}$ group, respectively. Furthermore, the methine H-6a and oxymethine H-10 appeared at δ_H 4.02 (1H, *m*) and 4.08 (1H, *brs*) respectively, while the methylene protons, H_2-4, H_2-5, H_2-7, H_2-8, H_2-9, H_2-11 and H_2-12 displayed a complex absorption pattern between δ_H 1.27-3.43. The placement of methoxyl group at C-2 was confirmed by the NOESY correlation (Figure 3.21) between H-3 and 2-OCH_3.

The ^{13}C NMR spectrum (Figure 3.18) and DEPT experiment (Figure 3.19) established the resonances of seventeen carbon signals, comprising one methyl, seven methylenes, three methines, and six quaternary carbons, consistent with the molecular formula and structure proposed for alkaloid **E**. The resonance of the quaternary spiro

carbon, C-7a, at δ_C 47.5 implied the proaporphinic nature of alkaloid **E** (Mukhtar et al., 2009). The carbon bearing the hydroxyl group, C-10 resonated at δ_C 65.8. The COSY experiment (Figure 3.20) showed all the correlations for vicinal protons; H-4/H-5, H-6a/H-7, H-8/H-9, H-10/H-9, H-10/H-11 and H-11/H-12, respectively. In the HMBC spectrum (Figure 3.23), correlation of H-7 to C-8 and C-12 can be observed, thus supporting the connectivity of ring C with ring D.

A full assignment of the ^{1}H and ^{13}C NMR was established by HSQC and HMBC correlation. By comparison of the observed data with the literature values (Veznik, Sedmera, Preininger, Simanek, & Slavik, 1981), alkaloid **E** was confirmed (+)-oridine **125** which has been previously isolated by Veznik et al., (1981) from *Papaver oreophilum* (Papaveraceae).

Table 3.6: ^{1}H NMR (400 MHz) and ^{13}C NMR (100 MHz) spectroscopic assignments of alkaloid **E** in $CDCl_3$

Position	δ_H (ppm, *J* in Hz)		δ_C (ppm)	
	Alkaloid **E**	(+)-Oridine **125** (Veznik et al., 1981) ($CDCl_3$+CD_3OD, 60 MHz)	Alkaloid **E**	(+)-Oridine **125** (Veznik et al., 1981) (DMSO-d_6, 15.036 MHz)
1	-	-	140.4	141.8
1a	-	-	134.6	136.2
1b	-	-	132.4	134.1
2	-	-	147.1	148.5
3	6.49 (1H, *s*)	6.49 (1H, *s*)	108.4	110.3
3a	-	-	122.1	122.4
4	α=2.72 (1H, *m*) β=2.61 (1H, *m*)	NR	25.9	27.4
5	α=3.43 (1H, *m*) β=3.11 (1H, *m*)	NR	45.0	45.6
6a	4.02 (1H, *m*)	NR	57.3	57.7
7	α=1.41 (1H, *m*) β=2.65 (1H, *m*)	NR	43.6	44.1
7a	-	NR	47.5	48.3
8	α=1.27 (1H, *m*) β=1.66 (1H, *m*)	NR	29.5	29.5
9	α=1.85 (1H, *m*) β=2.96 (1H, *m*)	NR	29.7	30.3
10	4.08 (1H, *brs*)	4.05 (1H, *m*)	65.8	64.3
11	1.79 (2H, *m*)	NR	30.6	30.8
12	α=1.46 (1H, *m*) β=2.16 (1H, *m*)	NR	26.9	26.8
2-OCH_3	3.83 (3H, *s*)	3.84 (3H, *s*)	56.5	57.3

*NR=none reported

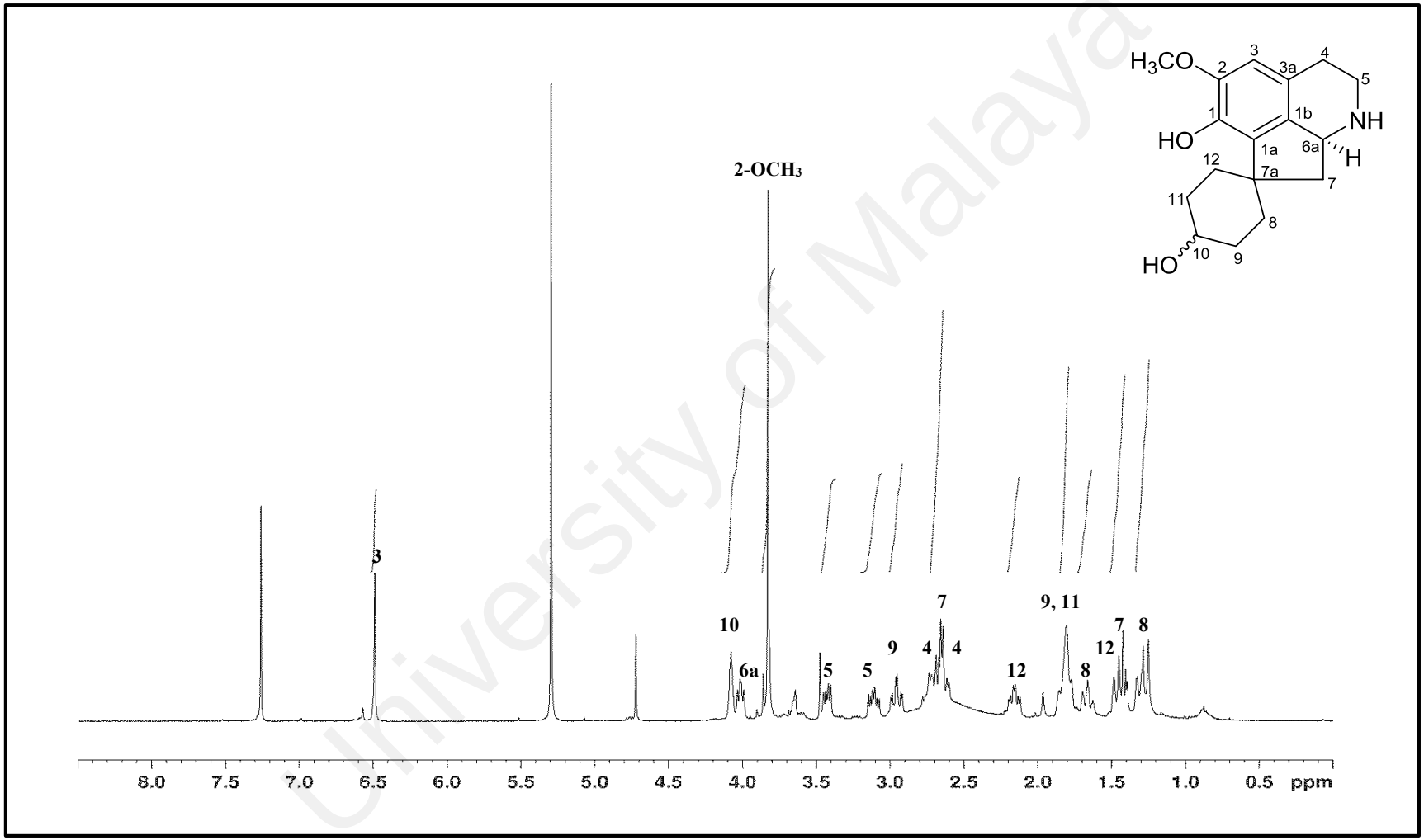

Figure 3.17: ^{1}H NMR spectrum of alkaloid **E**

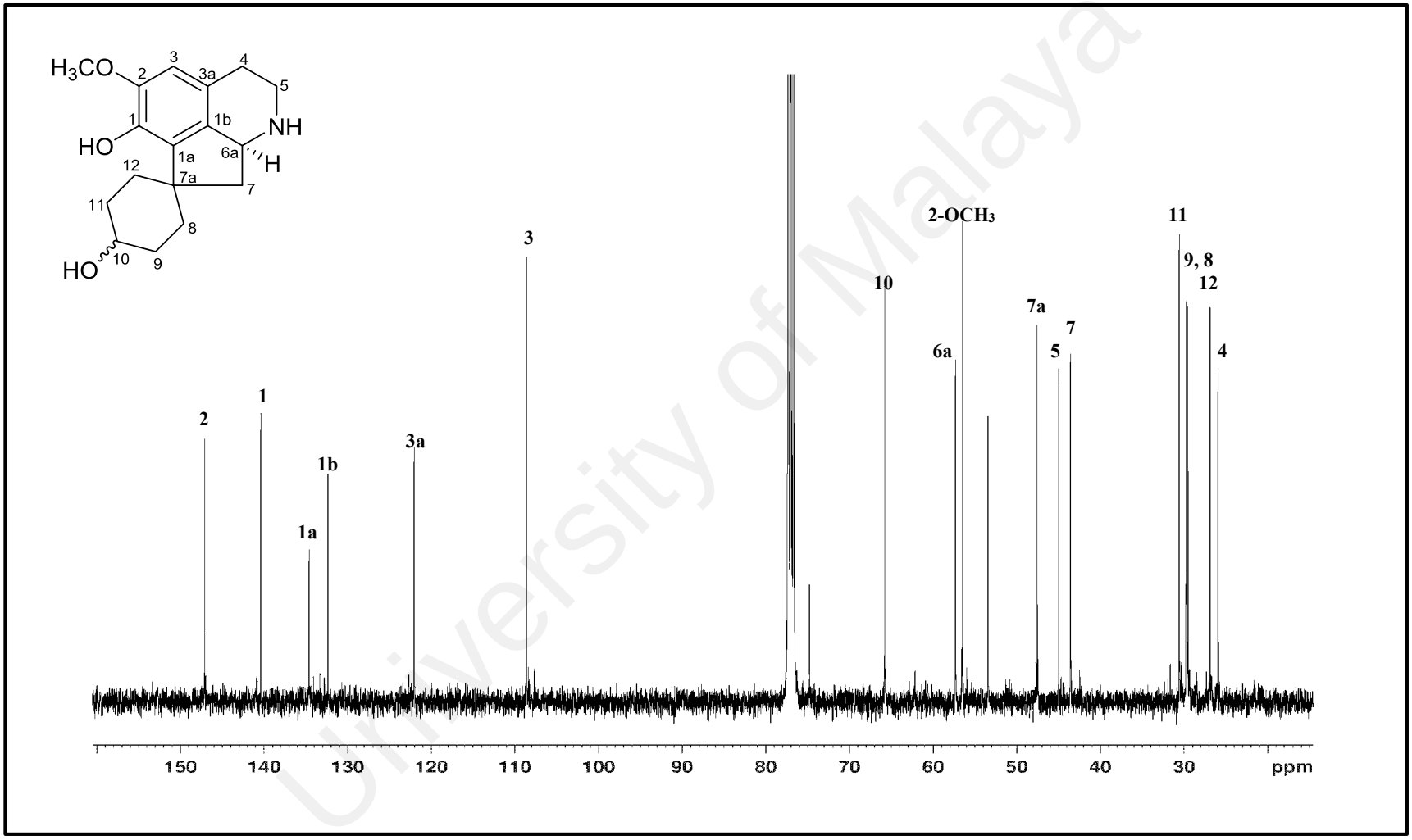

Figure 3.18: ^{13}C NMR spectrum of alkaloid **E**

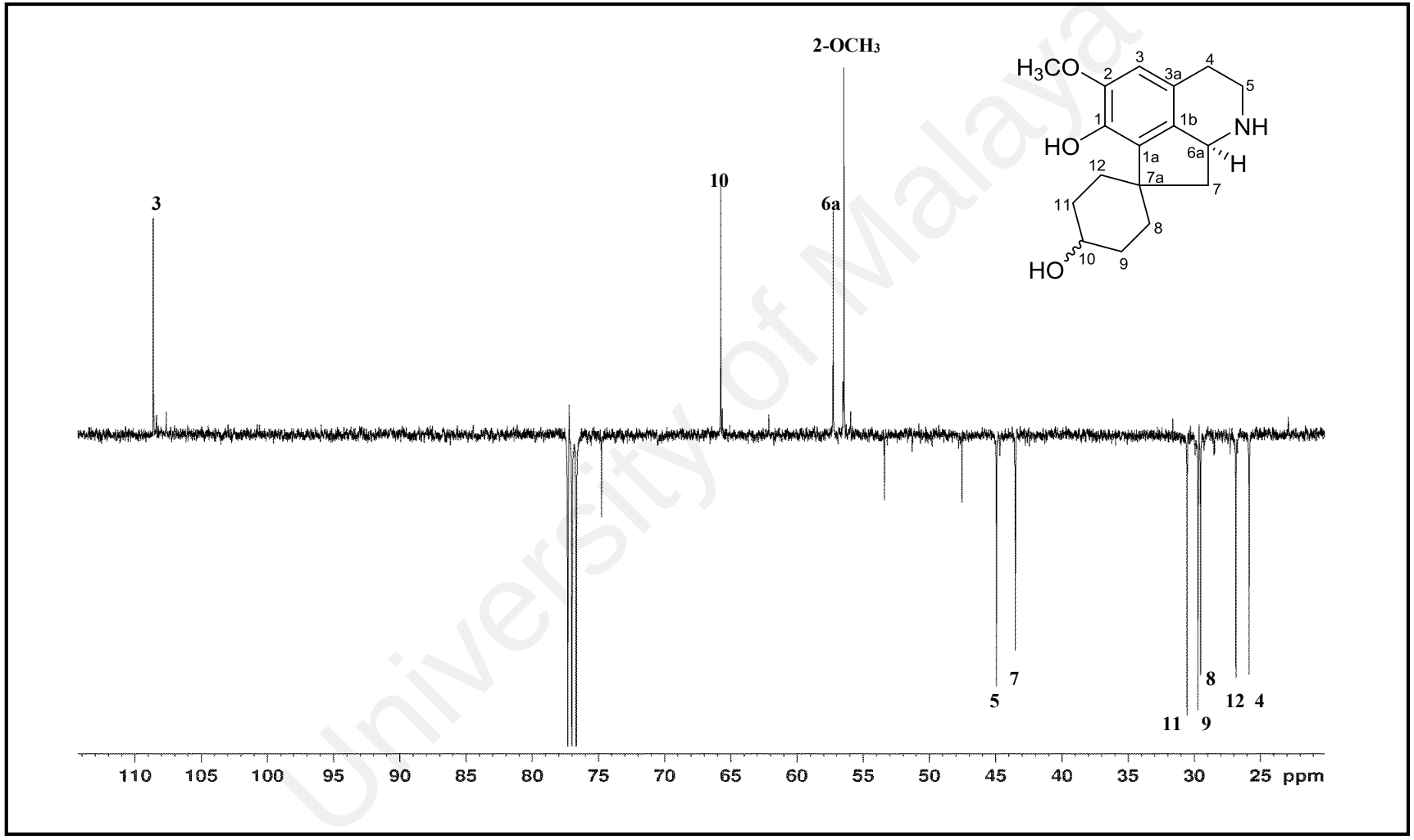

Figure 3.19: DEPT spectrum of alkaloid **E**

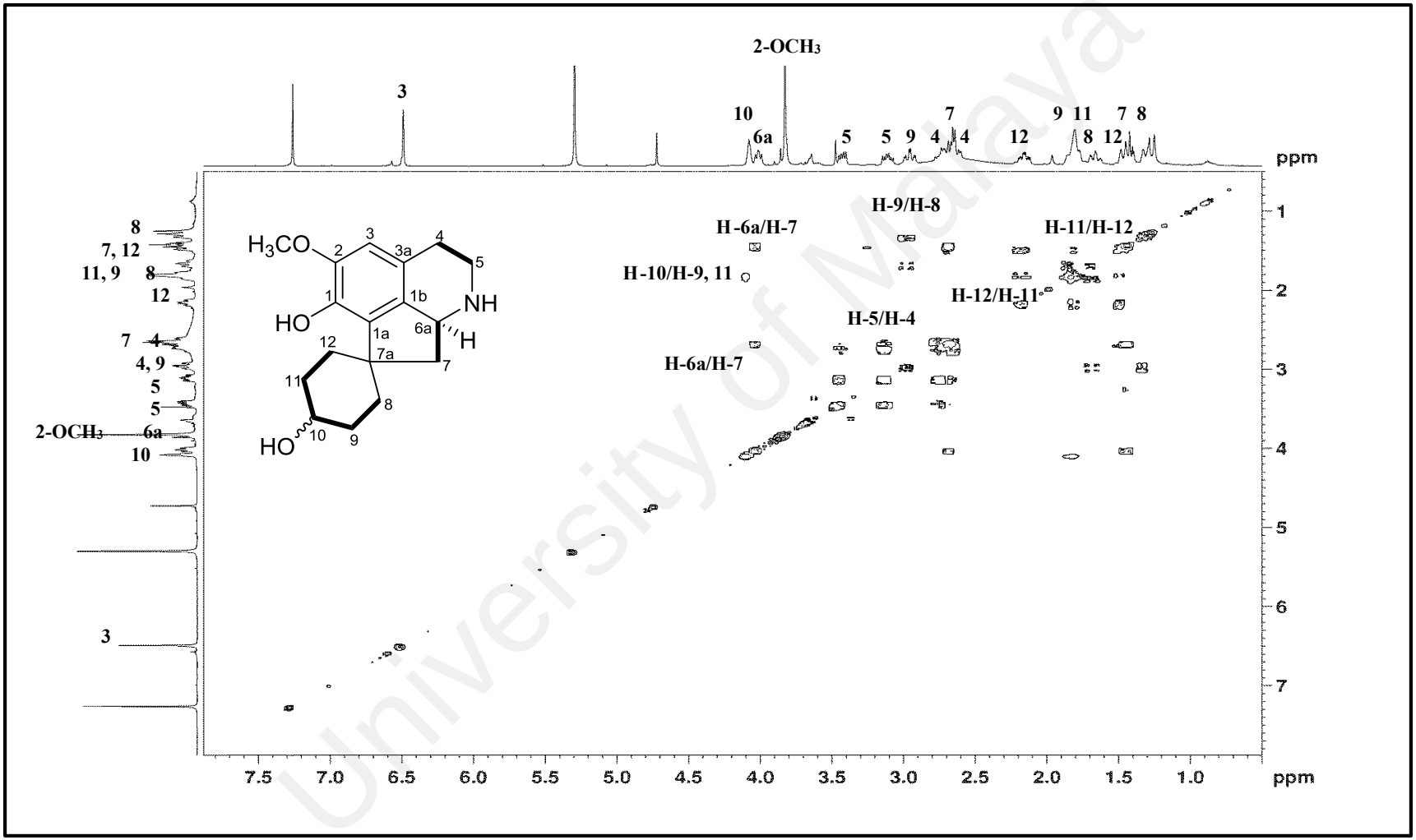

Figure 3.20: COSY spectrum of alkaloid **E**

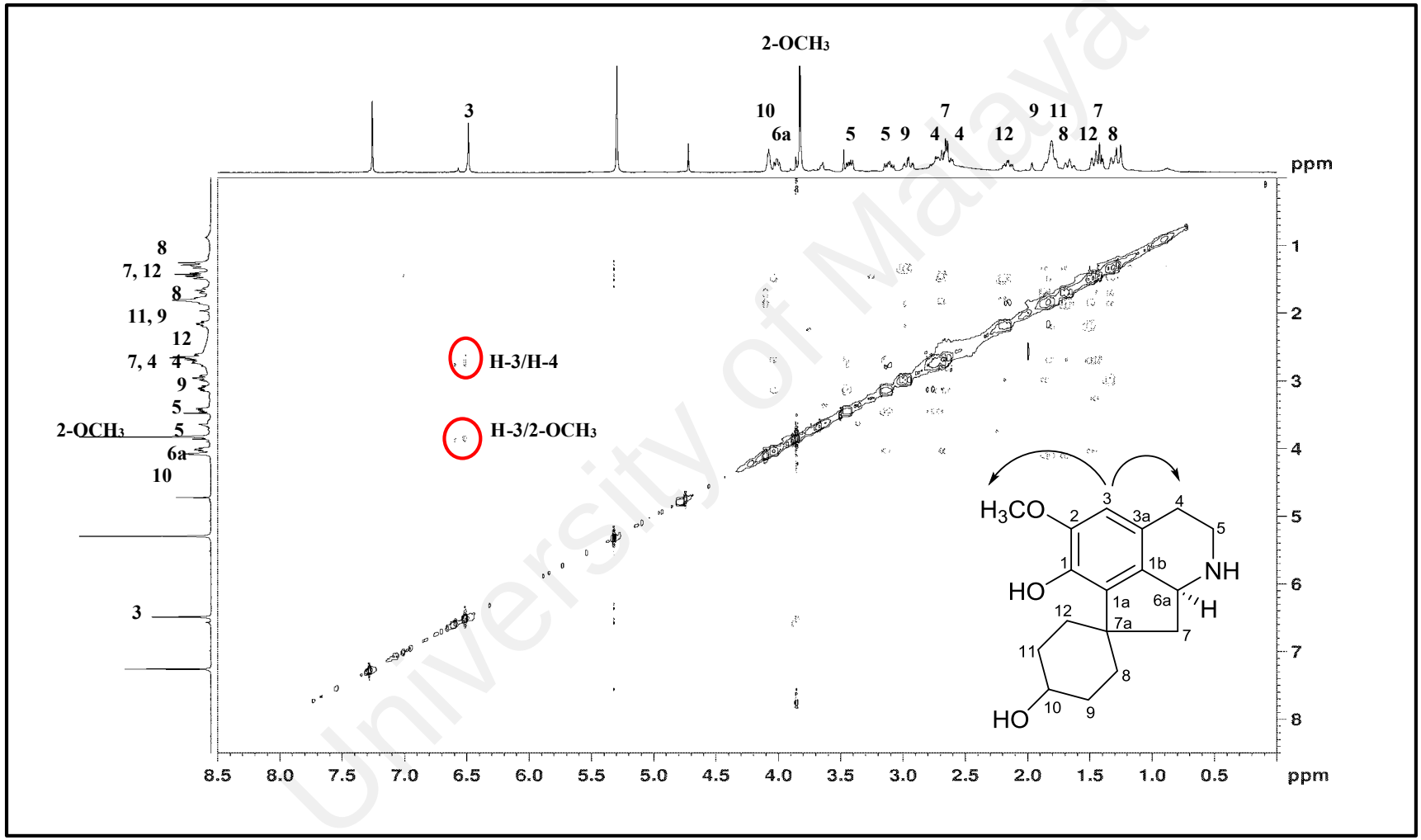

Figure 3.21: NOESY spectrum of alkaloid **E**

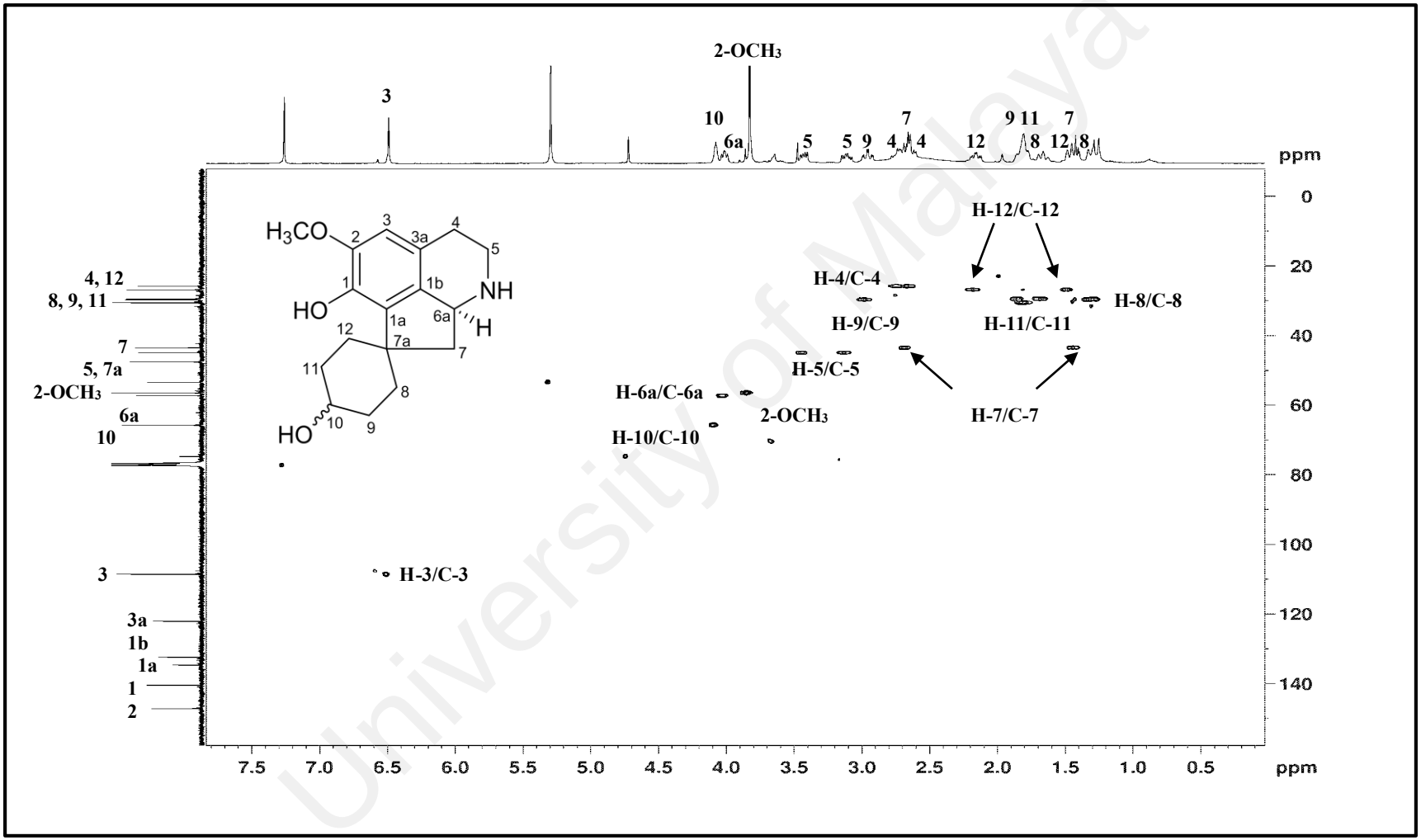

Figure 3.22: HSQC spectrum of alkaloid **E**

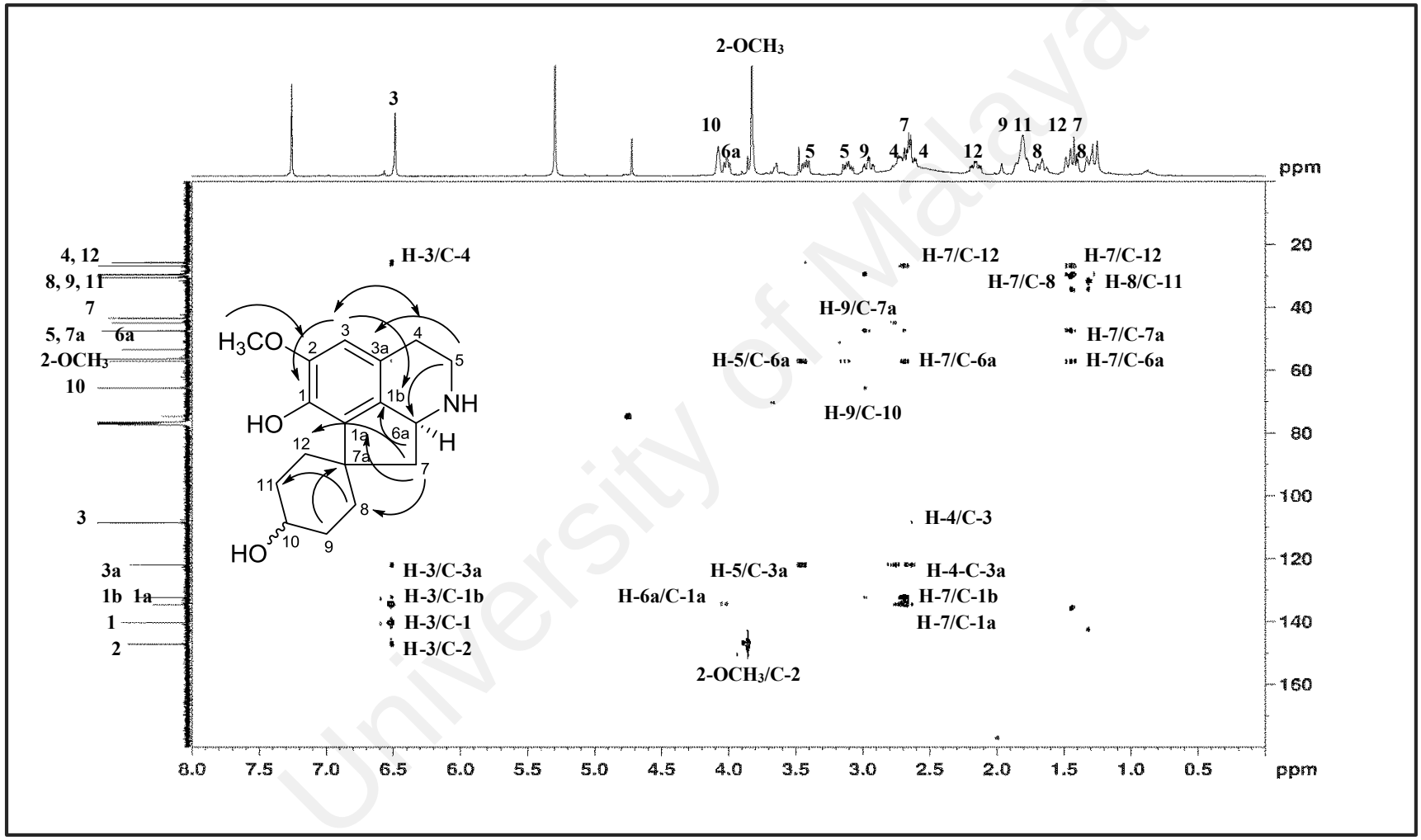

Figure 3.23: HMBC spectrum of alkaloid **E**

3.2.6 Alkaloid F: Prodensiflorin A 126

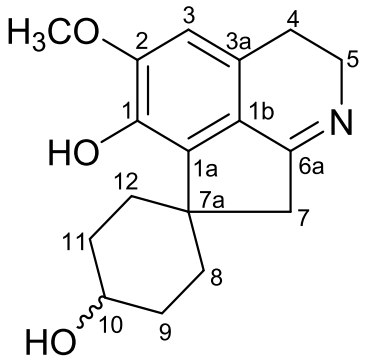

126

Alkaloid **F** was isolated as an optically inactive brownish amorphous. The positive LCMS-IT-TOF exhibited a pseudo-molecular ion peak, $[M+H]^+$ at *m/z* 288.1615 (calcd. for $C_{17}H_{22}NO_3$, 288.1594) that enabled a molecular formula of $C_{17}H_{21}NO_3$ to be proposed with eight degrees of unsaturation. The ^1H and ^{13}C NMR spectroscopic data (Table 3.7) of alkaloid **F** were comparable to those of alkaloid **E**, hence suggesting the possibility of alkaloid **F** being a proaporphine type alkaloid with a structure closely resembling that of alkaloid **E**. Nevertheless, an imine group was present in alkaloid **F** which was confirmed by the significant downfield shift (~120 ppm) in the carbon resonance at δ_C 172.6 (C-6a) and the absorption band at ν_{max} 1652 cm^{-1} in its ^{13}C NMR and IR spectra, respectively (Mahiou, Roblot, Fournet, & Hocquemiller, 2000). The absence of the H-6a multiplet at δ_H 4.02 along with the 115 ppm downfield shift in the resonance of the C-6a signal in the spectroscopic data of alkaloid **F** respective to the corresponding spectroscopic data of alkaloid **E**, unambiguously established the placement of the imine group in the molecule. Therefore, the additional degree of unsaturation in the proposed molecular formula of alkaloid **F** in relation to alkaloid **E** was attributed to the presence of the imine group in its skeleton. Based on this evidence, alkaloid **F** was an analogue of alkaloid **E** hence making it a new proaporphine alkaloid trivially named as prodensiflorin A, **126**.

Table 3.7: ^{1}H NMR (400 MHz), ^{13}C NMR (100MHz), COSY and HMBC spectroscopic assignments of alkaloid **F** in $CDCl_3$

Position	δ_H (ppm, *J* in Hz)	δ_C (ppm)	COSY	HMBC (H→C)
1	-	141.0	-	-
1a	-	137.9	-	-
1b	-	124.2	-	-
2	-	150.3	-	-
3	6.59 (1H, *s*)	108.2	-	1, 1b, 4
3a	-	125.0	-	-
4	2.66-2.68 (2H, *m*)	23.0	-	1b, 5
5	3.80-3.84 (2H, *t*, 7.8)	48.9	4	6a
6a	-	172.6	-	-
7	2.71-2.73 (2H, *m*)	43.7	-	1b, 6a, 8, 12
7a	-	45.9	-	-
8	1.31-1.35 (2H, *m*)	29.7	-	-
9	1.25-1.29 (2H, *m*)	29.4	-	11
10	4.16 (1H, *m*)	65.1	11	-
11	α=1.71 (1H, *m*) β=1.86 (1H, *m*)	30.0	-	-
12	2.64-2.65 (2H, *m*)	28.5	11	-
2-OCH_3	3.92 (3H, *s*)	56.6	-	2

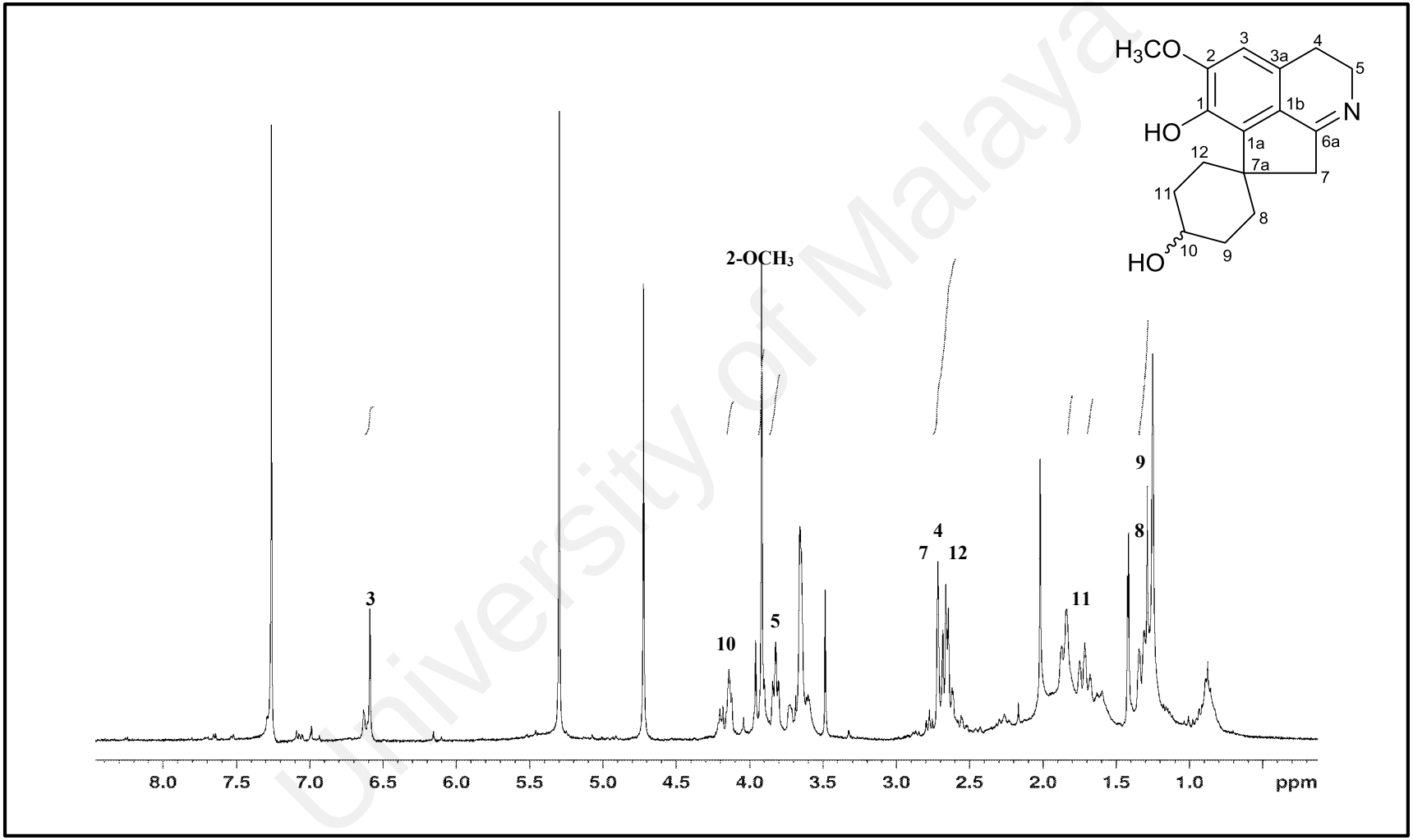

Figure 3.24: ^{1}H NMR spectrum of alkaloid **F**

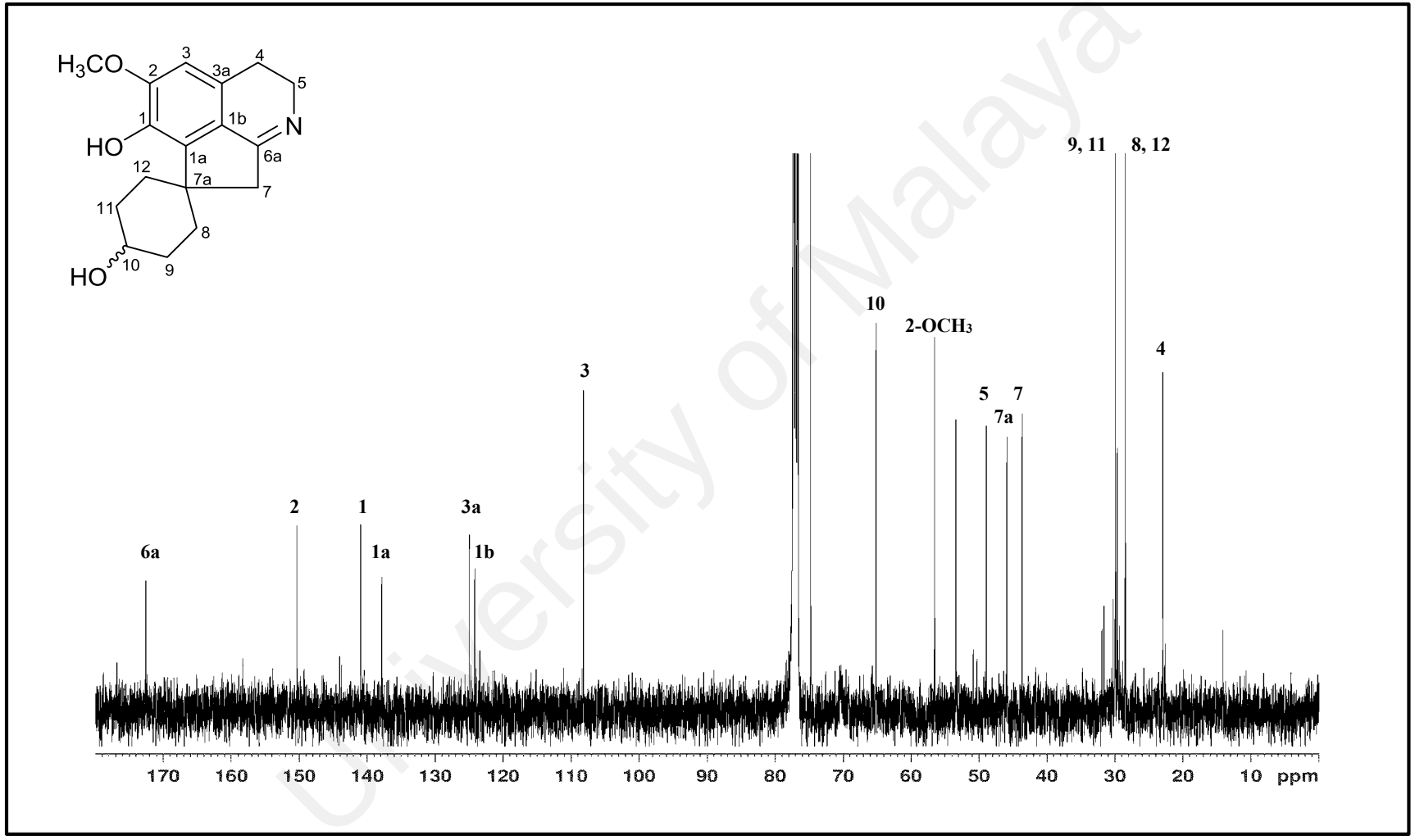

Figure 3.25: ^{13}C NMR spectrum of alkaloid **F**

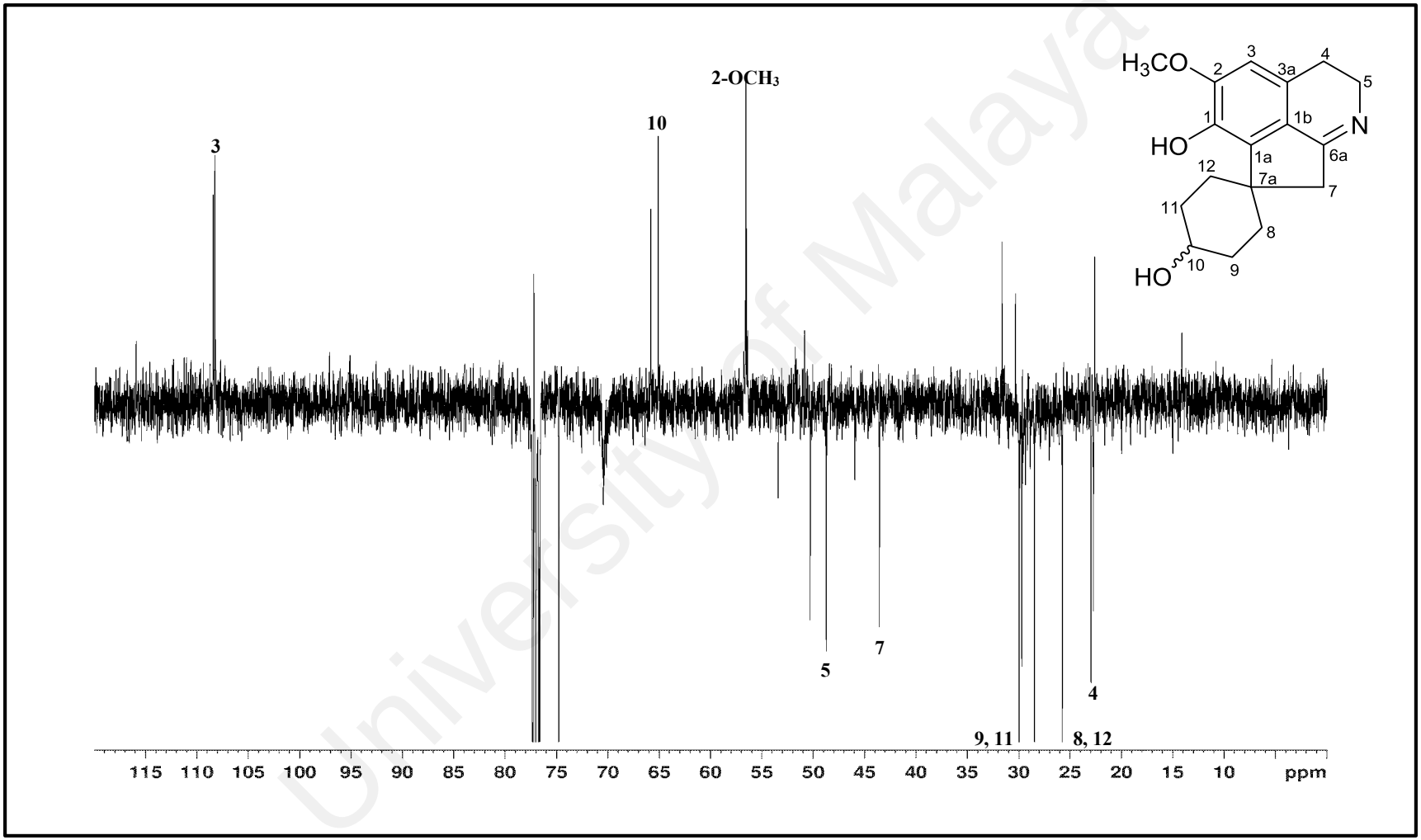

Figure 3.26: DEPT spectrum of alkaloid **F**

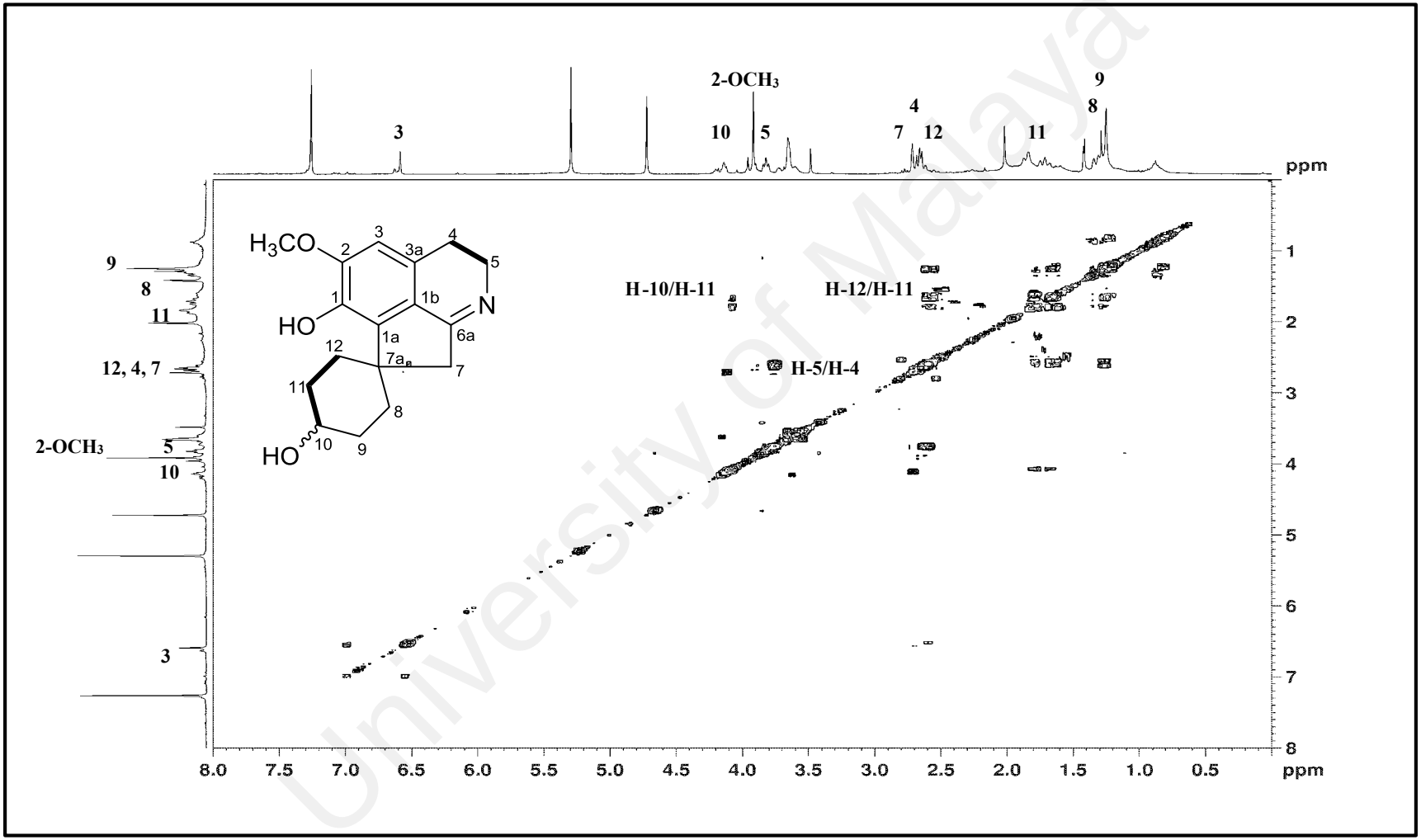

Figure 3.27: COSY spectrum of alkaloid **F**

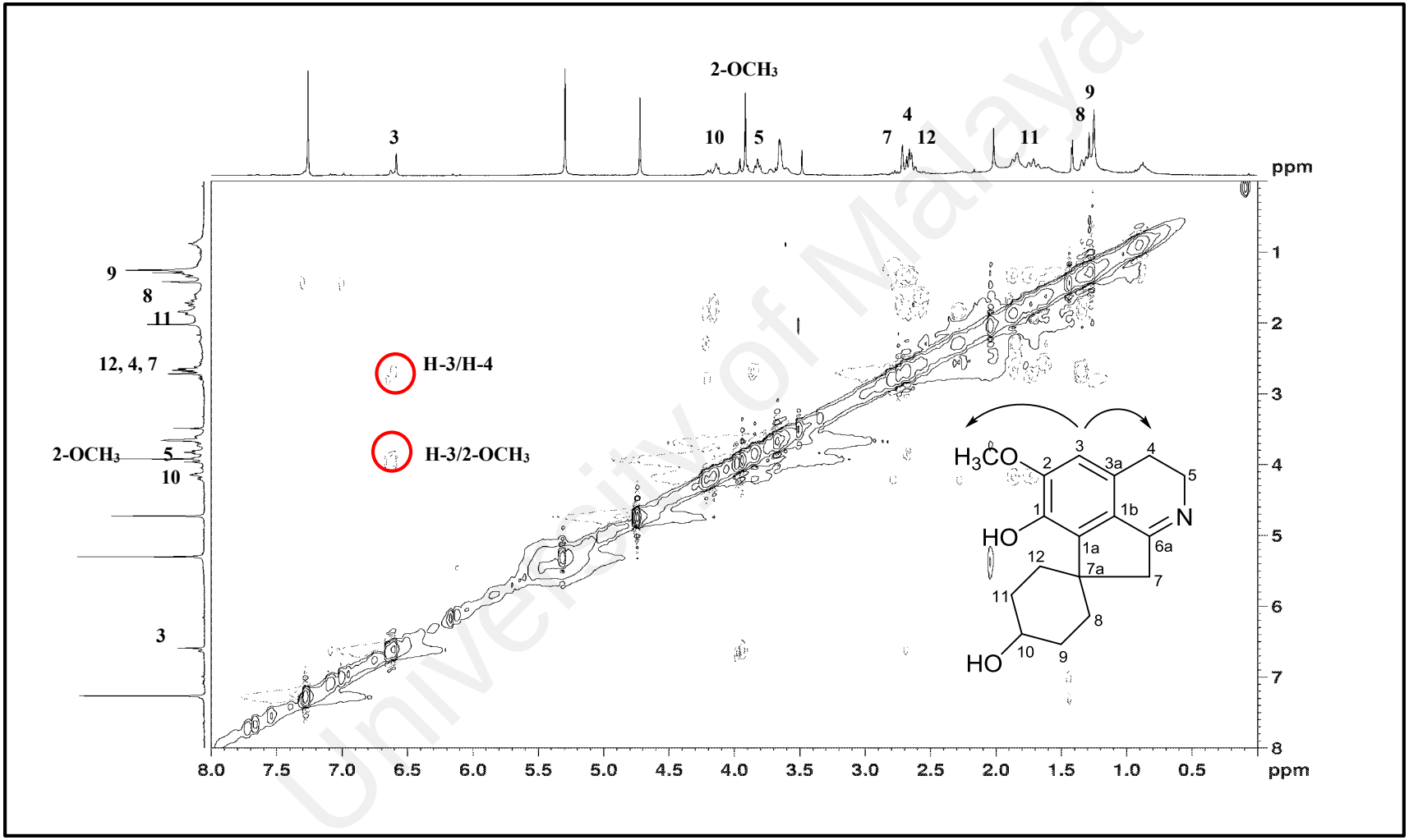

Figure 3.28: NOESY spectrum of alkaloid **F**

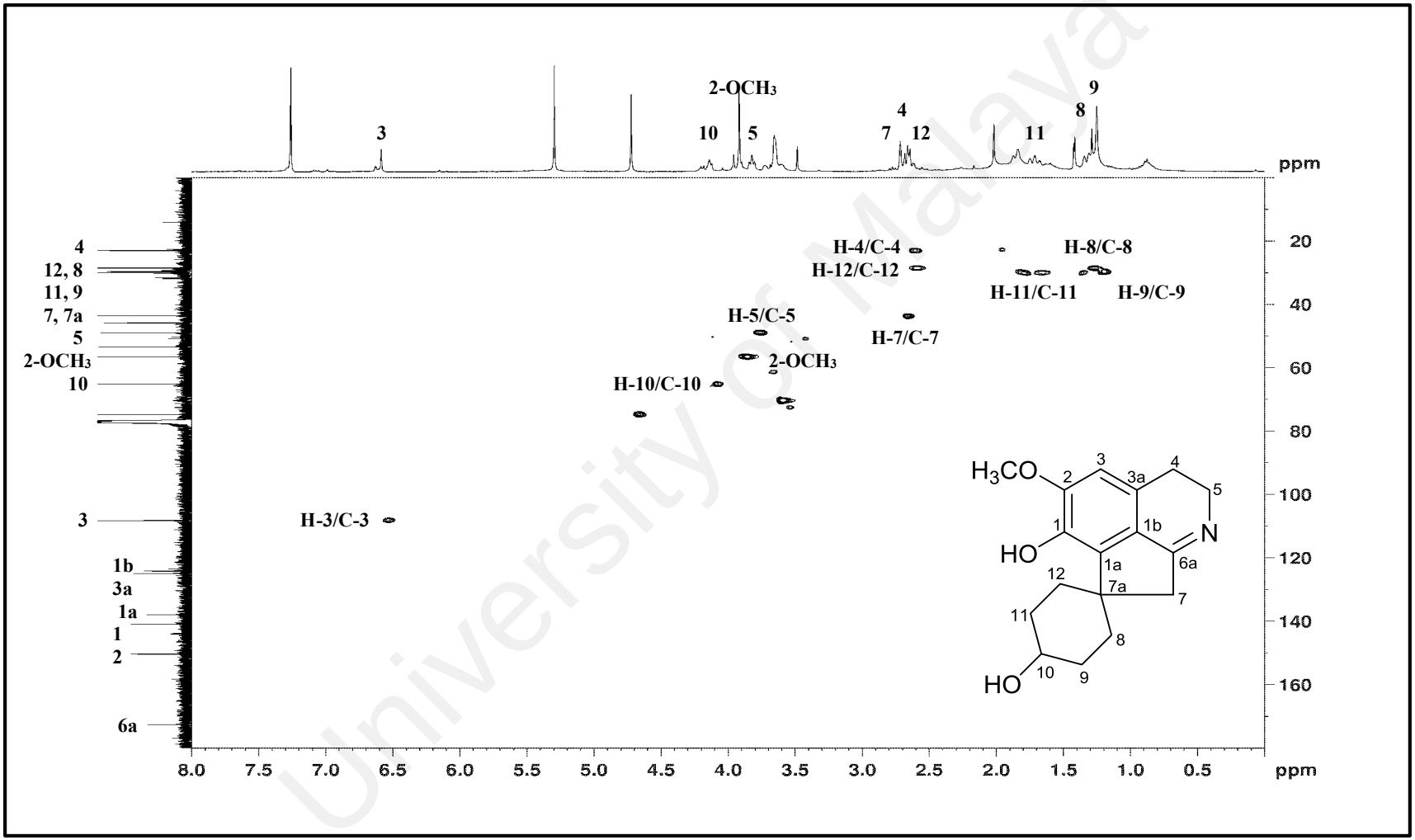

Figure 3.29: HSQC spectrum of alkaloid **F**

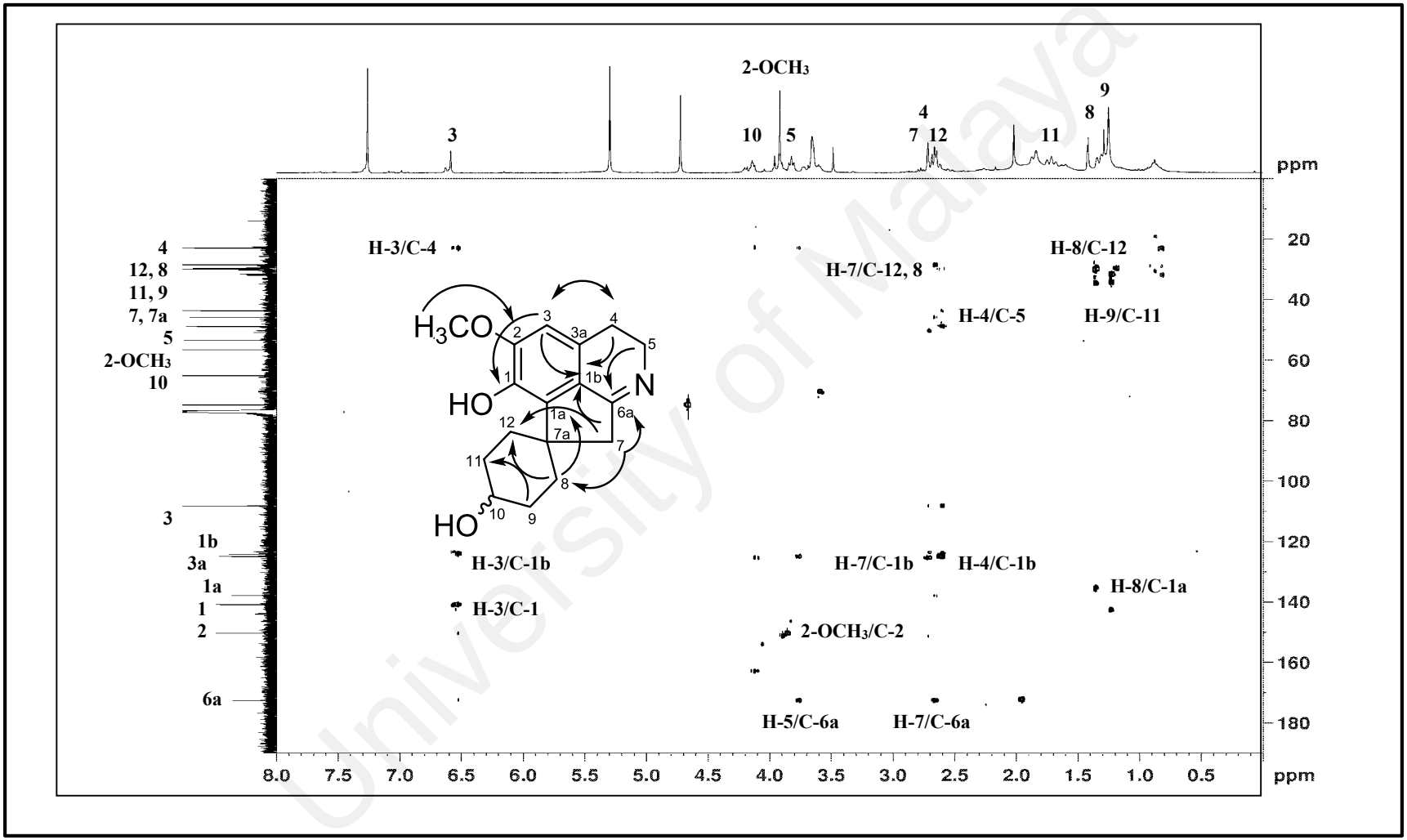

Figure 3.30: HMBC spectrum of alkaloid **F**

3.2.7 Alkaloid G: Prodensiflorin B 127

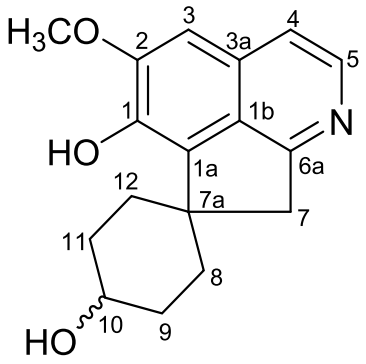

127

Alkaloid **G** was isolated as an optically inactive dark brownish amorphous. It was assigned a molecular formula of $C_{17}H_{19}NO_3$ as determined by its positive LCMS-IT-TOF {$[M+H]^+$, *m/z* 286.1503 (calcd. for $C_{17}H_{20}NO_3$ 286.1438)}, indicating nine degrees of unsaturation. The IR, UV and NMR spectroscopic data (Table 3.8) revealed close similarities with those of alkaloid **F**. However, the downfield shifts in the proton and carbon resonances of H-4 [(δ_H 7.25 *d*, *J*=5.9 Hz; δ_C 115.1 (C-4)] and H-5 [(δ_H 8.25 *d*, *J*=5.9 Hz; δ_C 143.1 (C-5)] upon comparison to the corresponding atoms in alkaloid **F** implied the presence of a double bond between these two carbon atoms, thus giving rise to the additional degree of saturation in the molecule. The position of the double bond was verified from the following HMBC cross peaks H-5/C-3a, C-6a and H-3/C-4 (Figure 3.37). Alkaloid **G**, an analogue of alkaloid **E**, was also determined to be a new proaporphine alkaloid and therefore named prodensiflorin B, **127**.

Table 3.8: ^{1}H NMR (400 MHz), ^{13}C NMR (100 MHz), COSY and HMBC spectroscopic assignments of alkaloid **G** in $CDCl_3$

Position	δ_H (*J* in Hz)	^{13}C (δ_C)	COSY	HMBC (H→C)
1	-	141.2	-	-
1a	-	134.1	-	-
1b	-	127.7	-	-
2	-	153.3	-	-
3	6.94 (1H, *s*)	100.8	-	1, 2, 1b, 4
3a	-	128.9	-	-
4	7.25 (1H, *d*, *J*=5.9)	115.1	5	1b, 3, 5
5	8.25 (1H, *d*, *J*=5.9)	143.1	-	3a, 4, 6a
6a	-	166.3	-	-
7	3.33 (2H, *s*)	44.3	-	1a, 1b, 6a, 7a, 8, 12
7a	-	46.7	-	-
8	α=1.45 (1H, *m*) β=2.76 (1H, *m*)	28.5	9	1a, 7, 9
9	α=1.27 (1H, *m*) β=1.87 (1H, *m*)	29.8	10	-
10	4.21 (1H, *brs*)	65.2	11	-
11	α=1.27 (1H, *m*) β=1.87 (1H, *m*)	29.8	12	-
12	α=1.45 (1H, *m*) β=2.76 (1H, *m*)	28.5	-	1a, 7, 11
2-OCH_3	4.04 (3H, *s*)	56.5	-	2

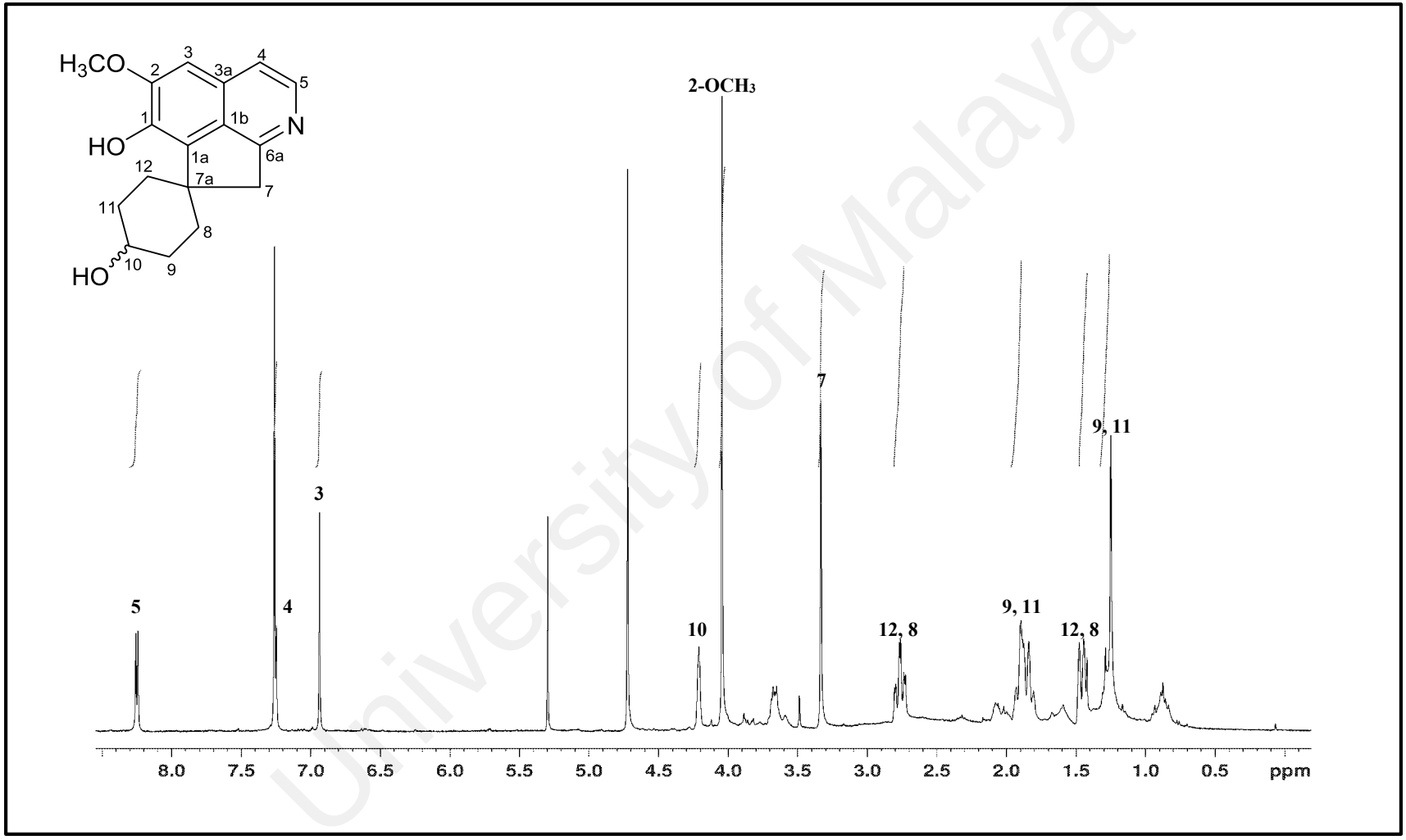

Figure 3.31: ^{1}H NMR spectrum of alkaloid **G**

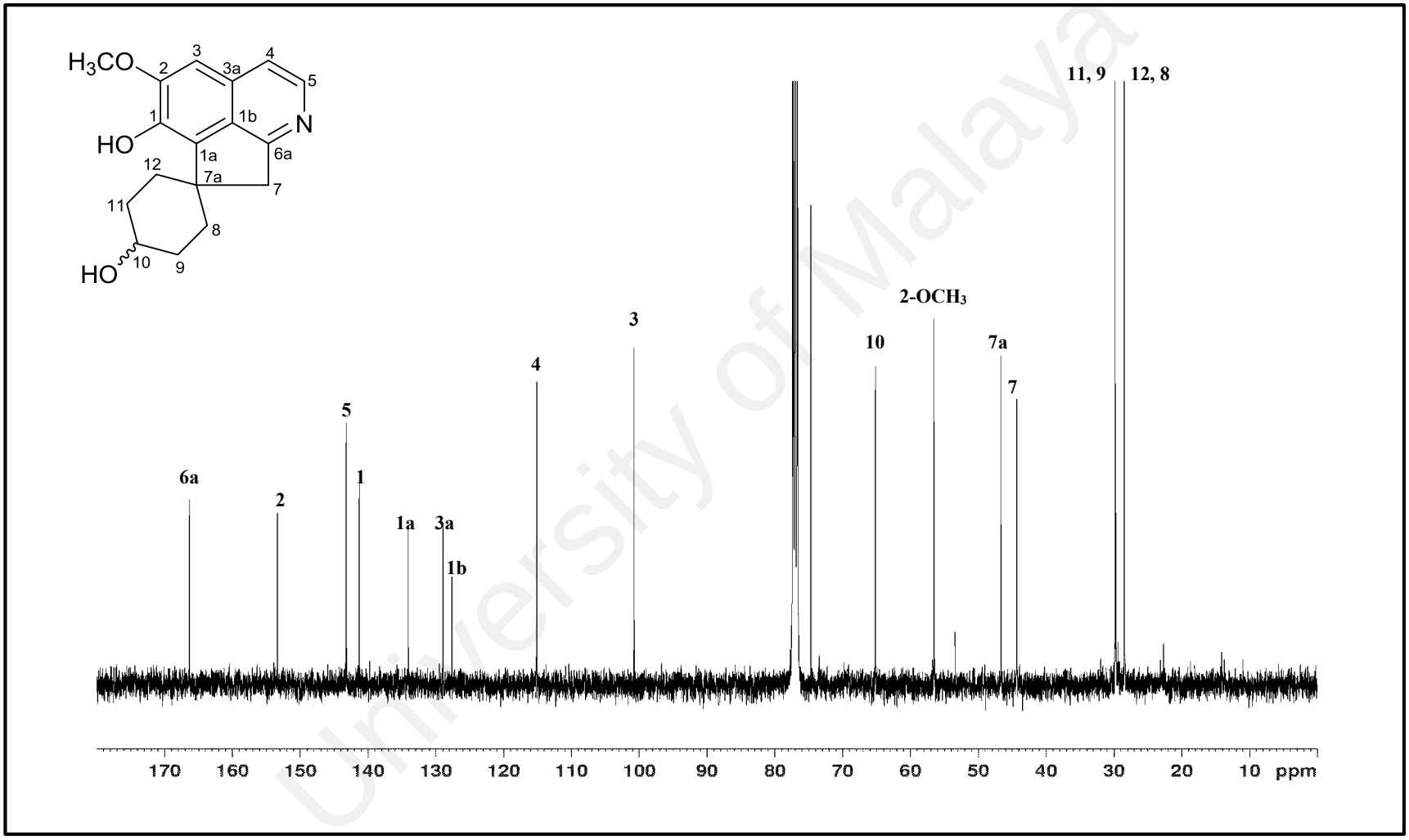

Figure 3.32: ^{13}C NMR spectrum of alkaloid **G**

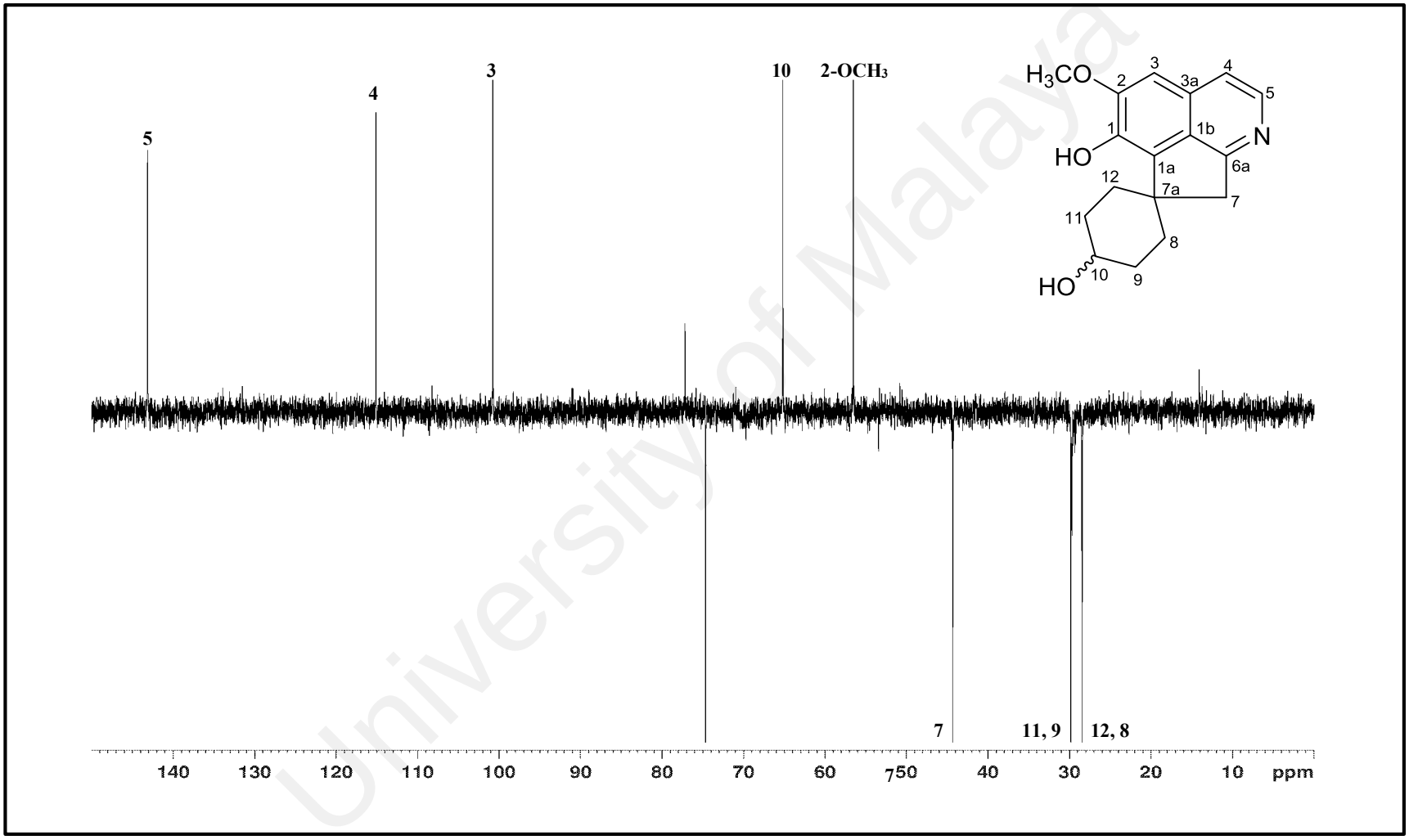

Figure 3.33: DEPT spectrum of alkaloid **G**

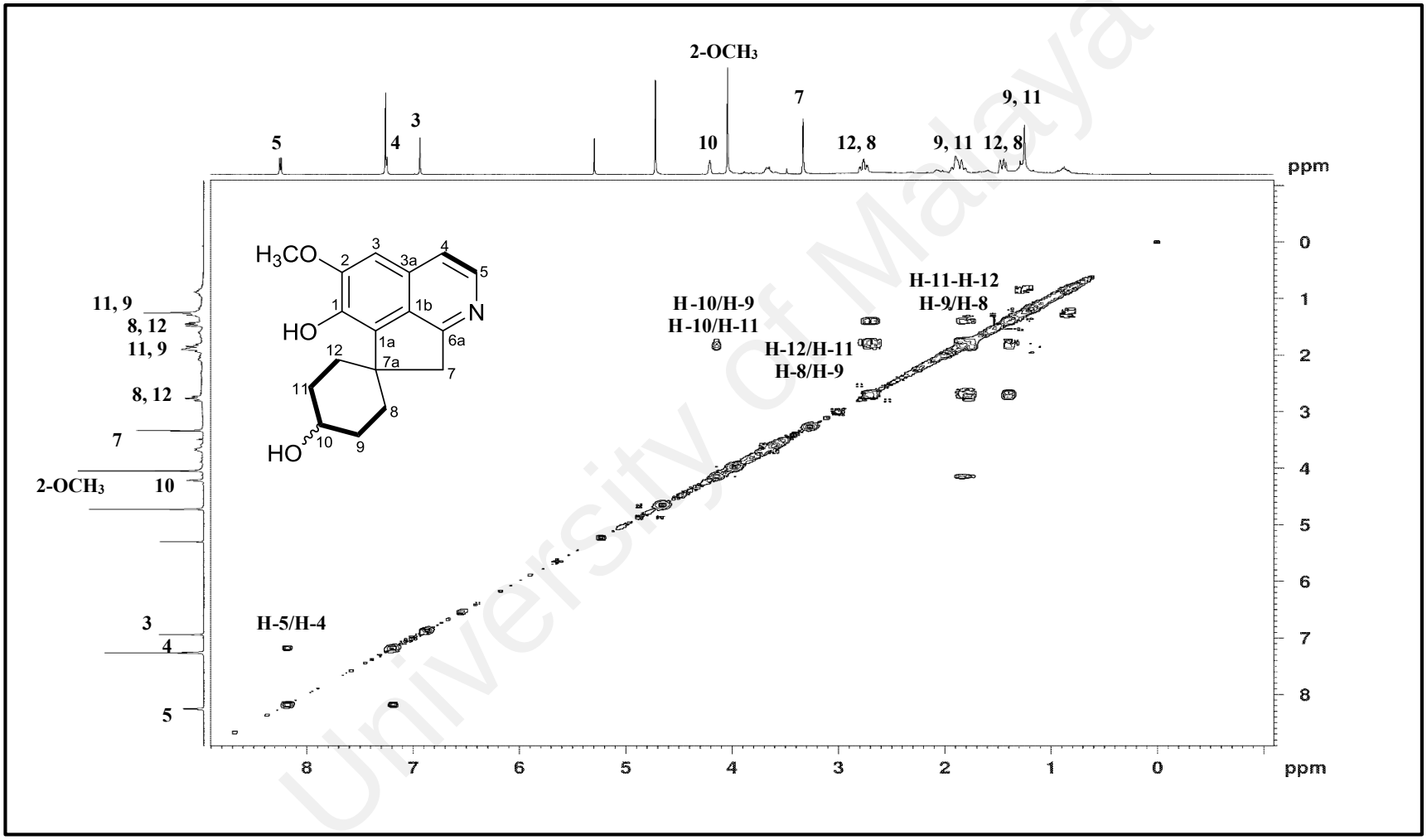

Figure 3.34: COSY spectrum of alkaloid **G**

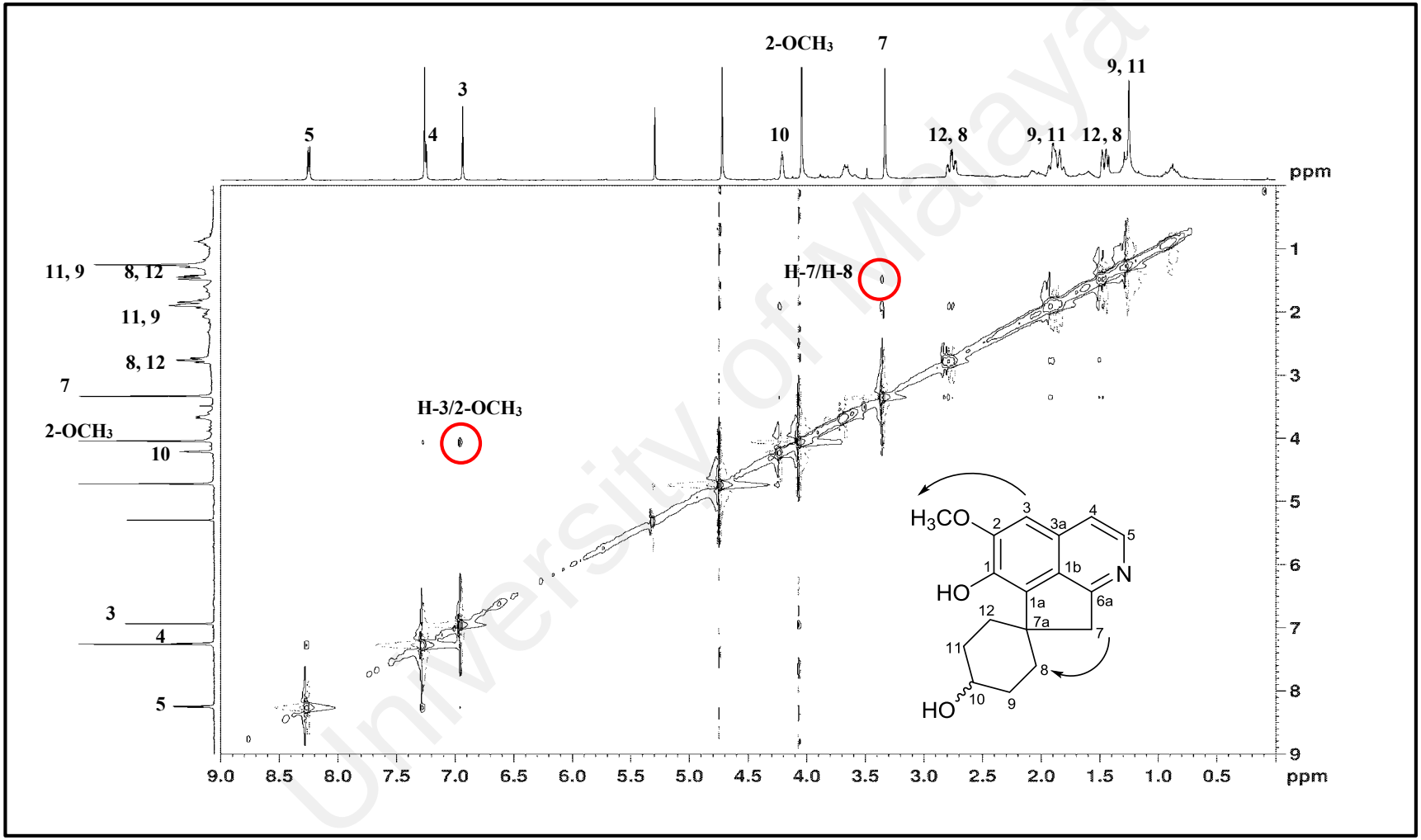

Figure 3.35: NOESY spectrum of alkaloid **G**

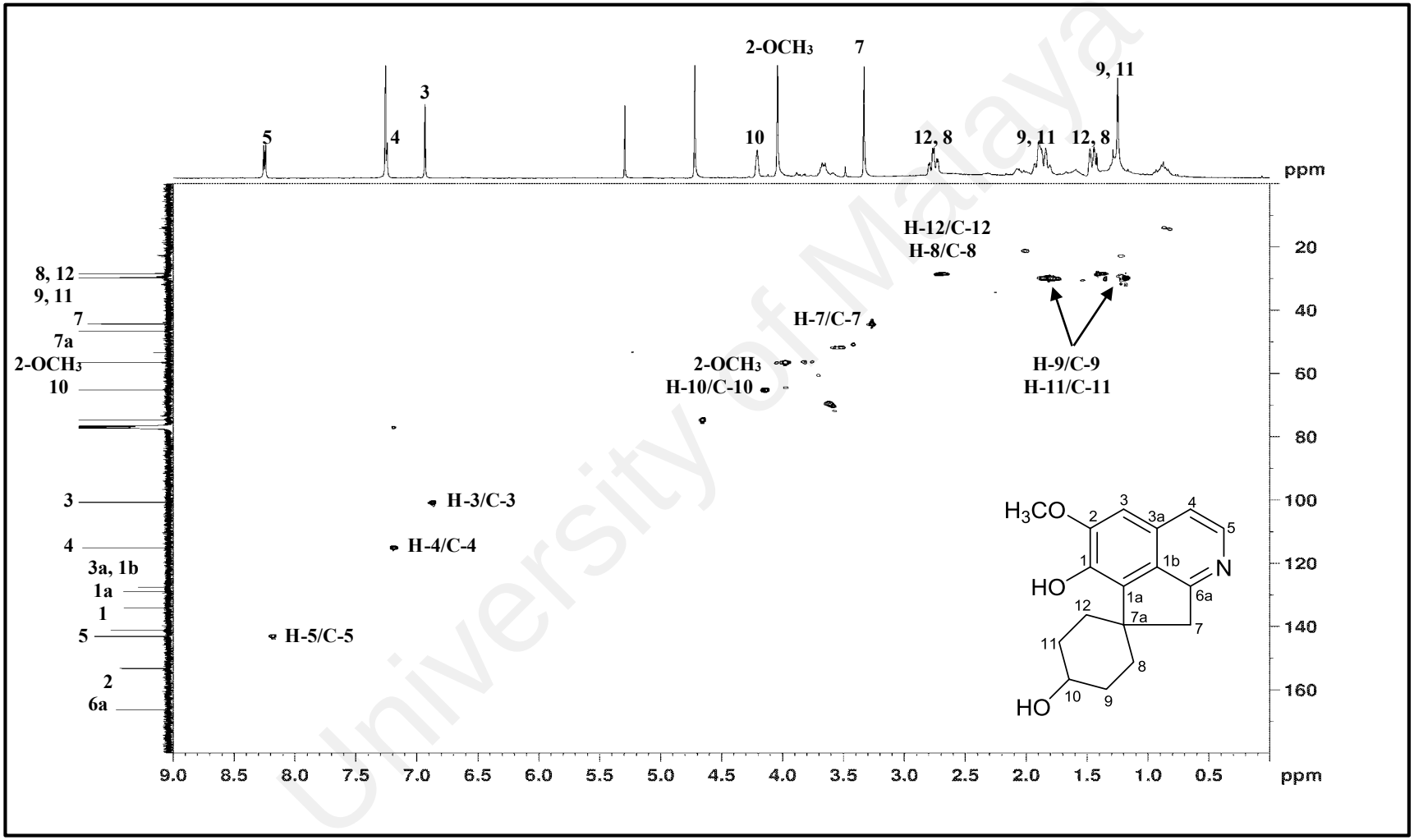

Figure 3.36: HSQC spectrum of alkaloid **G**

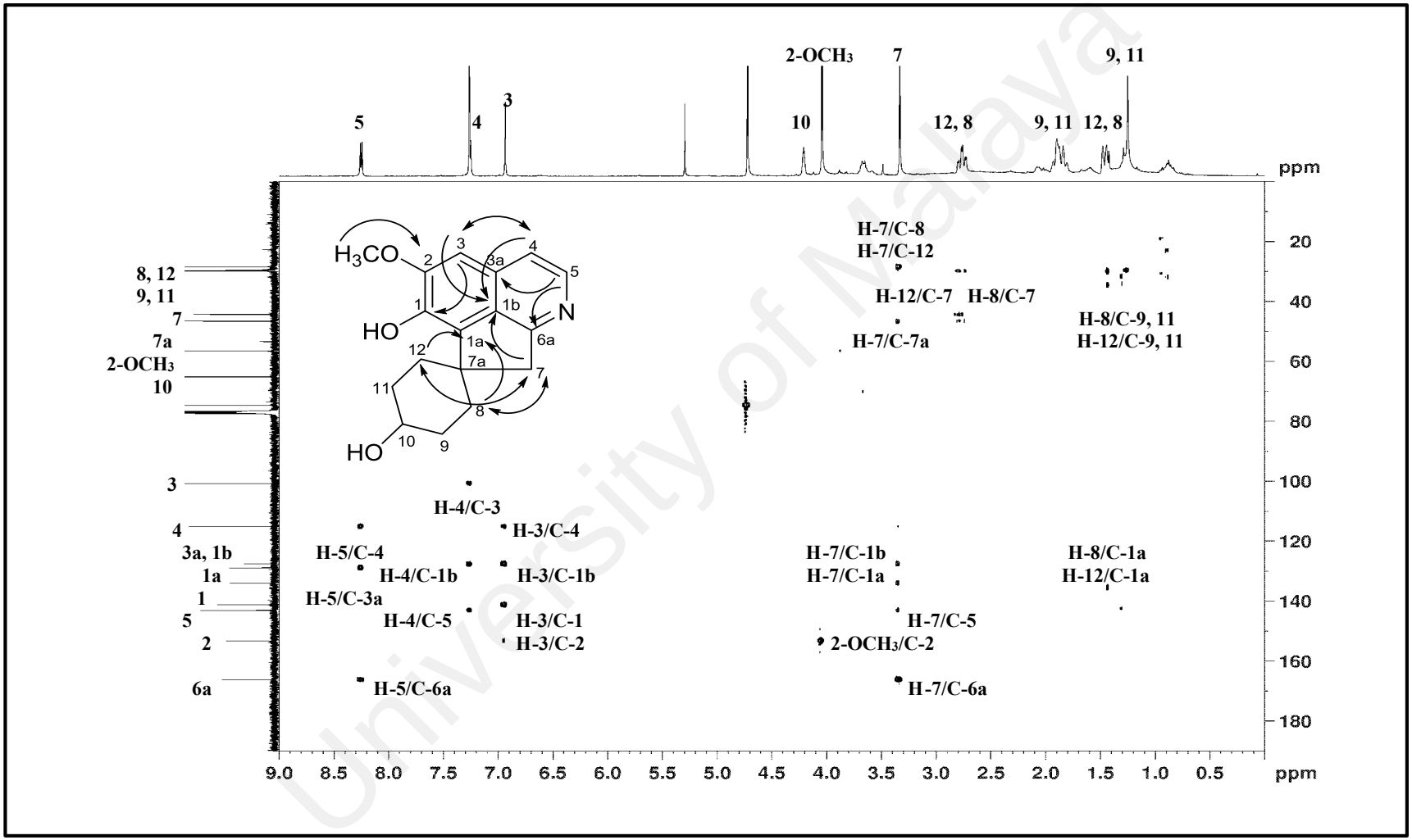

Figure 3.37: HMBC spectrum of alkaloid **G**

3.2.8 Alkaloid H: (-)-Antofine 6

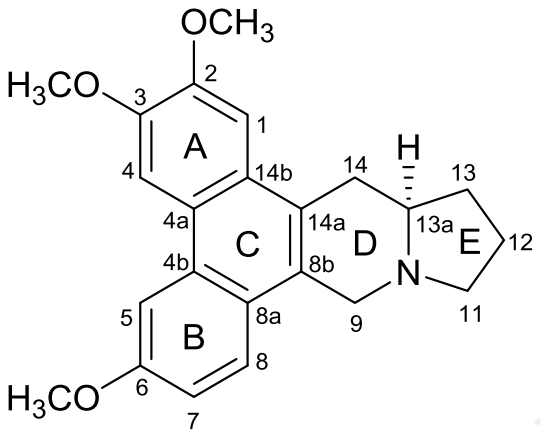

6

Alkaloid **H** was isolated as a brownish amorphous with $[\alpha]_D^{25}$ –15° (*c*=0.02, MeOH). The LCMS-IT-TOF spectrum showed an intense pseudomolecular ion peak, $[M+H]^+$ at *m/z* 364.1927 (calcd. for $C_{23}H_{26}NO_3$, 364.1907), in accordance with the molecular formula of $C_{23}H_{25}NO_3$. In the UV spectrum, absorption maxima were observed at λ_{max} 257, 284, 310 and 340 nm and were similar to those of phenanthroindolizidine skeleton (Damu et al., 2009). The IR spectrum revealed an absorption band due to CH aromatic (ν_{max} 1529 and 1512 cm^{-1}).

The ^1H NMR spectrum (Figure 3.38) exhibited two singlets for aromatic protons at δ_H 7.31 and 7.91 corresponding to H-1 and H-4, respectively. In addition, an ABX type spin system was observed in the ring B with resonances at δ_H 7.90 (1H, *d*, *J*=2.4 Hz, H-5), 7.20 (1H, *dd*, *J*=9.0, 2.4 Hz, H-7) and 7.81 (1H, *d*, *J*=9.0 Hz, H-8). Furthermore, three distinct methoxyl signals appeared at δ_H 4.06, 4.10 and 4.01 which were most probably positioned at C-2, C-3 and, C-6 respectively. The remaining aliphatic protons, H_2-9, H_2-11, H_2-12, H_2-13, H-13a and H_2-14 were observed in the range of δ_H 1.76-4.69. In the COSY spectrum (Figure 3.41), H-8 signal showed correlation with H-7 while H-14 signal showed a correlation with H-13a.

The ^{13}C NMR spectrum (Figure 3.39) showed the presence of twenty-three carbon signals, and the DEPT spectrum (Figure 3.40) indicated that six methines, five methylenes, three methyls and nine quaternary carbons were present. These characteristics of the NMR spectra and other physical data coincided well with the previous report by (Stærk et al., 2002) and the compound isolated was identified as a phenanthroindolizidine alkaloid type, (-)-antofine **6**, which has been previously isolated from *Ficus septica* Burm. F. (Moraceae) (Baumgartner, Erdelmeier, Wright, Rali, & Sticher, 1990).

Table 3.9: ^{1}H NMR (400 MHz) and ^{13}C NMR (100 MHz) spectroscopic assignments of alkaloid **H** in $CDCl_3$

Position	δ_H (ppm, *J* in Hz)		δ_C (ppm)	
	Alkaloid **H**	(-)-Antofine **6** (Stærk et al., 2002) ($CDCl_3$, 300 MHz)	Alkaloid **H**	(-)-Antofine **6** (Stærk et al., 2002) ($CDCl_3$,100 MHz)
1	7.31 (1H, *s*)	7.31 (1H, *s*)	103.9	104.1
2	-	-	149.4	149.6
3	-	-	148.4	148.6
4	7.91 (1H, *s*)	7.91 (1H, *s*)	103.8	103.9
4a	-	-	123.5	123.7
4b	-	-	130.1	130.4
5	7.90 (1H, *d*, *J*=2.4)	7.90 (1H, *d*, *J*=2.6)	104.7	104.8
6	-	-	157.5	157.8
7	7.20 (1H, *dd*, *J*=9.0, 2.4)	7.21 (1H, *dd, J*=9.1, 2.6)	114.8	115.1
8	7.81 (1H, *d*, *J*=9.0)	7.83 (1H, *d*, *J*=9.1)	124.2	124.5
8a	-	-	124.1	124.3
8b	-	-	126.6	126.7
9	α=3.70 (1H, *d*, *J*=14.9) β=4.69 (1H, *d*, *J*=14.9)	α=3.72 (1H, *d*, *J*=15.1) β=4.74 (1H, *d*, *J*=15.1)	53.8	53.8
11	2.47 (2H, *m*)	α=2.51 (1H, *q*, *J*=8.7) β=3.47 (1H, *dt*, *J*=8.7, 2.0)	54.9	55.1
12	α=1.90 (1H, *m*) β=1.99 (1H, *m*)	α=1.93 (1H, *m*) β=2.03 (1H, *m*)	21.5	21.6
13	α=1.76 (1H, *m*) β=2.24 (1H, *m*)	α=1.80 (1H, *m*) β=2.25 (1H, *m*)	31.1	31.3
13a	2.90 (1H, *m*)	2.53 (1H, *m*)	60.2	60.4
14	α=3.35 (1H, *m*) β=3.46 (1H, *m*)	α=2.92 (1H, *dd*, *J*=15.6, 10.5) β=3.35 (1H, *ddd, J*=15.6, 3.8, 1.4)	33.4	33.6
14a	-	-	125.4	125.7
14b	-	-	126.9	127.2
2-OCH_3	4.06 (3H, *s*)	4.07 (3H, *s*)	55.8	56.0
3-OCH_3	4.10 (3H, *s*)	4.11 (3H, *s*)	56.0	56.1
6-OCH_3	4.01 (3H, *s*)	4.02 (3H, *s*)	55.5	55.1

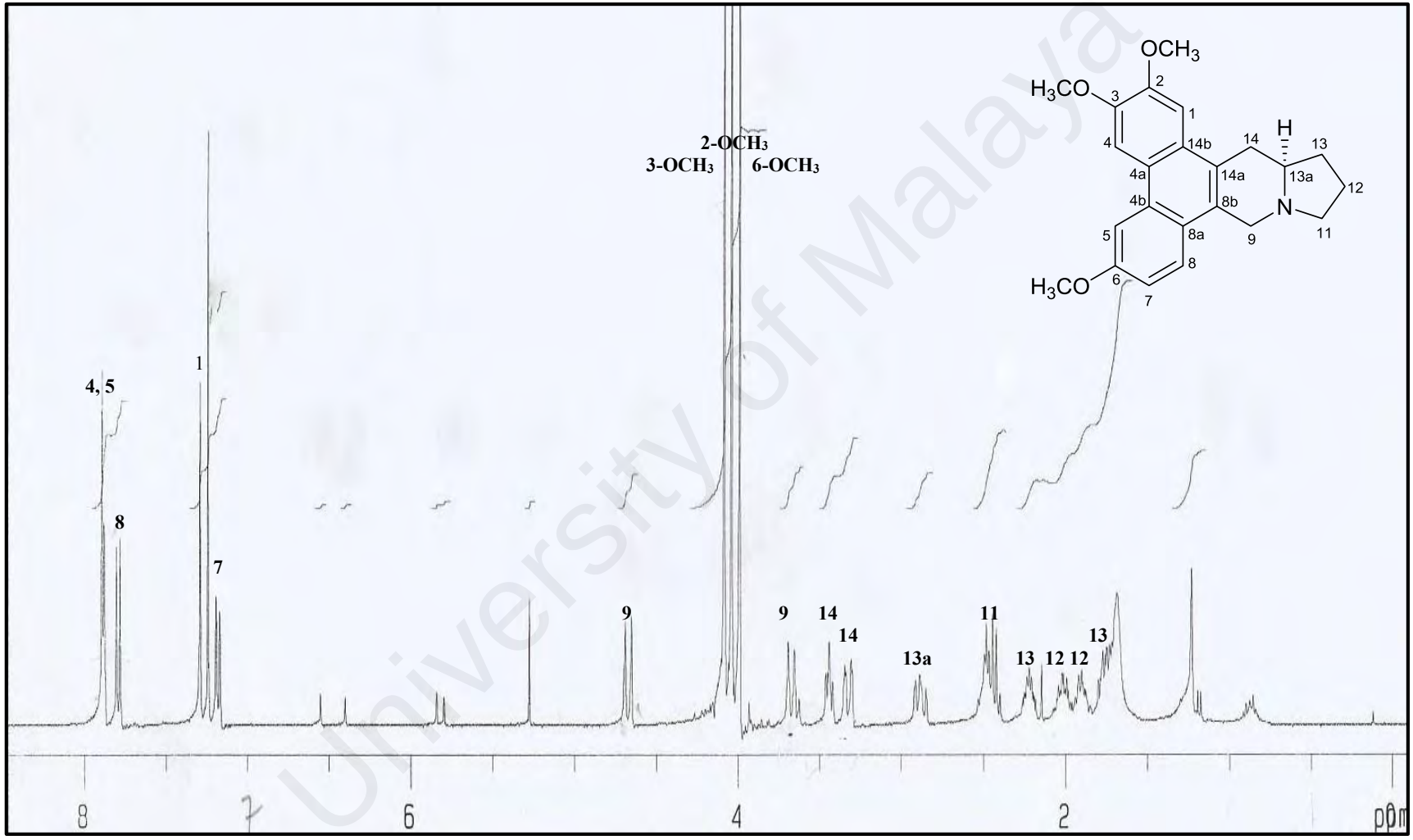

Figure 3.38: ^{1}H NMR spectrum of alkaloid **H**

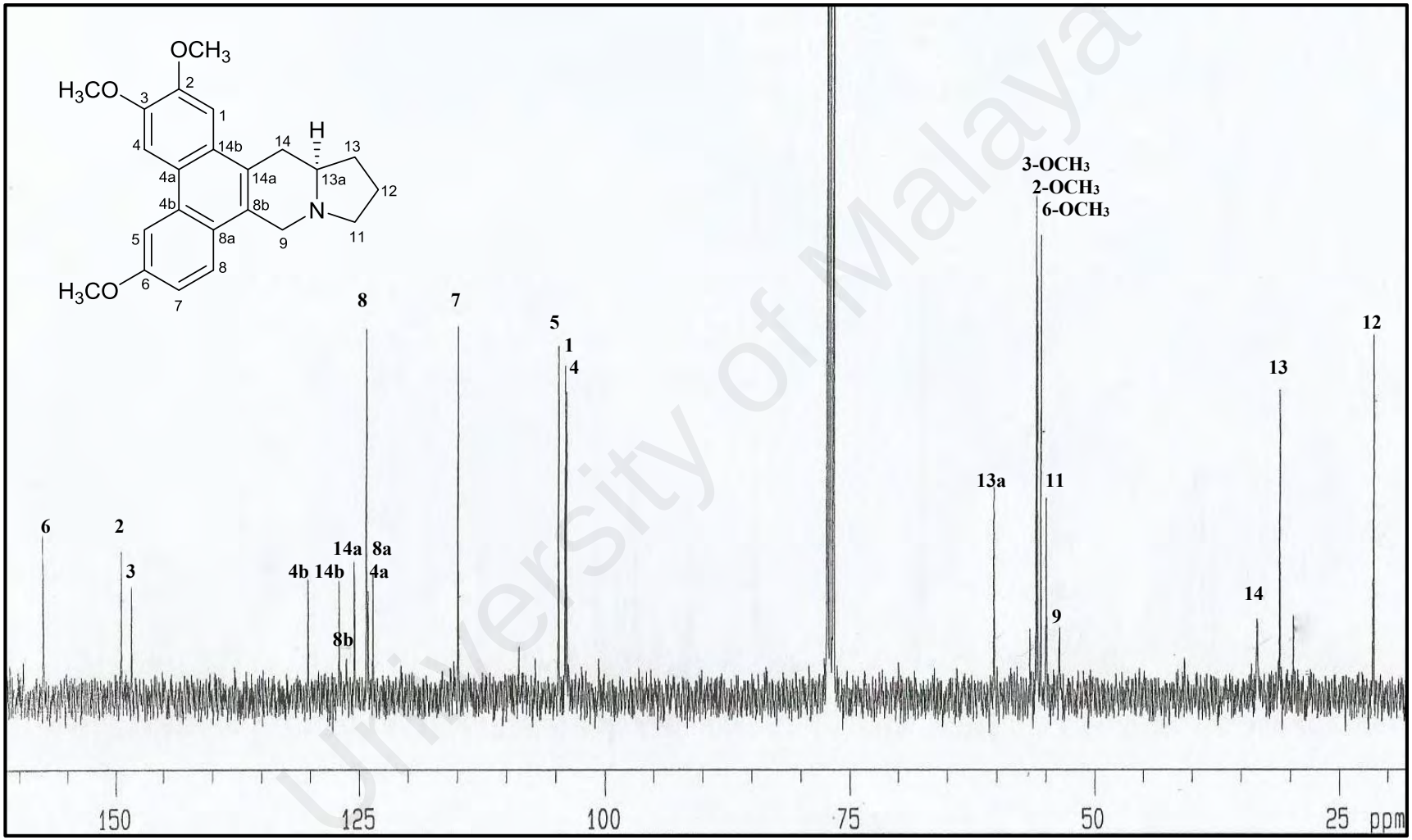

Figure 3.39: ^{13}C NMR spectrum of alkaloid **H**

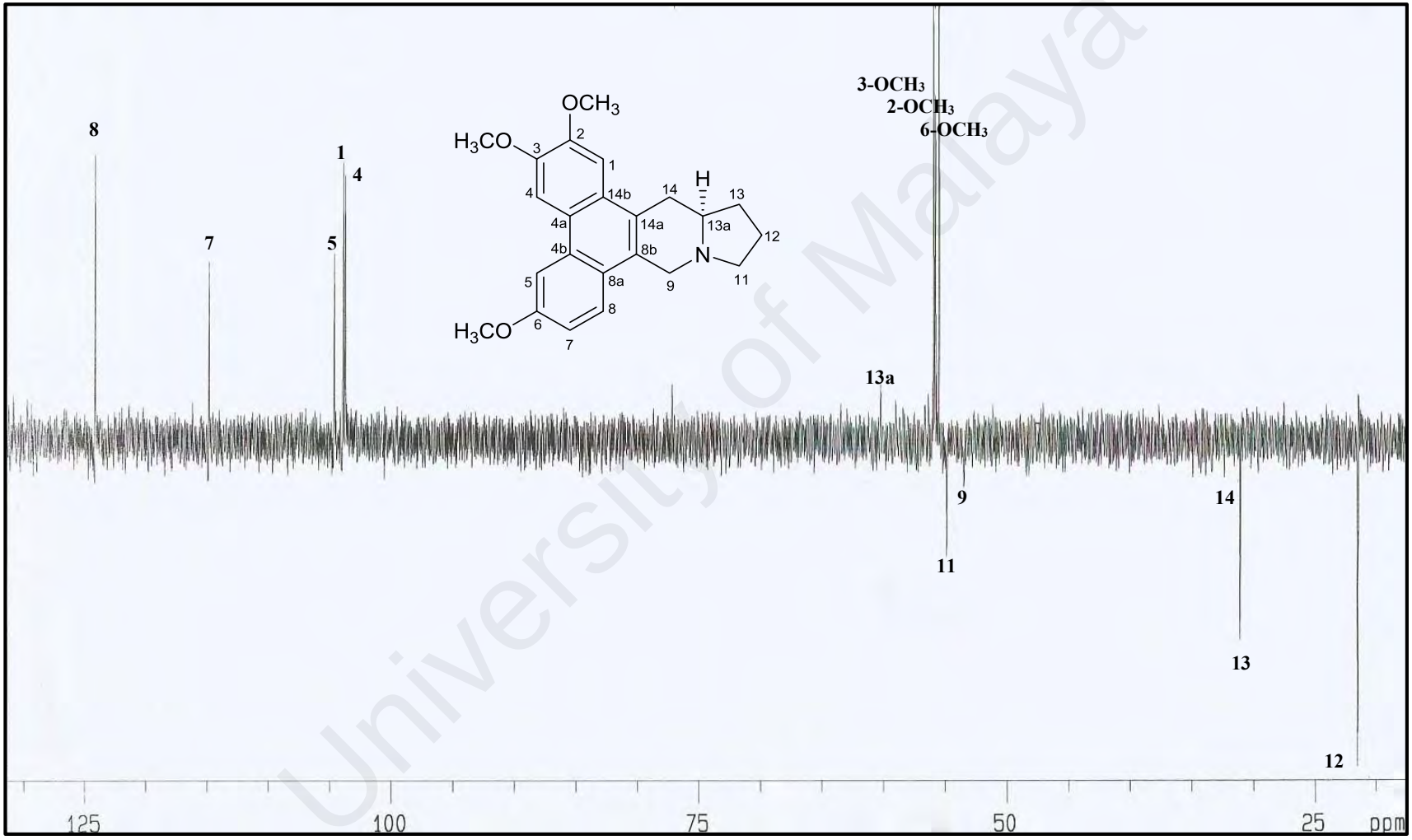

Figure 3.40: DEPT spectrum of alkaloid **H**

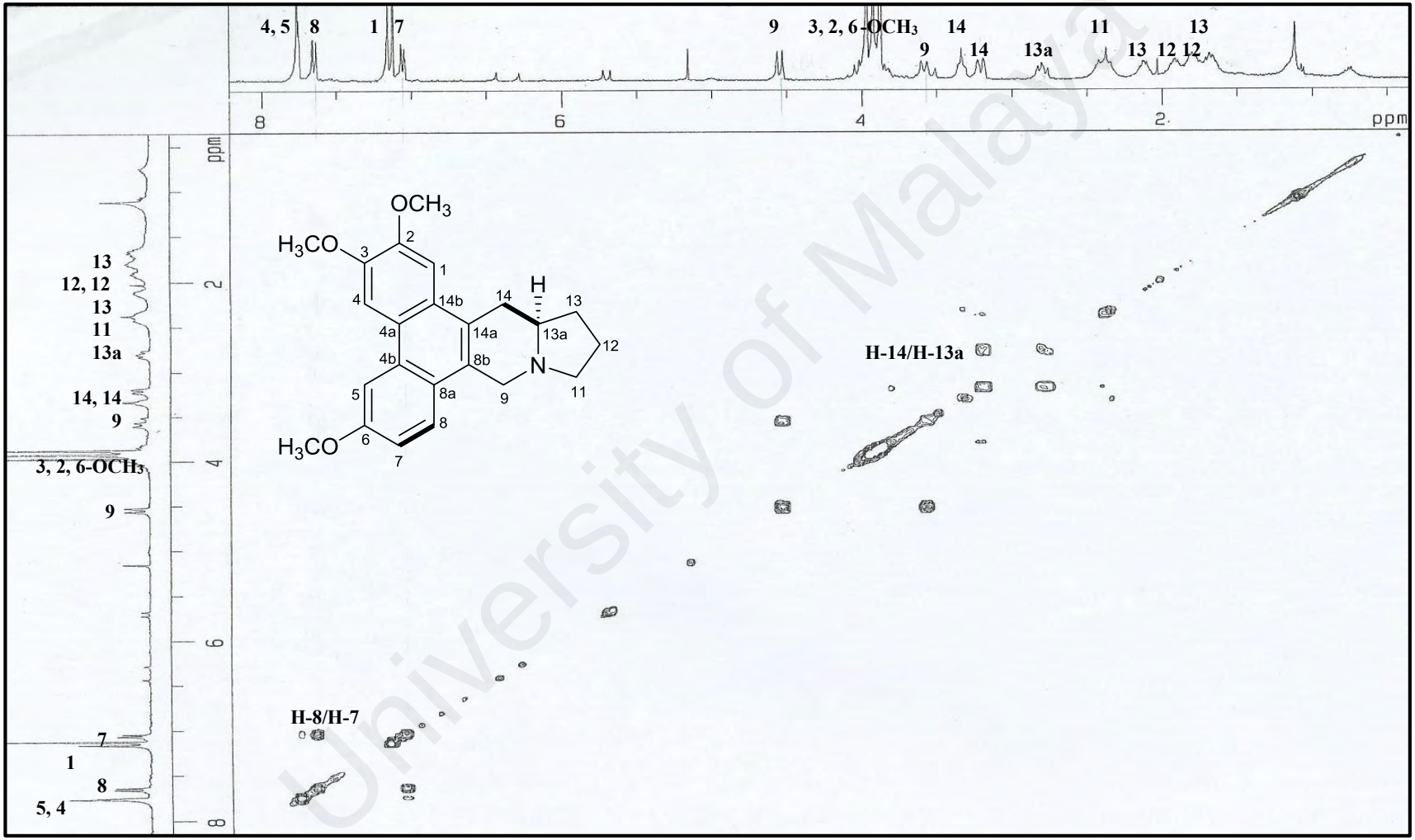

Figure 3.41: COSY spectrum of alkaloid **H**

3.2.9 Alkaloid I: (-)-Densiindolizidine 128

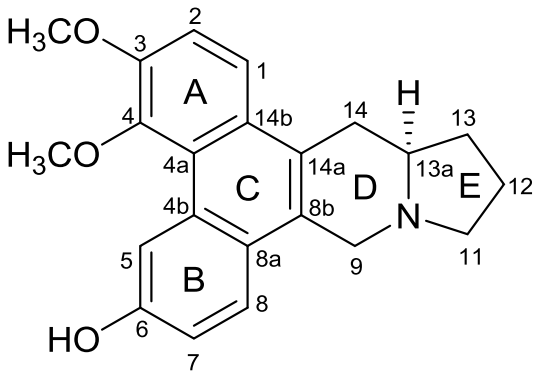

128

Alkaloid **I** was obtained as an optically active dark brownish amorphous with $[\alpha]_D^{25}$ –115° (*c*=1.1, MeOH). It was assigned a molecular formula of $C_{22}H_{23}NO_3$ with twelve degrees of unsaturation as deduced from its LCMS-IT-TOF analysis $[M+H]^+$, *m/z* 350.1759 (calcd. for $C_{22}H_{24}NO_3$, 350.1751). The UV spectrum exhibited characteristic absorption peaks of phenanthroindolizidine moiety at λ_{max} 252, 260, 280, 342 and 351 nm (Damu et al., 2009). The IR spectrum revealed absorption bands due to hydroxyl (OH) (ν_{max} 3340 cm^{-1}) and aromatic (ν_{max} 1596 and 1519 cm^{-1}) functional groups.

The ^1H NMR spectrum showed two mutually coupled doublets at δ_H 7.66 (1H, *d*, *J*=9.0 Hz) and 7.23 (1H, *d*, *J*=9.0 Hz), and a set of ABX signal patterns at δ_H 9.03 (1H, *s*), 7.06 (1H, *d*, *J*=7.8 Hz), and 7.51 (1H, *d*, *J*=7.8 Hz) which were attributed to H-1, H-2, H-5, H-7 and H-8, respectively. H-5 resonated more deshielded at δ_H 9.03 due to the presence of 4-OCH_3 group in ring A which caused the deshielding effect. Two singlets attributed to two methoxyl groups appeared at δ_H 3.96 and 3.81 were assignable to attached to C-3 and C-4 respectively. These assignments were confirmed by the HMBC correlations of H-1/3-OCH_3, 3-$OC\underline{H}_3$/C-3, H-2/4-OCH_3 and 4-$OC\underline{H}_3$/C-4. Analysis of the COSY experiment (Figure 3.45) showed all the correlations of vicinal protons; H-1/H-2, H-8/H-7, H-11/H-12, H-12/H-13, H-13a/H-13 and H-14/H-13a in the structure.

The ^{13}C NMR (Figure 3.43) and DEPT spectrum (Figure 3.44) of alkaloid **I** revealed the presence of twenty-two carbons inclusive of five aromatic protons, two methoxyl groups, one methine, five methylenes and nine quaternary carbons which validated the molecular formula. The HMBC spectrum (Figure 3.47) revealed cross-peak of H-13 to C-14 and H-9 to C-13a indicating that ring E was fused to ring D through C-13a.

Through analysis of all the data obtained (Table 3.10) and comparison with it close analogue, ficuseptine D **129**, alkaloid **I** was identified as a new chemical entity and therefore named (-)-densiindolizidine **128**.

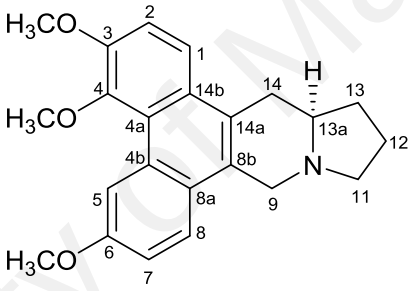

129

Table 3.10: ^{1}H NMR (400 MHz) and ^{13}C NMR (100 MHz) spectroscopic assignments of alkaloid **I** in $CDCl_3$

Position	δ_H (ppm, *J* in Hz)		δ_C (ppm)
	Alkaloid **I**	Ficuseptine D **129** (Damu et al., 2005) (acetone-d6, 400 MHz)	Alkaloid **I**
1	7.66 (1H, *d*, *J*=9.0)	7.83 (1H, *d*, *J*=8.4)	112.9
2	7.23 (1H, *d*, *J*=9.0)	7.49 (1H, *d*, *J*=8.4)	119.4
3	-	-	150.7
4	-	-	147.1
4a	-	-	123.6
4b	-	-	130.0
5	9.03 (1H, *s*)	9.31 (1H, *d*, *J*=2.8)	112.7
6	-	-	154.6
7	7.06 (1H, *d*, *J*=7.8)	7.25 (1H, *dd*, *J*=7.2, 2.8)	116.6
8	7.51 (1H, *d*, *J*=7.8)	7.87 (1H, *d*, *J*=7.2)	123.2
8a	-	-	124.8
8b	-	-	125.7
9	α=3.64 (1H, *m*) β=4.60 (1H, *d*, *J*=15.4)	α=3.57 (1H, *d*, *J*=14.6) β=4.58 (1H, *d*, *J*=14.6)	53.3
11	α=2.51 (1H, *m*) β=3.51 (1H, *m*)	α =2.41 (1H, *q*, *J*=14.8) β= 3.25 (1H, *td*, *J*=14.8, 3.2)	54.7
12	2.04 (2H, *m*)	α=1.82 (1H, *m*) β=2.01 (1H, *m*)	21.4
13	α=1.81 (1H, *m*) β=2.25 (1H, *m*)	α=1.70 (1H, *m*) β=2.20 (1H, *m*)	30.8
13a	2.55 (1H, *m*)	2.34 (1H, *m*)	60.3
14	α=2.93 (1H, *brt*, *J*=11.3) β=3.26 (1H, *brd*, *J*=15.0)	α=2.94 (1H, *dd*, *J*=15.0, 11.0) β=3.32 (1H, *dd*, *J*=15.0, 3.0)	32.9
14a	-	-	125.2
14b	-	-	127.8
3-OCH_3	3.96 (3H, *s*)	3.98 (3H, *s*)	56.4
4-OCH_3	3.81 (3H, *s*)	4.05 (3H, *s*)	59.8
6-OCH_3	-	3.92 (3H, *s*)	-

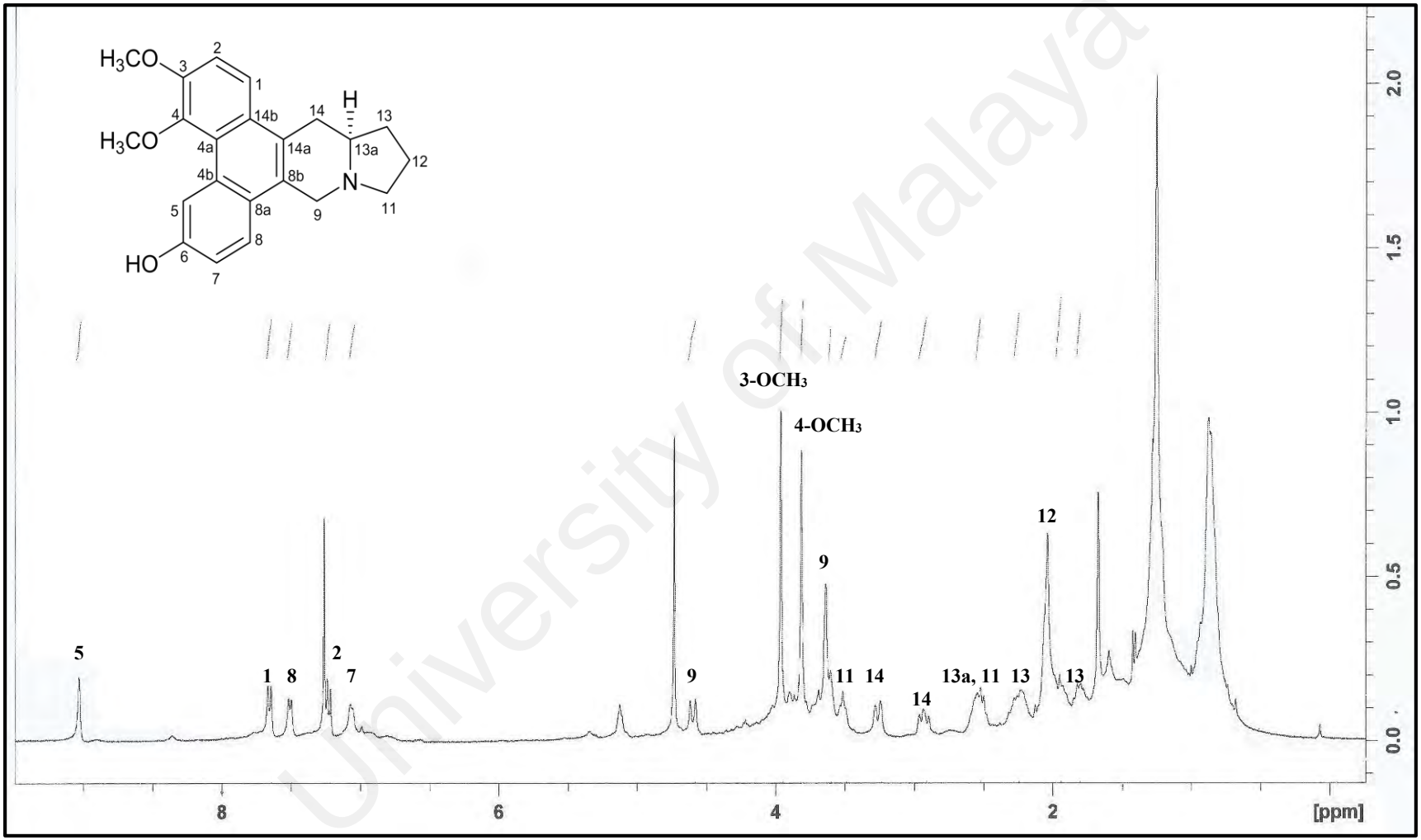

Figure 3.42: ^{1}H NMR spectrum of alkaloid **I**

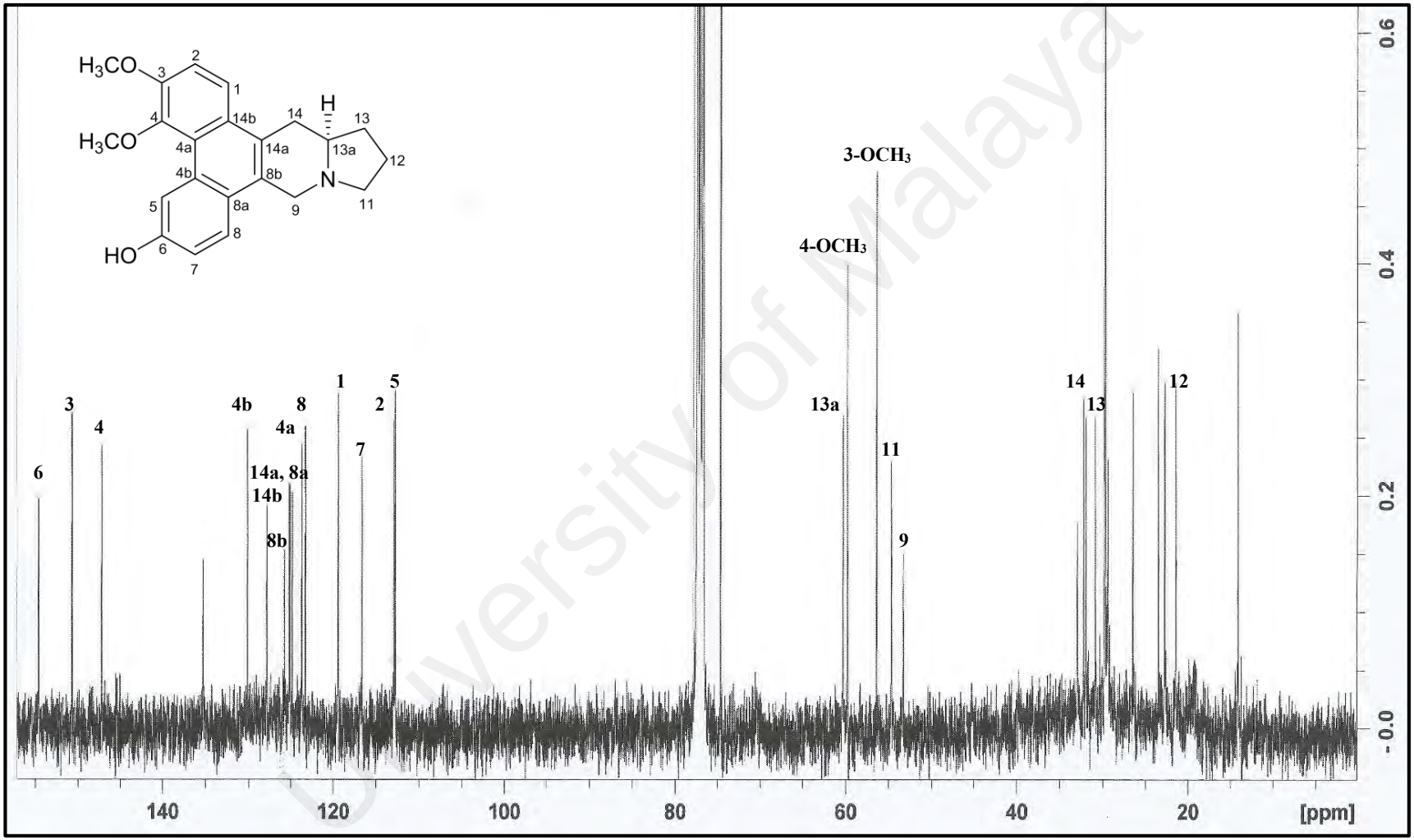

Figure 3.43: ^{13}C NMR spectrum of alkaloid **I**

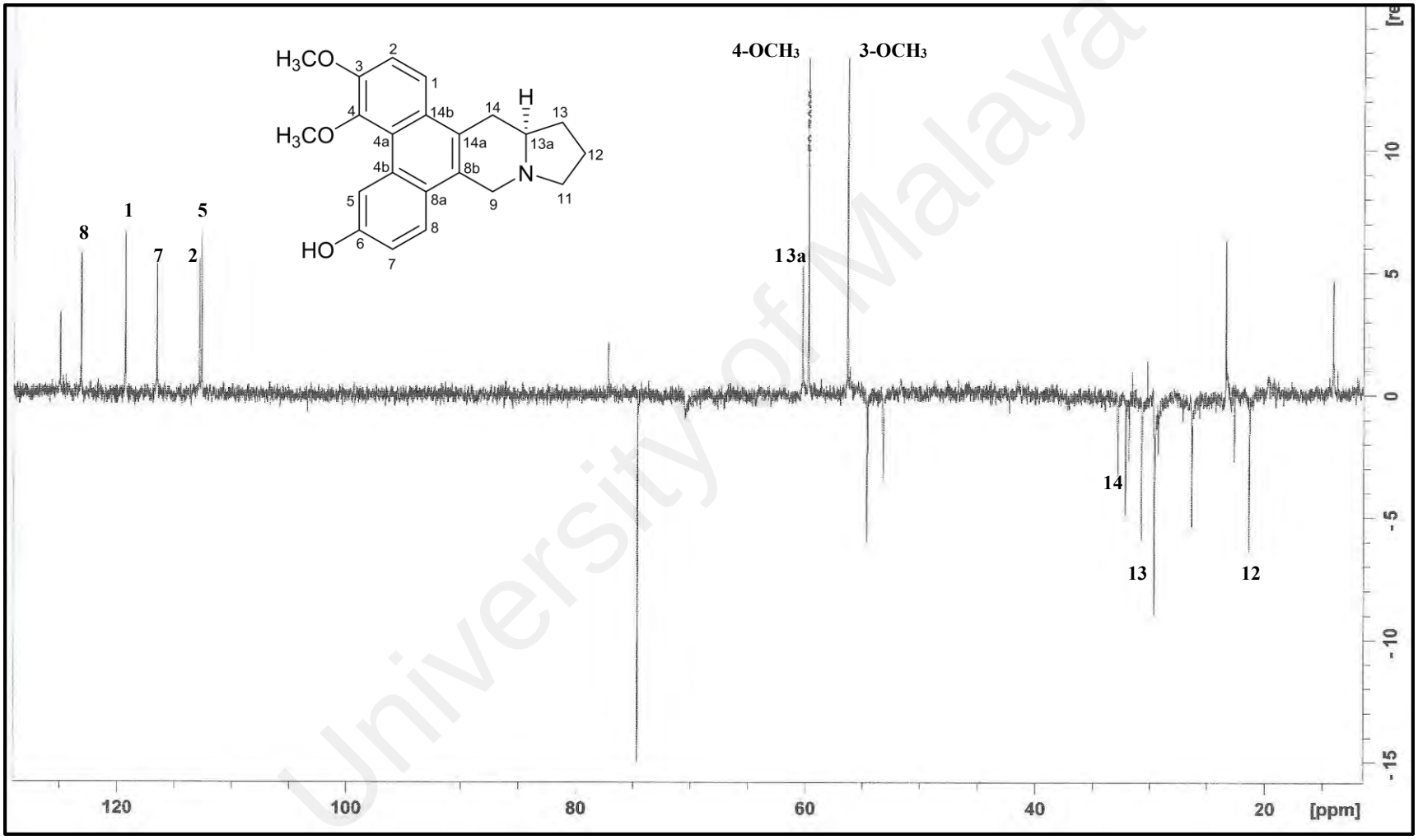

Figure 3.44: DEPT spectrum of alkaloid **I**

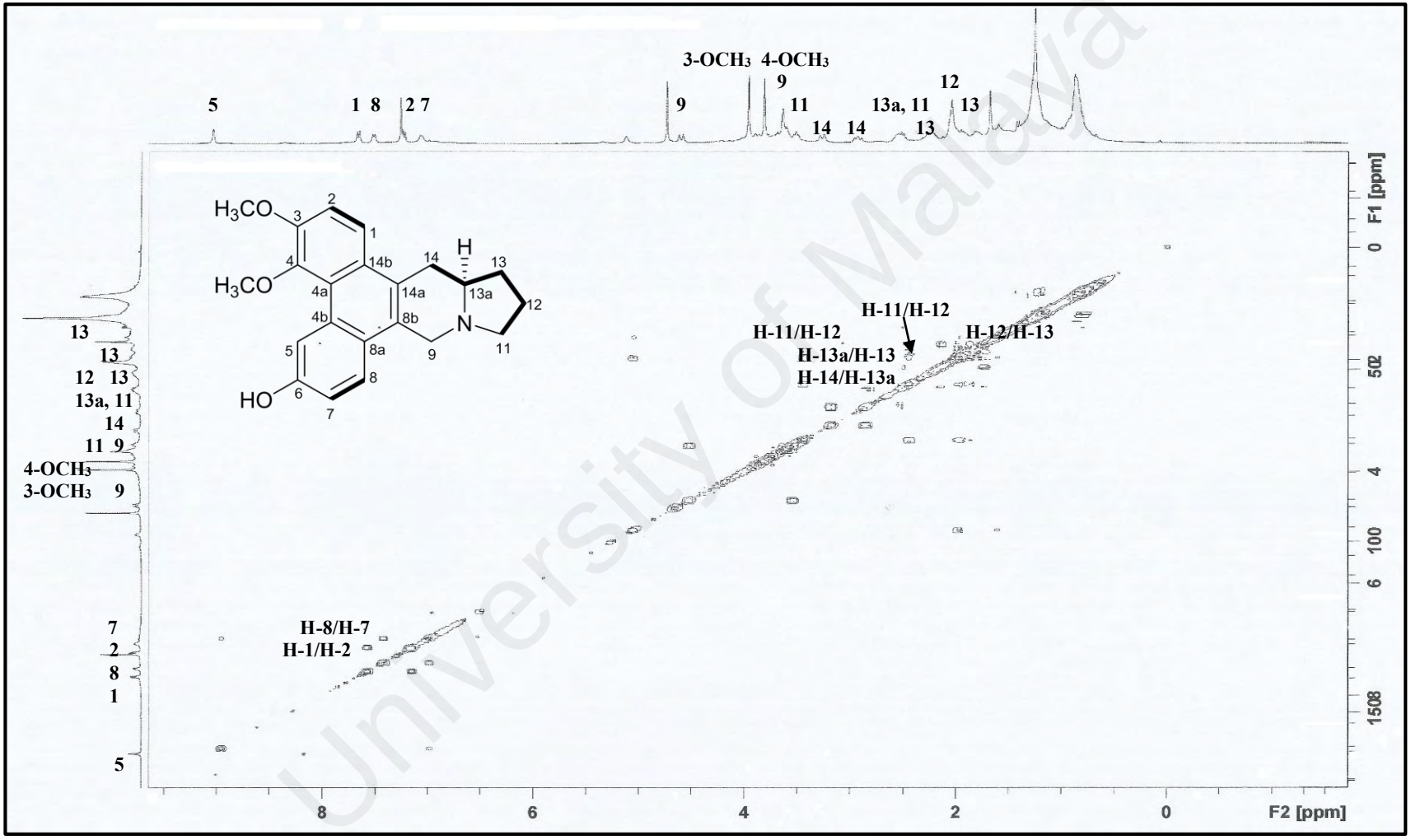

Figure 3.45: COSY spectrum of alkaloid **I**

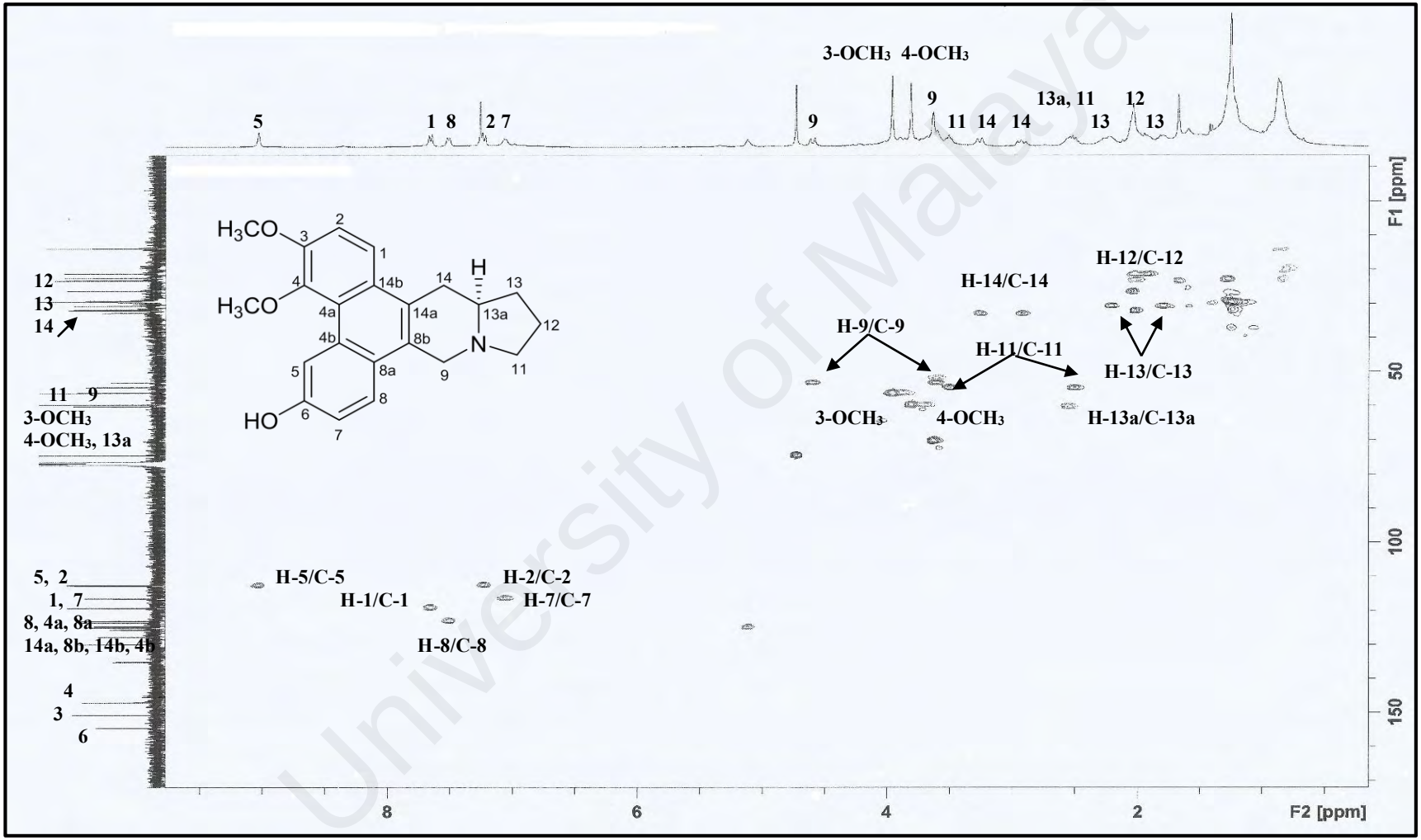

Figure 3.46: HSQC spectrum of alkaloid **I**

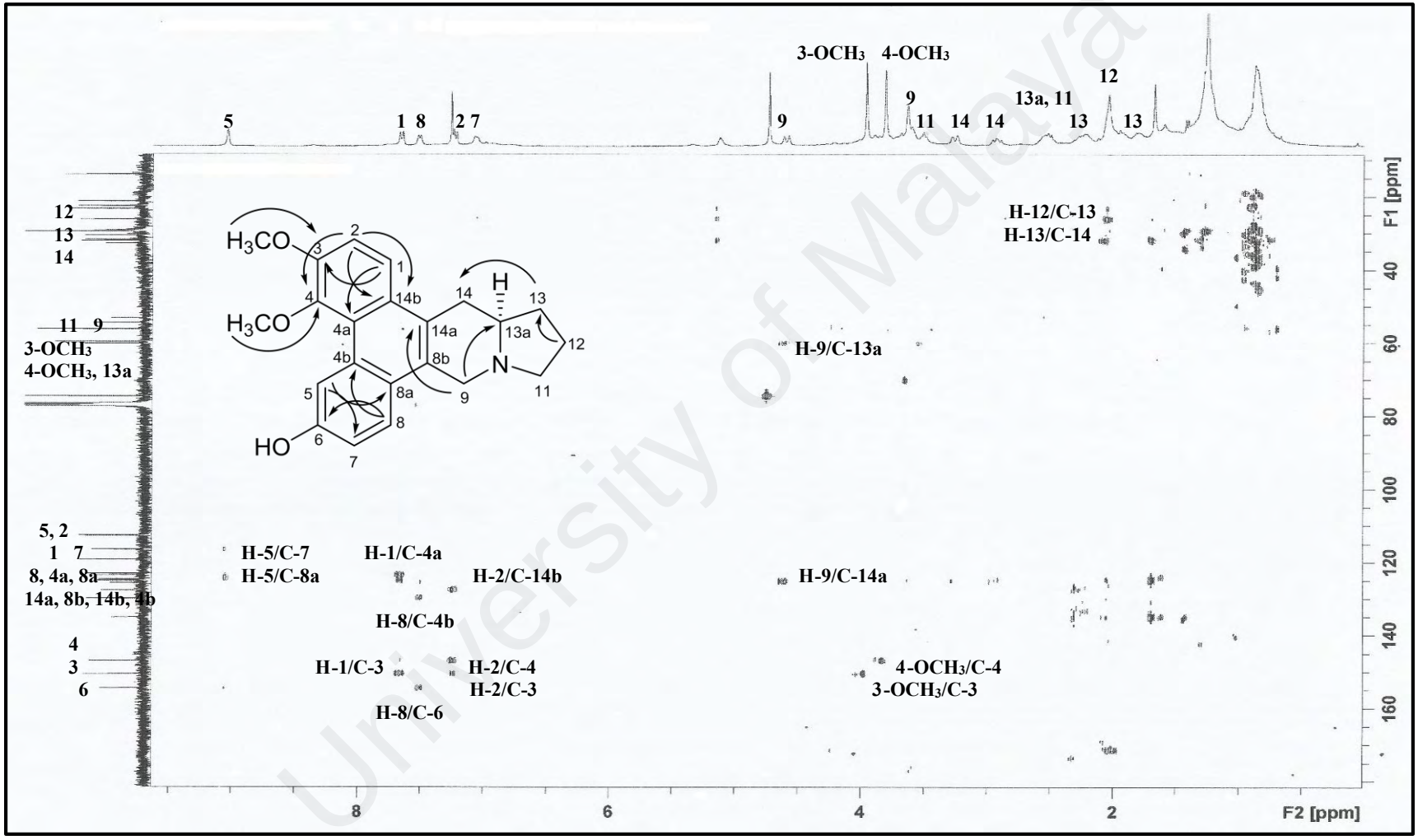

Figure 3.47: HMBC spectrum of alkaloid **I**

3.2.10 Alkaloid J: (-)-Desmethylsecoantofine 130

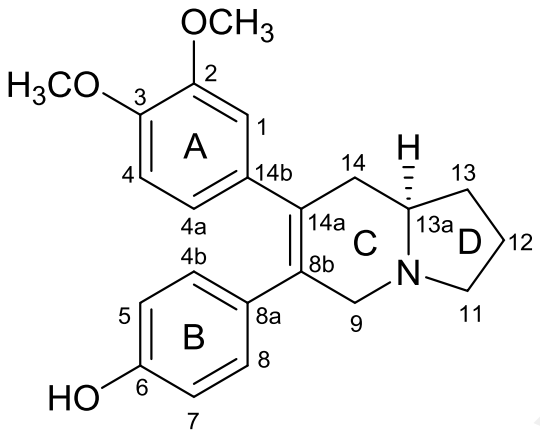

130

Alkaloid **J** was purified as an optically active dark brownish amorphous with $[\alpha]_D^{25}$ –20° (*c*=0.02, MeOH). The positive LCMS-IT-TOF spectrum gave a pseudomolecular ion peak $[M+H]^+$ at *m/z* 352.1981 (calcd. for $C_{22}H_{26}NO_3$, 352.1907), therefore suggesting a molecular formula of $C_{22}H_{25}NO_3$, consistent with eleven degrees of unsaturation. The UV spectrum showed absorptions at λ_{max} 225, 260 and 281 nm while its IR spectrum implied the presence of hydroxyl (OH) and aromatic rings at ν_{max} 3448 and (1516, 1642) cm^{-1} respectively.

The ^1H NMR spectrum (Figure 3.48) of alkaloid **J** exhibited two sets of aromatic spin systems, ABX and A_2B_2. The ABX spin system was assigned to H-1 (δ_H 6.87, *d*, *J*=1.6 Hz), H-4 (δ_H 6.78, *d*, *J*=8.2 Hz) and H-4a (δ_H 6.91, *dd*, *J*=8.2, 1.6 Hz) of ring A while the A_2B_2 spin system was ascribed to H-8/H-4b (δ_H 7.19, *d*, *J*=8.5 Hz) and H-5/H-7 (δ_H 7.04, *d*, *J*=8.5 Hz) of ring B. The linkage between C-4a and C-4b has lost therefore, suggesting a *seco*-phenanthroindolizidine skeleton. Two methoxyl groups at δ_H 3.59 and 3.62 were evident from the ^1H NMR spectrum. The 2-OC<u>H</u>$_3$/C-2 and 3-OC<u>H</u>$_3$/C-3 heteronuclear couplings established the position of these OCH_3 groups on ring A, thus in turn enabling us to place the hydroxyl group at position C-6 of ring B. The aliphatic protons were observed in the range of δ_H 1.50 to 3.98. The COSY spectrum (Figure 3.51)

displayed the correlations of all the vicinal protons; H-4/H-4a, H-5/H-4b, H-7/H-8, H-11/H-12, H-12/H-13, H-13/H-13a and H-13a/H-14 in the structure.

The ^{13}C NMR spectrum (Figure 3.49) revealed the presence of twenty carbon signals instead of twenty-two due to two overlapping signals of C-4b/C-8 and C-5/C-7 carbons, which appeared at δ_C 130.7 and 115.7, respectively. Three oxygenated carbons resonated at δ_C 148.9, 148.0 and 157.3 which were assignable to C-2, C-3 and C-6 respectively.

The HMBC spectrum (Figure 3.54) revealed cross-peak of H-1 to C-14a and H-4b to C-8b indicated that ring A and B was fused to ring C through C-14a and C-8b junction respectively. Furtheremore, the ring D closure was found to attach at C-13a and *N* by observing the correlations of H-11 to C-9 and H-13 to C-14.

Comprehensive study of the 1D and 2D NMR spectra (Table 3.11) and comparison with the literature values led to the conclusion that the investigated compound was indeed (-)-desmethylsecoantofine **130**, which has been previously isolated from *Cynanchum vincetoxicum* (Staerk et al., 2002). It should be noted that, the difference in NMR values of the indicated compound with that of the reference is due to the different solvent used in recording the spectral data.

Table 3.11: ^{1}H NMR (600 MHz) and ^{13}C NMR (150 MHz) spectroscopic assignments of alkaloid **J** in C_5D_5N

Position	δ_H (ppm, *J* in Hz)		δ_C (ppm)	
	Alkaloid **J**	Desmethylsecoantofine **130** (Stærk et al., 2002) (C_6D_6+$CDCl_3$, 7:9, 400 MHz)	Alkaloid **J**	Desmethylseco-antofine **130** (Stærk et al., 2002) (C_6D_6+$CDCl_3$ 7:9, 100 MHz)
1	6.87 (1H, *d*, *J*=1.6)	6.33 (1H, *d*, *J*=1.7)	114.0	112.9
2	-	-	148.9	148.0
3	-	-	148.0	147.5
4	6.78 (1H, *d*, *J*=8.2)	6.38 (1H, *d*, *J*=8.3)	111.7	110.6
4a	6.91 (1H, *dd*, *J*=8.2, 1.6)	6.46 (1H, *dd*, *J*=8.3, 1.7)	121.4	120.7
4b	7.19 (1H, *d*, *J*=8.5)	6.67 (1H)	130.7	130.2
5	7.04 (1H, *d*, *J*= 8.5)	6.47 (1H)	115.7	115.3
6	-	-	157.3	155.2
7	7.04 (1H, *d*, *J*=8.5)	6.47 (1H)	115.7	115.3
8	7.19 (1H, *d*, *J*=8.5)	6.67 (1H)	130.7	130.2
8a	-	-	132.5	131.6
8b	-	-	132.1	132.6
9	α=3.12 (1H, *dt*, *J*=16.0, 2.9) β=3.98 (1H, *d*, *J*=16.0)	α=3.00 (1H, *d*, *J*=15.4) β=3.67 (1H, *d*, *J*=15.4)	58.5	56.2
11	α=2.12 (1H, *m*) β=3.23 (1H, *m*)	α=1.81 (1H, *m*) β=3.14 (1H, *m*)	54.3	53.7
12	α=1.81 (1H, *m*) β=1.67 (1H, *m*)	α=1.56 (1H, *m*) β=1.77 (1H, *m*)	21.7	21.4
13	α=1.97 (1H, *m*) β=1.50 (1H, *m*)	α=1.49 (1H, *m*) β=1.84 (1H, *m*)	31.0	30.1
13a	2.35 (1H, *m*)	2.19 (1H, *m*)	60.5	60.8
14	α=2.81 (1H, *m*) β=2.51 (1H, *m*)	2.46 (2H, *m*)	38.8	36.6
14a	-	-	132.1	132.6
14b	-	-	133.4	134.0
2-OCH_3	3.59 (3H, *s*)	3.30 (3H, *s*)	55.4	55.6
3-OCH_3	3.62 (3H, *s*)	3.45 (3H, *s*)	55.4	55.7

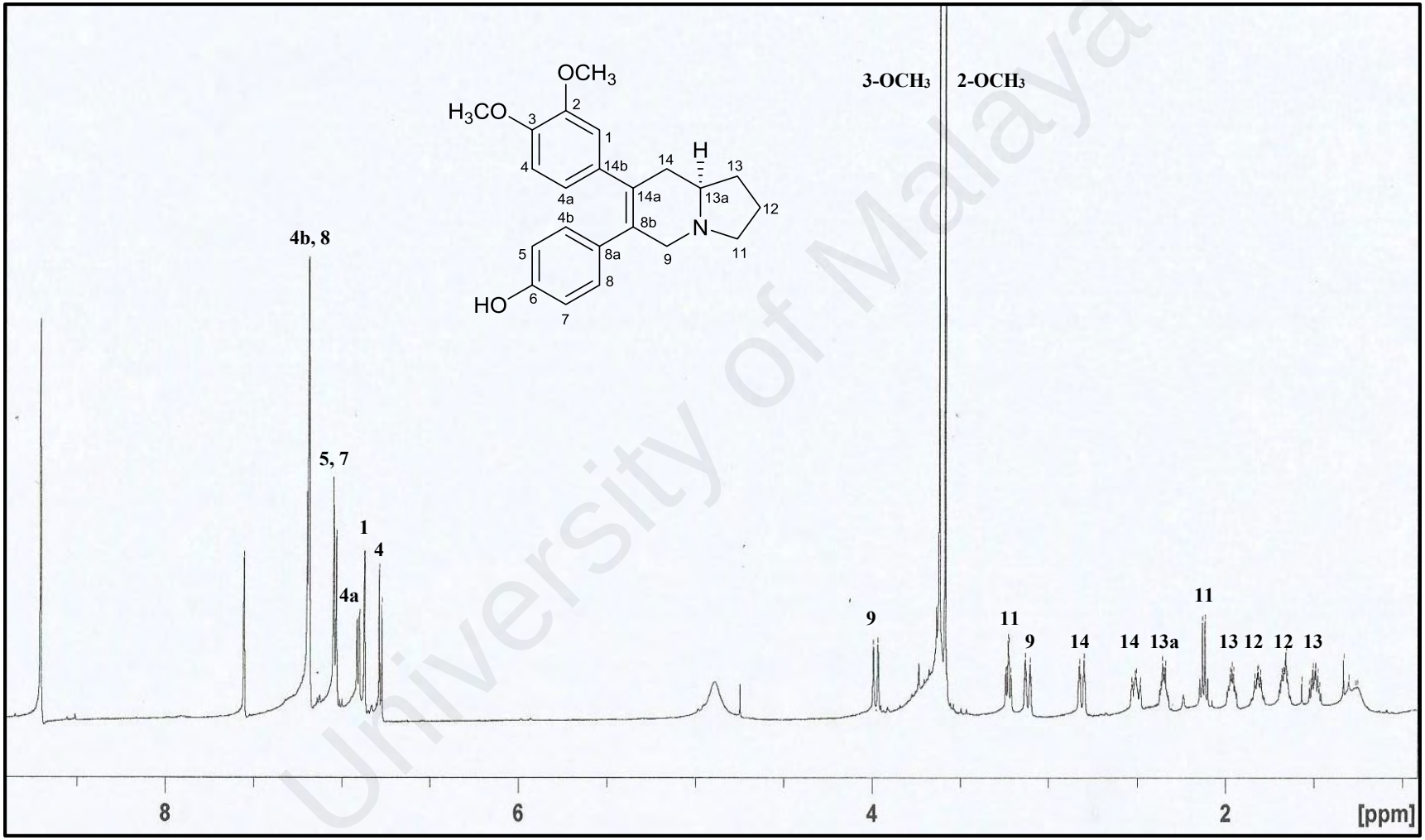

Figure 3.48: ^{1}H NMR spectrum of alkaloid **J**

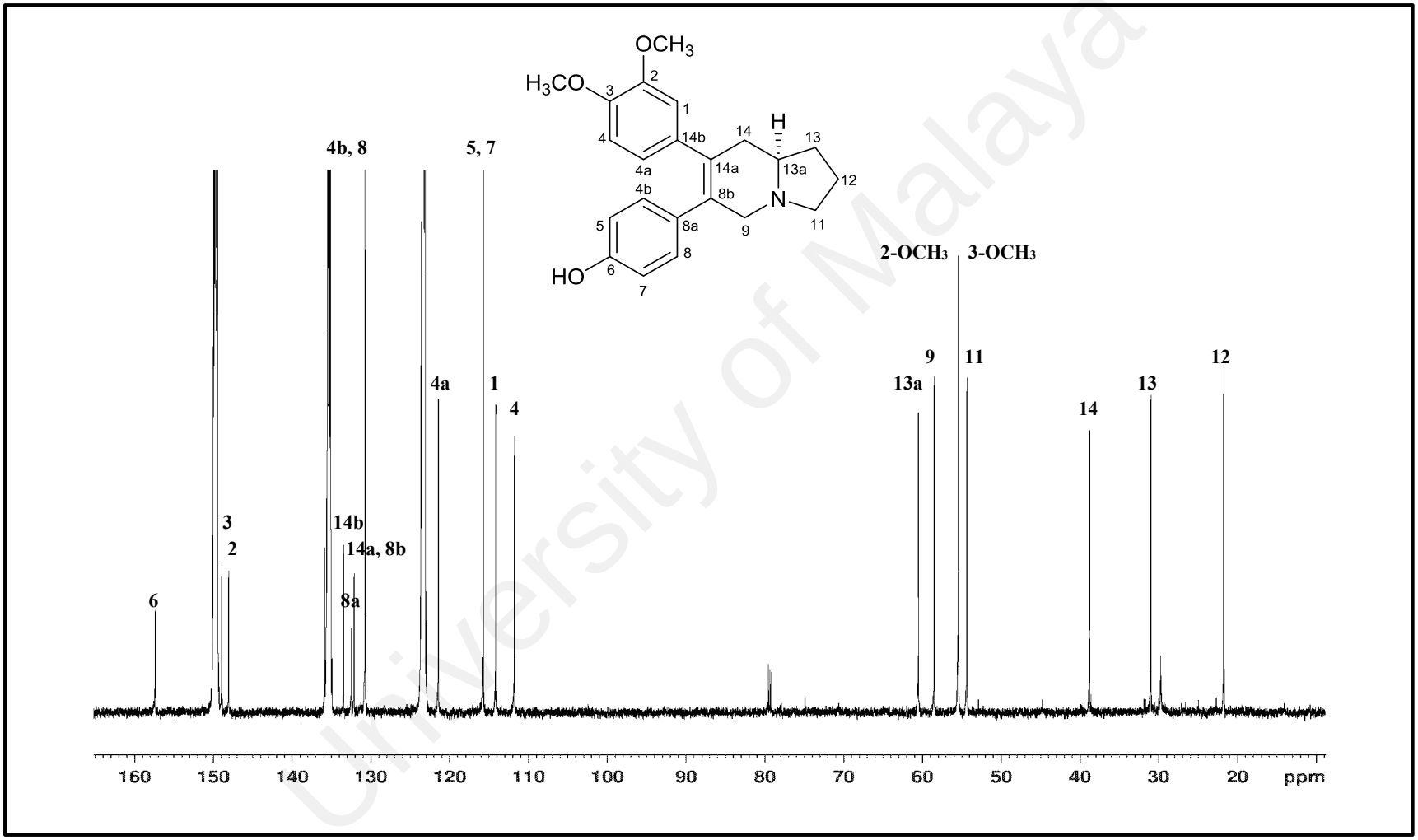

Figure 3.49: ^{13}C NMR spectrum of alkaloid **J**

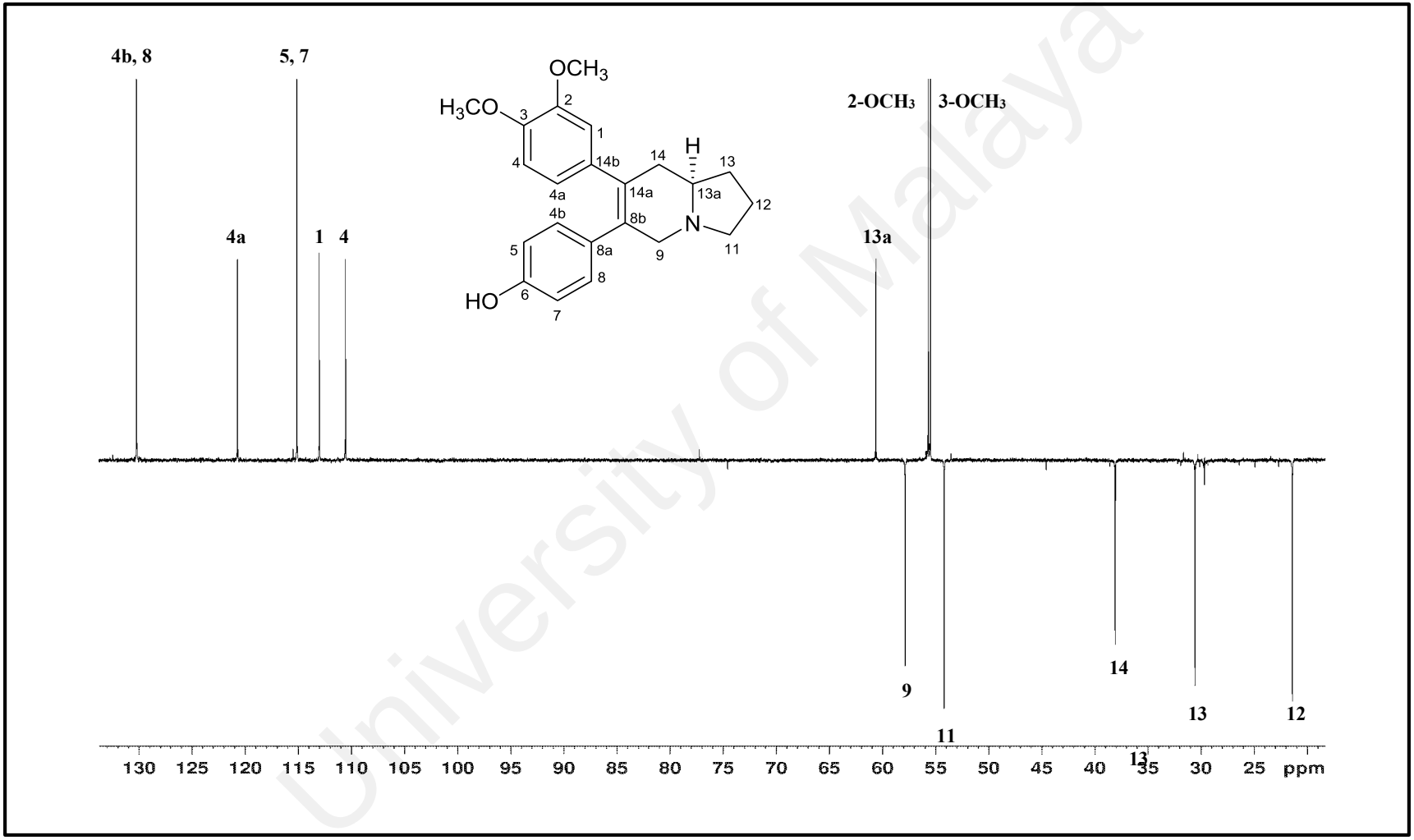

Figure 3.50: DEPT spectrum of alkaloid **J**

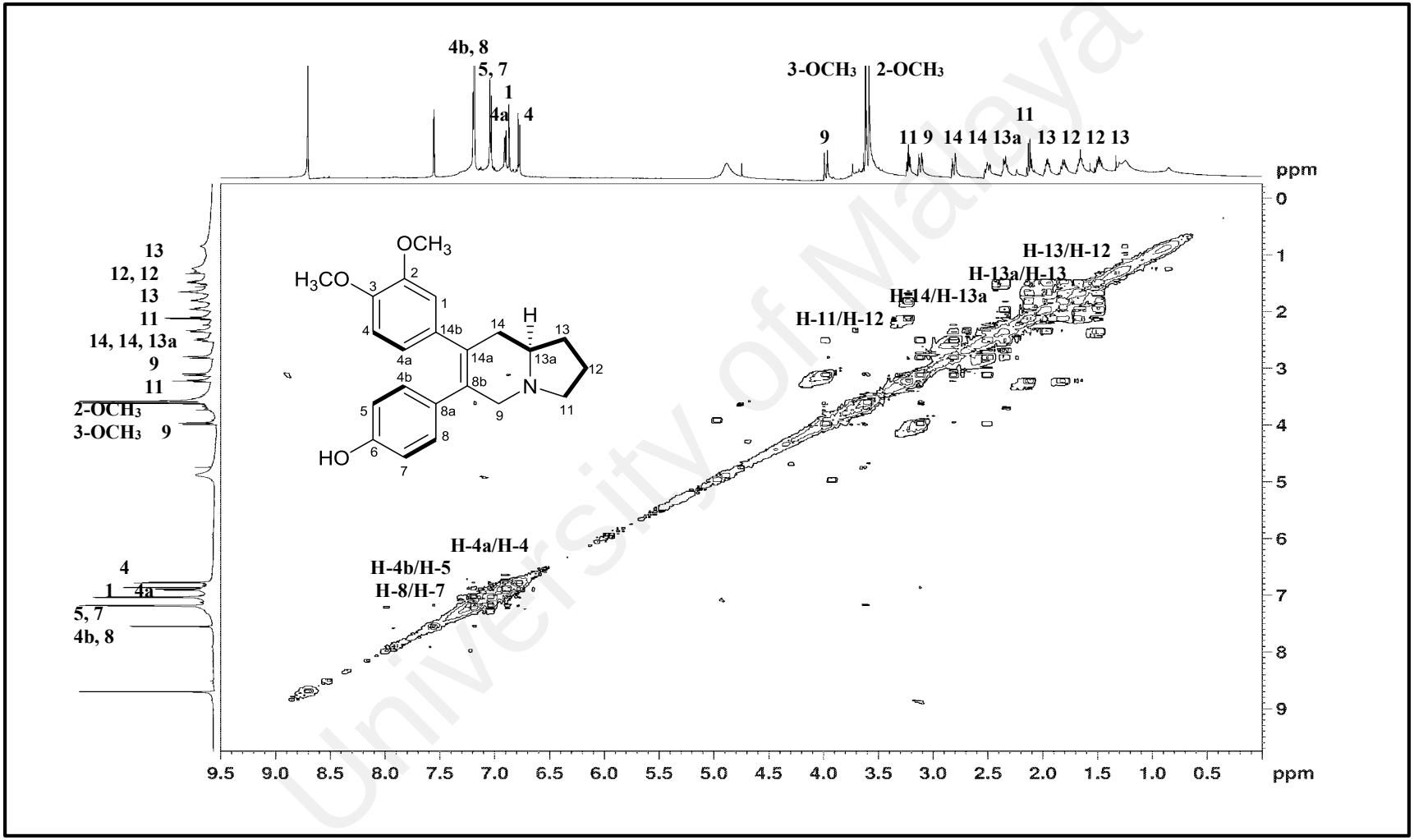

Figure 3.51: COSY spectrum of alkaloid **J**

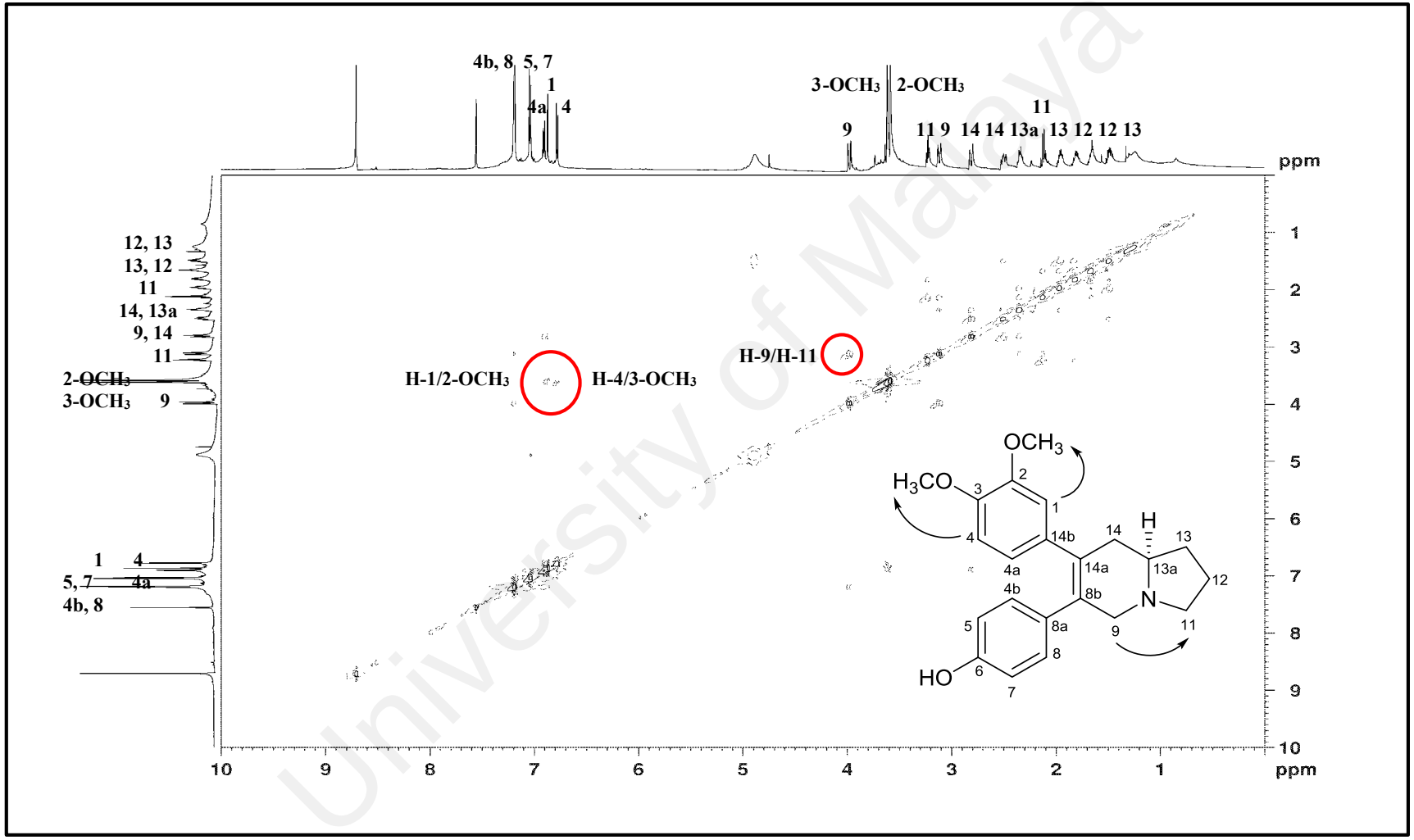

Figure 3.52: NOESY spectrum of alkaloid **J**

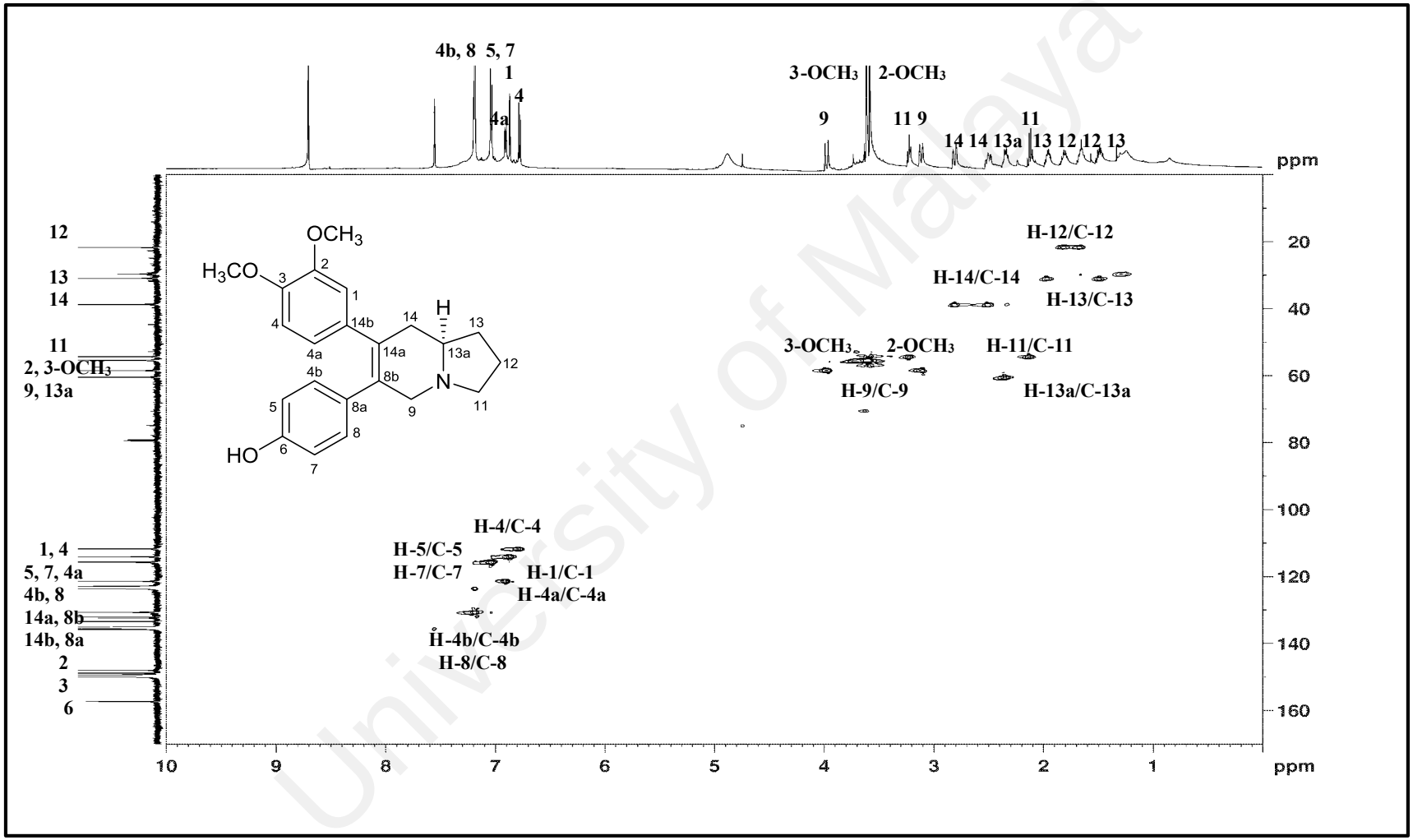

Figure 3.53: HSQC spectrum of alkaloid **J**

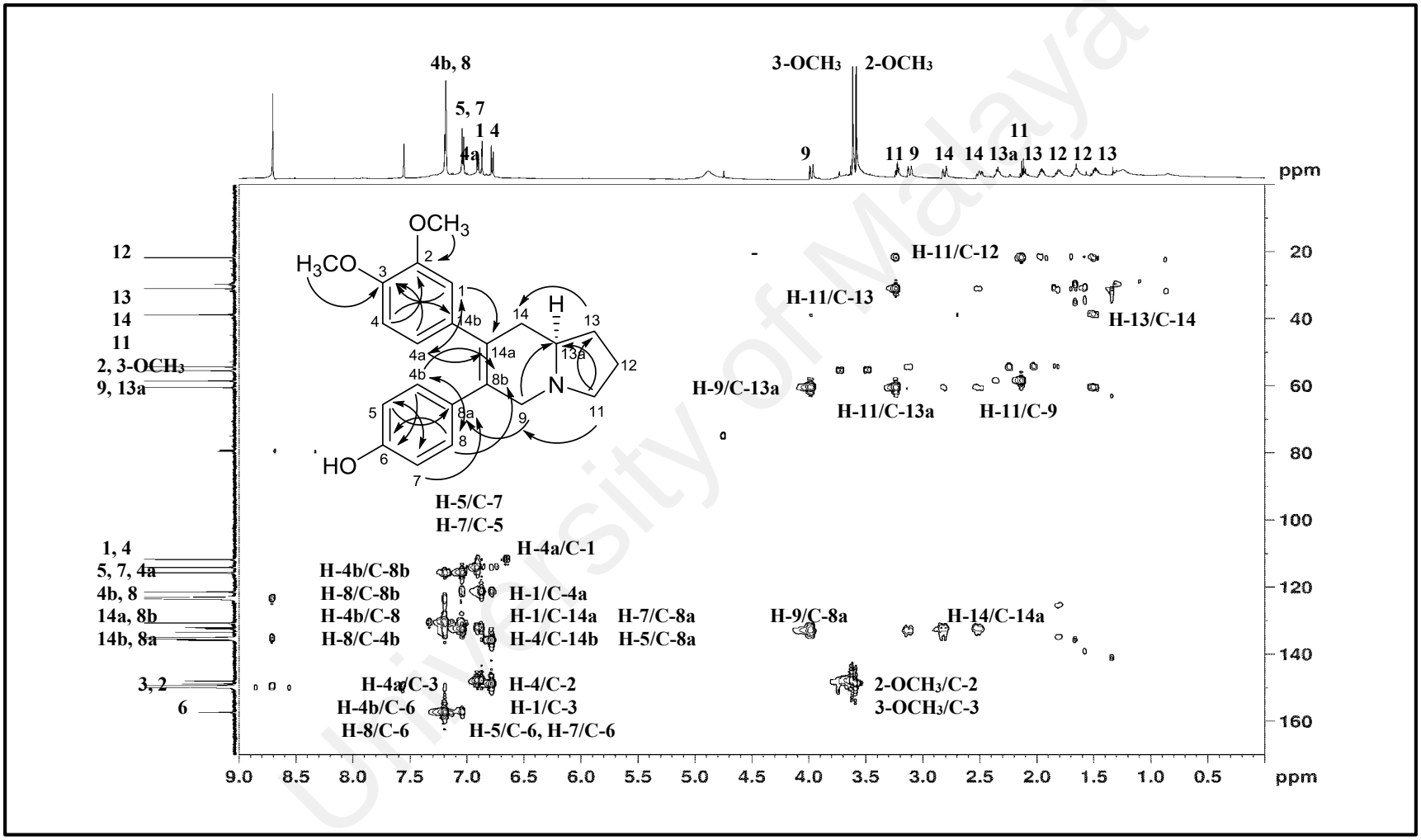

Figure 3.54: HMBC spectrum of alkaloid **J**

3.2.11 Alkaloid K: (-)-Desmethylsecoantofine-*N*-oxide 131

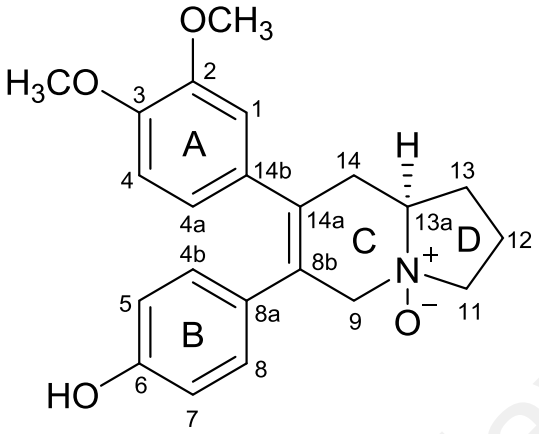

131

Alkaloid **K** was assigned a molecular formula $C_{22}H_{25}NO_4$ as deduced from its ^{13}C NMR spectrum (Table 3.12) and positive LCMS-IT-TOF {$[M+H]^+$ *m/z* 368.1855 (calcd. for $C_{22}H_{26}NO_4$, 368.1856)}, consistent with eleven degrees of unsaturation. The UV, IR, ^1H NMR and ^{13}C NMR spectra (Table 3.12) of alkaloid **K** were almost superimposable with those of alkaloid **J** (Table 3.11), thus implying that alkaloid **K** was also a *seco*-phenanthroindolizidine type alkaloid which was structurally related to alkaloid **J**. There was however a significant difference between the indolizidine moiety of alkaloid **K** with that of alkaloid **J**. Unlike that of the latter, the above mentioned substructure in alkaloid **K** was an indolizidine *N*-oxide moiety. This was evident from the downfield shift in the resonances of C-9 (δ_C 68.6), C-11 (δ_C 68.2) and C-13a (δ_C 70.6) upon comparison to the corresponding atoms in alkaloid **J**. Similar downfield shifts were also observed when a comparison was made between the carbon framework of (-)-13aα-secoantofine **132** and (-)-13aα-secoantofine-*N*-oxide **133** (Stærk et al., 2000; Stærk et al., 2002). Thus, the structure of alkaloid **K** was established as (-)-desmethylsecoantofine-*N*-oxide **131**, a new *seco*-phenanthroindolizidine alkaloid. Alkaloid **K** is most probably naturally occurs in *C. densiflora* as it was isolated along with other free bases and these free bases were not

converted into *N*-oxides. These compounds were all subjected to the same/similar procedure of extraction and isolation. In addition, there was no heat involved during the isolation procedure; therefore, the possibility of the formation of an artifact within the process could be mitigated. Furthermore, there have been a number of reports of plants containing naturally occurring isoquinoline *N*-oxide alkaloids which provides strong justification as to why alkaloid **K** is most probably naturally occurring compound (Dembitsky, Gloriozova, & Poroikov, 2015).

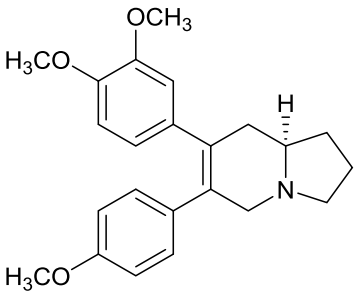

132

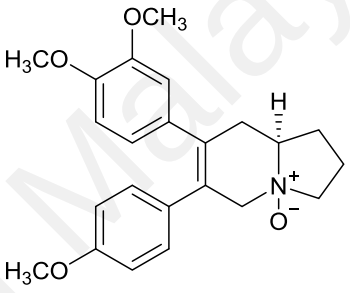

133

Table 3.12: ^{1}H NMR (600 MHz) and ^{13}C NMR (150 MHz) spectroscopic assignments of alkaloid **K** in C_5D_5N

Position	δ_H (ppm, *J* in Hz)		δ_C (ppm)	
	Alkaloid **K**	(-)-13aα-secoantofine-*N*-oxide **133** (Stærk et al., 2000) (C_6D_6+$CDCl_3$,7:9, 800 MHz)	Alkaloid **K**	(-)-13aα-secoantofine-*N*-oxide **133** (Stærk et al., 2000) (C_6D_6+$CDCl_3$ 7:9, 100 MHz)
1	6.88 (1H, *d*, *J*=1.6)	6.29 (1H, *d*, *J*=1.9)	114.0	113.1
2	-	-	148.9	148.4
3	-	-	148.3	148.1
4	6.74 (1H, *d*, *J*=8.8)	6.39 (1H, *d*, *J*=8.2)	111.6	110.7
4a	6.89 (1H, *dd J* =8.8, 1.6)	6.43 (1H, *dd*, *J*=8.2, 1.9)	121.6	120.8
4b	7.14 (1H, *d*, *J*=8.4)	6.97 (1H, *d*, *J*=8.5)	130.8	130.6
5	7.08 (1H, *d*, *J*=8.4)	6.50 (1H, *d*, *J*=8.5)	116.3	113.8
6	-	-	158.7	158.9
7	7.08 (1H, *d*, *J*=8.4)	6.50 (1H, *d*, *J*=8.5)	116.3	113.8
8	7.14 (1H, *d*, *J*=8.4)	6.97 (1H, *d*, *J*=8.5)	130.8	130.5
8a	-	-	129.6	130.4
8b	-	-	127.8	126.2
9	α=4.33 (1H, *d*, *J*=15.3) β=4.59 (1H, *d*, *J*=15.3)	α=4.69 (1H, *brs*) β=5.28 (1H, *brs*)	68.6	66.6
11	α=3.39 (1H, *m*) β=3.94 (1H, *m*)	α=2.92 (1H, *brm*) β=4.46 (1H, *brs*)	68.2	67.1
12	α=2.36 (1H, *m*) β=1.77 (1H, *m*)	α=1.54 (1H, *m*) β=1.98 (1H, *m*)	20.1	19.6
13	α=2.15 (1H, *m*) β=1.97 (1H, *m*)	α=1.62 (1H, *m*, overlap with H-13β) β=1.66 (1H, *m*, overlap with H-13α)	26.9	26.4
13a	3.69 (1H, *m*)	2.82 (1H, *m*)	70.6	70.2
14	α=3.24 (1H, *m*) β=2.69 (1H, *d*, *J*=16.3)	α=2.35 (1H, *dd*, *J*=17.6, 3.9) β=2.51 (1H, *dd*, *J*=17.6, 11.8)	32.4	31.9
14a	-	-	131.2	131.7
14b	-	-	134.3	132.6
2-OCH_3	3.51 (3H, *s*)	3.27 (3H, *s*)	55.4	55.4
3-OCH_3	3.61 (3H, *s*)	3.41 (3H, *s*)	55.4	55.4
6-OCH_3	-	3.31 (3H, *s*)	-	54.8

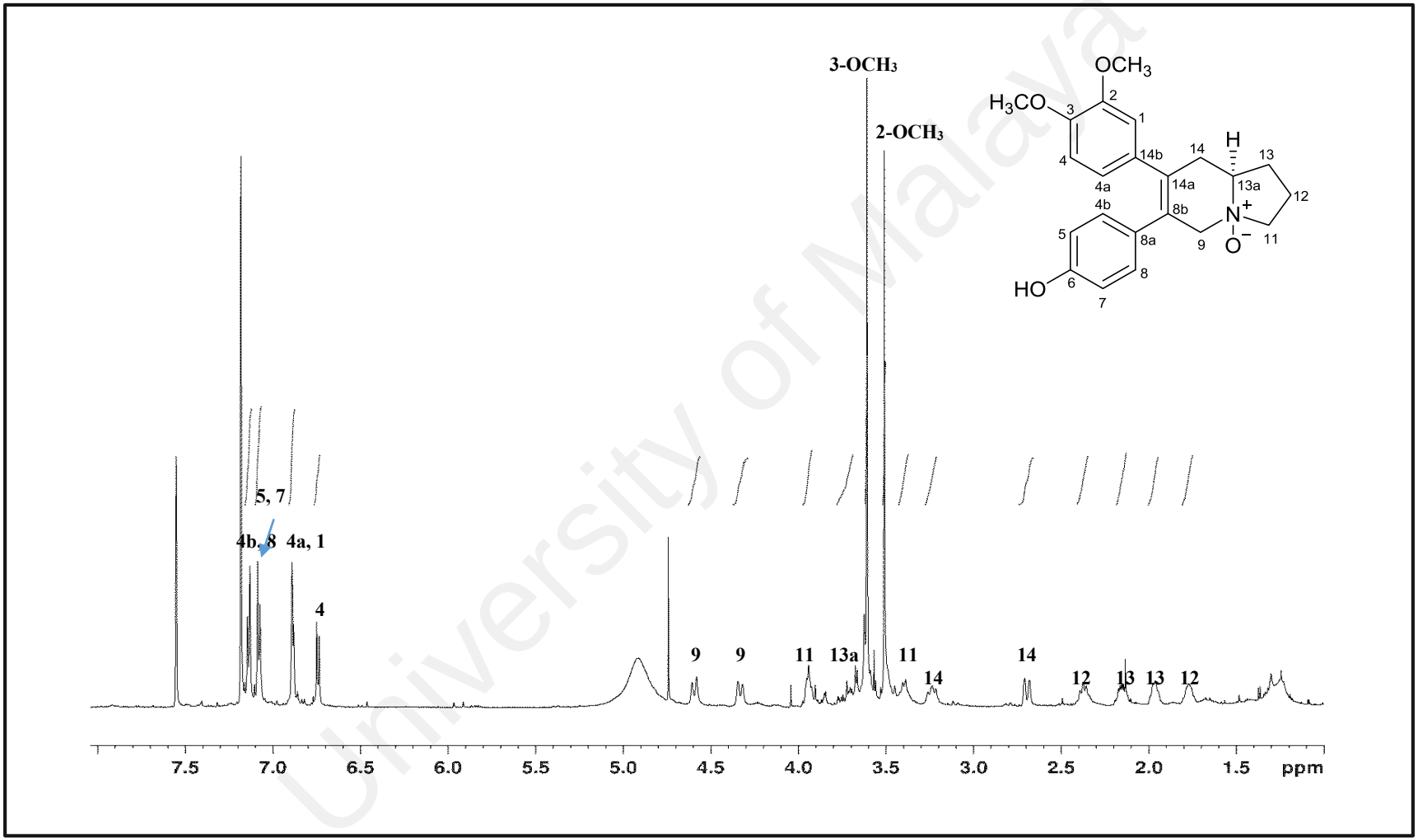

Figure 3.55: ^{1}H NMR spectrum of alkaloid **K**

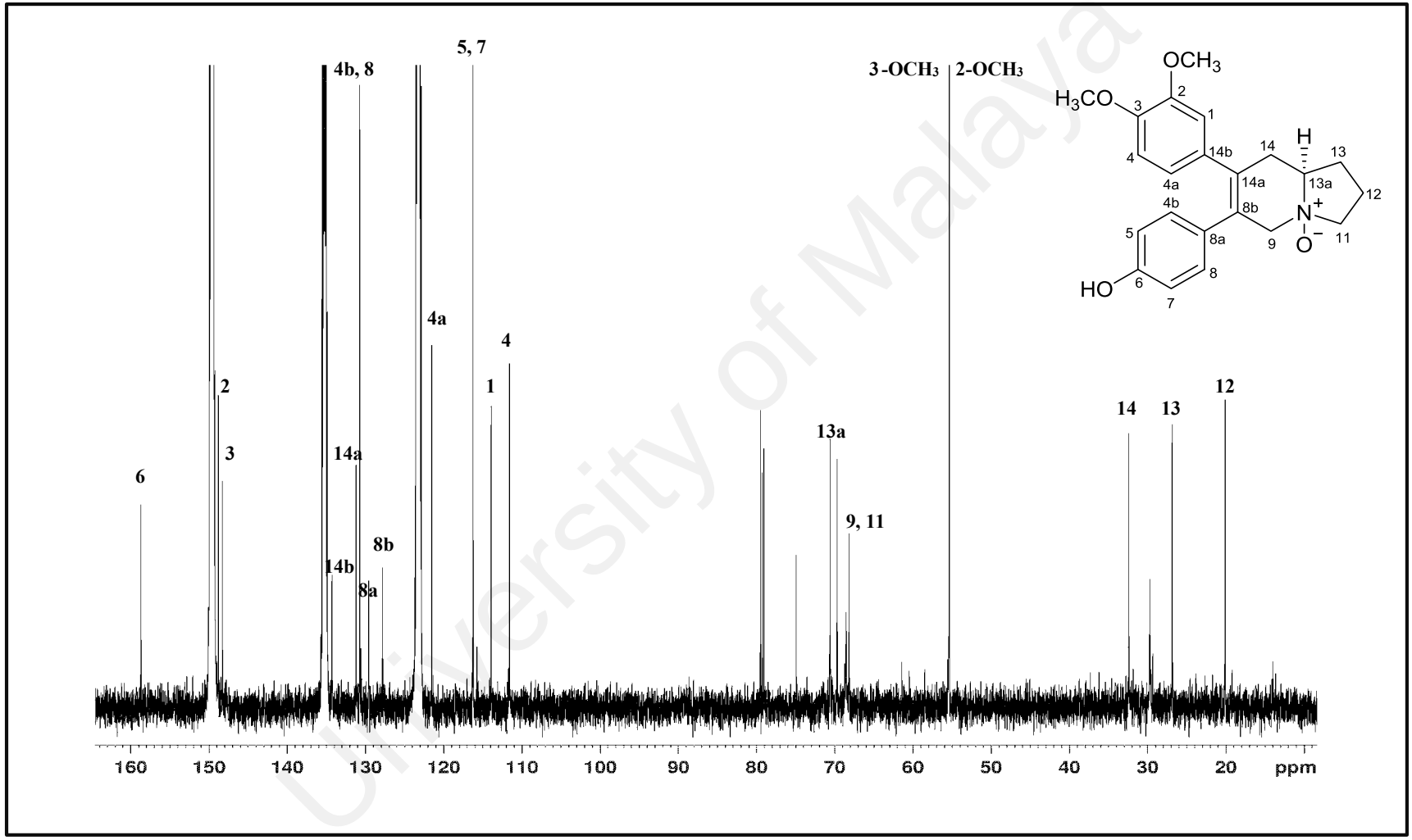

Figure 3.56: ^{13}C NMR spectrum of alkaloid **K**

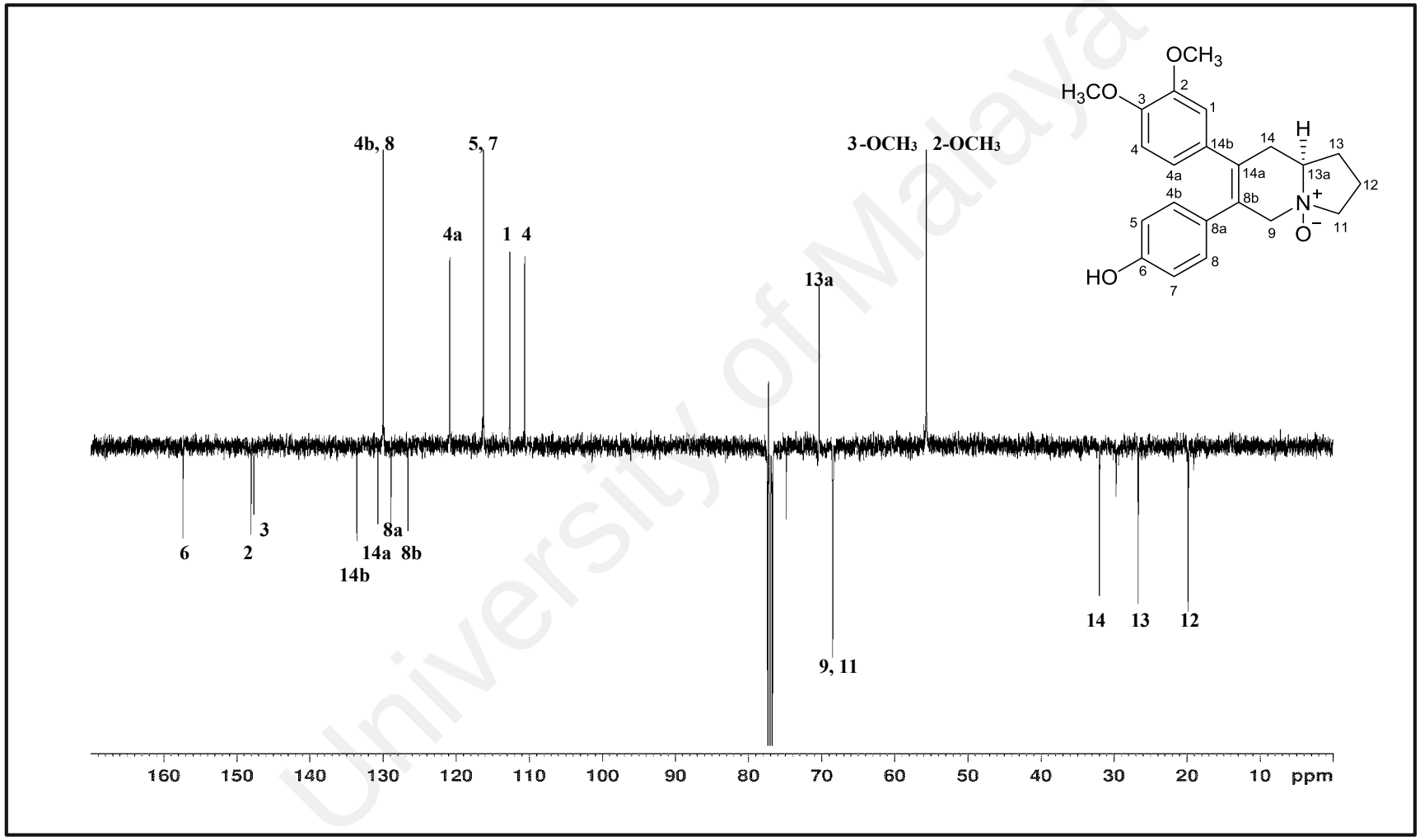

Figure 3.57: DEPT spectrum of alkaloid **K**

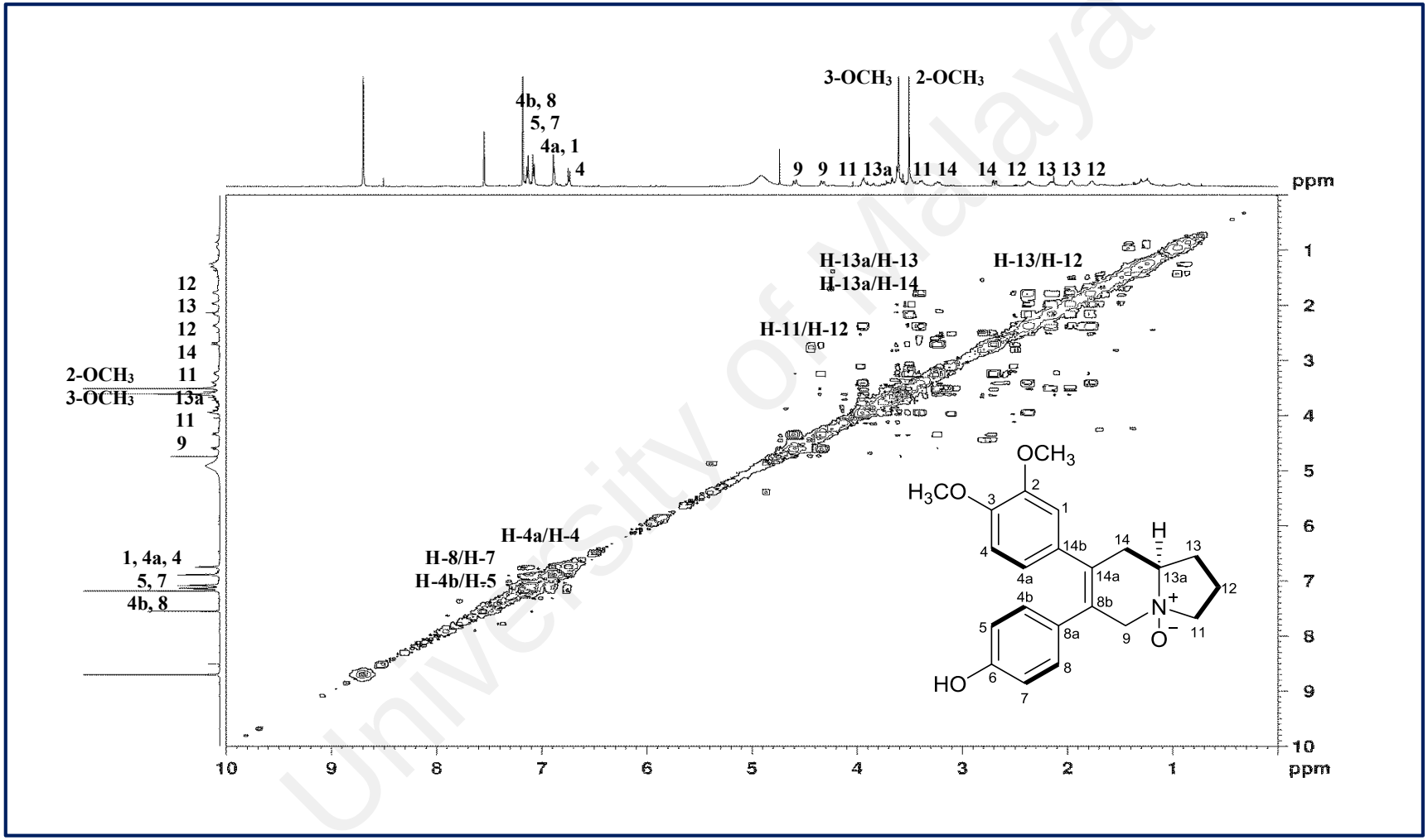

Figure 3.58: COSY spectrum of alkaloid **K**

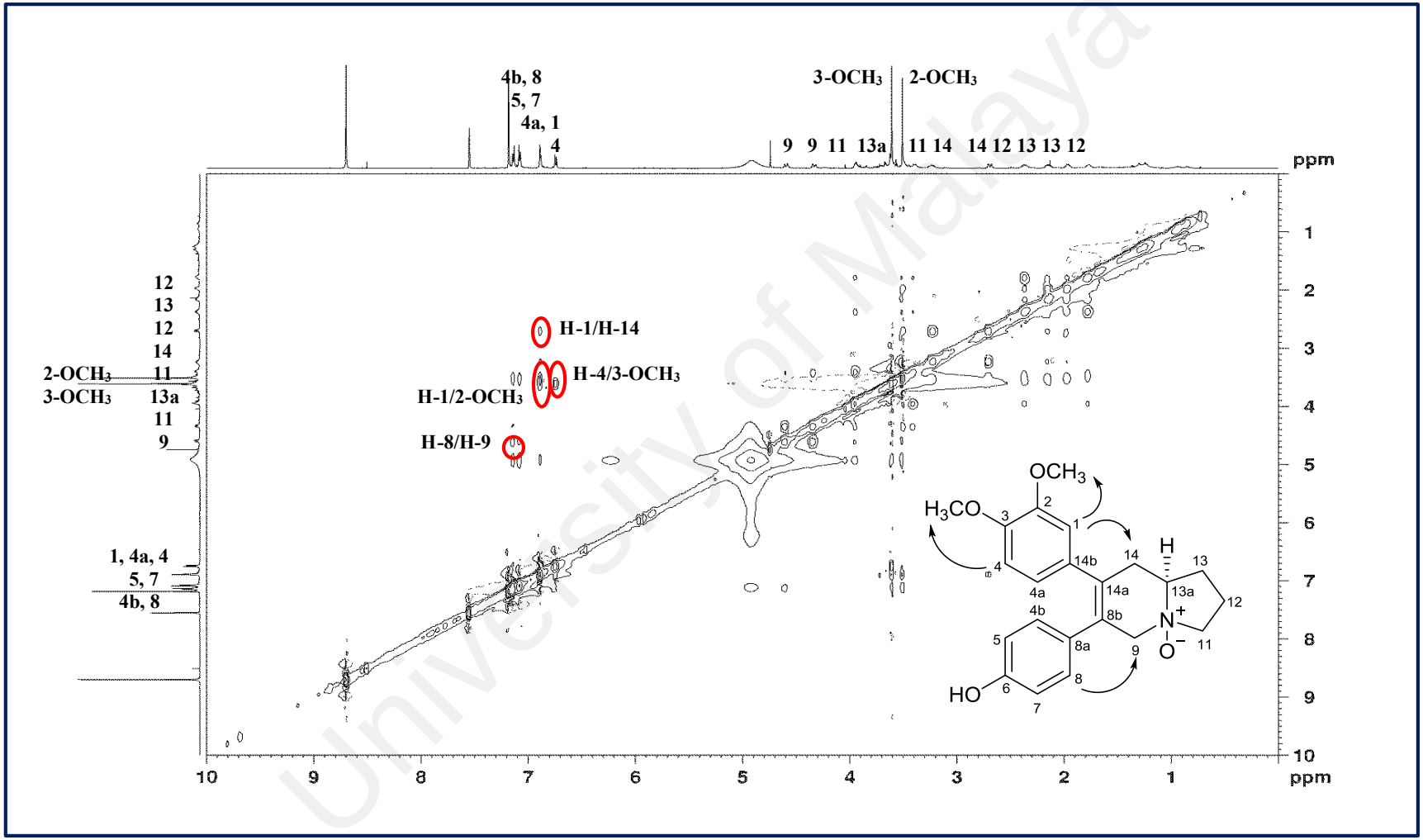

Figure 3.59: NOESY spectrum of alkaloid **K**

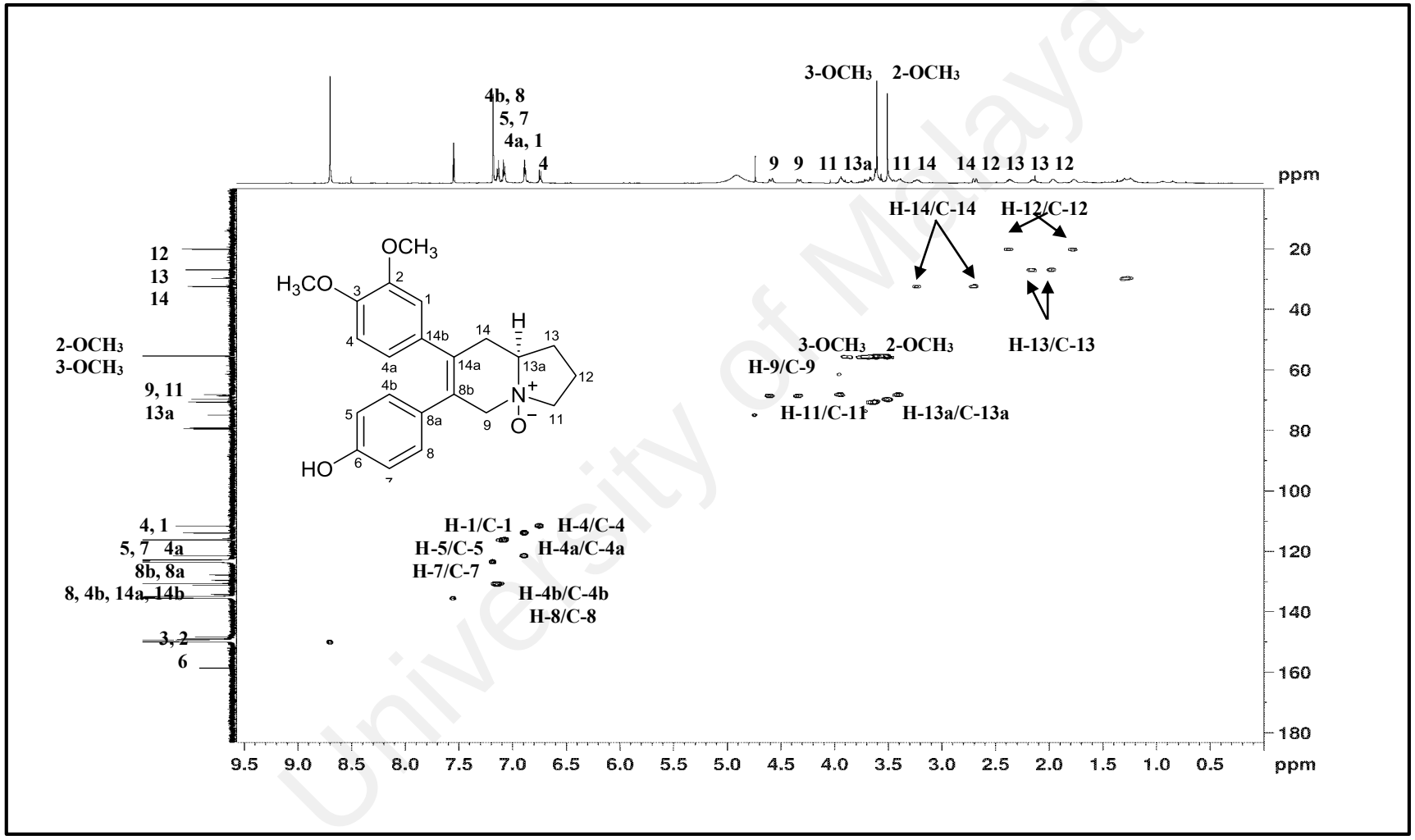

Figure 3.60: HSQC spectrum of alkaloid **K**

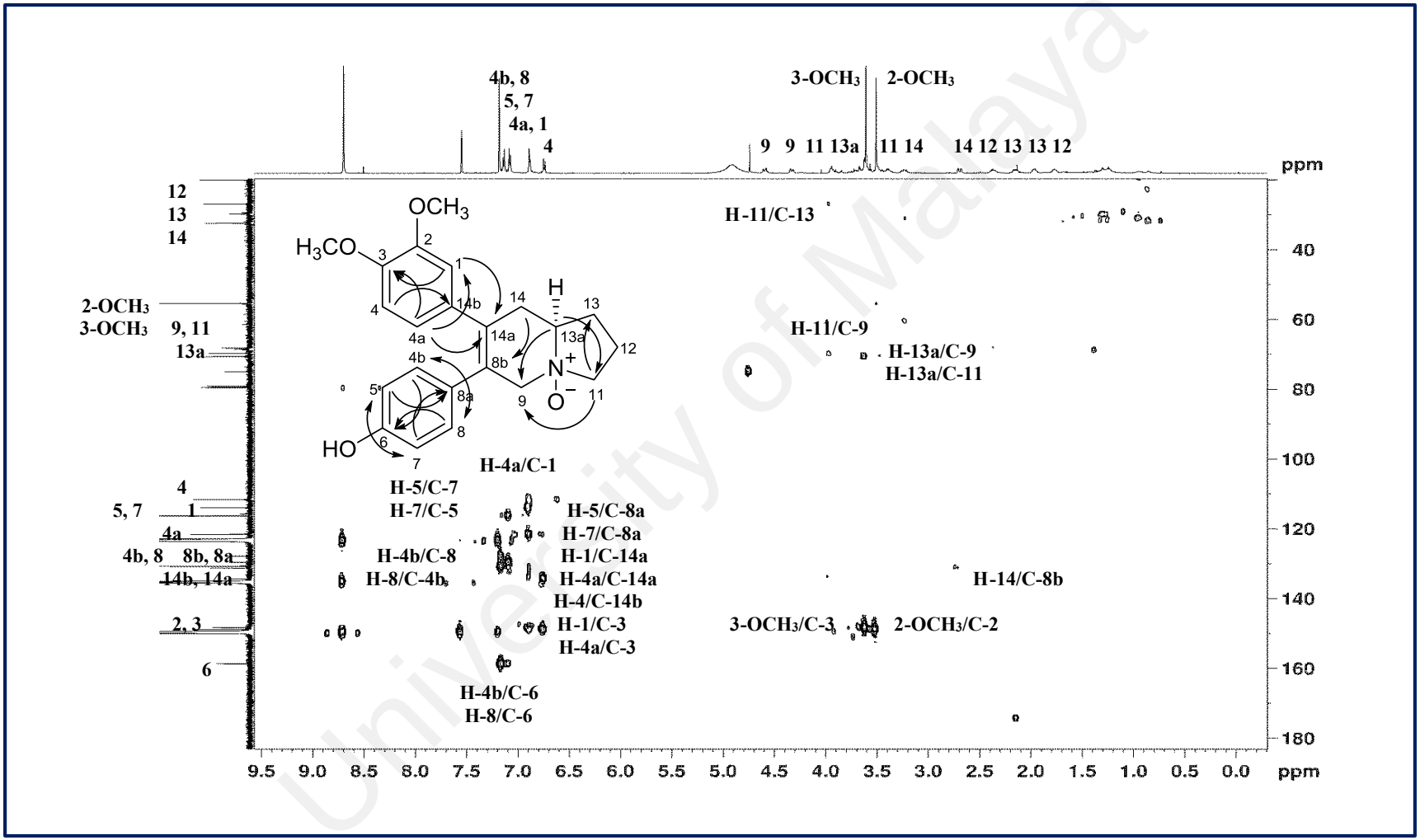

Figure 3.61: HMBC spectrum of alkaloid **K**

3.2.12 Alkaloid L: (+)-Reticuline 76

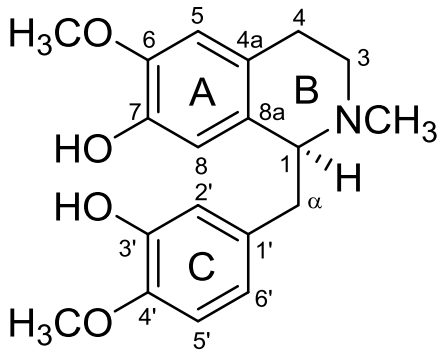

76

Alkaloid **L** was isolated as an optically active brownish amorphous with $[\alpha]_D^{25}$ + 55° (*c*=0.02, MeOH). Analysis of the LCMS-IT-TOF spectrum showed a pseudomolecular ion peak, $[M+H]^+$ at *m/z* 330.0860 suggesting a molecular formula of $C_{19}H_{23}NO_4$ (calcd. for $C_{19}H_{24}NO_4$, 330.1700), consistent with nine degrees of unsaturation. The UV spectrum showed characteristic absorption bands at λ_{max} 231 and 288 nm suggesting the presence of a benzylisoquinoline moiety (Shamma, 1972). Its IR spectrum showed strong absorption bands at ν_{max} 3299 and 1637 cm^{-1} corresponding to hydroxyl (OH) and C=C functional group, respectively.

The ^1H NMR spectrum (Figure 3.62) revealed a sharp singlet attributed to six protons of methoxyl signals at δ_H 3.85 which were attached to C-6 and C-4' respectively. Furthermore, the spectrum gave two doublets at δ_H 6.77 (1H, *d*, *J*=1.9 Hz) and 6.73 (1H, *d*, *J*=8.2 Hz) which belonged to H-2' and H-5' respectively. Doublet of doublets (*dd*) corresponding to H-6' was observed at δ_H 6.60 (1H, *dd*, *J*=8.2, 1.9 Hz). In addition, two singlets assignable to the isolated aromatic protons, H-5 and H-8 appeared at δ_H 6.54 and 6.41 respectively. An *N*-methyl proton resonating as singlet was observed at δ_H 2.45. The chemical shift values of the aliphatic proton appeared as multiplets in the region of δ_H

2.49-3.65. The COSY spectrum (Figure 3.64) showed that H-5' was correlated with H-6'while in a shielded area, H-3 correlated with H-4.

The ^{13}C NMR experiments (Figure 3.63) further confirmed the presence of a total nineteen carbon atoms which was in agreement with the molecular formula of alkaloid **L**. The HMBC spectrum (Figure 3.66) revealed correlations of H-1 to C-1' suggesting the connectivity of ring B with ring C. In addition, the correlations of H-8 to C-4a and H-5 to C-8a proved that ring A and ring B are fused together via C-4a and C-8a.

The complete assignments of the ^{1}H and ^{13}C NMR spectroscopic data of alkaloid **L** were achieved with the aid of the COSY, HSQC and HMBC experiments (Figure 3.64-3.66). All of the above mentioned spectroscopic data of alkaloid **L** were in accordance with those reported for (+)-reticuline **76** (Saidi et al., 2011b).

Table 3.13: ^{1}H NMR (400 MHz) and ^{13}C NMR (100 MHz) spectroscopic assignments of alkaloid **L** in $CDCl_3$

Position	δ_H (ppm, *J* in Hz)		δ_C (ppm)	
	Alkaloid **L**	Reticuline **76** (Castro, López, & Vergara, 1985) ($CDCl_3$)	Alkaloid **L**	(+)-Reticuline **76** (Saidi et al., 2011a) ($CDCl_3$)
1	3.65 (1H, *m*)	2.55-3.25 (1H, *m*)	64.5	64.5
3	α=2.57 (1H, *m*) β=3.16 (1H, *m*)	2.55-3.25 (2H, *m*)	46.9	46.5
4	α=2.49 (1H, *m*) β=2.74 (2H, *m*)	2.55-3.25 (2H, *m*)	25.2	24.7
4a	-	-	128.8	130.0
5	6.54 (1H, *s*)	6.54 (1H, *s*)	110.4	110.5
6	-	-	144.9	145.3
7	-	-	143.3	143.3
8	6.41 (1H, *s*)	6.39 (1H, *s*)	113.6	113.7
8a	-	-	125.6	124.7
α	α=2.62 (1H, *dd*, *J*=14.0, 6.9) β=3.01 (1H, *dd*, *J*=14.0, 6.9)	2.55-3.25 (2H, *m*)	41.0	40.9
1’	-	-	133.5	132.7
2’	6.77 (1H, *d*, *J*=1.9)	6.77 (1H, *d*, *J*=1.5)	115.6	115.6
3’	-	-	145.1	145.1
4’	-	-	145.2	145.3
5’	6.73 (1H, *d*, *J*=8.2)	6.73 (1H, *d*, *J*=8.0)	110.6	110.4
6’	6.60 (1H, *dd*, *J*=8.2, 1.9)	6.60 (1H, *dd*, *J*=8.0, 1.5)	120.9	120.9
NCH_3	2.45 (3H, *s*)	2.47 (3H, *s*)	42.6	42.1
6-OCH_3	3.85 (3H, *s*)	3.85 (3H, *s*)	55.9	55.8
4’-OCH_3	3.85 (3H, *s*)	3.85 (3H, *s*)	55.9	55.8

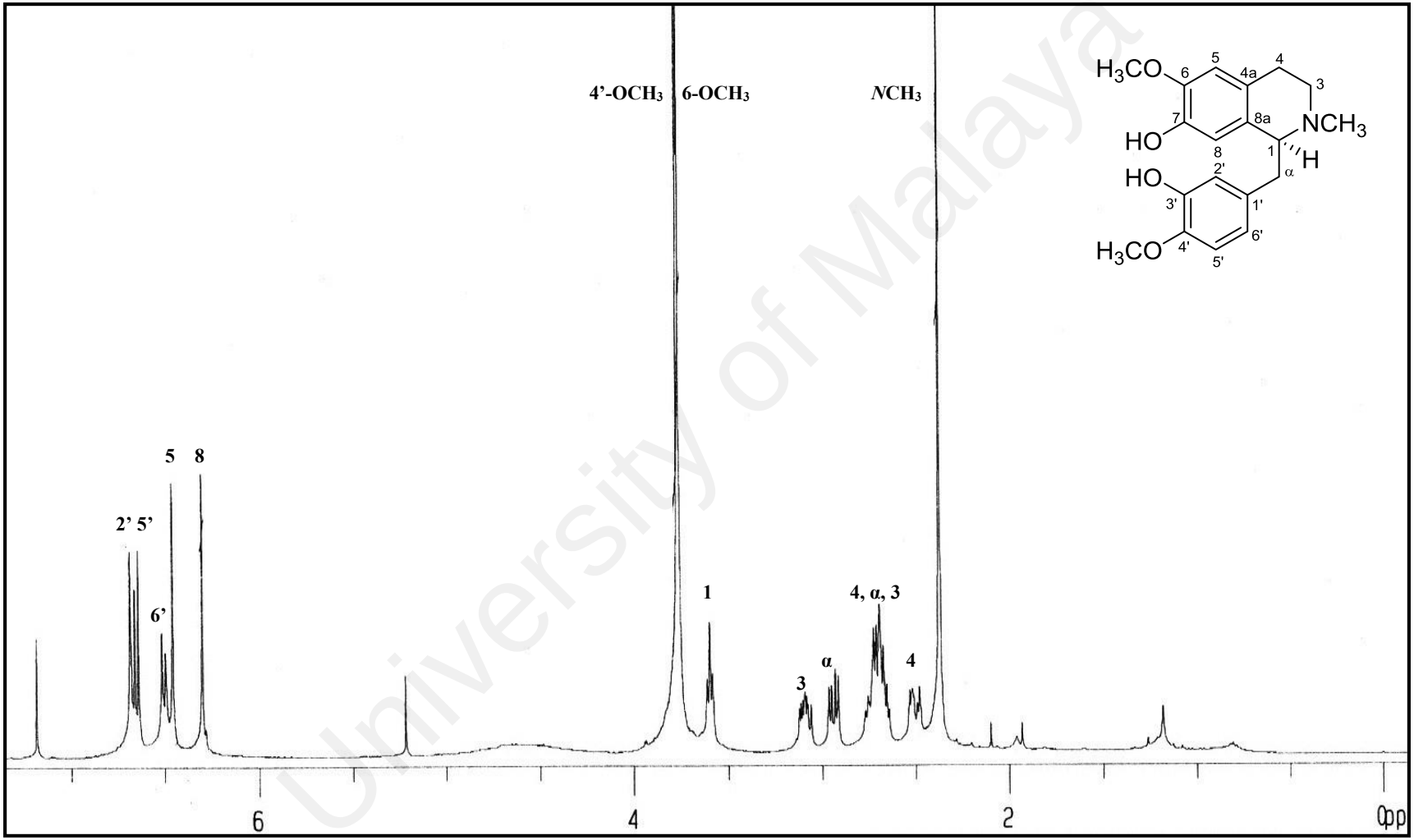

Figure 3.62: ^{1}H NMR spectrum of alkaloid **L**

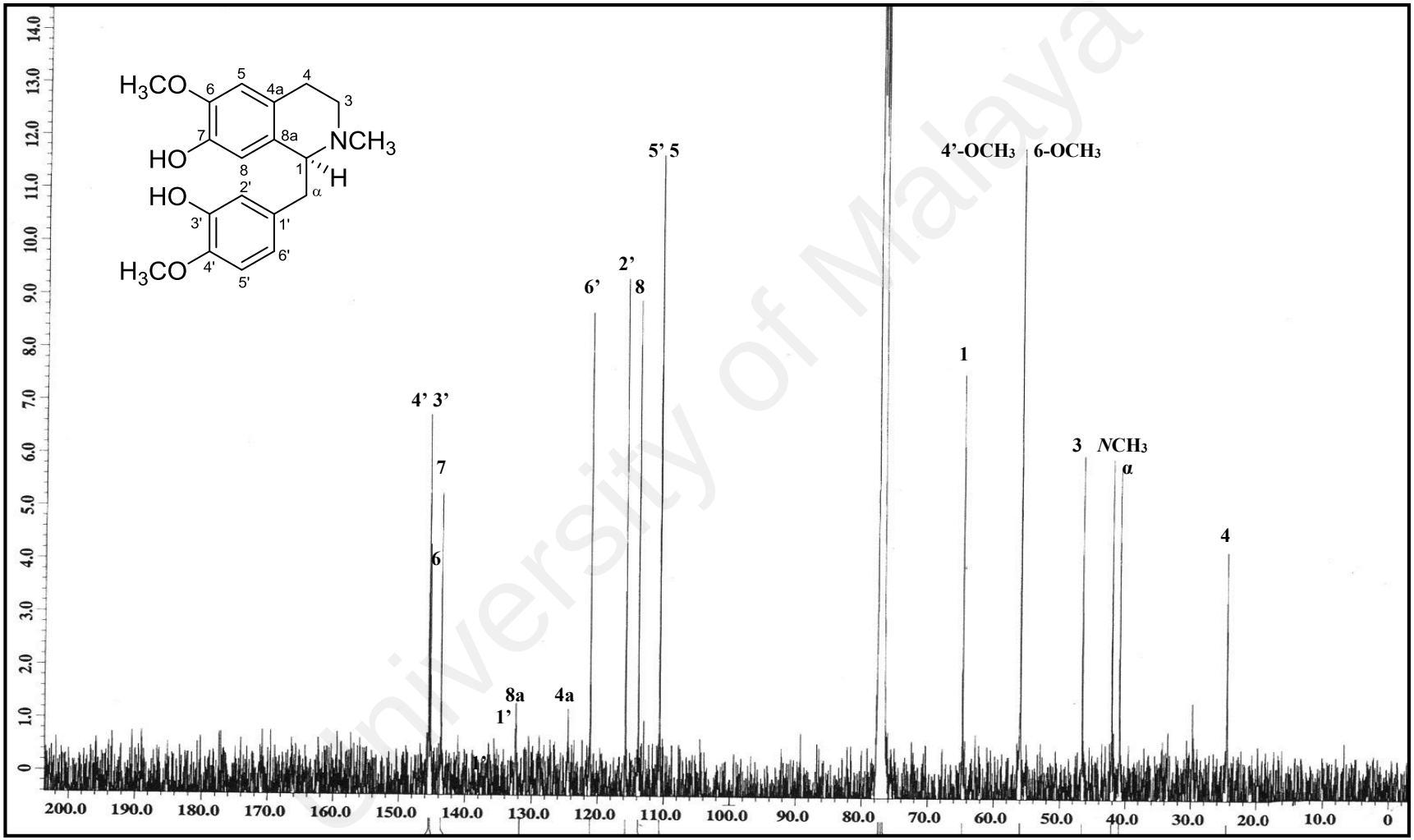

Figure 3.63: ^{13}C NMR spectrum of alkaloid **L**

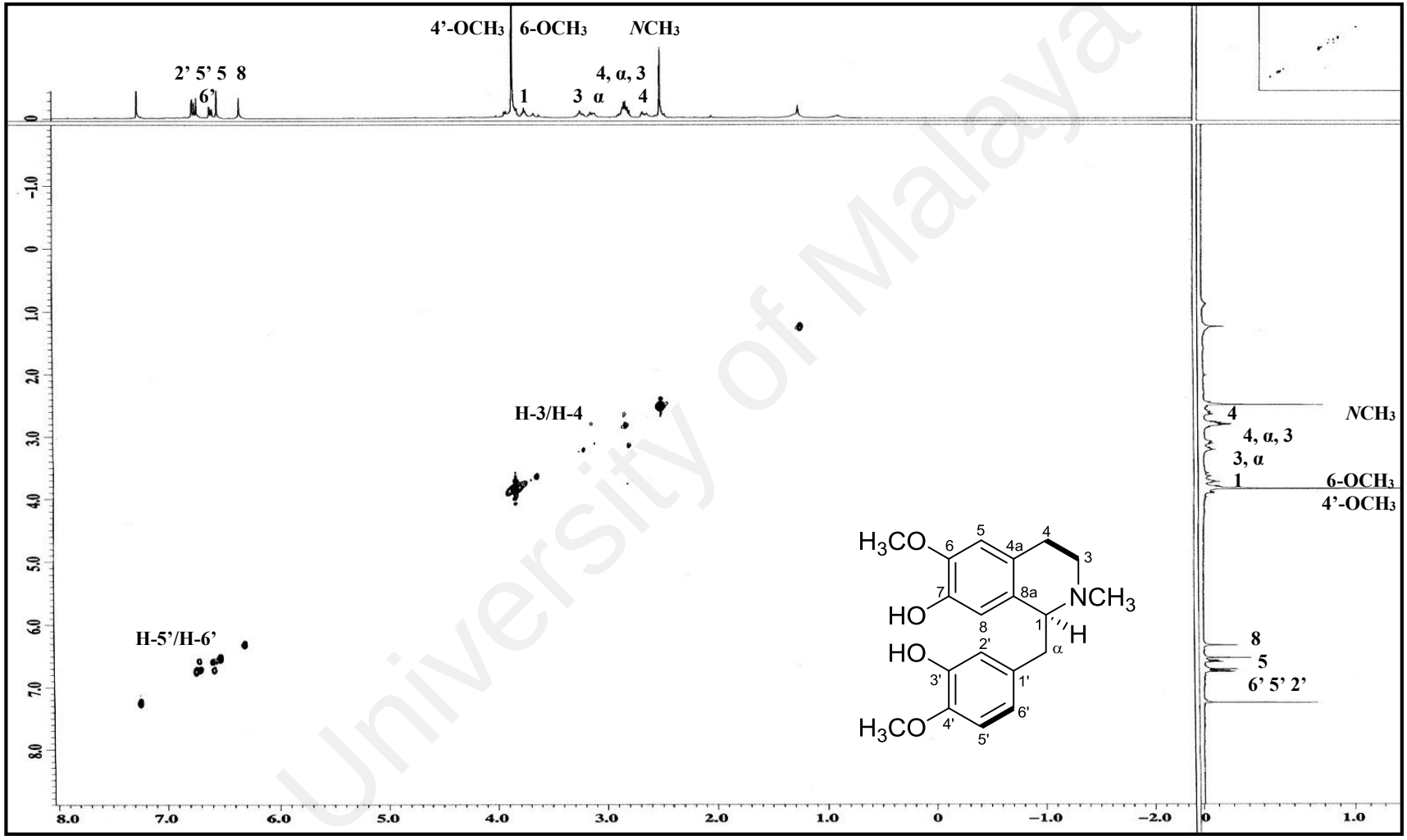

Figure 3.64: COSY spectrum of alkaloid **L**

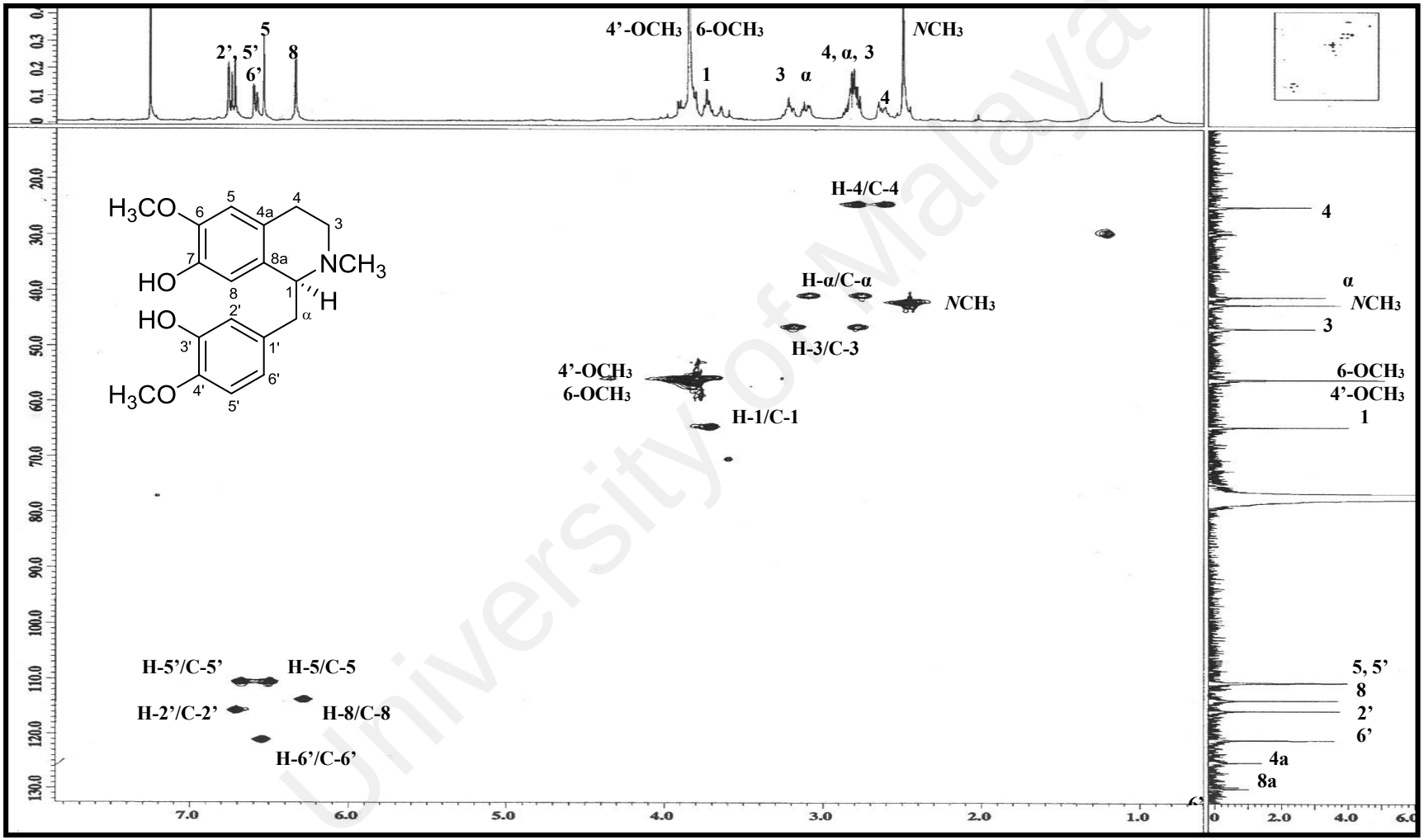

Figure 3.65: HSQC spectrum of alkaloid

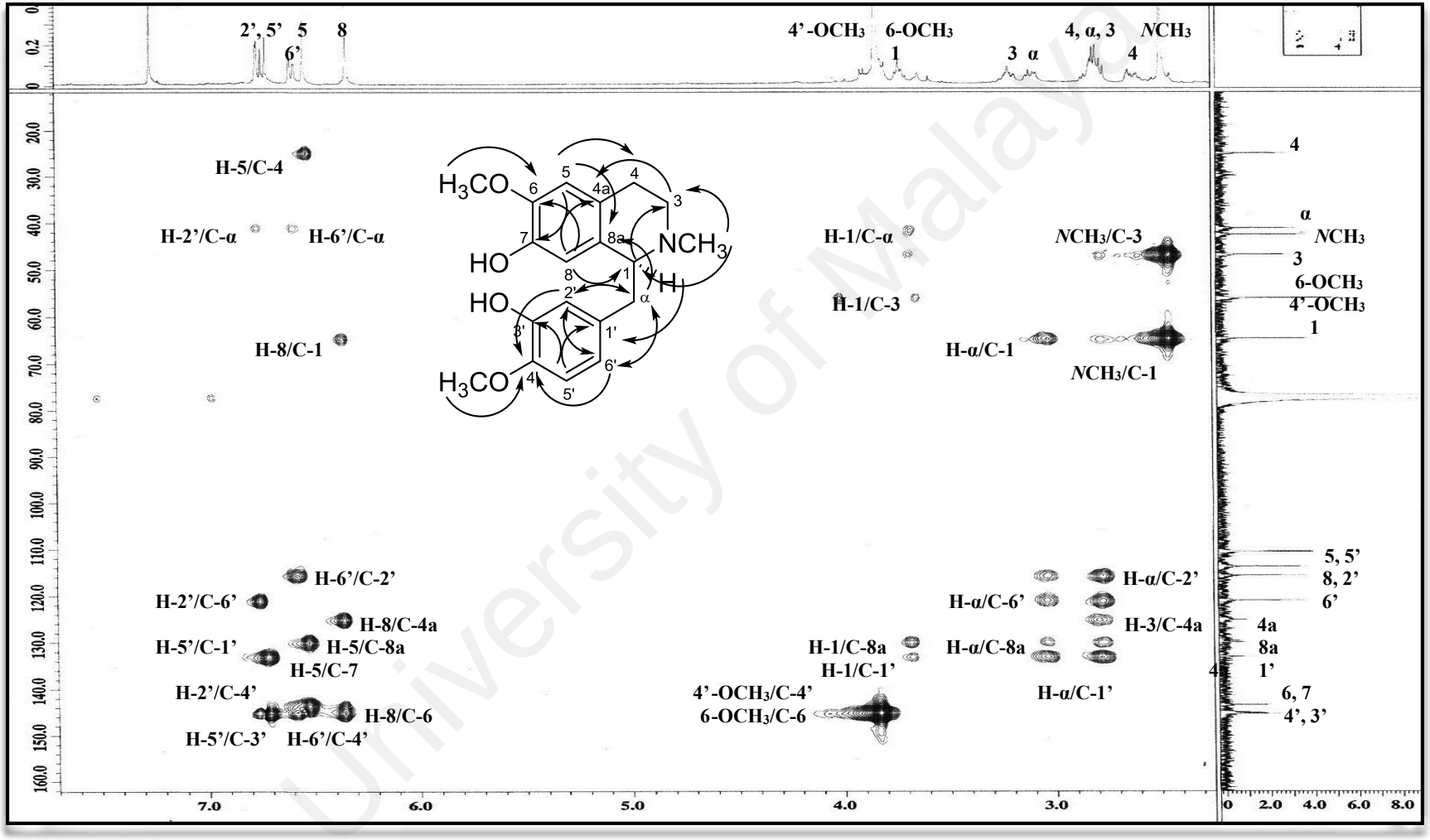

Figure 3.66: HMBC spectrum of alkaloid **L**

3.2.13 Alkaloid M: Crychine 134

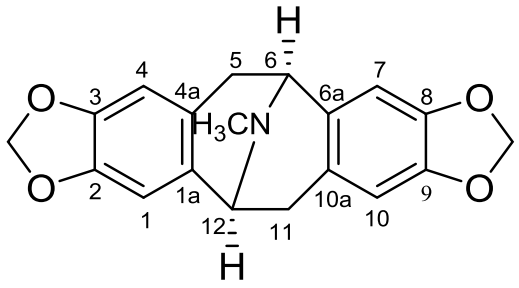

134

Alkaloid **M** was isolated as an optically inactive brownish amorphous. The positive LCMS-IT-TOF analysis revealed a pseudomolecular ion peak $[M+H]^+$ at *m/z* 324.1216 (calcd. for $C_{19}H_{18}NO_4$, 324.1230), corresponding to a molecular formula of $C_{19}H_{17}NO_4$, thus, implying twelve degrees of unsaturation. The UV spectrum showed absorptions at λ_{max} 238, 290 and 294 nm. The presence of a methylenedioxy group in IR spectrum was proven by its characteristic absorption at ν_{max} 1040 and 936 cm^{-1}.

Analysis of ^1H NMR spectrum (Figure 3.67) revealed two overlapped aromatic singlets at δ_H 6.42 and 6.57 which could be belonged to H-4/10 and H-1/7 respectively. AMX patterns at δ_H 3.96 (1H, *d*, *J*=5.8 Hz, H-6, H-12), 2.54 (1H, *d*, *J*=16.4 Hz, H-5α/H-11α), 3.36 (1H, *dd*, *J*=16.4, 5.8 Hz, H-5β, H-11β) and OCH_2O signals at δ_H 5.84 (2H, *dd*, *J*=18.1, 1.5 Hz) indicated a highly symmetrical pavine structure (T.-S. Wu & Lin, 2001). In addition, the *N*C<u>H</u>$_3$ group resonated as a singlet at δ_H 2.51. The assignment of protons was further ascertained by a complete COSY experiment (Figure 3.70). The spectrum showed the correlations between H-5/H-6 and H-11/H-12.

The ^{13}C NMR (Figure 3.68) and DEPT (Figure 3.69) spectrum revealed the presence of ten signals attributed to nineteen carbons. Two of them were *N*<u>C</u>H$_3$ (δ_C 40.9) and overlapped O<u>C</u>H$_2$O (δ_C 100.7), and the rest were overlapped carbon signals which corresponded to C-5/C-11 (δ_C 34.1), C-6/C-12 (δ_C 56.7), C-1/C-7 (δ_C 107.1), C-4/C-10

(δ_C 108.7), C-4a/C-10a (δ_C 124.9), C-1a/C-6a (δ_C 130.9), C-2/C-8 (δ_C 146.1) and C-3/C-9 (δ_C 146.5) due to their equivalent environment. The symmetrical of this compound clearly shown by cross-peaks seen in HMBC spectrum (Figure 3.72). For instance, H-1/H-7 correlated to C-3, C-4a, or C-9, C-10a respectively.

From the analysis of the spectroscopic data obtained (Table 3.14) and comparison with its close analogue, (-)-*N*-demethylcrychine **47**, the structure of crychine **134** was established without doubt.

Table 3.14: ^{1}H NMR (400 MHz) and ^{13}C NMR (100 MHz) spectroscopic assignments of alkaloid **M** in $CDCl_3$

Position	**δ_H (ppm, *J* in Hz)**		**δ_C (ppm)**	
	Alkaloid **M**	(-)-*N*-demethyl crychine **47** (T.-S. Wu & Lin, 2001) ($CDCl_3$, 400 MHz)	Alkaloid **M**	Crychine **134** (Lee, Liu, & Chen, 1989) ($CDCl_3$, 75.47, MHz)
1	6.57 (1H, *s*)	6.58 (1H, *s*)	107.1	106.7
1a	-	-	130.9	130.7
2	-	-	146.1	145.8
3	-	-	146.4	146.1
4	6.42 (1H, *s*)	6.42 (1H, *s*)	108.7	108.3
4a	-		124.9	124.6
5	α=2.54 (1H, *d*, *J*=16.4) β=3.36 (1H, *dd*, *J*=16.4, 5.8)	α=2.68 (1H, *d*, *J*=14.3) β=3.35 (1H, *dd*, *J*=14.3, 5.5)	34.1	33.8
6	3.96 (1H, *d*, *J*=5.8)	4.42 (1H, *d*, *J*=5.5)	56.7	56.4
6a	-	-	130.9	130.7
7	6.57 (1H, *s*)	6.58 (1H, *s*)	107.1	106.7
8	-	-	146.1	145.8
9	-	-	146.4	146.1
10	6.42 (1H, *s*)	6.42 (1H, *s*)	108.7	108.3
10a	-		124.9	124.6
11	α=2.54 (1H, *d*, *J*=16.4) β=3.36 (1H, *dd*, *J*=16.4, 5.8)	α=2.68 (1H, *d*, *J*=14.3) β=3.35 (1H, *dd*, *J*=14.3, 5.5)	34.1	33.8
12	3.96 (1H, *d*, *J*=5.8)	4.42 (1H, *d*, *J*=5.5)	56.7	56.4
6, 12-*N*CH_3	2.51 (3H, *s*)	-	40.9	40.4
2, 3 and 8, 9-OCH_2O	5.84 (2H, *dd*, *J*=18.1, 1.5)	5.84 (2H, *d*, *J*=1.6)	100.7	100.3

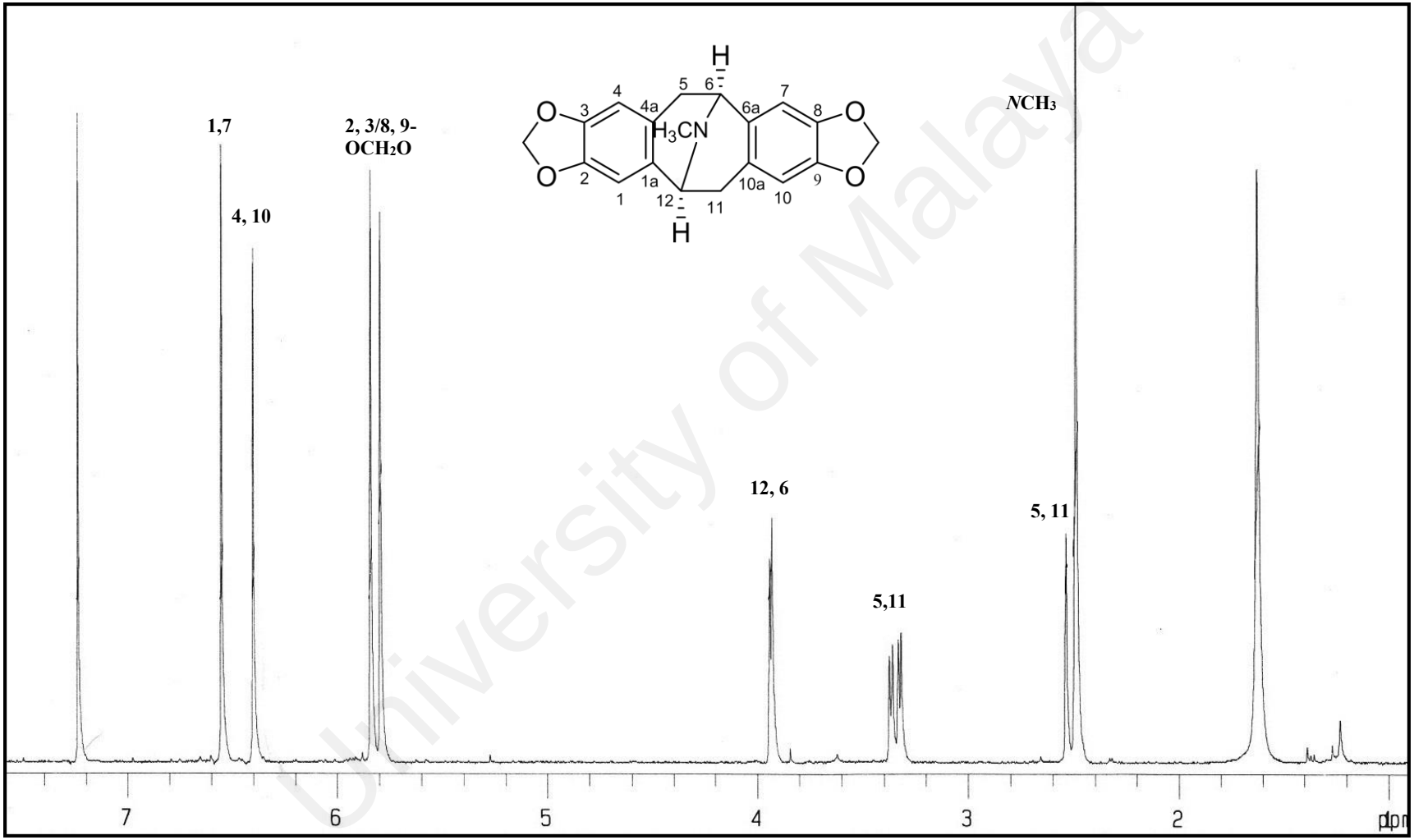

Figure 3.67: ^{1}H NMR spectrum of alkaloid **M**

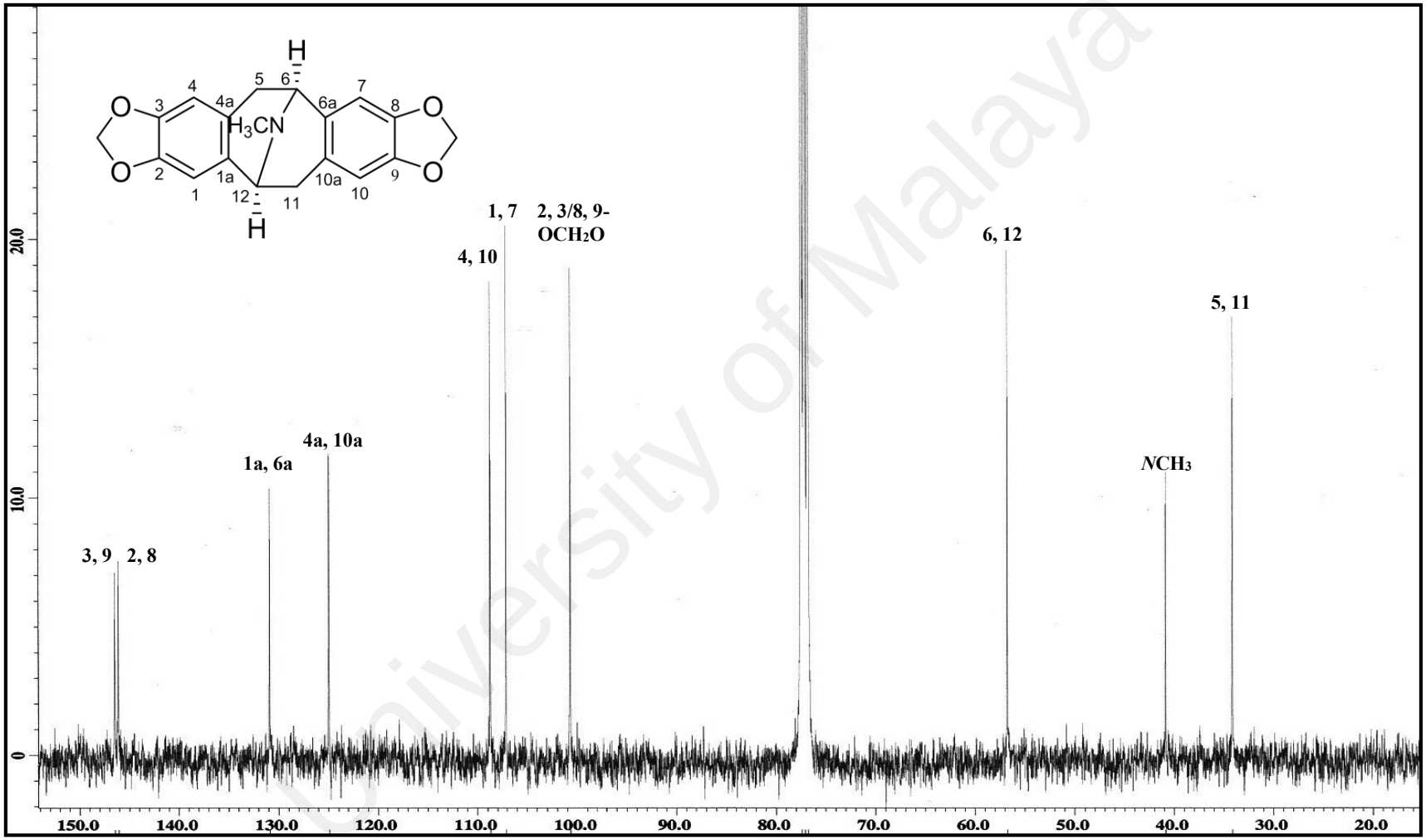

Figure 3.68: ^{13}C NMR spectrum of alkaloid **M**

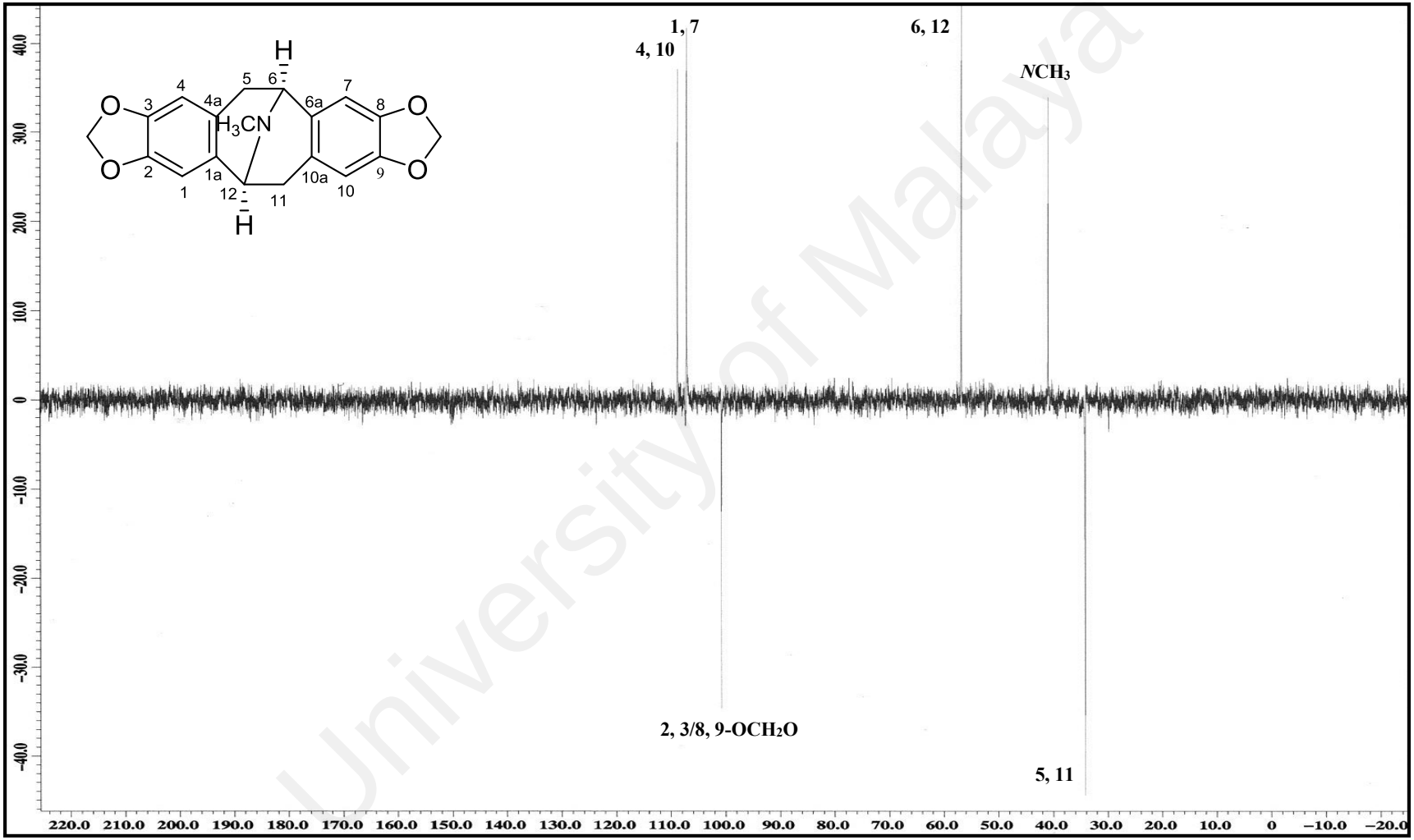

Figure 3.69: DEPT spectrum of alkaloid **M**

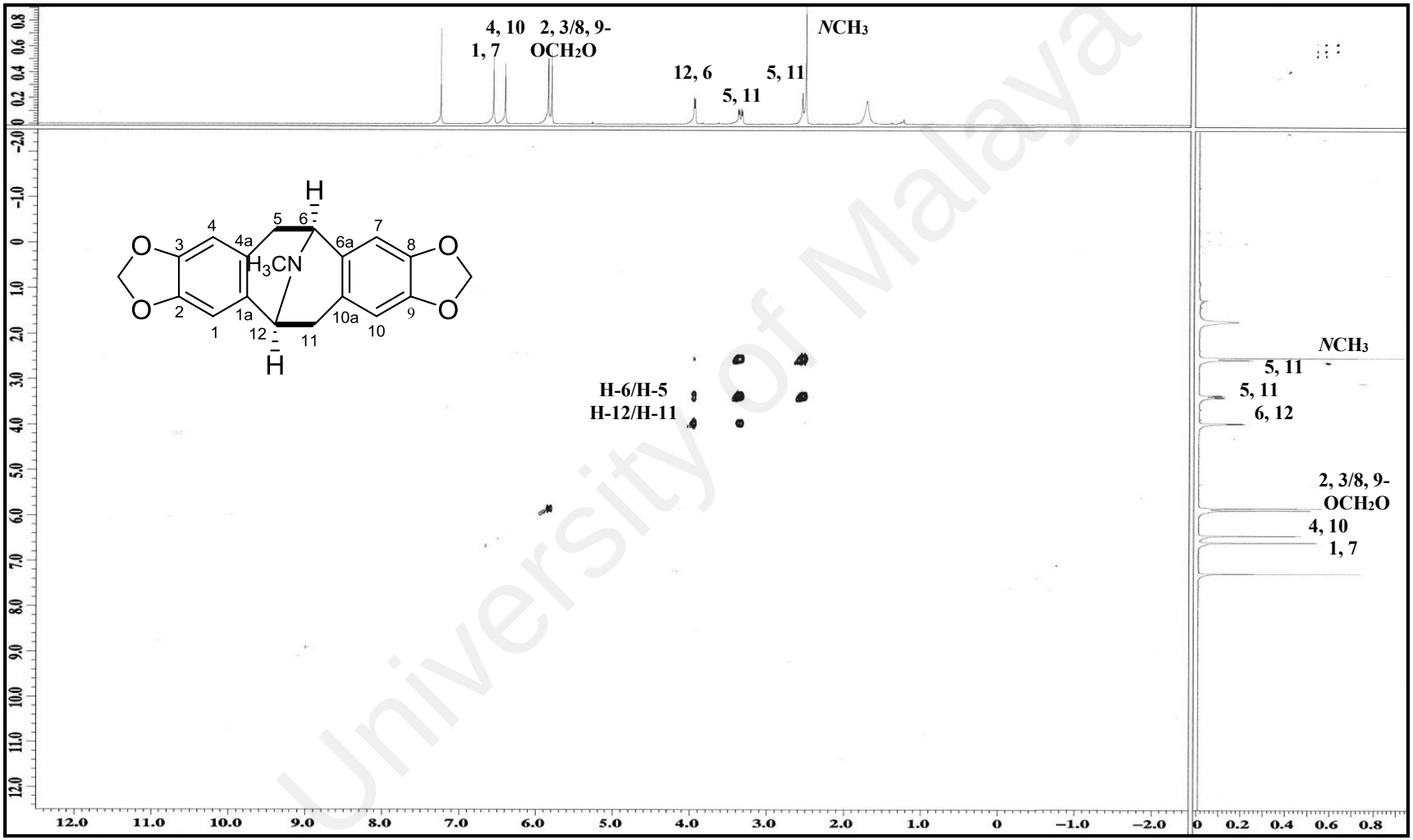

Figure 3.70: COSY spectrum of alkaloid **M**

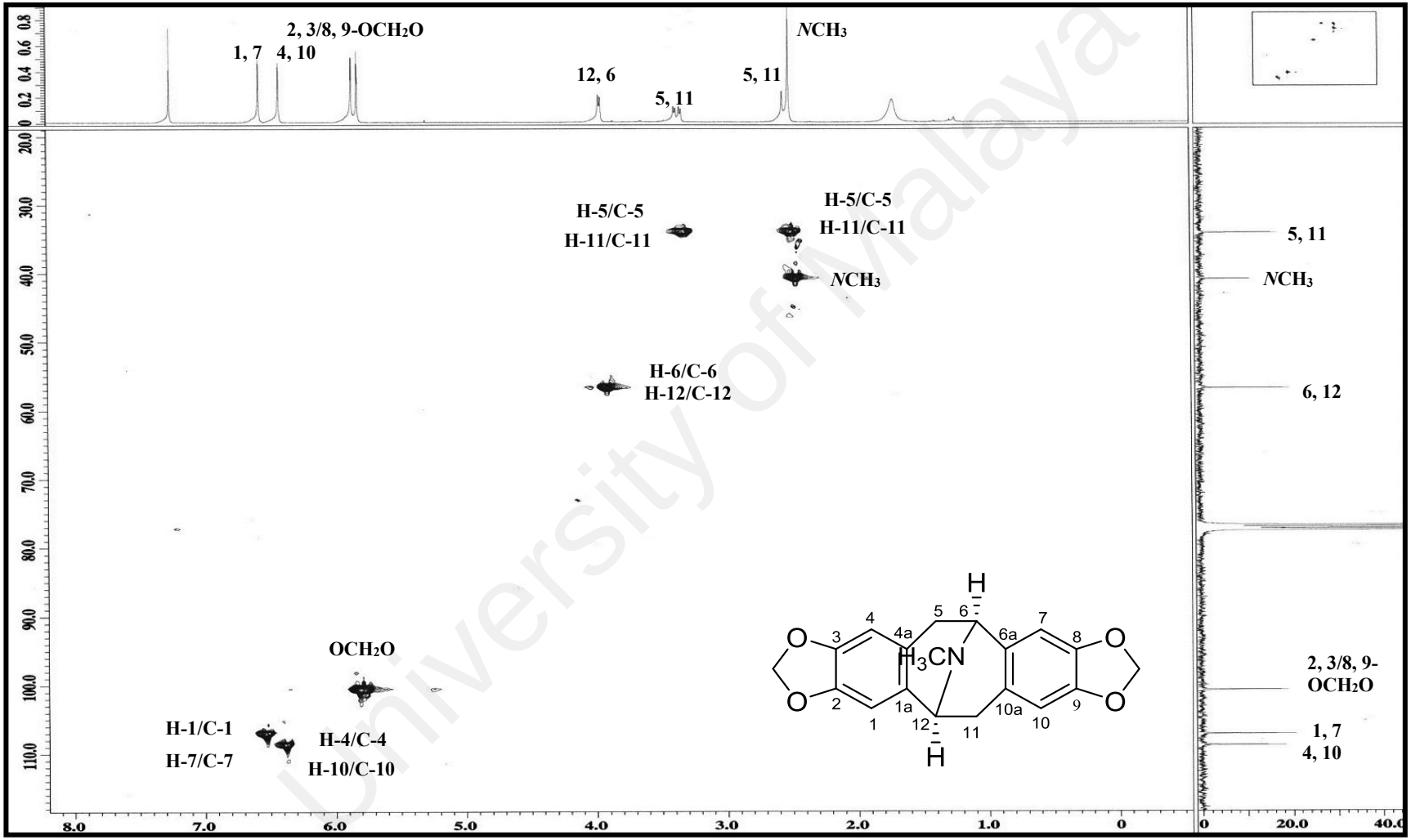

Figure 3.71: HSQC spectrum of alkaloid **M**

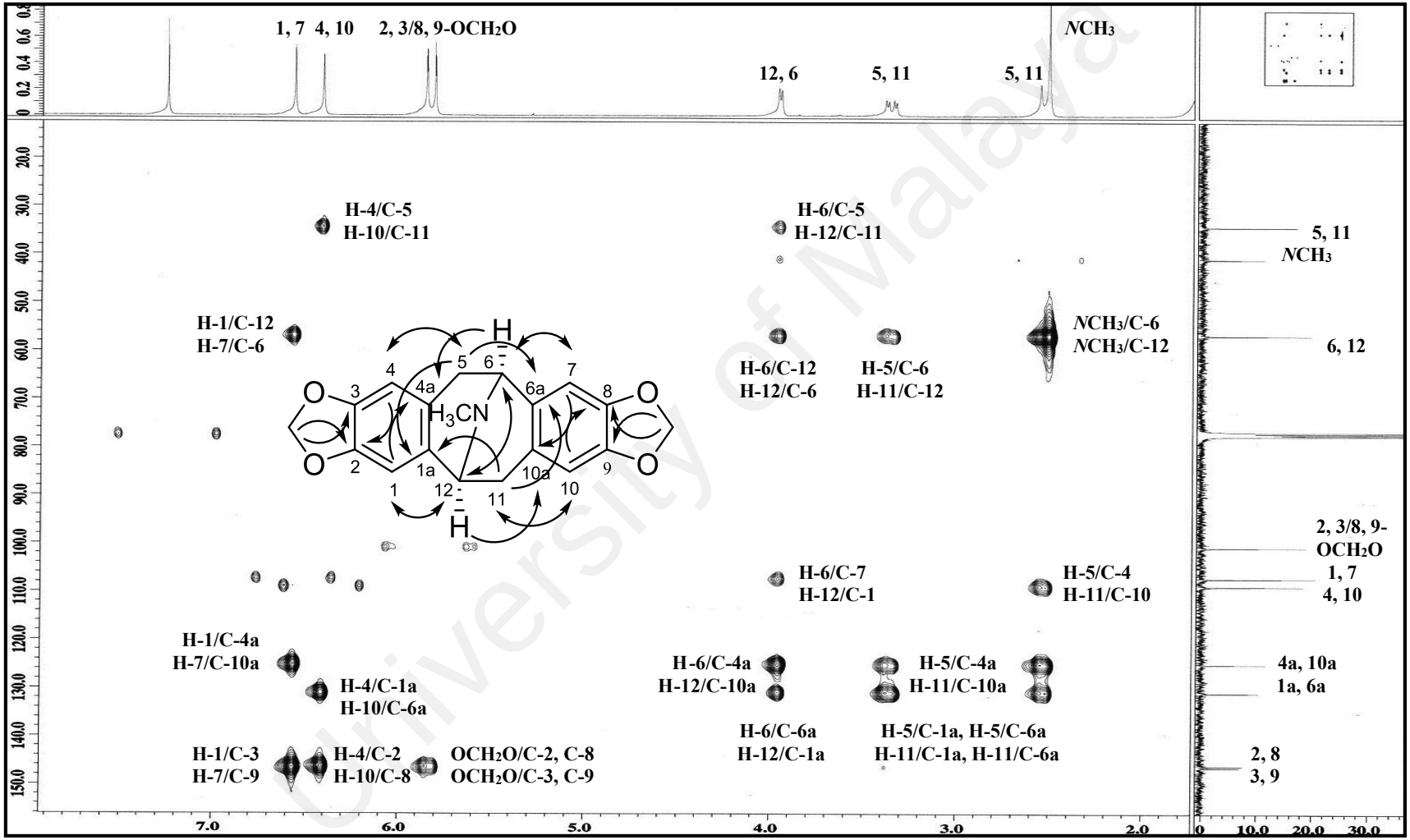

Figure 3.72: HMBC spectrum of alkaloid **M**

3.2.14 Alkaloid N: (-)-Isocaryachine 61

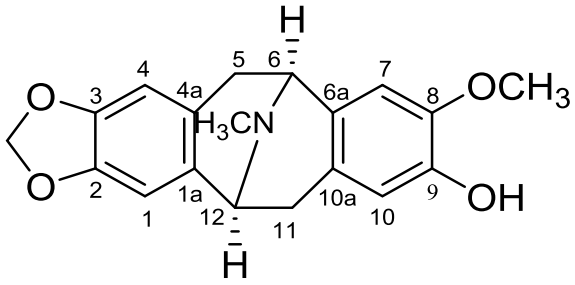

61

Alkaloid **N** was purified as a dark brownish amorphous with $[\alpha]_D^{25}$ –125 (*c*=0.02, MeOH). The LCMS-IT-TOF spectrum exhibited a pseudomolecular ion peak, $[M+H]^+$ at *m/z* 326.1000 (calcd. for $C_{19}H_{20}NO_4$, 326.1387), suggesting a molecular formula of $C_{19}H_{19}NO_4$ which corresponded with eleven degrees of unsaturation. The UV spectrum exhibited absorptions at λ_{max} 280 and 283 nm indicated the presence of a phenolic function. The IR spectrum showed absorption at ν_{max} 3436 cm^{-1} due to the presence of a hydroxyl group in the structure. The presence of a methylenedioxy group was proven by its characteristic absorptions at 1230 and 925 cm^{-1}.

Alkaloid **N** displayed similar ^1H (Figure 3.73) and ^{13}C (Figure 3.74) NMR spectral features with those of alkaloid **M**. However, the only difference was the presence of methoxyl and hydroxyl group at C-8 and C-9 replacing the methylenedioxy group in alkaloid **M**. The methoxyl group was resonated as a singlet at δ_H 3.84.

Analysis of the ^{13}C NMR spectrum (Figure 3.74) was in agreement with the molecular formula deduced from the mass spectrum, accounting for all nineteen carbons. The O<u>C</u>H_3 and O<u>C</u>H_2O groups were resonated at δ_C 55.7 and 100.3 respectively.

Based on the above findings and other spectroscopic data available, alkaloid **N** was identified as (-)-isocaryachine **61**.

Table 3.15: ^{1}H NMR (400 MHz) and ^{13}C NMR (100 MHz) spectroscopic assignments of alkaloid **N** in $CDCl_3$

Position	δ_H (ppm, *J* in Hz)		δ_C (ppm)	
	Alkaloid **N**	Isocaryachine-*N*-oxide **58** (Lin, Wang, & Wu, 2002) (CD_3OD, 400 MHz)	Alkaloid **N**	Isocaryachine **61** (Lee, Liu, & Chen, 1990) ($CDCl_3$, 20.14 MHz)
1	6.57 (1H, *d*, *J*=4.1)	6.69 (1H, *s*)	106.8	106.8
1a	-	-	130.9	131.0
2	-	-	145.7	145.8
3	-	-	146.0	146.1
4	6.48 (1H, *s*)	6.48 (1H, *s*)	108.4	108.4
4a	-	-	124.3	124.9
5	α=2.55 (1H, *d*, *J*=16.1) β=3.35 (1H, *dd*, *J*=16.1, 5.8)	α= 2.77 (1H, *d*, *J*=16.4) β= 3.91 (1H, *dd*, *J*=16.4, 5.6)	34.2	34.2
6	3.96 (1H, *d*, *J*=5.8)	4.54 (1H, *d*, *J*=5.6)	56.5	56.2
6a	-		129.0	129.0
7	6.57 (1H, *d*, *J*=4.1)	6.83 (1H, *s*)	109.0	109.6
8	-	-	145.0	145.6
9	-	-	144.2	144.7
10	6.44 (1H, *s*)	6.49 (1H, *s*)	114.2	114.8
10a	-	-	124.7	124.4
11	α=2.55 (1H, *d*, *J*=16.1) β=3.35 (1H, *dd*, *J*=16.1, 5.8)	α= 2.99 (1H, *d*, *J*=17.6) β= 3.54 (1H, *dd*, *J*=17.6, 5.6)	32.9	33.0
12	3.96 (1H, *d*, *J*=5.8)	4.52 (1H, *d*, *J*=5.6)	56.1	56.7
NCH_3	2.51 (3H, *s*)	3.26 (3H, *s*)	40.6	40.5
8-OCH_3	3.84 (3H, *s*)	3.84 (3H, *s*)	55.7	55.8
2, 3-OCH_2O	5.83 (2H, *dd*, *J*=20.8, 1.5)	5.90 (2H, *d*, *J*=1.2)	100.3	100.3

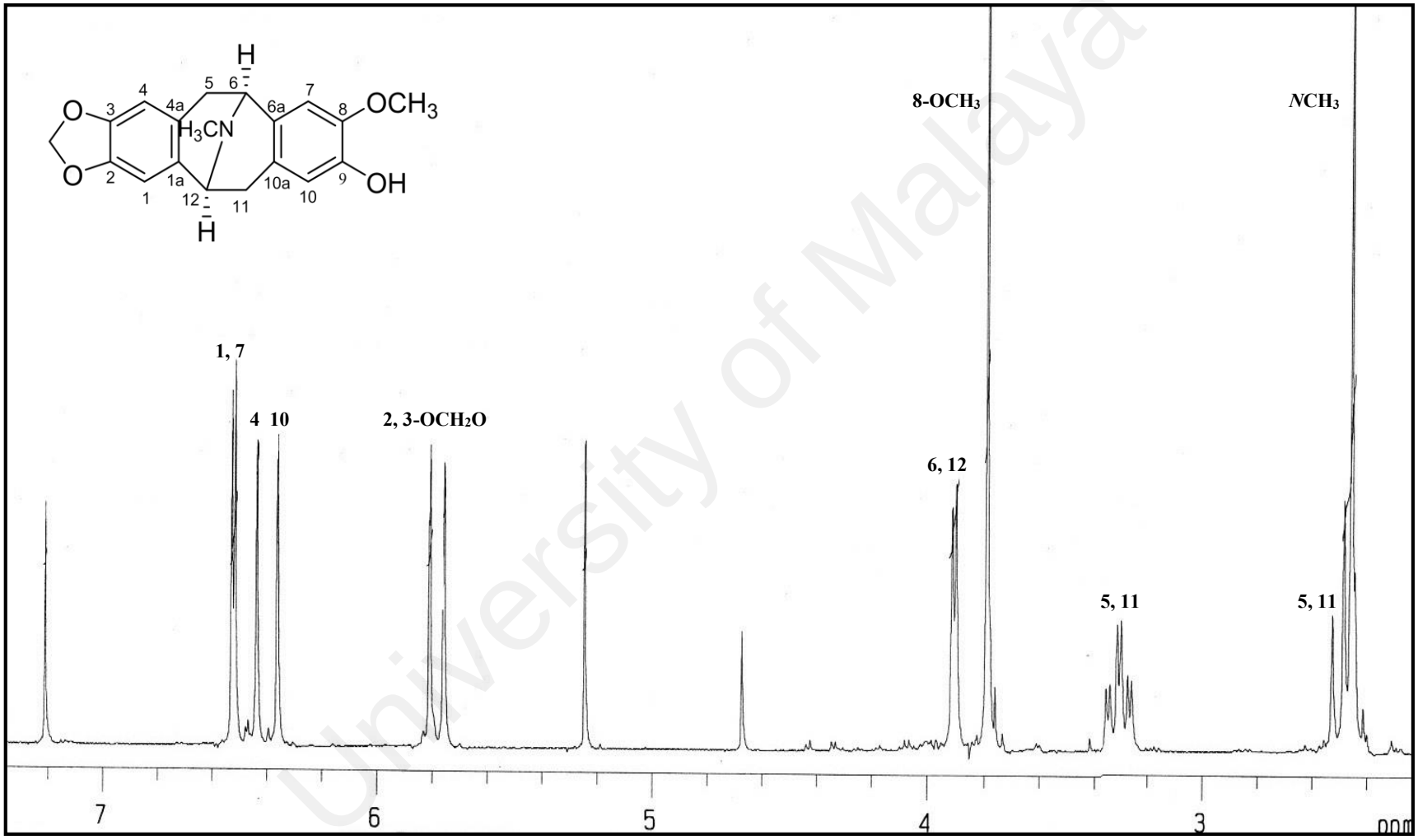

Figure 3.73: ^{1}H NMR spectrum of alkaloid **N**

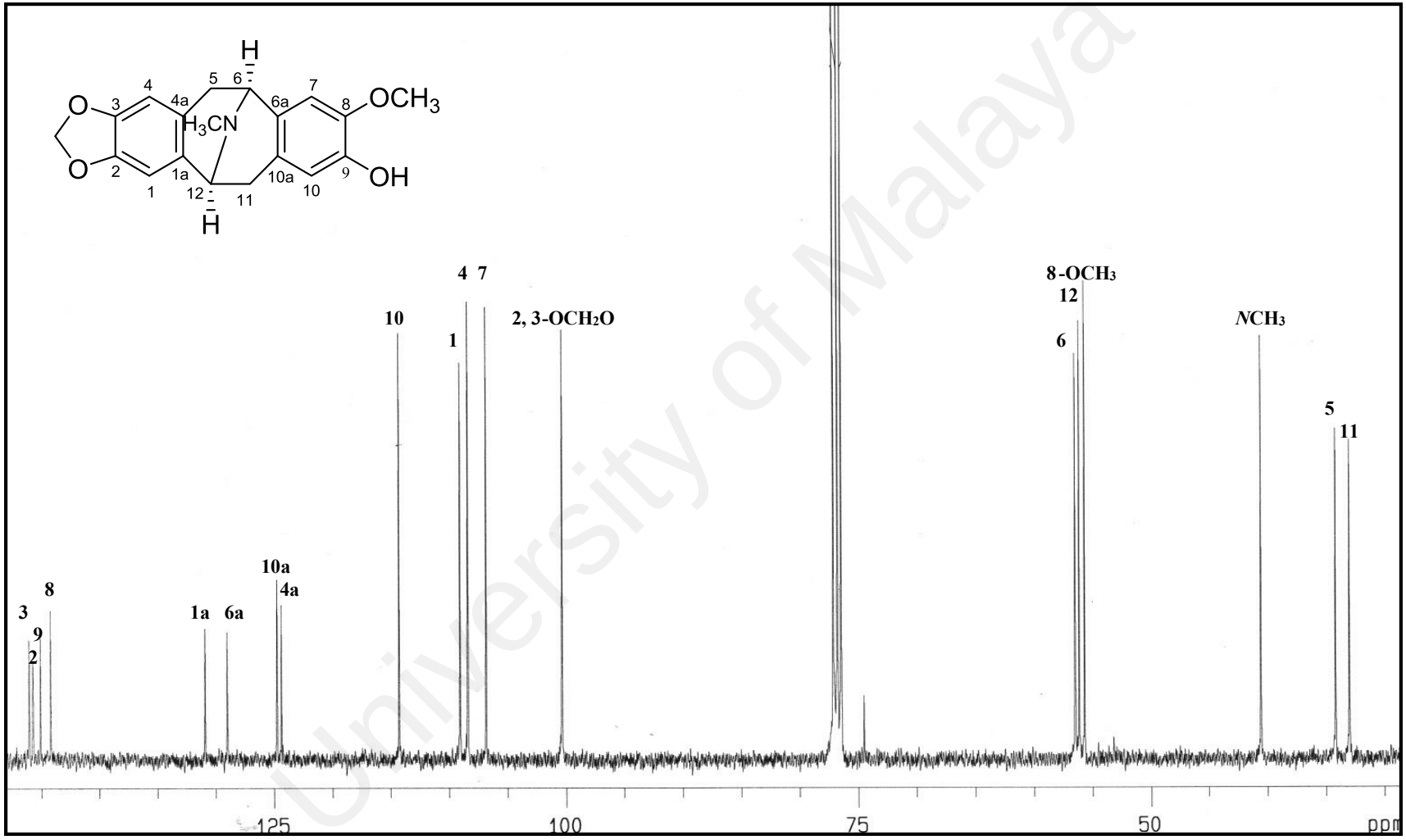

Figure 3.74: ^{13}C NMR spectrum of alkaloid **N**

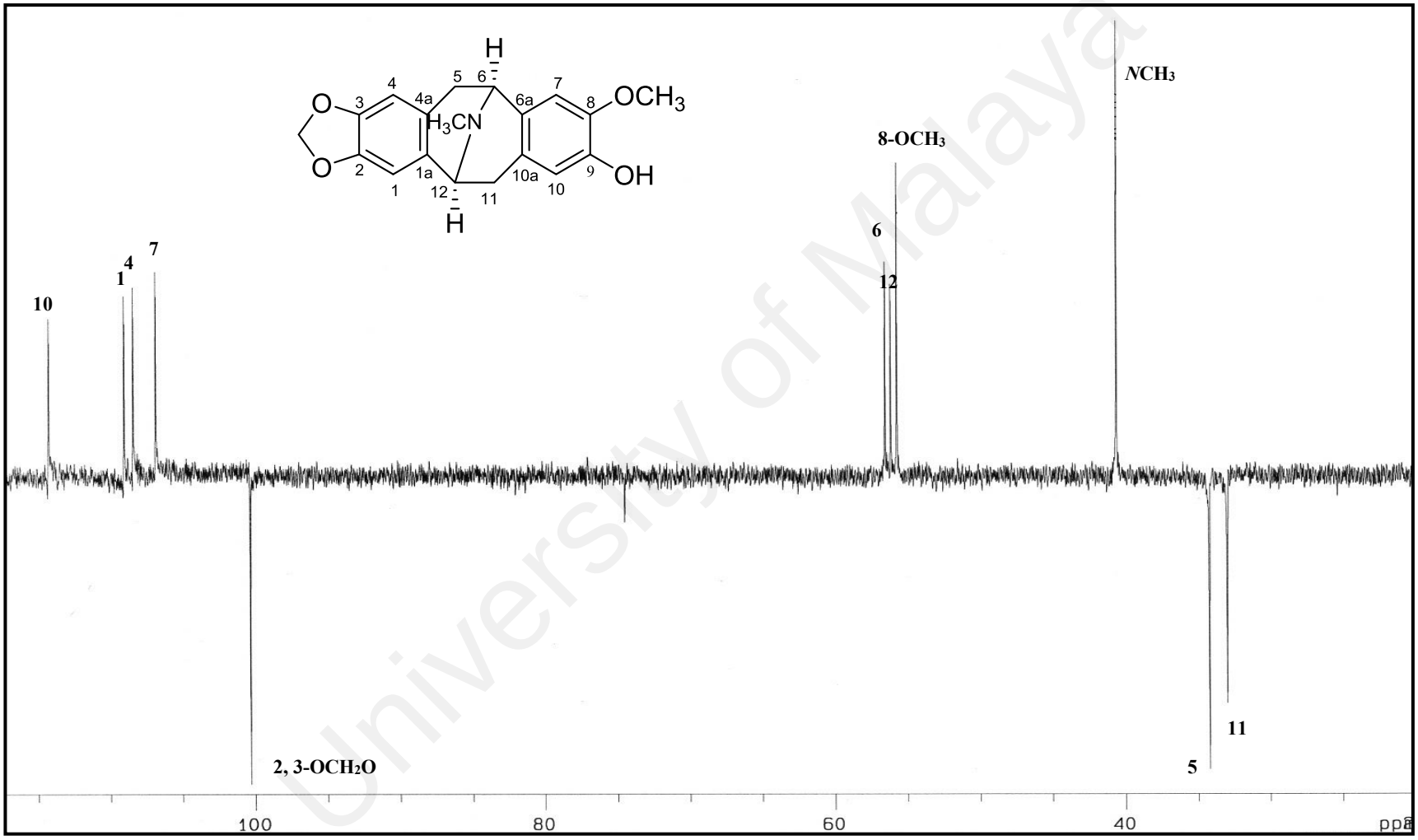

Figure 3.75: DEPT spectrum of alkaloid **N**

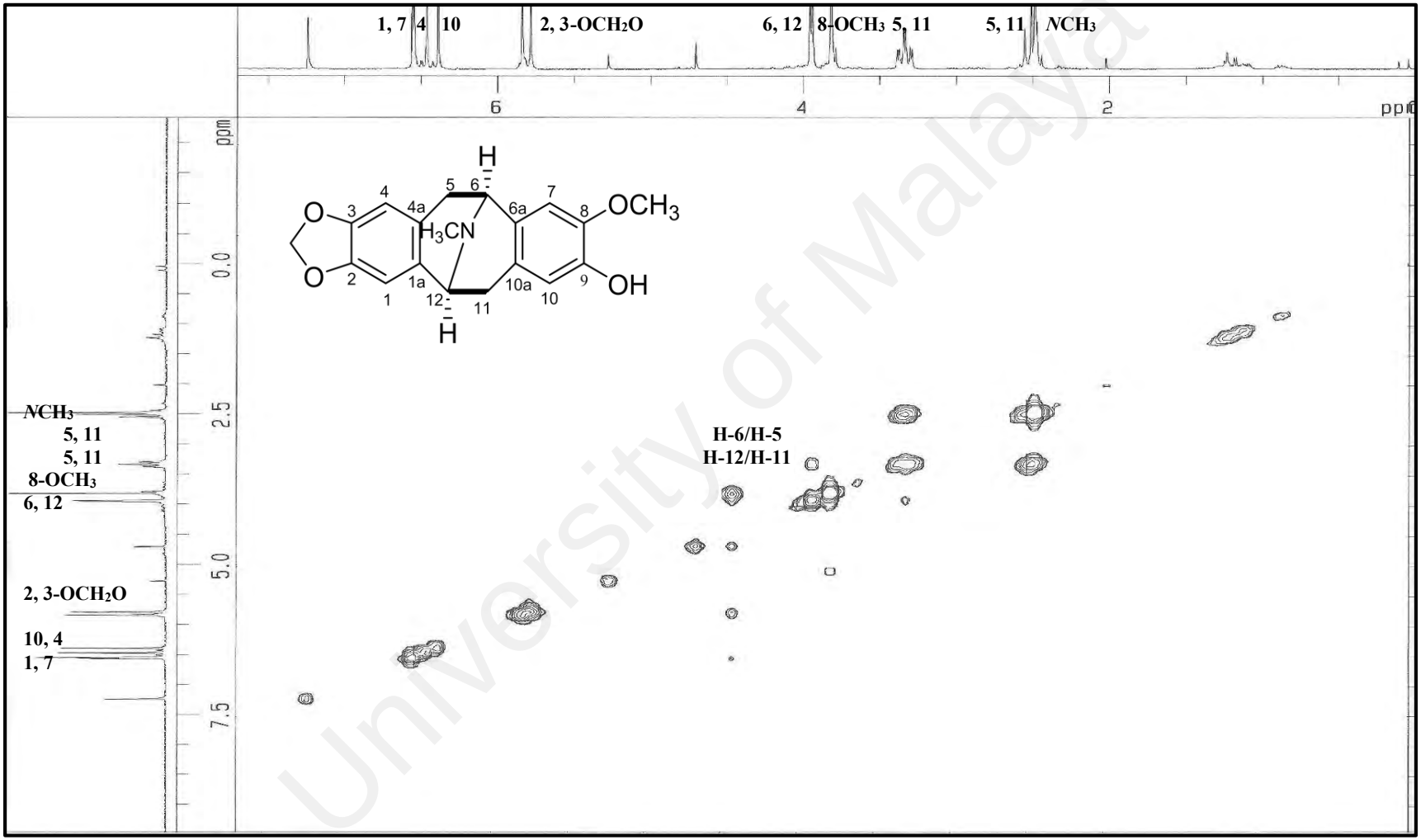

Figure 3.76: COSY spectrum of alkaloid **N**

3.2.15 Alkaloid O: Argentinine 135

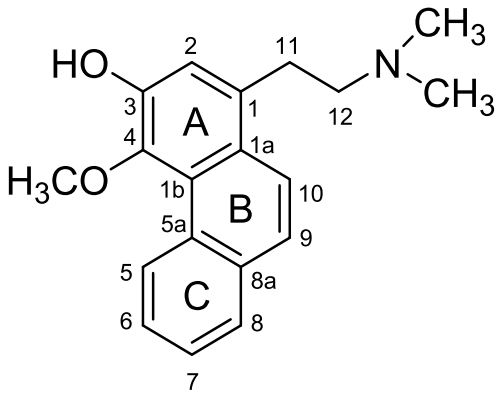

135

Alkaloid **O** was obtained as an optically inactive brownish amorphous. The LCMS-IT-TOF spectrum revealed a pseudomolecular ion peak, $[M+H]^+$ at *m/z* 296.1627 (calcd. for $C_{19}H_{22}NO_2$, 296.1645), compatible with the molecular formula of $C_{19}H_{21}NO_2$ with ten degrees of unsaturation. The UV spectrum showed absorptions at λ_{max} 218, 223, 258, 304 and 338 nm which suggested alkaloid **O** being a phenanthrene type alkaloid (Kini & Ramana, 2004). The IR spectrum exhibited an absorption bands at ν_{max} 3392 and 1600 cm^{-1}, indicated the presence of a hydroxyl (OH) group and C=C respectively.

The ^1H NMR spectrum (Figure 3.77) revealed the presence of two singlets at δ_H 2.38 and 3.83, which corresponded to 2-*N*-C<u>H</u>$_3$ and 4-OC<u>H</u>$_3$ respectively. In addition, two aromatic protons appeared as a doublet at δ_H 7.61 (1H, *d*, *J*=8.5 Hz) and overlapping signals at δ_H 7.87 (1H, *m*) which were attributed to two mutually *ortho*-located protons at H-9 and H-10 respectively. Furthermore, the proton signal at δ_H 9.41 (1H, *d*, *J*=8.0 Hz, H-5), which falls appreciably downfield, was a characteristic for this type of compounds (M. Shamma 1972). Another aromatic proton corresponding to H-6, H-7 (δ_H 7.61) and H-8 (δ_H 7.87) were observed as multiplets. This proved that ring of C was not substituted. A singlet proton at δ_H 7.23 corresponded to H-2 was observed in the spectrum, thus implying that C-3 and C-4 were substituted. Two batches of multiplets were observed, at

δ_H 2.66 and 3.24, which were assignable to the typical of methylene protons H-12 and H-11 respectively.

The COSY spectrum (Figure 3.80) was made possible for the assignment of group of aromatic proton at positions H-5/H-6, H-8/H-7 and H-10/H-9. In addition, the spectrum also showed the correlations between H-11/H-12 of the aliphatic proton. The position of methoxyl group was assigned based on the NOESY cross-peak (Figure 3.81) between H-5/4-OC$\underline{H}_3$.

The ^{13}C NMR (Figure 3.78) and DEPT (Figure 3.79) spectra exhibited nineteen signals among which three were methyls, two methylenes, seven methines, and seven quarternary carbons. The signal of 4-O$\underline{C}H_3$ carbon resonated at δ_C 60.1. In addition, *N*-$\underline{C}H_3$ group was observed at δ_C 45.4. The signals of substituted aromatic carbon were observed at higher chemical shift for C-3 and C-4 at δ_C 147.5 and 142.5 respectively. It was due to the affected by the presence of electronegative substituents effect. Furthermore, the typical of C-11 and C-12 methylene carbon were observed at δ_C 31.8 and 60.8 respectively. C-12 resonated more downfield compared to C-11 due to the fact that C-12 was adjacent to *N* atom. The HMBC experiment (Figure 3.83) further confirmed the structure of alkaloid **O**, which showed the connectivity of aliphatic chain with ring A via the correlation between H-11 to C-1a and C-2.

Analysis of the spectral data and comparison with the literature review (López-Martín, Anam, Boira, Sanz, & Blázquez, 2002, Sari, Gray, & Sariyar, 2004), alkaloid **O** was determined as argentinine **135**, which has been previously discovered from the family of Annonaceae (López-Martín et al., 2002) and Papaveraceae (Sari, Gray, & Sariyar, 2004).

Table 3.16: ^{1}H NMR (600 MHz) and ^{13}C NMR (150 MHz) spectroscopic assignments of alkaloid **O** in $CDCl_3$

Position	δ_H (ppm, *J* in Hz)		δ_C (ppm)	
	Alkaloid **O**	Argentinine **135** (López-Martín et al., 2002) ($CDCl_3$, 400 MHz)	Alkaloid **O**	Argentinine **135** (Sari et al., 2004). $CDCl_3$, 100 MHz
1	-	-	134.3	133.8
1a	-	-	126.0	126.0
1b	-	-	124.2	124.7
2	7.23 (1H, *s*)	7.28 (1H, *s*)	117.3	118.0
3	-	-	147.5	148.1
4	-	-	142.5	143.1
5	9.41 (1H, *d*, *J*=8.0)	9.42 (1H, *brd*, *J*=9.2)	127.2	127.5
5a	-	-	129.2	129.5
6	7.61 (1H, *m**)	7.86 (1H, *brd*, *J*=9.2)	126.6	126.6
7	7.61 (1H, *m**)	7.61 (1H, *td*, *J*=8.6, 1.6)	126.4	126.8
8	7.87 (1H, *m**)	7.53 (1H, *brd*, *J*=8.6)	128.2	128.3
8a	-	-	132.7	132.9
9	7.61 (1H, *m**)	7.68 (1H, *d*, *J*=9.2)	125.1	125.3
10	7.87 (1H, *m**)	7.91 (1H, *d*, *J*=9.2)	122.6	122.7
11	3.24 (2H, *m*)	3.59 (2H, *ddd, J*=16.8, 11.6, 5.2)	31.8	31.6
12	2.66 (2H, *m*)	3.21 (2H, *ddd*, *J*=16.8, 11.6, 5.2)	60.8	60.7
2-*N*CH_3	2.38 (6H, *s*)	2.84 (6H, *s*)	45.4	45.2
4-OCH_3	3.83 (3H, *s*)	3.84 (3H, *s*)	60.1	60.1

* overlapping signals

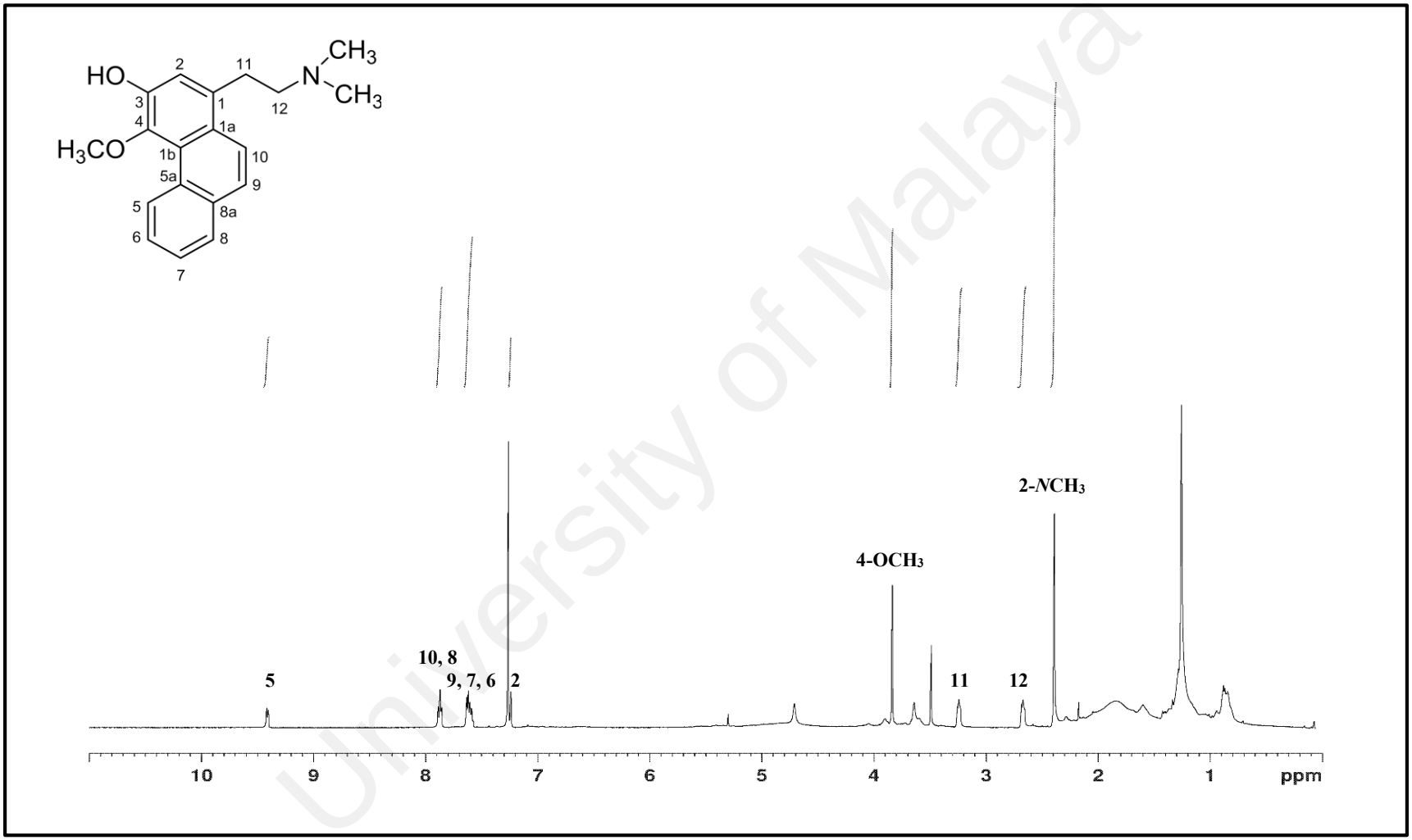

Figure 3.77: ^{1}H NMR spectrum of alkaloid **O**

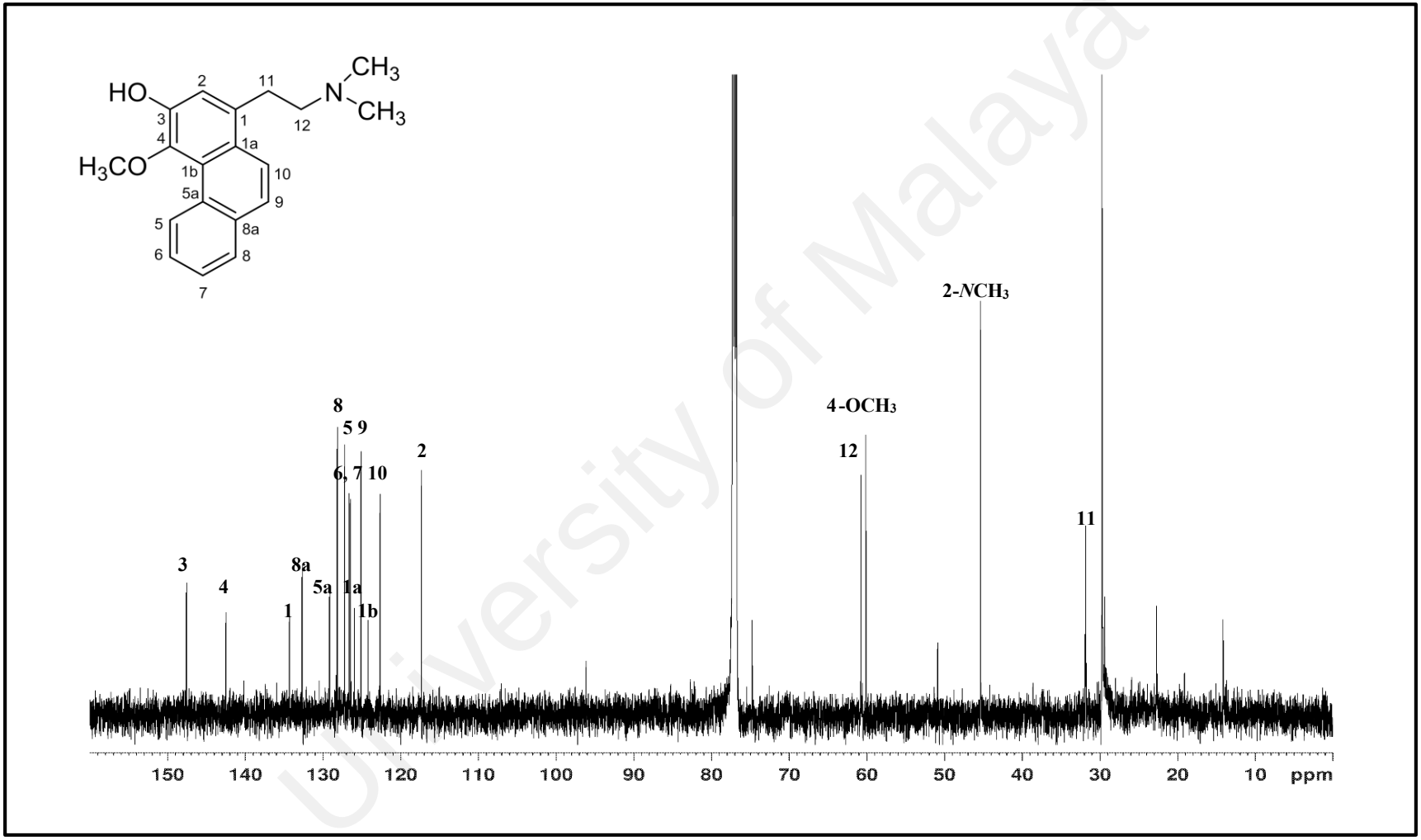

Figure 3.78: ^{13}C NMR spectrum of alkaloid **O**

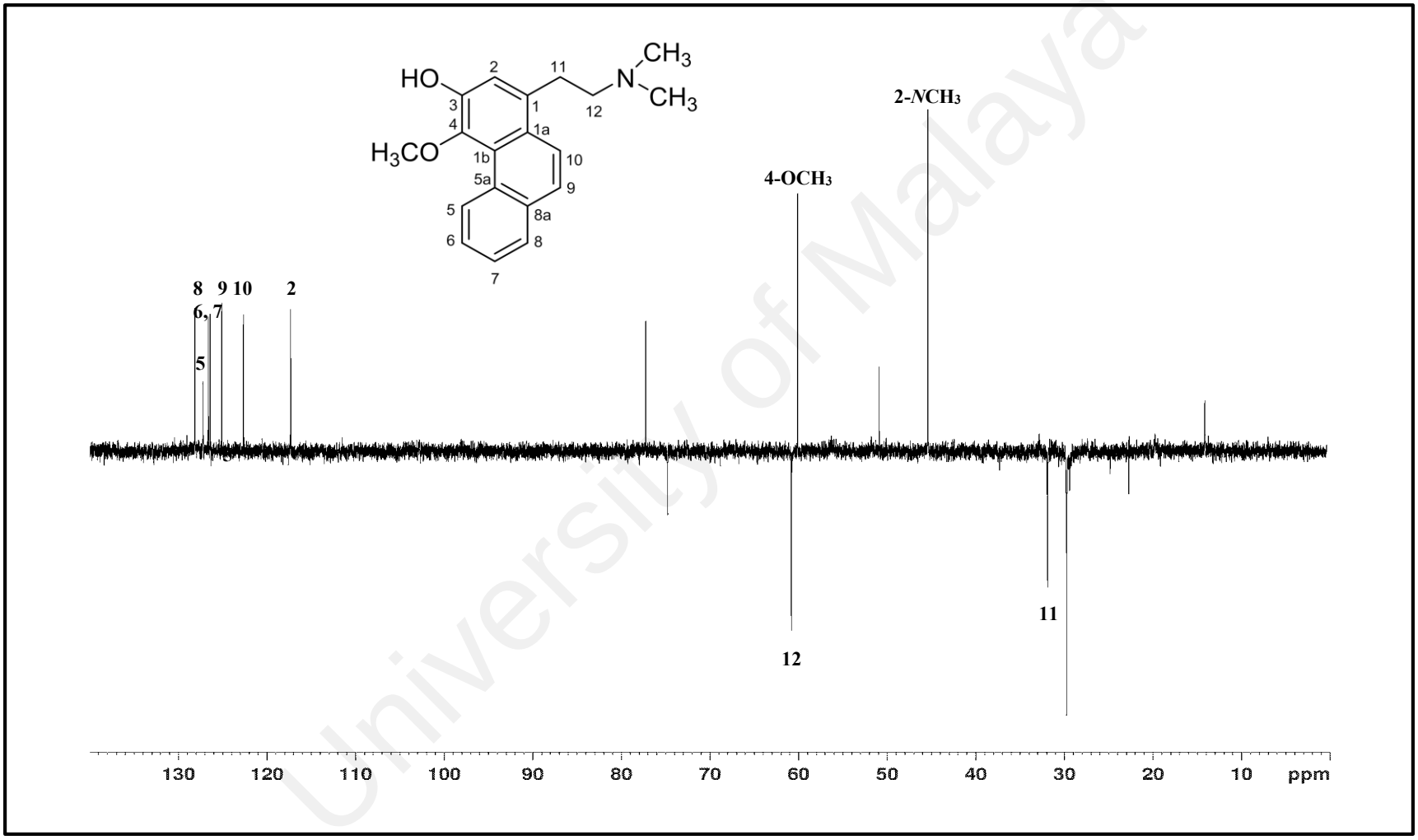

Figure 3.79: DEPT spectrum of alkaloid **O**

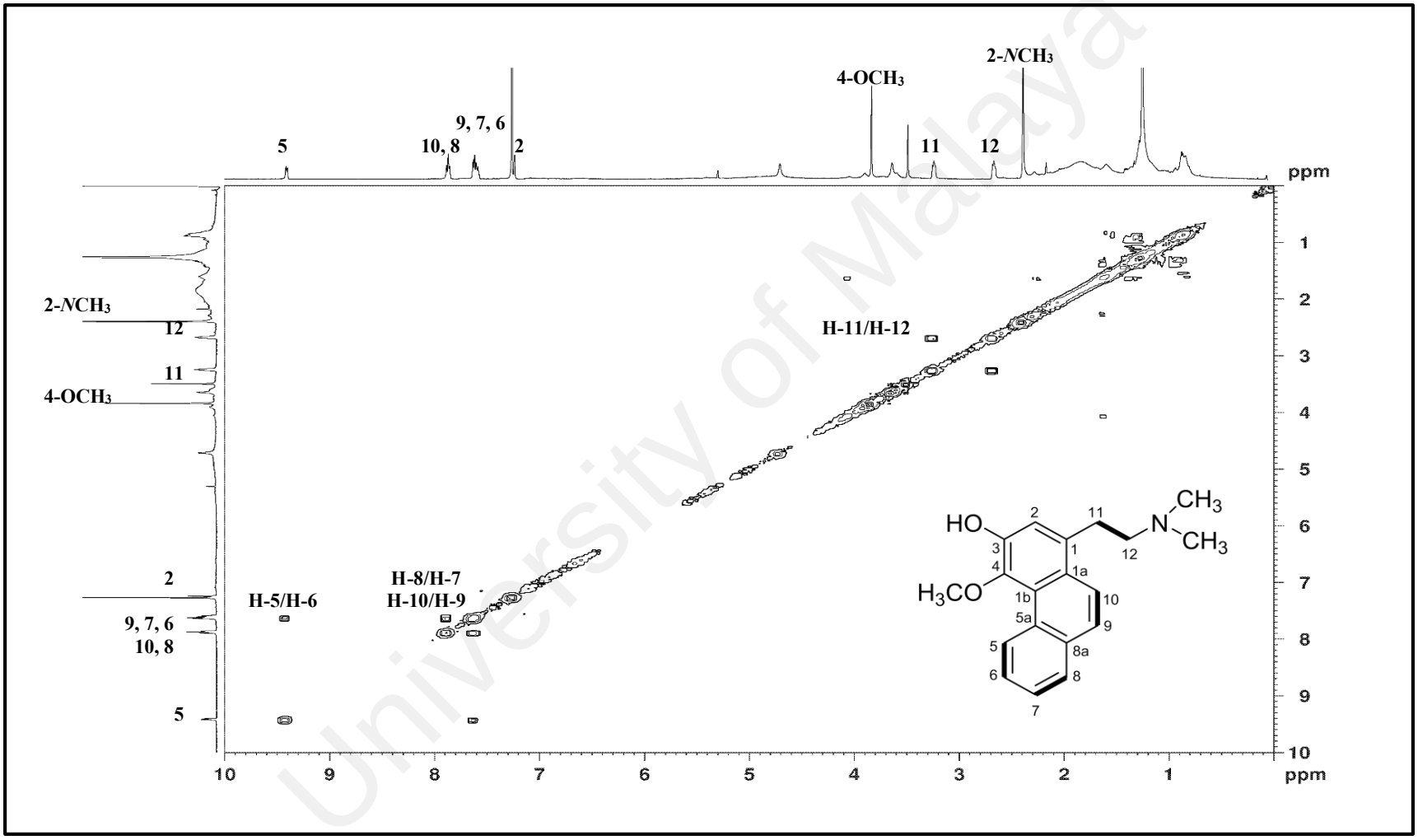

Figure 3.80: COSY spectrum of alkaloid **O**

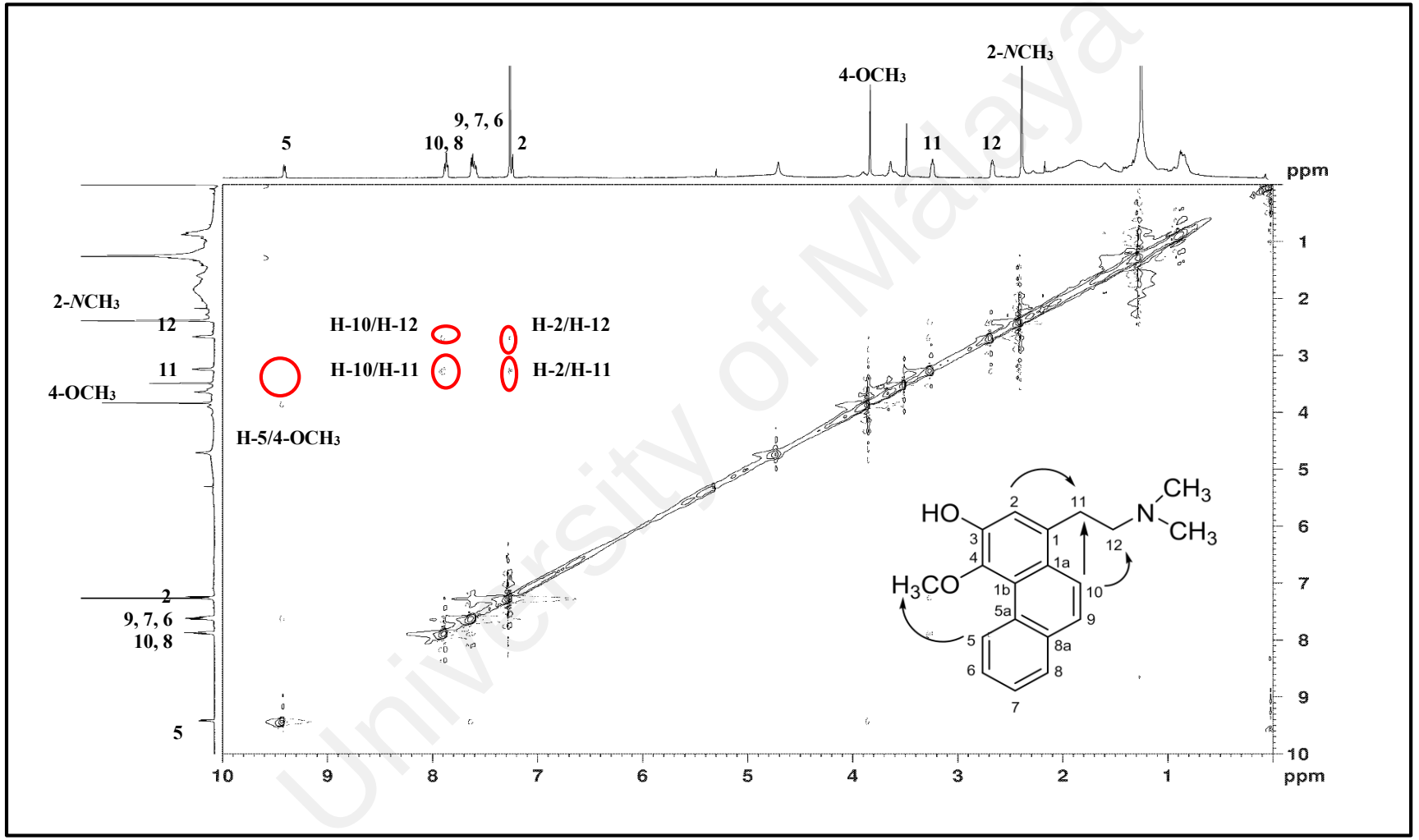

Figure 3.81: NOESY spectrum of alkaloid **O**

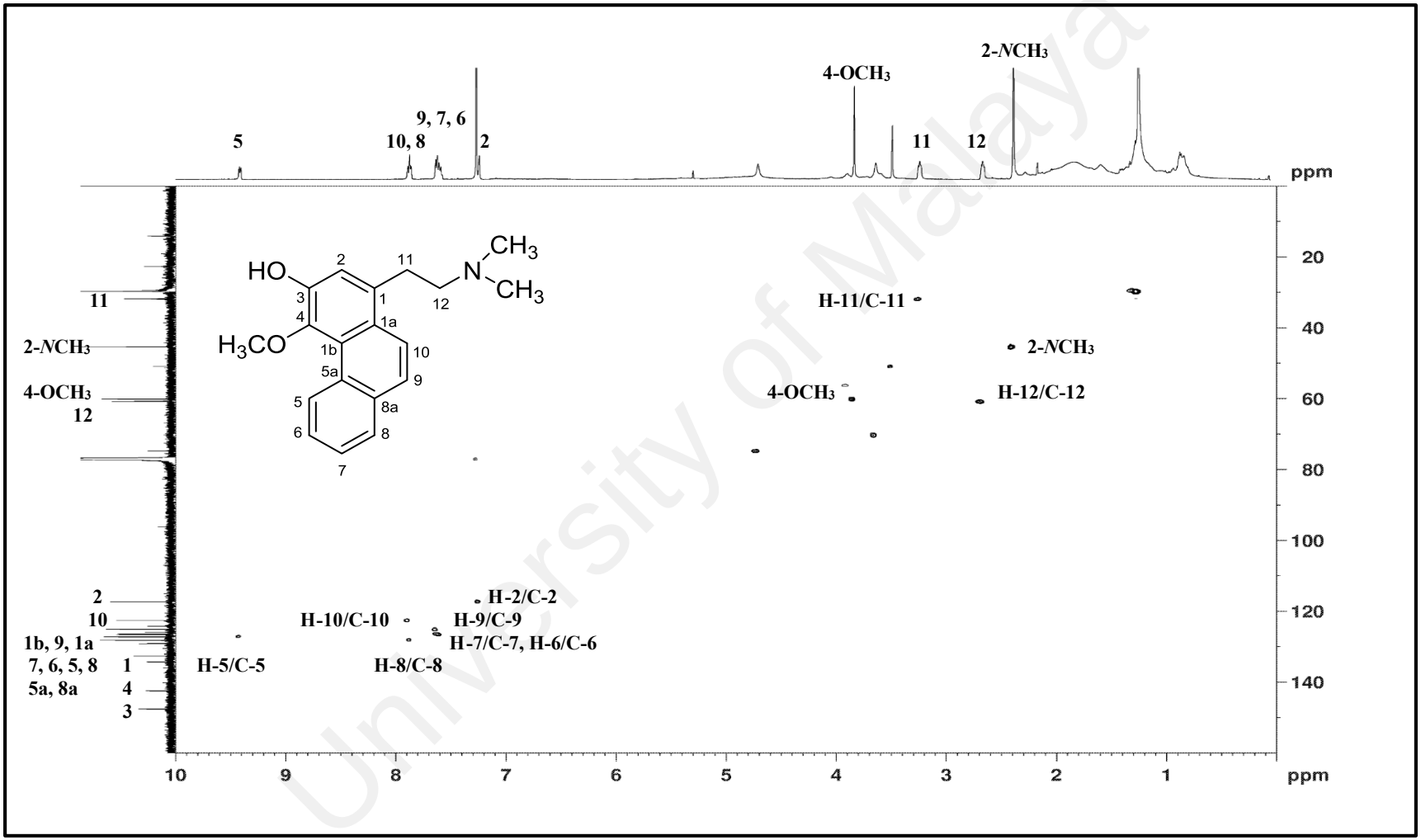

Figure 3.82: HSQC spectrum of alkaloid **O**

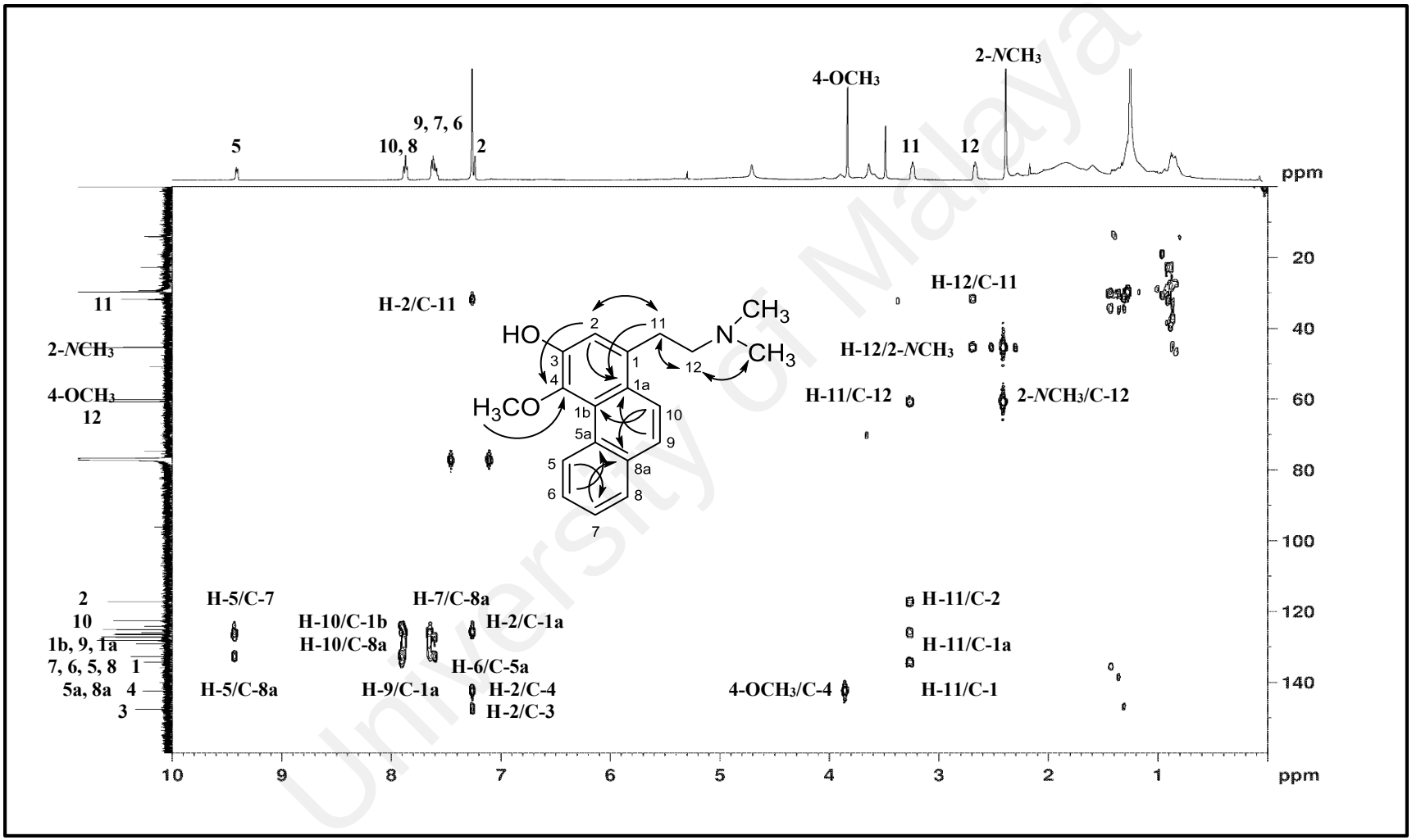

Figure 3.83: HMBC spectrum of alkaloid **O**

3.2.16 Alkaloid P: Atherosperminine 15

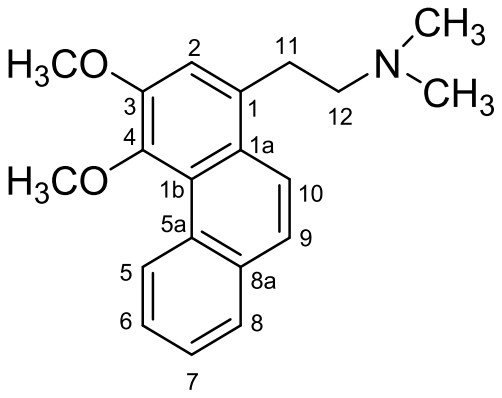

15

Alkaloid **P** was isolated as an optically inactive brownish amorphous. Its molecular formula was established as $C_{20}H_{23}NO_2$ by LCMS-IT-TOF spectrum, which showed an intense pseudomolecular ion peak, $[M+H]^+$ at *m/z* 310.1795 (calcd. for $C_{20}H_{24}NO_2$, 310.1802). The UV spectrum showed absorptions maxima at 218, 220, 256, 308 and 342 nm and were characteristic of phenanthrene alkaloids (Kini & Ramana, 2004). The IR spectrum showed an absorption at ν_{max} 1610 cm^{-1} due to the stretching of aromatic C=C.

The ^1H (Figure 3.84) and ^{13}C (Figure 3.85) NMR spectrum of alkaloid **P** was identical to that of alkaloid **O**, except for the additional methoxyl signal resonated at δ_H 4.03 which located at C-3 replacing the hydroxyl group in alkaloid **O**. A singlet peak appeared at δ_H 7.23 which could be belonged to H-2. In addition, a very typical downfield doublet-doublet signal resonated at δ_H 9.66 corresponded to H-5 with the coupling constants of 7.8 and 1.4 Hz due to this signal is *ortho* to H-6 and *metha* to H-7. Analysis of ^{13}C NMR spectrum (Figure 3.85) revealed the presence of twenty carbon signals which validated the molecular formula, $C_{20}H_{23}NO_2$. Due to paucity of sample, we were unable to get its 2D NMR spectrum including HMBC spectrum.

Comparison of the empirical data obtained with the literature values (Guinaudeau, Leboeuf, & Cavé, 1988; Kini & Ramana, 2004), alkaloid **P** was identified as atherosperminine **15**.

Table 3.17: ^{1}H NMR (400 MHz) and ^{13}C NMR (100 MHz) spectroscopic assignments of alkaloid **P** in $CDCl_3$

Position	δ_H (ppm, *J* in Hz)		δ_C (ppm)	
	Alkaloid **P**	Atherosperminine **15** (Kini & Ramana, 2004) ($CDCl_3$ 60 MHz)	Alkaloid **P**	Atherosperminine **15** (Guinaudeau et al., 1988) ($CDCl_3$)
1	-	-	130.2	130.1
1a	-	-	126.2	126.1
1b	-	-	125.3	125.2
2	7.23 (1H, *s*)	7.20-7.50 (1H, *m*)	114.8	114.8
3	-	-	150.9	162.5
4	-	-	146.0	150.8
5	9.66 (1H, *dd*, *J*=7.8, 1.4)	9.67 (1H, *m*)	128.2	122.3
5a	-	-	132.9	132.7
6	7.61 (1H, *m**)	7.20-7.50 (1H, *m*)	126.6	126.5
7	7.61 (1H, *m**)	7.20-7.50 (1H, *m*)	125.8	126.5
8	7.85 (1H, *m**)	7.65 (1H, *m*)	128.2	125.7
8a	-	-	133.3	132.7
9	7.61 (1H, *m**)	7.65 (1H, *m*)	126.6	128.1
10	7.85 (1H, *m**)	7.65 (1H, *m*)	122.5	128.1
11	3.33 (2H, *m*)	2.30-3.85 (2H, *m*)	32.6	32.2
12	2.69 (2H, *m*)	2.30-3.85 (2H, *m*)	61.1	60.7
2-*N*CH_3	2.41 (6H, *s*)	2.25 (6H, *s*)	45.6	45.2
3-OCH_3	4.03 (3H, *s*)	3.90 (3H, *s*)	56.7	56.6
4-OCH_3	3.91 (3H, *s*)	3.88 (3H, *s*)	59.9	59.7

* overlapping signals

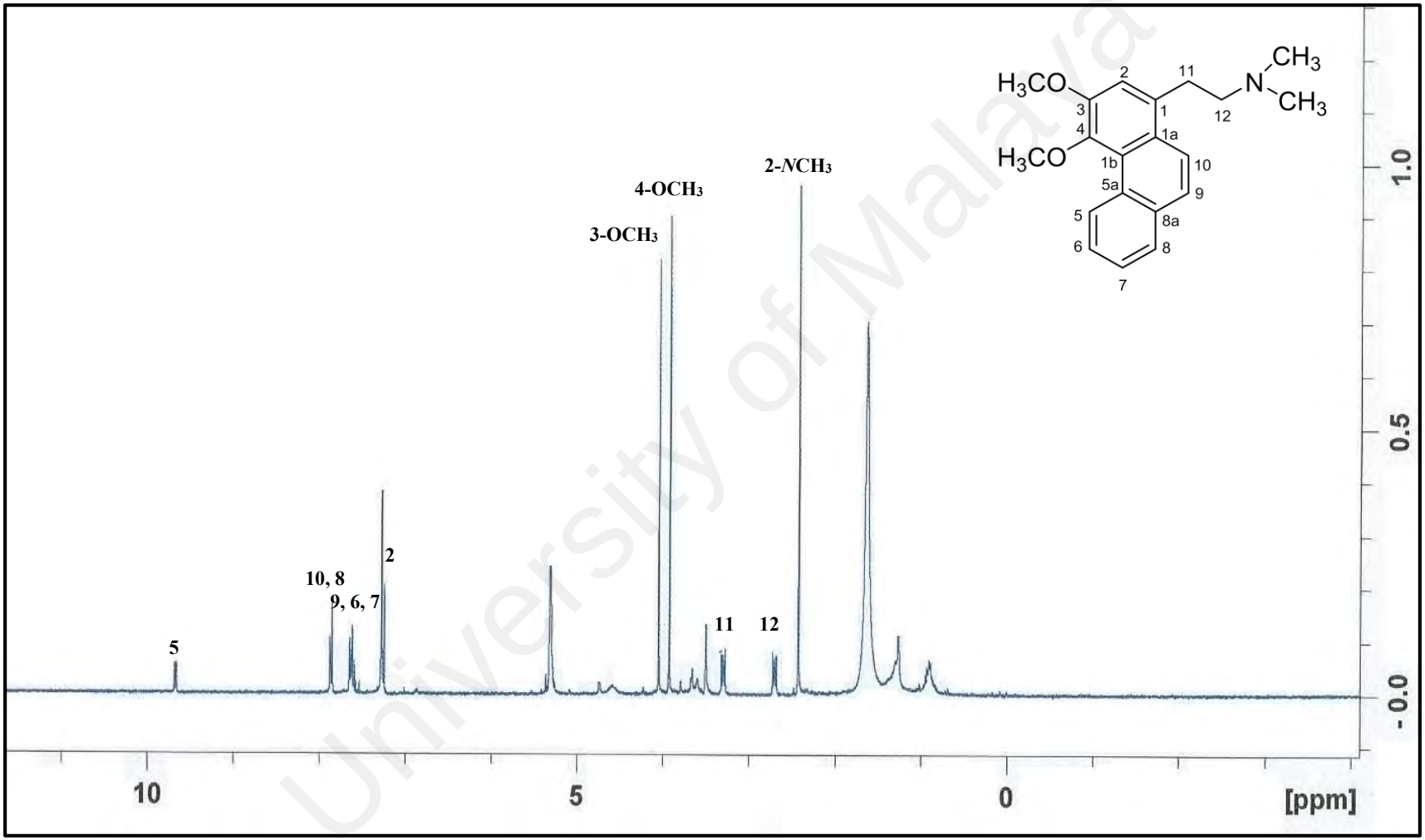

Figure 3.84: ^{1}H NMR spectrum of alkaloid **P**

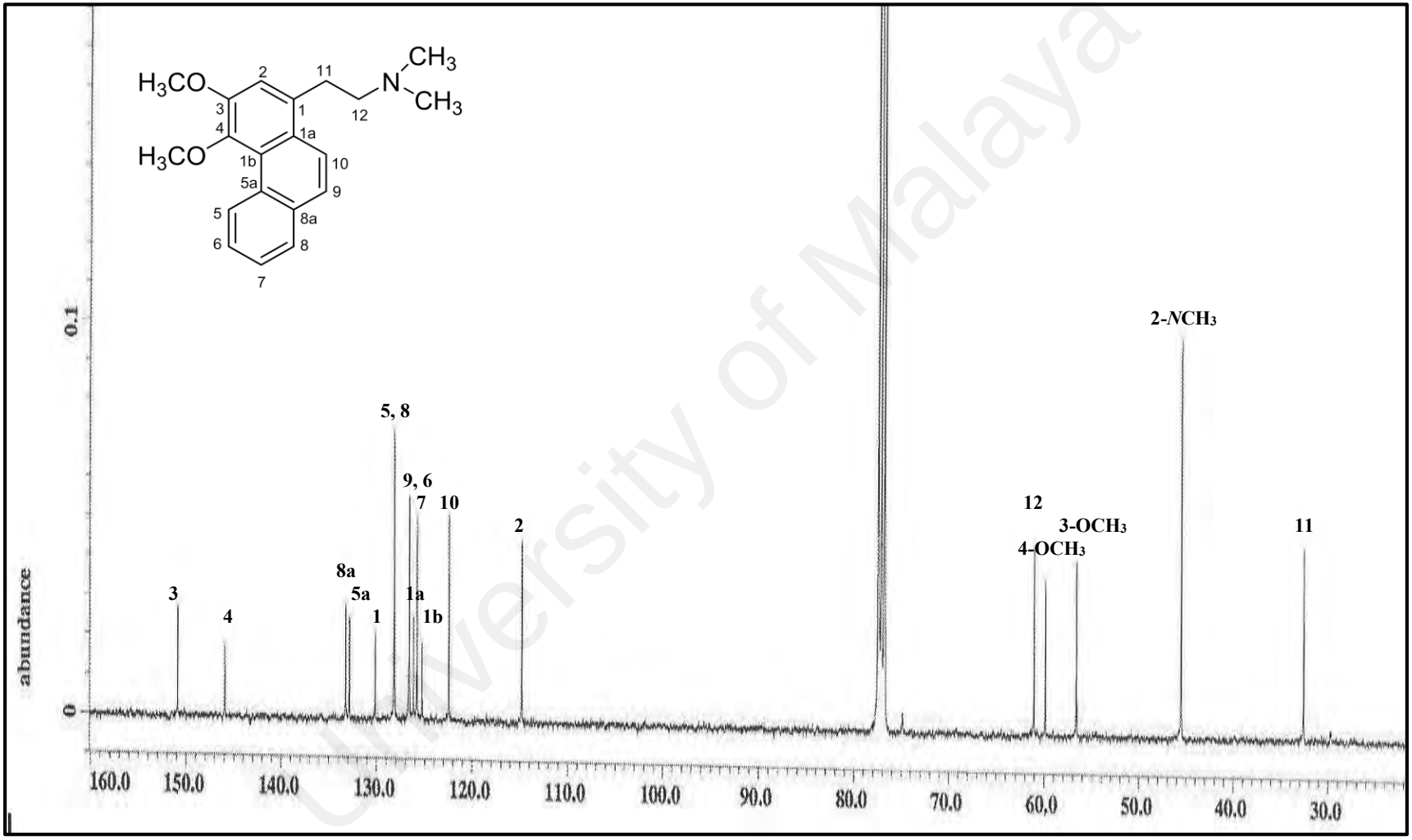

Figure 3.85: ^{13}C NMR spectrum of alkaloid **P**

3.2.17 Alkaloid Q: (+)-*N*-methylisococlaurine 14

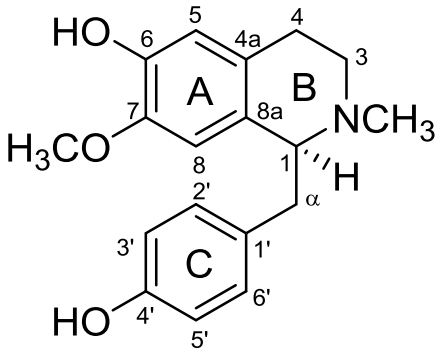

14

Alkaloid **Q** was purified as an optically active brownish amorphous with $[\alpha]_D^{25}$ +67° (*c*=0.02 MeOH). The positive LCMS-IT-TOF exhibited a pseudomolecular ion peak, $[M+H]^+$ at *m/z* 300.1573 (calcd. for $C_{18}H_{22}NO_3$, 300.1594), thus giving the possibility of the molecular formula to be $C_{18}H_{21}NO_3$ corresponding with nine degrees of unsaturation. The UV spectrum showed absorption bands at λ_{max} 228 and 293 nm which were a characteristic of a benzylisoquinoline moiety (Shamma, 1972). The IR spectrum showed absorptions at ν_{max} 3303 and 2337 cm^{-1} due to the presence of a hydroxyl (OH) group and stretching of C-H aromatic respectively.

In the ^1H NMR spectrum (Figure 3.86), two singlets were apparent at δ_H 3.85 and 2.46 ascribable to 7-OC<u>H</u>$_3$ and *N*-C<u>H</u>$_3$ group respectively. In addition, two singlets aromatic protons appeared at δ_H 6.53 and 6.42 which belonged to H-5 and H-8 respectively. Another four of the aromatic protons were observed at δ_H 6.68 (1H, *d*, *J*=8.2 Hz, H-3'and H-5') and δ_H 6.98 (1H, *d*, *J*=8.2 Hz, H-2'and H-6'). The chemical shift values of the aliphatic protons appeared as multiplet in the region of δ_H 2.54-3.66. The COSY assignment (Figure 3.88) indicated the correlations between the vicinal proton of H-3/H-4, H-1/H-α, H-2'/H-3'and H-5'/H-6'.

The ^{13}C NMR spectrum (Figure 3.87) displayed sixteen carbon signals instead of eighteen, due to two overlapping signals of C-2'/C-6' and C-3'/C-5' carbons, which

appeared at δ_C 130.5 and 115.0, respectively. The HMBC spectrum (Figure 3.90) revealed the correlation of H-1 to C-1' thus, supporting the connectivity of ring B with ring C. Furthermore, the correlations of H-1 to *N*C$\underline{H}_3$ and *N*$\underline{C}H_3$ to C-3 confirmed that this group was located at ring B of the structure.

From the analysis of the spectroscopic data obtained (Table 3.18) and comparison with the literature values (Saidi et al., 2011a), thus the structure of (+)-*N*-methylisococlaurine **14** was identified. This alkaloid have been previously isolated from the bark of *Cryptocarya nigra* (Nasrullah, Zahari, Mohamad, & Awang, 2013).

Table 3.18: ^{1}H NMR (600 MHz) and ^{13}C NMR (150 MHz) spectroscopic assignments of alkaloid **Q** in $CDCl_3$

Position	**δ_H (ppm, *J* in Hz)**		**δ_C (ppm)**	
	Alkaloid **Q**	*N*-methylisococlaurine **14** (Saidi et al., 2011a) ($CDCl_3$, 400 MHz)	Alkaloid **Q**	*N*-metylisococlaurine **14** (Saidi et al., 2011a) ($CDCl_3$, 400 MHz)
1	3.66 (1H, *m*)	3.67-3.79 (1H, *t*,)	64.7	64.7
3	α=2.72 (1H, *m*) β=3.17 (1H, *m*)	α =2.74-2.77 (1H, *m*) β=2.98-3.03 (1H, *dd*)	47.0	46.0
4	α=2.54 (1H, *m*) β=2.77 (1H, *m*)	α=2.53-2.60 (1H, *m*) β=3.17-3.24 (1H, *m*)	25.2	24.2
4a	-	-	125.7	124.5
5	6.53 (1H, *s*)	6.51 (1H, *s*)	110.5	110.7
6	-	-	145.0	145.5
7	-	-	143.3	143.4
8	6.42 (1H, *s*)	6.29 (1H, *s*)	113.6	114.0
8a	-	-	130.4	130.4
α	α=2.84 (1H, *dd*, *J*=14.3, 6.1) β=3.01 (1H, *dd*, *J*=14.3, 6.1)	2.80-2.86 (2H, *m*)	40.7	40.5
1'	-	-	132.0	129.3
2'	6.98 (1H, *d*, *J*=8.2)	6.86-6.88 (1H, *d*, *J*=8.3)	130.5	130.3
3'	6.68 (1H, *d*, *J*=8.2)	6.54-6.56 (1H, *d*, *J*=8.3)	115.0	115.5
4'	-	-	153.8	154.8
5'	6.68 (1H, *d*, *J*=8.2)	6.54-6.56 (1H, *d*, *J*=8.3)	115.0	115.5
6'	6.98 (1H, *d*, *J*=8.2)	6.86-6.88 (1H, *d*, *J*=8.3)	130.5	130.3
NCH_3	2.46 (3H, *s*)	2.37 (3H, *s*)	42.6	41.8
7-OCH_3	3.85 (3H, *s*)	3.74 (3H, *s*)	55.8	55.7

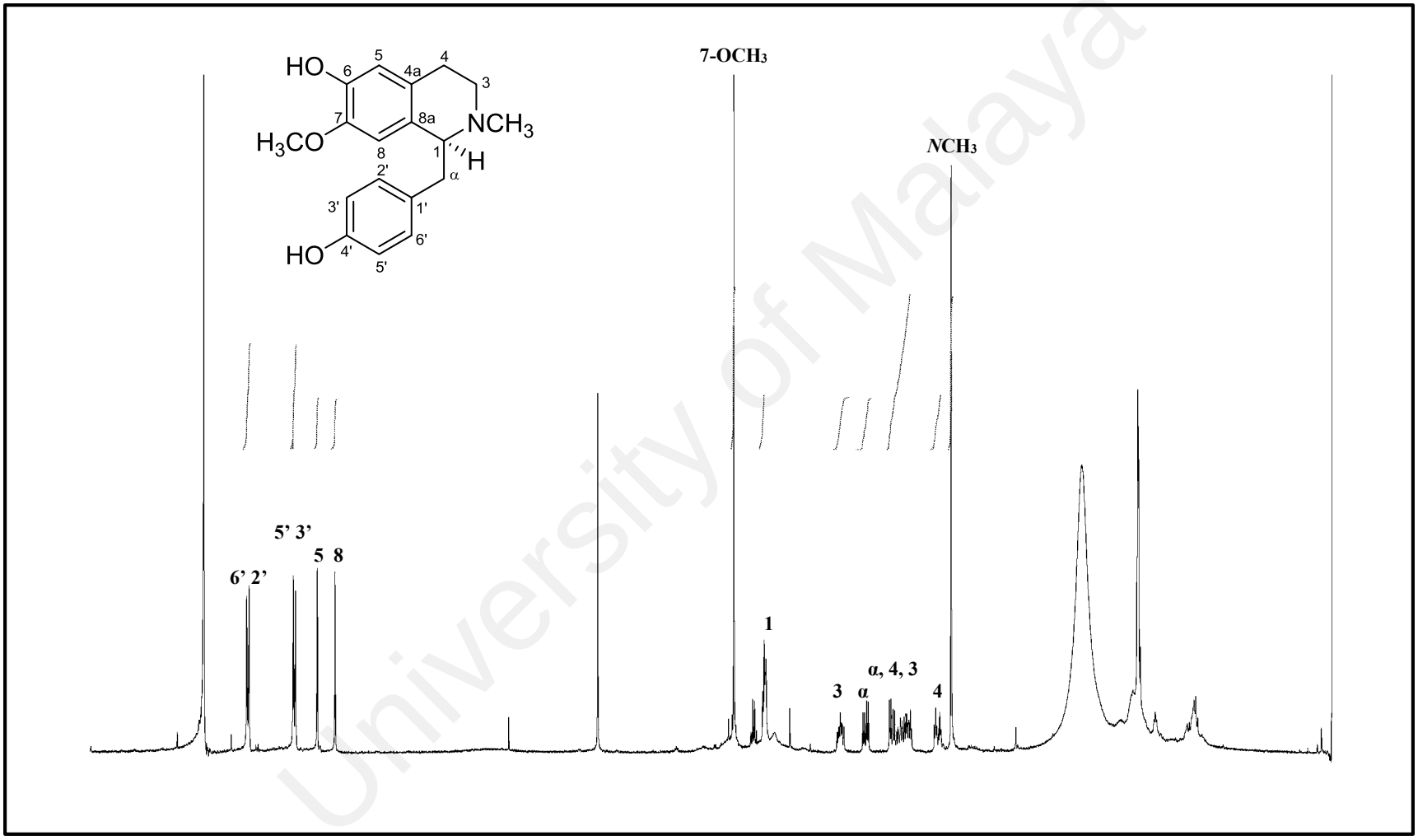

Figure 3.86: ^{1}H NMR spectrum of alkaloid **Q**

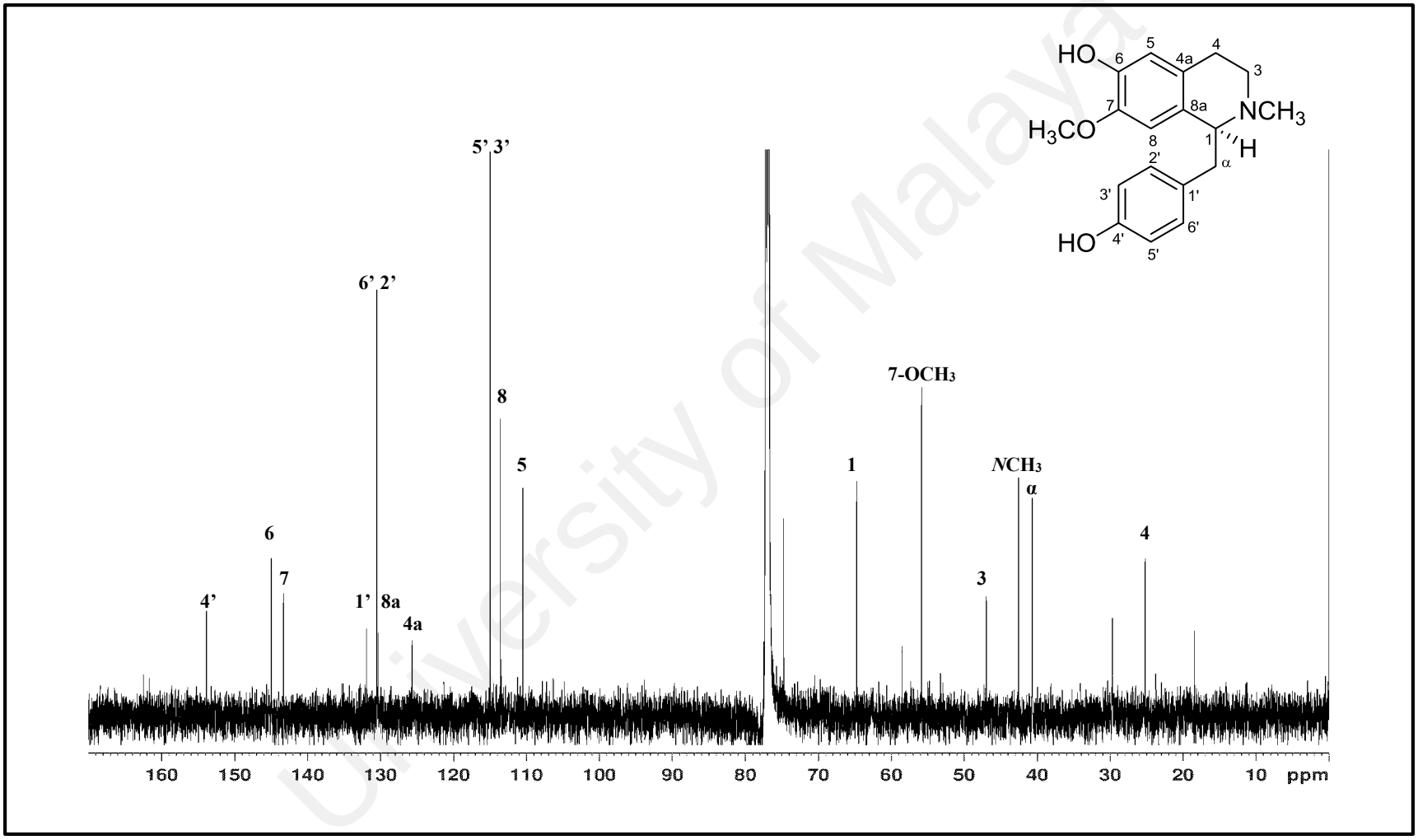

Figure 3.87: ^{13}C NMR spectrum of alkaloid **Q**

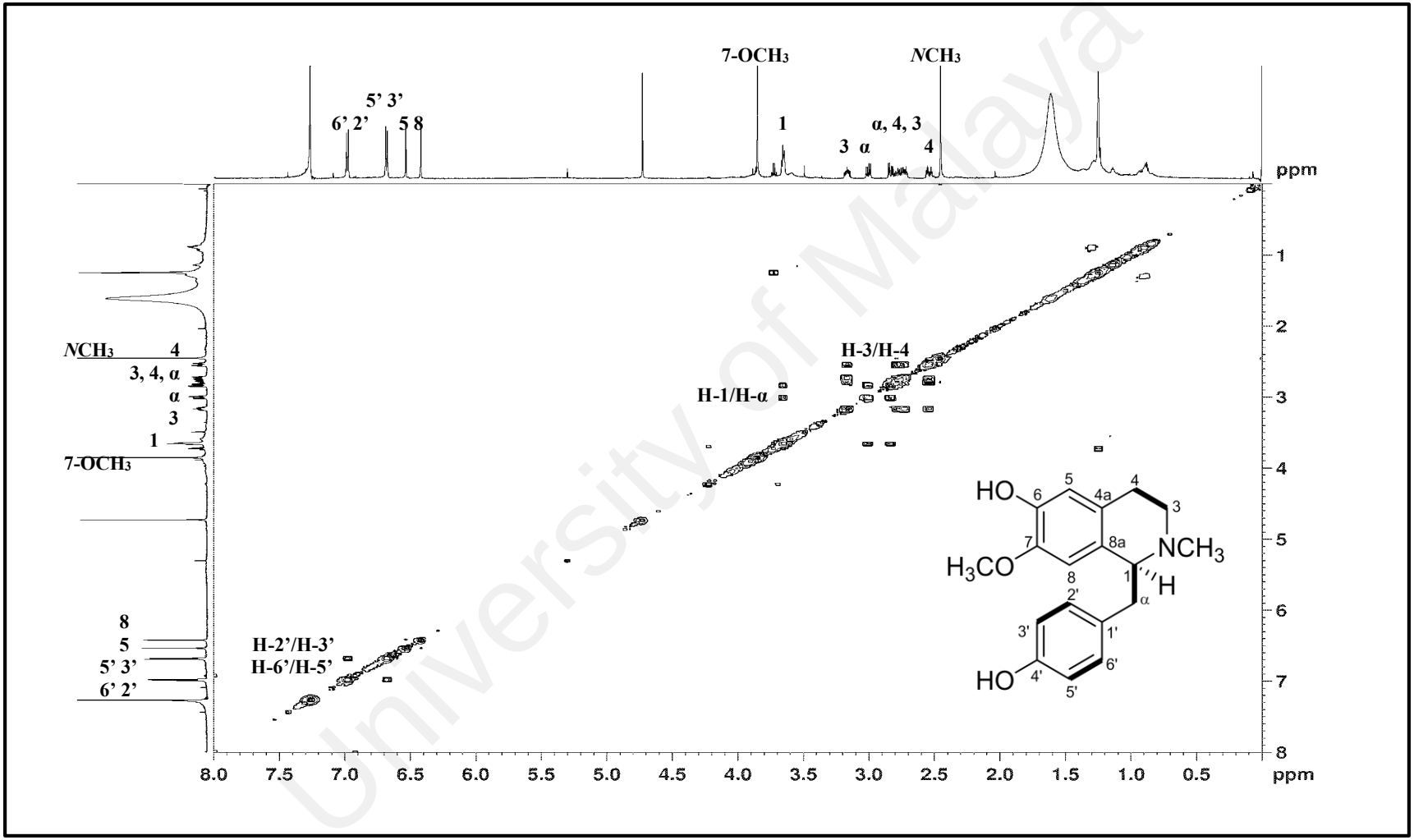

Figure 3.88: COSY spectrum of alkaloid **Q**

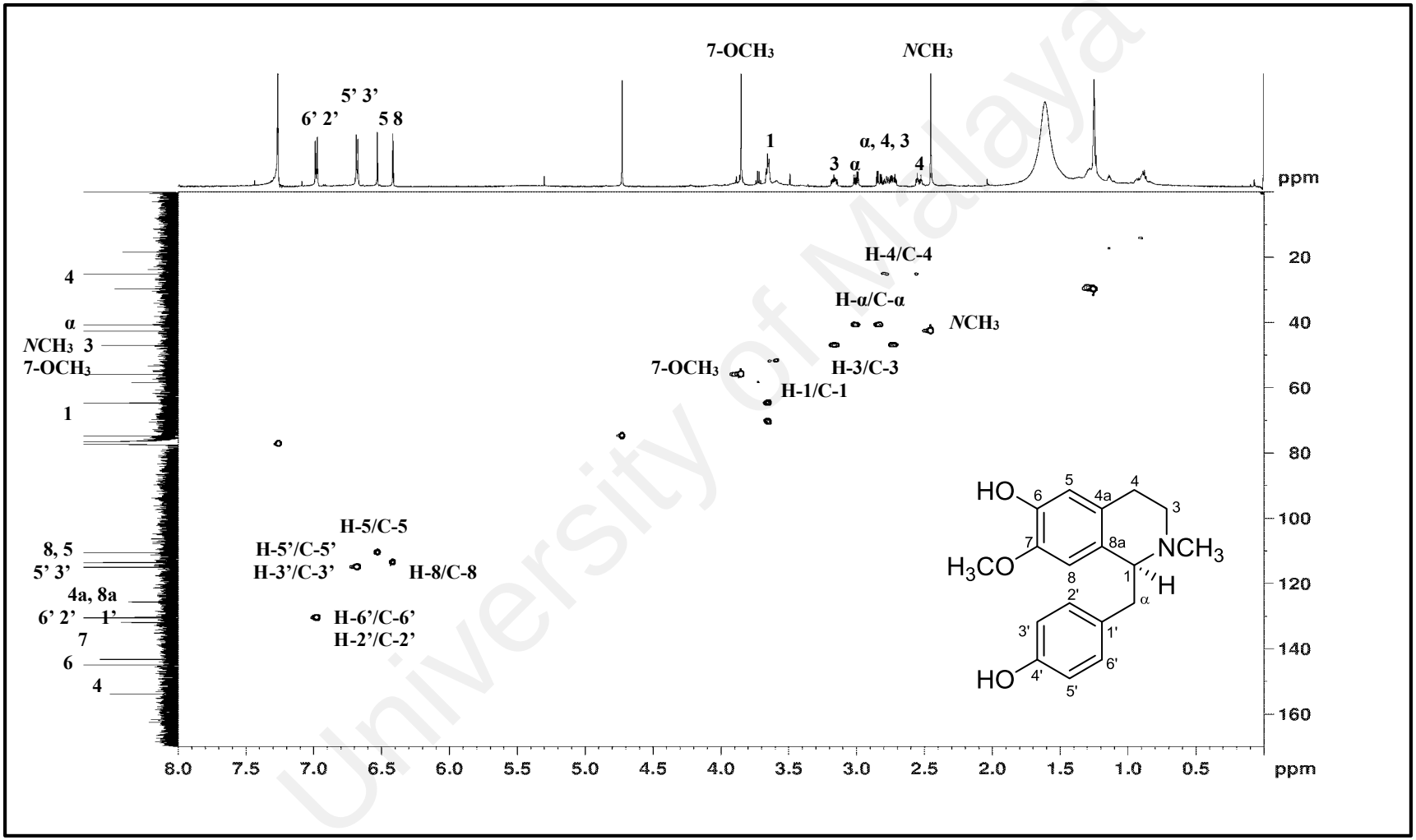

Figure 3.89: HSQC spectrum of alkaloid **Q**

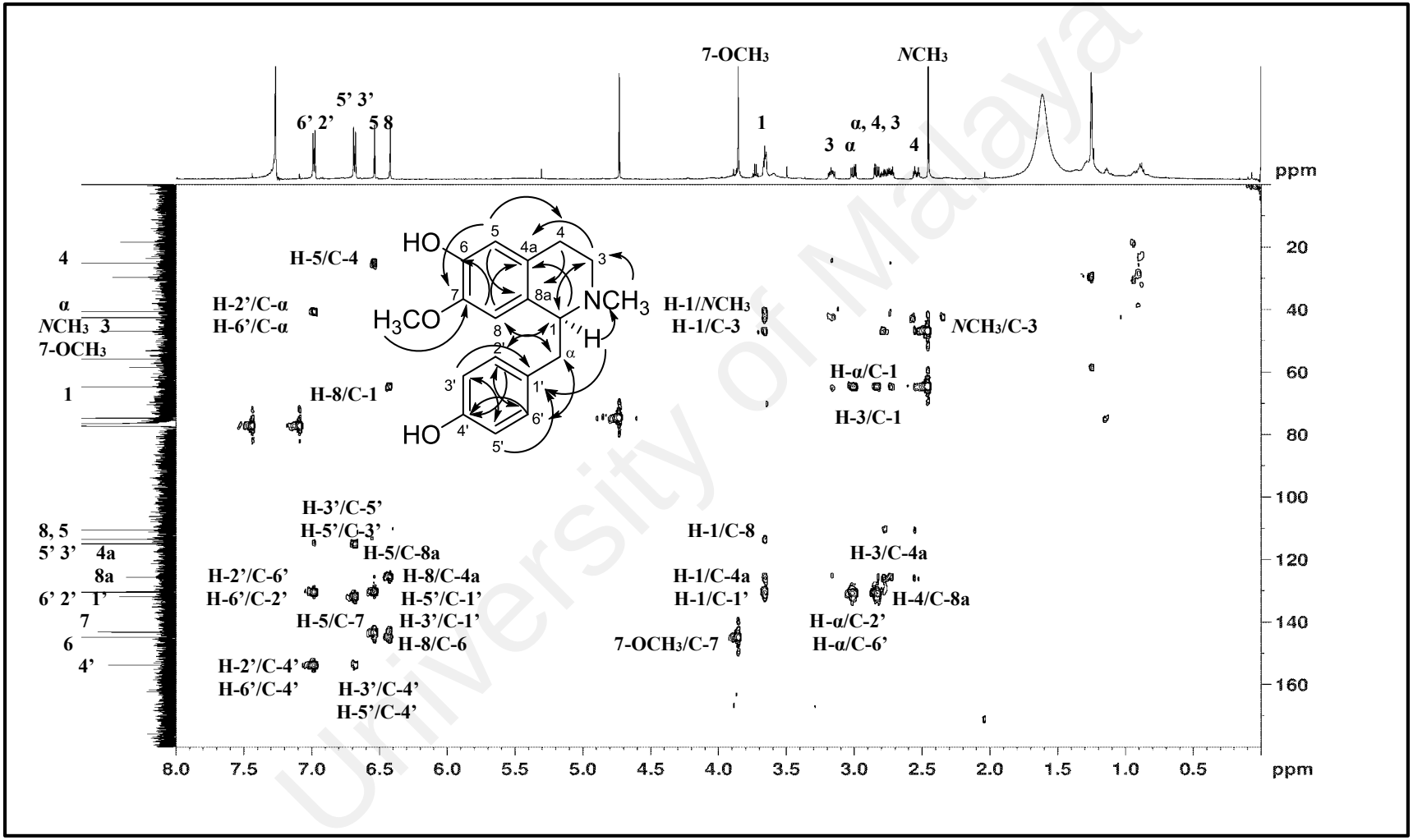

Figure 3.90: HMBC spectrum of alkaloid **Q**

3.2.18 Alkaloid R: Liriodenine 136

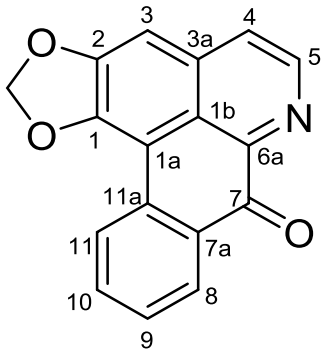

136

Alkaloid **R** was obtained as an optically inactive yellowish amorphous. It has a molecular formula of $C_{17}H_9NO_3$ as deduced from the LCMS-IT-TOF spectrum which showed an intense pseudomolecular ion peak, $[M+H]^+$ at *m/z* 276.0651 (calcd. $C_{17}H_{10}NO_3$, 276.0655), consistent with fourteen degrees of unsaturation. In the UV spectrum, maxima absorptions were observed at λ_{max} 238, 295, 308 and 405 nm, indicated that it possessed highly conjugated oxoaporphine system (Harrigan, Gunatilaka, Kingston, Chan, & Johnson, 1994). The IR spectrum revealed absorption bands due to conjugated carbonyl (ν_{max} 1649 cm^{-1}), C=C (ν_{max} 1561 cm^{-1}) and methylenedioxy (ν_{max} 1264 and 982 cm^{-1}) functional groups.

In the ^1H NMR spectrum (Figure 3.91), a singlet signals were observed at δ_H 6.39 and 7.20 due to the resonances of methylenedioxy group and H-3 respectively. The aromatic protons of ring D were resonated at δ_H 8.60 (1H, *dd*, *J*=8.1, 1.4 Hz, H-8), 7.59 (1H, *t*, *J*=8.1 Hz, H-9), 7.76 (1H, *dd*, *J*=8.1, 1.4 Hz, H-10) and 8.69 (1H, *d*, *J*=8.1 Hz, H-11). H-11 has the highest chemical shift compared to the other aromatic protons due to the deshielding effect of the facing ring A and hydrogen bonding with the methylenedioxy group. In addition, two sets of doublets with coupling constant of 5.1 Hz were observed at δ_H 7.80 and 8.90 which were attributable to H-4 and H-5 respectively.

Due to the limited amounts of samples, we were unable to get its 2D NMR spectrum including HMBC spectrum. Comparison of the empirical data obtained (Table 3.19) with the literature values of the known compound (Guinaudeau et al., 1994), confirmed that alkaloid **R** was liriodenine **136**, which widely distributed among the family of Annonaceae (Y.-C. Wu, Chang, Chang-Yih, & Shang-Kwei, 1993) and Magnoliaceae (Pyo, Yun-Choi, & Hong, 2003).

Table 3.19: ^{1}H NMR (600 MHz) spectroscopic assignments of alkaloid **R** in $CDCl_3$

Position	**δ_H (ppm, *J* in Hz)**	
	Alkaloid **R**	Liriodenine **136** (Guinaudeau et al., 1994) ($CDCl_3$, 400 MHz)
1	-	-
1a	-	-
1b	-	-
2	-	-
3	7.20 (1H, *s*)	7.22 (1H, *brs*)
3a	-	-
4	7.80 (1H, *d*, *J*=5.1)	7.80 (1H, *d*, *J*=5.0)
5	8.90 (1H, *d*, *J*=5.1)	8.90 (1H, *d*, *J*=5.0)
6a	-	-
7	-	-
7a	-	-
8	8.60 (1H, *dd*, *J*=8.1, 1.4)	8.60 (1H, *dd*, *J*=8.0, 2.0)
9	7.59 (1H, *t*, *J*=8.1)	7.59 (1H, *dt*, *J*=8.0, 2.0)
10	7.76 (1H, *dd*, *J*=8.1, 1.4)	7.78 (1H, *dt*, *J*=8.0, 2.0)
11	8.69 (1H, *d*, *J*=8.1)	8.68 (1H, *d*, *J*=8.0)
11a	-	-
1, 2-OCH_2O	6.39 (2H, *s*)	6.38 (2H, *s*)

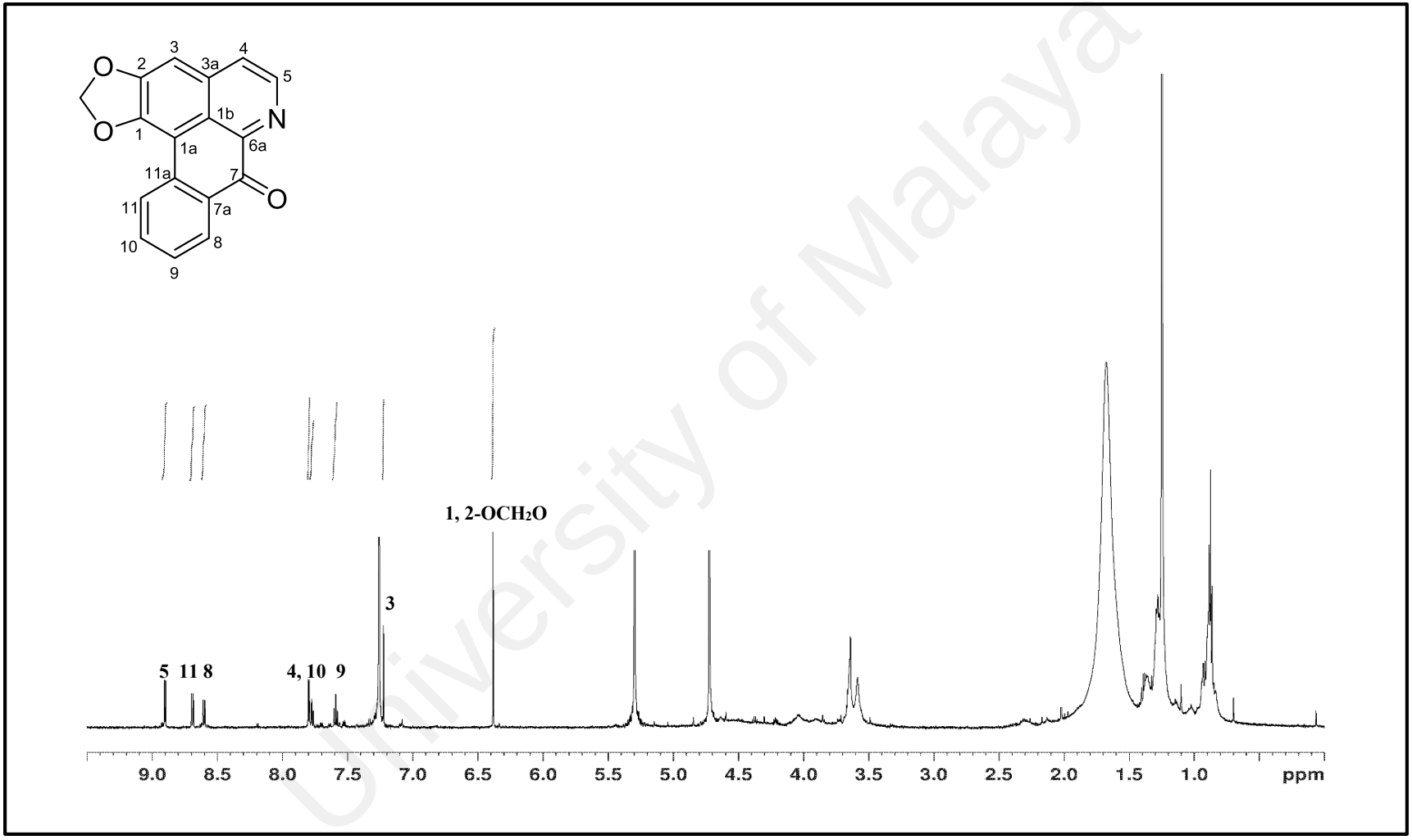

Figure 3.91: ^{1}H NMR spectrum of alkaloid **R**

3.2.19 Alkaloid S: 2-Methoxyatherosperminine 72

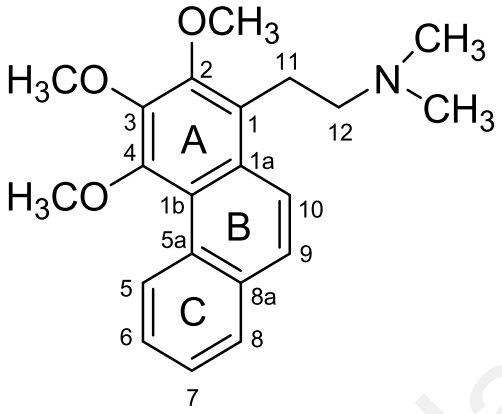

72

Alkaloid **S** was obtained as an optically inactive dark brownish amorphous. The LCMS-IT-TOF spectrum revealed a pseudomolecular ion peak, $[M+H]^+$ at *m/z* 340.1076 (calcd. for $C_{21}H_{26}NO_3$, 340.1907), hence gave possible the molecular formula of $C_{21}H_{25}NO_3$, which can deduce ten degrees of unsaturation.

The UV, IR, ^{1}H NMR (Figure 3.92) and ^{13}C NMR (Figure 3.93) spectra indicated that alkaloid **S** was structurally related to those of alkaloid **P**. However, alkaloid **S** revealed an additional methoxyl signal which resonated as a singlet at δ_H 4.01 assignable to C-2. The position of methoxyl group was determined *via* HMBC correlation between 2-OC<u>H</u>$_3$ and C-2. The COSY (Figure 3.94) experiment displayed correlations of H-5/H-6, H-6/H-7 and H-7/H-8, thus, proved that ring C was not substituted. The ^{13}C NMR spectra (Figure 3.93) established the presence of twenty-one carbon signals which comprising of *N*-methyls, three methoxyls, two methylenes, six methines and eight quaternary carbons.

Comparison of the observed data with its close analogue, *N*-demethyl-2-methoxyatherosperminine **71** (Awang et al., 2008), confirmed that alkaloid **S** was 2-methoxyatherosperminine.

Table 3.20: ^{1}H NMR (400 MHz) and ^{13}C NMR (100 MHz) spectroscopic assignments of alkaloid **S** in $CDCl_3$

Position	δ_H (ppm, *J* in Hz)		δ_C (ppm)	
	Alkaloid **S**	*N*-demethyl-2-methoxyatherosperminine **71** (Awang et al., 2008) ($CDCl_3$, 400 MHz)	Alkaloid **S**	*N*-demethyl-2-methoxy atherosperminine **71** (Awang et al.,2008) ($CDCl_3$, 100 MHz)
1	-	-	128.4	128.3
1a	-	-	124.5	123.2
1b	-	-	121.8	131.9
2	-	-	150.8	150.9
3	-	-	146.1	151.5
4	-	-	151.3	146.0
5	9.57 (1H, *dd*, *J*=8.4, 0.7)	9.52-9.54 (1H, *d*, *J*=8.6)	127.2	127.3
5a	-	-	130.1	121.8
6	7.62 (1H, *m*)	7.56-7.60 (1H, *m*)	126.7	126.7
7	7.56 (1H, *m*)	7.50-7.54 (1H, *m*)	126.1	126.1
8	7.85 (1H, *dd*, *J*=7.7, 1.6)	7.78-7.80 (1H, *dd*, *J*=9.3, 1.7)	128.2	128.4
8a	-	-	131.9	130.0
9	7.70 (1H, *d*, *J*=9.1)	7.65-7.68 (1H, *d*, *J*=9.3)	127.3	127.4
10	7.89 (1H, *d*, *J*=9.1)	7.92-7.94 (1H, *d*, *J*=9.3)	122.3	122.2
11	3.30 (2H, *m*)	3.40-3.45 (2H, *dd*, *J*=15.8, 7.1)	24.2	25.1
12	2.55 (2H, *m*)	2.95-2.99 (2H, *m*)	60.0	51.3
NCH_3	-	2.58 (3H, *s*)		
2-*N*CH_3	2.41 (6H, *s*)	-	45.2	35.0
2-OCH_3	4.01 (3H, *s*)	3.98 (3H, *s*)	61.2	61.4
3-OCH_3	4.07 (3H, *s*)	3.94 (3H, *s*)	61.5	60.2
4-OCH_3	3.98 (3H, *s*)	4.03 (3H, *s*)	60.3	61.1

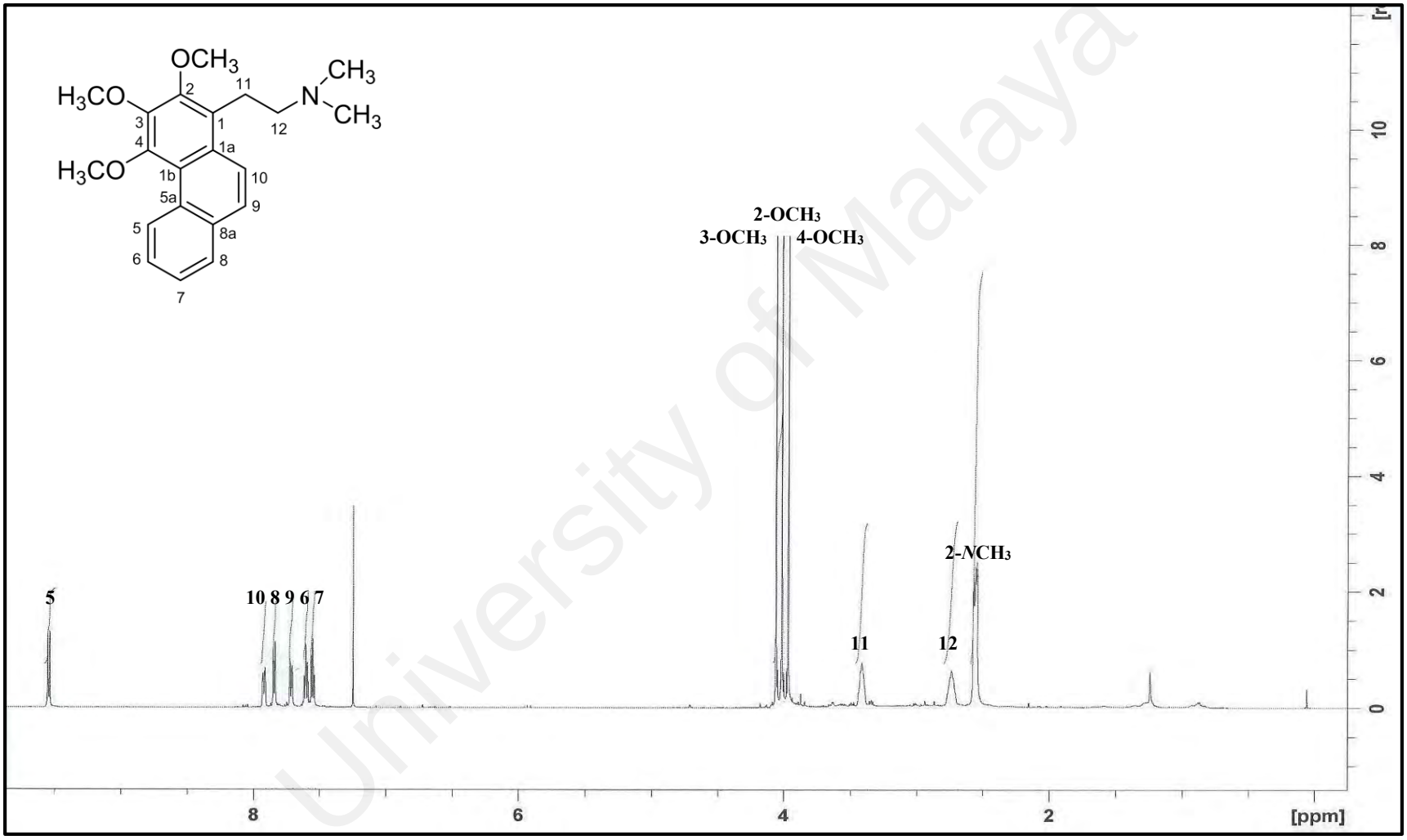

Figure 3.92: ^{1}H NMR spectrum of alkaloid **S**

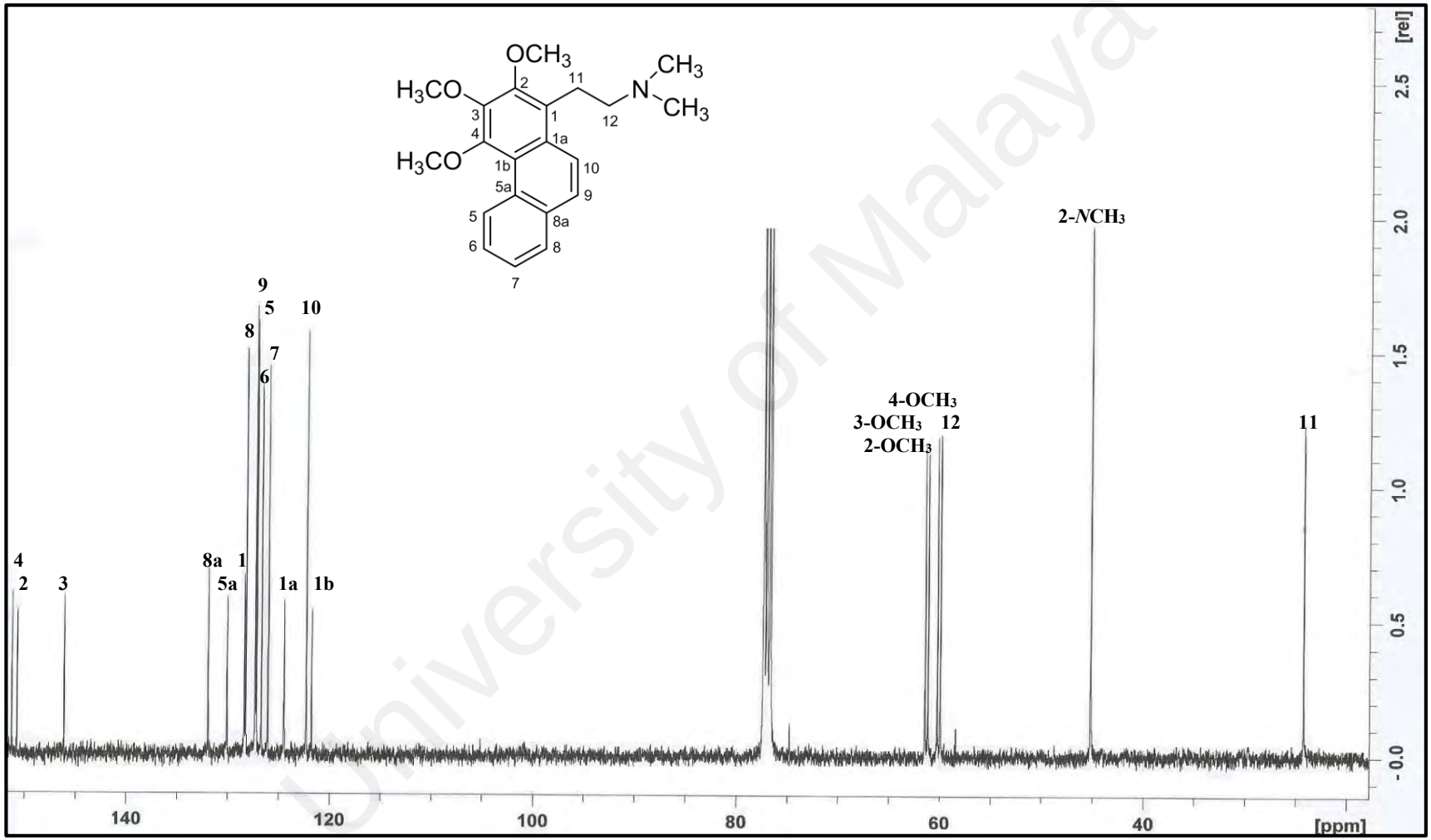

Figure 3.93: ^{13}C NMR spectrum of alkaloid **S**

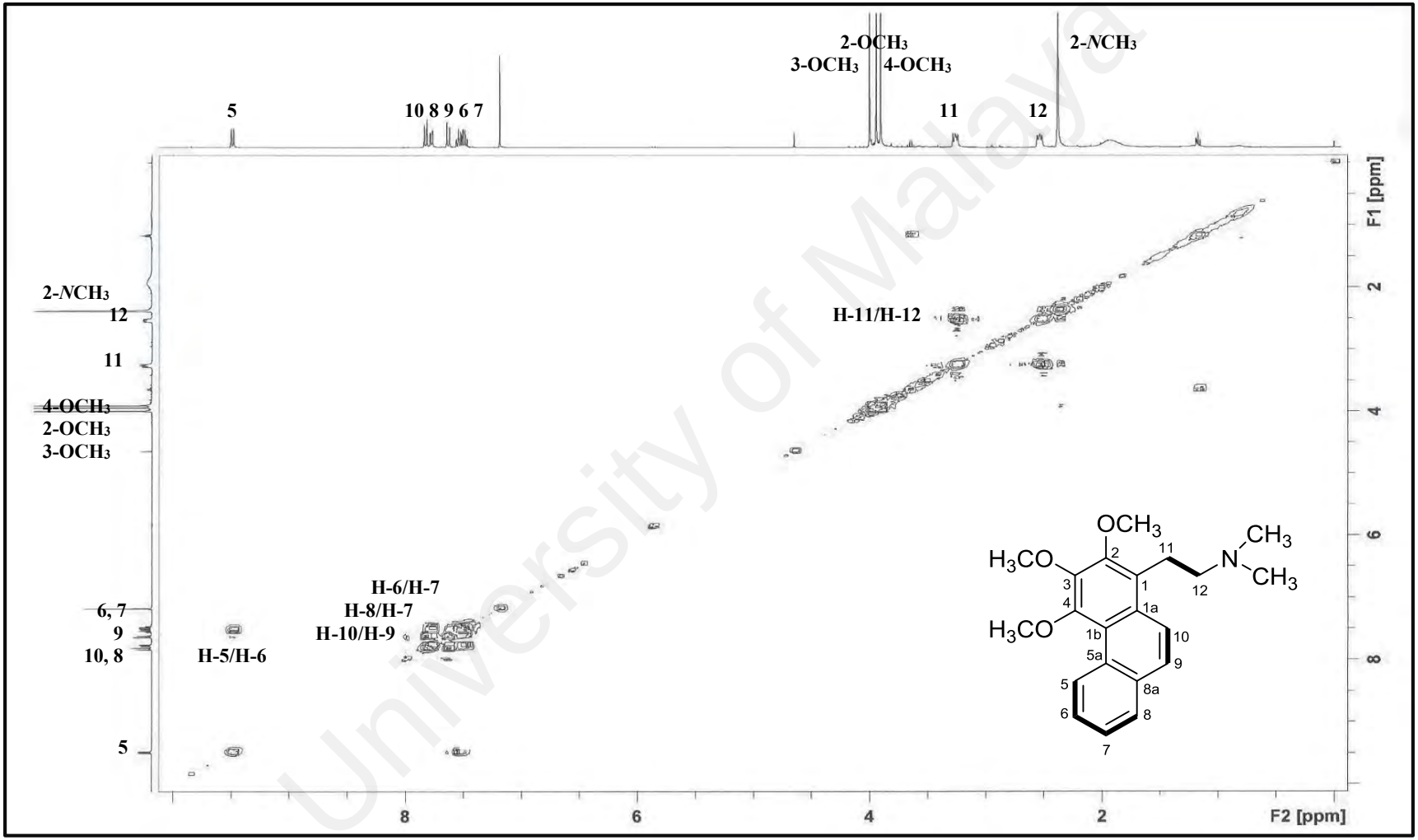

Figure 3.94: COSY spectrum of alkaloid **S**

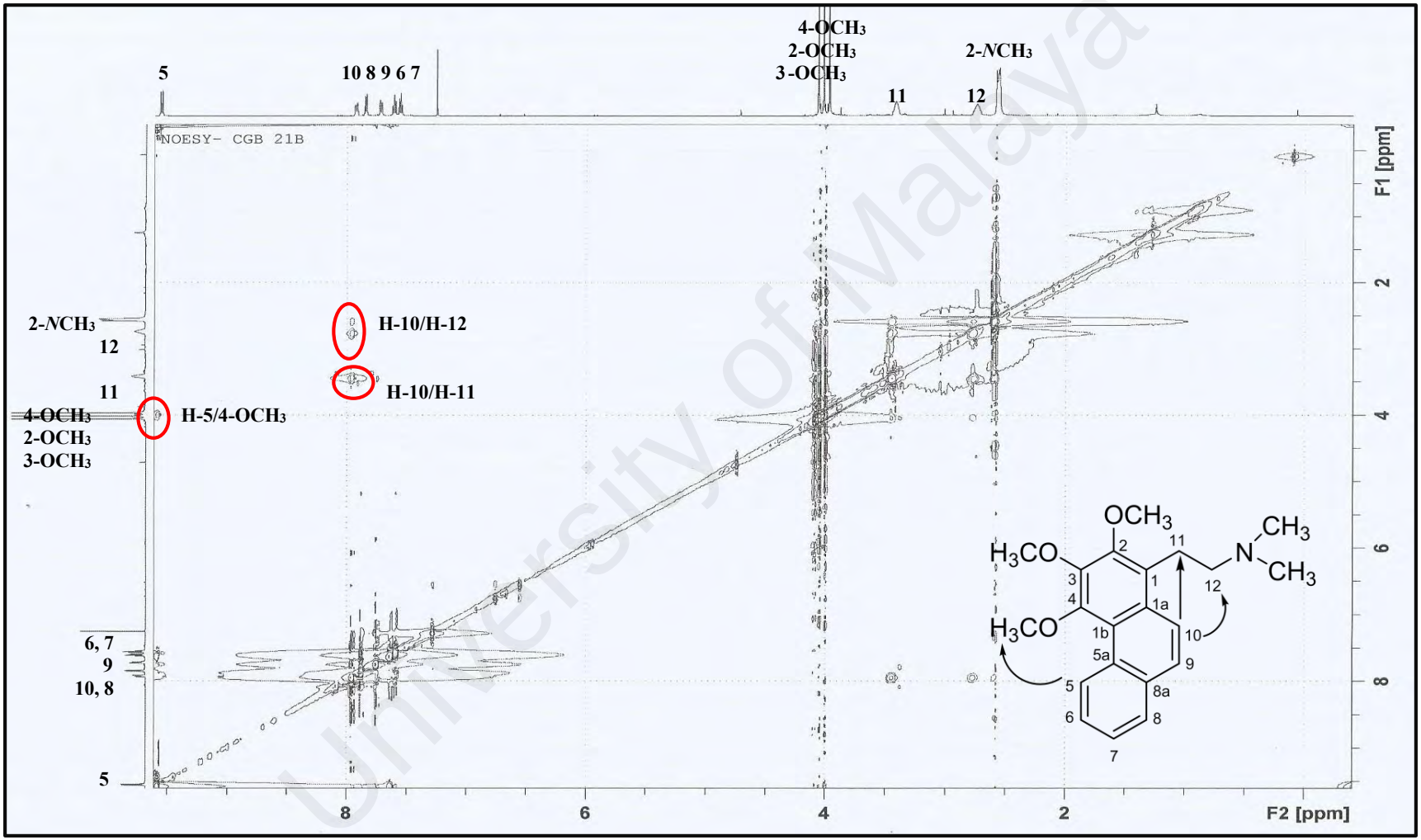

Figure 3.95: NOESY spectrum of alkaloid **S**

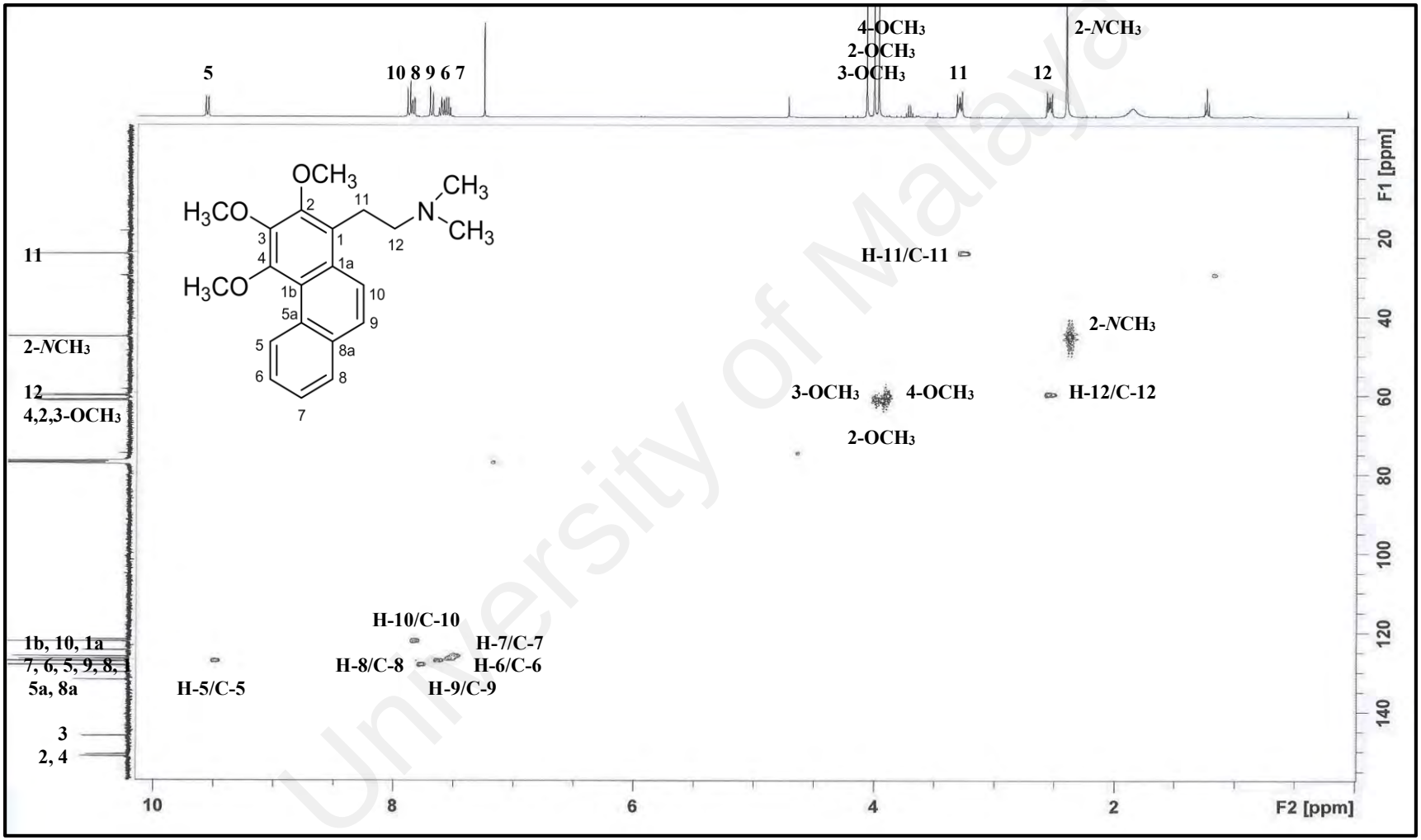

Figure 3.96: HSQC spectrum of alkaloid **S**

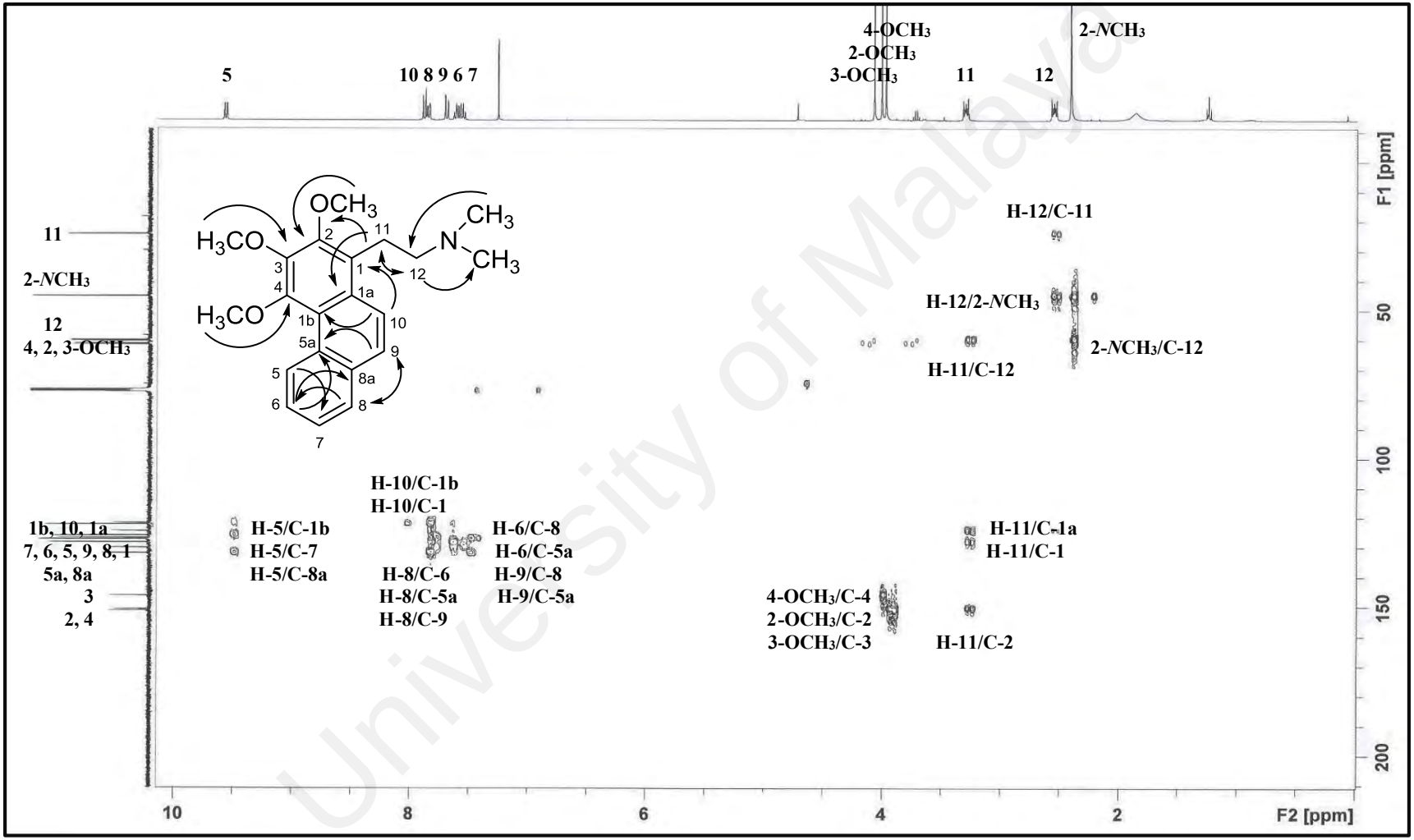

Figure 3.97: HMBC spectrum of alkaloid **S**

3.2.20 Alkaloid T: 2-Hydroxyatherosperminine 13

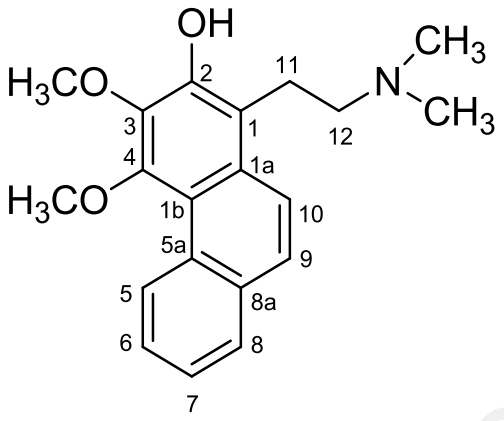

13

Alkaloid **T** was isolated as a brownish amorphous. The LCMS-IT-TOF spectrum gave a pseudomolecular ion peak, $[M+H]^+$, *m/z* 326.0934, (calcd. for $C_{20}H_{24}NO_3$, 326.1751), which indicated the molecular formula of $C_{20}H_{23}NO_3$, thus, implying ten degrees of unsaturation. The IR spectrum revealed an important peak at 3394 cm^{-1} due to hydrogen-bonded OH (phenolic) stretching vibrations.

Alkaloids **T** exhibited a ^1H NMR spectrum (Figure 3.98) which closely resembled that of alkaloid **S**, except for the absence of one methoxyl signal located at C-2 in alkaloid **T**. Two distinct methoxyl signals appeared as singlet at δ_H 4.02 and 3.87, which were attached to C-3 and C-4 respectively. A sharp peak attributed to the six methyl hydrogen groups attached to the nitrogen was observed at δ_H 2.41. The ^{13}C NMR spectrum was very weak due to paucity of sample and some quaternary carbons could not be detected.

On the basis of the analyzed spectral data and comparison with the literature, the structure of alkaloid **T** was elucidated as 2-hydroxyatherosperminine **13**, which was previously isolated from *Cryptocarya crassinervia* (Awang et al., 2008).

Table 3.21: ^{1}H NMR (400 MHz) spectroscopic assignments of alkaloid **T** in $CDCl_3$

Position	**δ_H (ppm, *J* in Hz)**	
	Alkaloid **T**	2-hydroxyatherosperminine **13** (Awang et al., 2008) ($CDCl_3$, 400 MHz)
1	-	-
1a	-	-
1b	-	-
2	-	-
3	-	-
4	-	-
5	9.39 (1H, *dd*, *J*=7.6, 0.8)	9.31-9.32 (1H, *d*, *J*=7.3)
5a	-	-
6	7.60 (1H, *m**)	7.47-7.52 (1H, *m*)
7	7.56 (1H, *m**)	7.47-7.52 (1H, *m*)
8	7.84 (1H, *dd, J*=8.0, 1.8)	7.83-7.85 (1H, *dd*, *J*=7.8, 1.7)
8a	-	-
9	7.65 (1H, *d*, *J*=9.2)	7.68-7.71 (1H, *d*, *J*=9.0)
10	7.87 (1H, *d, J*=9.2)	7.95-7.98 (1H, *d*, *J*=9.0)
11	3.31 (2H, *m*)	3.61 (2H, *m*)
12	2.57 (2H, *m*)	3.04 (2H, *m*)
2-*N*CH_3	2.41 (6H, *s*)	2.80 (6H, *s*)
3-OCH_3	4.02 (3H, *s*)	4.04 (3H, *s*)
4-OCH_3	3.87 (3H, *s*)	3.84 (3H, *s*)

*m**= overlapping signals.

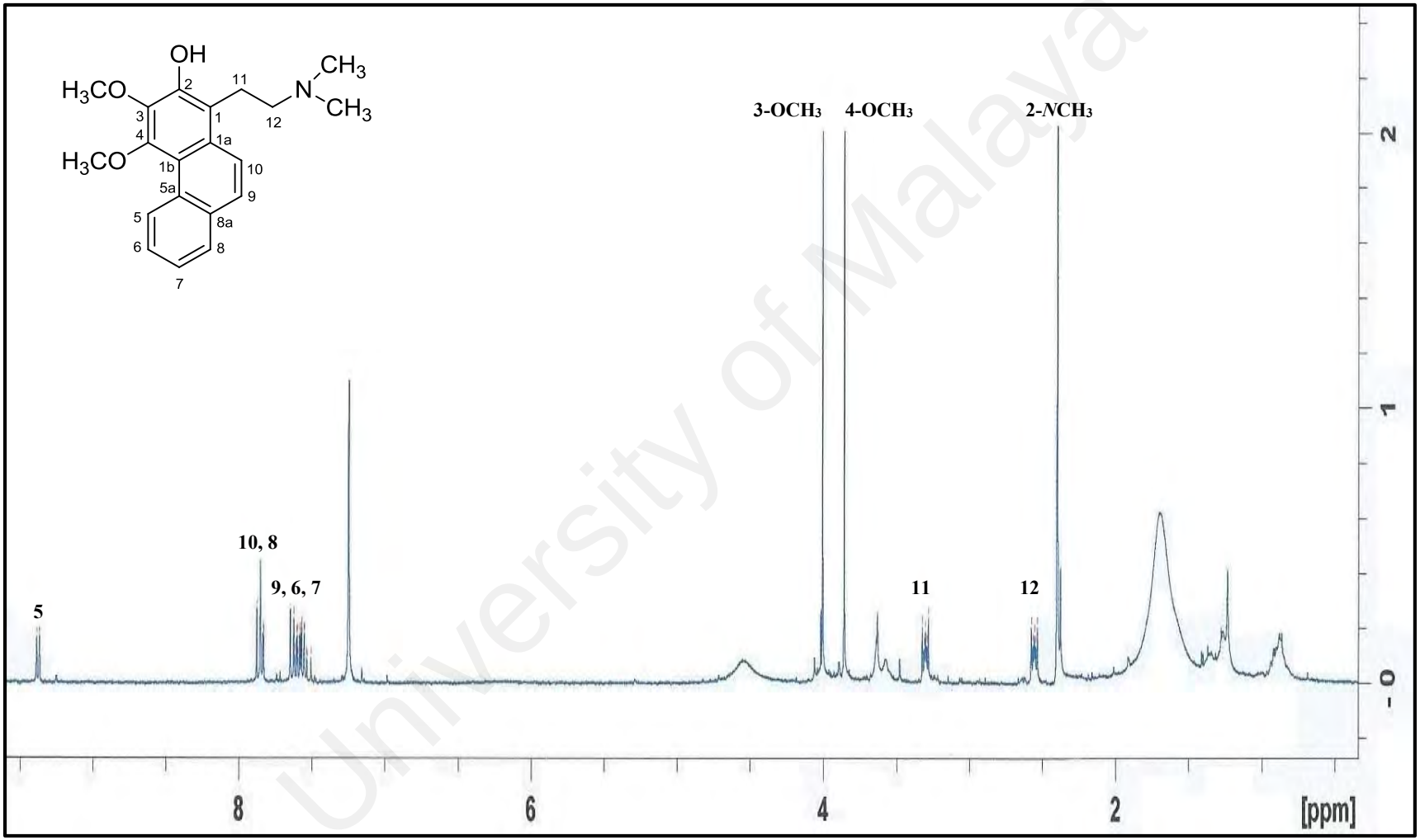

Figure 3.98: ^{1}H NMR spectrum of alkaloid **T**

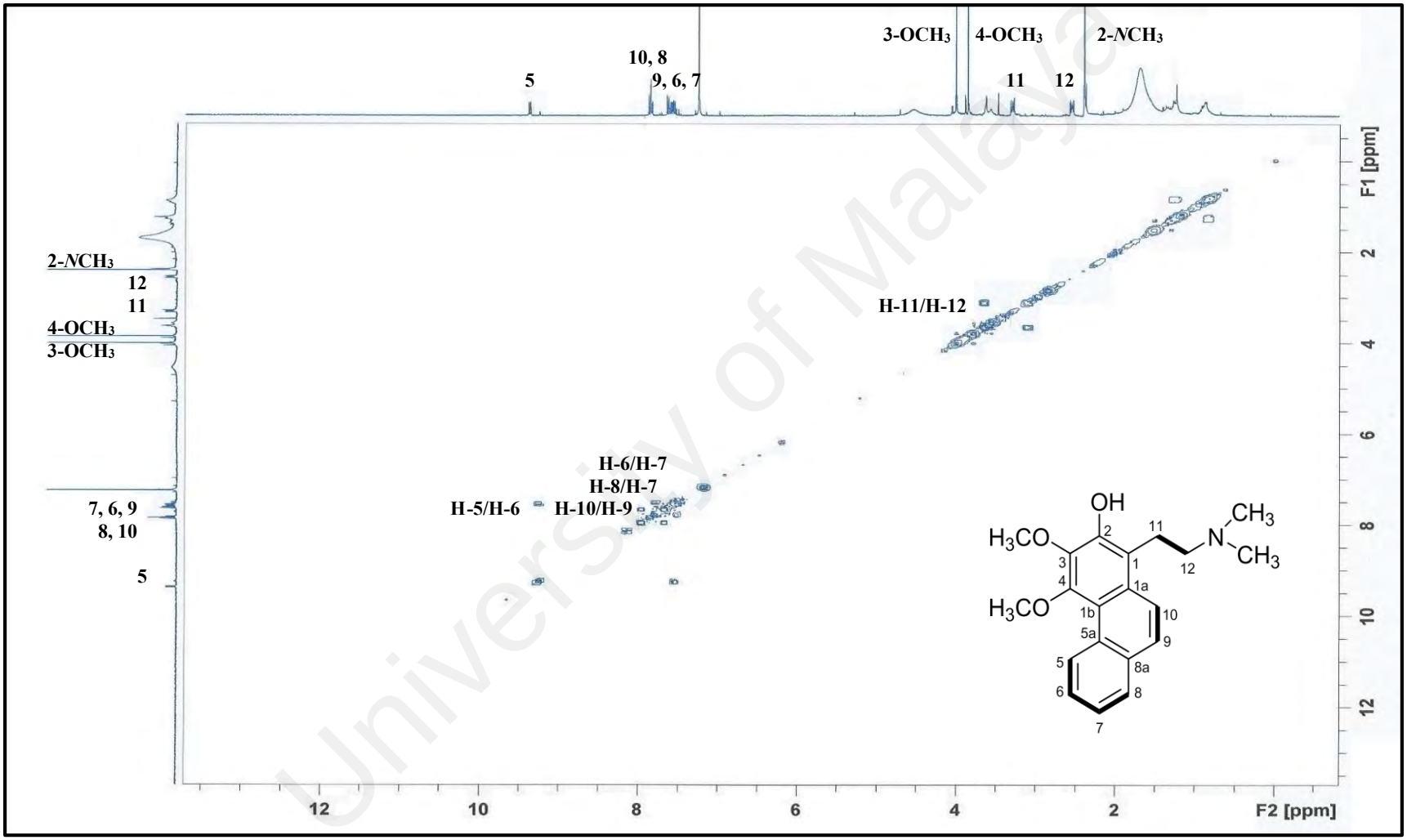

Figure 3.99: COSY spectrum of alkaloid **T**

CHAPTER 4: BIOLOGICAL ACTIVITIES

4.1 General

Plants have served as a source of medicinally important bioactive compounds against numerous ailments for centuries (Subbulakshmi, Thalavaipandian, Bagyalakshmi, & Rajendran, 2012). Until today, natural products have served as the mainstay of all medicines world-wide. According to WHO, over 70% of the world population still relies on herbal remedies for their health care needs. The systematic drug development programs from natural sources are based on the bioassay-guided isolation of natural products, taking into consideration the folklore uses (ethnopharmacological applications) of local plants. A number of bioassays have been developed recently to direct the isolation work (Choudhary, 1999).

In this study, the isolated alkaloids were evaluated for two bioassays; antioxidant and cholinesterase inhibitory activity, exemplify the importance and potential of bioactivity-directed phytochemical investigations. The following subchapters will discuss briefly the DPPH antioxidant activity and acetyl and butyrylcholinesterase activities.

4.2 Antioxidants DPPH Activity

Free radicals are molecules which contains one or more unpaired electron and are important intermediates in natural processes involving cytotoxicity, control of vascular tone, and neurotransmission (Sarma, Mallick, & Ghosh, 2010). Free radicals are formed naturally in the human body and produced especially when our cells create energy from food and oxygen and when we are exposed to microbial infections, extensive exercise, or pollutants/toxins such as cigarette smoke, alcohol, ionizing and UV radiations, pesticides, and ozone (Poljsak, Šuput, & Milisav, 2013). Any free radical involving oxygen can be referred to as a reactive oxygen species (ROS). In healthy individuals,

the production of free radicals is balanced by the antioxidative defense system; however, oxidative stress arises as a result of an imbalance between the production of ROS and the biological system's ability to detoxify the reactive intermediates (Ienco et al., 2011). At high concentrations, free radicals can be hazardous to the body and damage all major components of cells, including DNA, proteins, and cell membranes. The damage to cells caused by free radicals, especially the damage to DNA, may play a role in the development of cancer and other health conditions (Valko et al., 2007).

To counteract oxidative stress, the body produces an armoury of antioxidants to defend itself. Antioxidants reduce the oxidative stress in cells by neutralizing or scavenging of reactive species by hydrogen donation, therefore useful in the treatment of many human diseases. One solution to this problem is to supplement the diet with antioxidant compounds that are contained in natural plant sources (Knekt, Jarvinen, Reunanen, & Maatela, 1996). These natural plant antioxidants can therefore serve as a type of preventive medicine. Medicinal plants contain some organic compounds which produce definite physiological action in the human body and these bioactive substances include tannins, alkaloids, carbohydrates, terpenoids, steroids and flavonoids. The major plant antioxidants are phenolic compounds with their large known number exceeding 8000 molecules (Elansary, 2014). Phenolics have been known to possess a capacity to scavenge free radicals. The antioxidant activity of phenolics is principally due to their redox properties, which allow them to act as reducing agents, hydrogen donors (Soni & Sosa, 2013).

4.2.1 Solvents and Chemicals

1,1-Diphenyl-2-picrylhydrazyl (DPPH), and ascorbic acid were obtained from Sigma-Aldrich (Germany). Analytical grade ethanol (EtOH) was purchased from Merck (Darmstadt, Germany).

4.2.2 *In vitro* Antioxidant DPPH Assay

The free radical scavenging activity of alkaloids, (+)-*N*-methyllaurotetanine **87**, dicentrinone **124**, (-)-desmethylsecoantofine **130** and crychine **134** were measured in terms of hydrogen donating ability using DPPH radical as described (Shimada, Fujikawa, Yahara, & Nakamura, 1992). Briefly, 0.1 mM of DPPH (1 mL) dissolved in ethanol was added to an ethanol solution (3 mL) of the tested alkaloids at different concentrations (25, 50, 100, 200 µg/mL). An equal volume of ethanol was added in the control test. The mixture was shaken vigorously and allowed to stand in the dark at room temperature for 30 mins. The decrease in the absorbance was measured at 517 nm with a microplate reader (Tecan Sunrise, Austria). Ascorbic acid (20.8-333.3 µg/mL) was used as the standard and the control was ethanol. The percentage of inhibitory activity of alkaloids (+)-*N*-methyllaurotetanine **87**, dicentrinone **124**, (-)-desmethylsecoantofine **130** and crychine **134** was calculated according to the following equation:

$$\% \text{ of DPPH radical scavenging effect activity} = [A_o\text{-}A_1/A_o] \times 100$$

where A_o is the absorbance of the control and A_1 is the absorbance of the compound or standard. The concentration of the compound required to scavenge 50% of the DPPH radical (IC_{50}) was estimated from the graph plotted against the percentage inhibition and compared with the standard. All tests were carried out in triplicates, and the results were expressed in µg/mL.

4.2.3 Results and Discussion

Alkaloids (+)-*N*-methyllaurotetanine **87**, dicentrinone **124**, (-)-desmethylsecoantofine **130** and crychine **134** were screened for their *in vitro* DPPH free radical scavenging activity in order to evaluate their antioxidant potential. Ascorbic acid

137 was used as the positive control (IC_{50} = 13.16 ± 0.25 µg/mL). The results in Figure 4.1 and Table 4.1 revealed that alkaloids (-)-desmethylsecoantofine **130** (IC_{50} = 62.40 ± 0.05 µg/mL) and (+)-*N*-methyllaurotetanine **87** (IC_{50} = 130.00 ± 0.07 µg/mL) were more effective free radical scavengers compared to crychine **134** and dicentrinone **124** (IC_{50} > 200 µg/mL). It has been reported that phenolic compounds which are capable of donating hydrogen atoms are known to be effective in scavenging radicals (Nasrullah, Zahari, Mohamad, & Awang, 2013; Zahari et al., 2014). The higher radical scavenging activities of (-)-desmethylsecoantofine **130** and (+)-*N*-methyllaurotetanine **87** in contrast to crychine **134** and dicentrinone **124** may have been attributed to the presence of a phenolic chromophore in the structure of the former two alkaloids and the absence of it in the latter two.

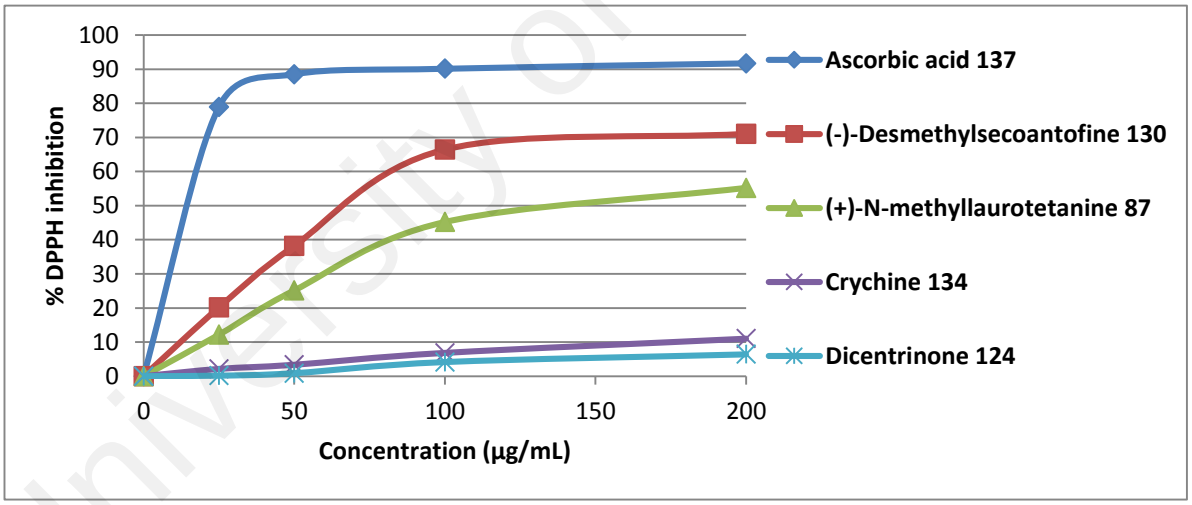

Figure 4.1: Antioxidant activity of isolated alkaloids

Table 4.1: DPPH radical scavenging activity of isolated alkaloids and ascorbic acid.

Alkaloids	(+)-*N*-methyllaurotetanine **87**	Crychine **134**	(-)-Desmethyl-secoantofine **130**	Dicentrinone **124**	Ascorbic acid **137**
IC_{50} (µg/mL)	130.00 ± 0.07	> 200	62.40 ± 0.05	> 200	13.16 ± 0.25

4.3 Cholinesterase Inhibitory Activity

Alzheimer's disease (AD), a common neurodegenerative disease, is characterized by low levels of the neurotransmitter, acetylcholine (ACh) in the brain region involved with cognition. AD is one of the most common forms of dementia affecting many elderly people. Clinical treatment of this disease among other include enhancement of cholinergic function by prolonging the availability of ACh released into the neuronal synaptic cleft. This is achieved by the use of cholinesterase inhibitors, which inhibit the enzyme responsible for breaking down ACh. There are two types of cholinesterase, namely acetylcholinesterase (AChE) and butyrylcholinesterase (BChE). A potential source of AChE and BChE inhibitors is certainly provided by the abundance of plants in nature (Adewusi, Moodley, & Steenkamp, 2010). Up to date, several potent AChE and BChE inhibitors has been originally isolated from plants and fungi such as physostigmine **138** and galantamine **139** which were isolated from the seeds of *Physostigma venenosum* (Leguminosae) and the bulbs of *Galanthus nivalis* (Amaryllidaceae), respectively. These inhibitors were reported to be more selective for AChE (Mukherjee, Kumar, Mal, & Houghton, 2007). Plant-derived cholinesterase inhibitors are mainly divided into alkaloids, terpenoids and shikimate-derived group of compounds. Among them, alkaloids are regarded as the strongest inhibitors, and AChE inhibitors marketed to treat AD contain nitrogen atoms in their molecule (Houghton, Ren, & Howes, 2006). For example, huperzine A **140**, a quinolizidine related alkaloid from the clubmoss *Huperzia serrata* (Lycopodiaceae) is an AChE commercialized as a dietary supplement for memory support and it is used to treat AD symptoms in China (Murray, Faraoni, Castro, Alza, & Cavallaro, 2013).

4.3.1 Solvents and Chemicals

Acetylcholinesterase (AChE) was obtained from electric eel, 5,5′-dithiobis (2-nitrobenzoic acid) (DTNB), acetylthiocholine iodide (ATCI), butyrylcholineterase (BChE) was collected from equine serum, *S*-butyrylthiocholine chloride, physostigmine **138** and galantamine **139** were purchased from Sigma (St. Louis, MO, USA). Sodium dihydrogen phosphate anhydrous was purchased from R&M Chemicals (Essex, UK) while disodium hydrogen phosphate anhydrous was purchased from Merck (Darmstadt, Germany). All the other solvents and reagents used were of analytical grade.

4.3.2 *In vitro* Cholinesterase Inhibitory Assay

Cholinesterase inhibitory activity of the isolated alkaloids was evaluated following Ellman's microplate assay with modification as described by Khaw et al. (Khaw et al., 2014). Briefly, for AChE inhibitory assay, 140 µL of 0.1 M sodium phosphate buffer (pH 8) was first added into each well of a 96-well microplate followed by 20 µL of the test sample; (+)-nornantenine **123**, (-)-desmethylsecoantofine **130**, desmethylsecoantofine-*N*-oxide **131**, (+)-oridine **125**, prodensiflorin A **126**, prodensiflorin B **127**, (+)-laurotetanine **86**, atherosperminine **15**, (+)-*N*-methylisococlaurine **14**, (+)-*N*-methyllaurotetanine **87**, 2-methoxyatherosperminine **72** and (+)-reticuline **76** (in 10 % methanol) and 20 µL of 0.09 unit/mL AChE. After 15 minutes of pre-incubation at 25 °C, 10 µL of 10 mM 5,5′-dithiobis (2-nitrobenzoic acid) was added into each well followed by 10 µL of 14 mM acetylthiocholine iodide (ATCI). The absorbance of the colored end-product was measured at 412 nm at designated intervals for 30 minutes after the initiation of enzymatic reaction using Tecan Infinite 200 ProMicroplate Spectrometer (Switzerland). For BChE inhibitory assay, the same procedure was followed except that the enzyme and substrate used were BChE from the equine serum and *S*-butyrylthiocholine chloride, respectively. Physostigmine **138** and

galantamine **139** were used as the reference standard. Each test sample was conducted in triplicate. Absorbance of the test sample was corrected by subtracting the absorbance of its respective blank. A set of five concentrations was used to estimate the 50 % inhibitory concentration (IC_{50}) for the active compounds.

4.4 Enzyme Inhibition Kinetic

Mode of BChE inhibition and enzyme kinetics of 2-methoxyatherosperminine **72** were determined by analyses of Lineweaver-Burk (LB) plot and secondary plot of LB as described by Liew et al. (Liew et al., 2015). The enzyme activity was evaluated in the absence and presence of different concentrations of 2-methoxyatherosperminine **72** (0.00, 1.47, 2.95 μM) at various concentration of substrate (1.75, 3.50, 7.00, 14.00 mM).

4.5 Results and Discussion

4.5.1 Cholinesterase Inhibition Studies

All the alkaloid tested exhibited a wide range of AChE and BChE inhibitory activity with IC_{50} values, within the range of 3.95-301.01 μM (Table 4.2). In general, the isolated alkaloids were found to be moderate to weak inhibitors of AChE, with IC_{50} values in the range of 83.26 – 301.01 μM. In contrast, eight alkaloids showed more than 50% inhibition against BChE at 100 μg/mL. Among them, alkaloids (+)-nornantenine **123**, atherosperminine **15**, 2-methoxyatherosperminine **72** and (+)-reticuline **76** showed potent to moderate BChE inhibition, with IC_{50} lower than 100 μM. The difference in the activity towards the cholinesterase could be contributed, at least in part, by the bulkiness of the alkaloids isolated in this study. Due to the different amino acid residues underlying the active site, BChE but not AChE could accommodate bulkier alkaloids into its active site (Khaw et al., 2014).

The enzyme inhibition data indicated that alkaloid 2-methoxyatherosperminine **72** had the most potent BChE inhibitory activity with only 6.8 times less potent than that of physostigmine **138**. However, alkaloid 2-methoxyatherosperminine **72** showed more potency than galantamine **139**, a clinically used cholinesterase inhibitor, which was reported as having IC_{50} value of 28.29 μM (Liew et al., 2015). In addition, both alkaloids 2-methoxyatherosperminine **72** and atherosperminine 1**5** were found to be selective towards BChE inhibition. Some studies revealed that BChE level in specific brain region is increased with progression of AD while AChE level decreases (Greig et al., 2005; Lam, Hollingdrake, Kennedy, Black, & Masellis, 2009). Hence, a BChE selective inhibitor would be useful in the later stages of AD. There is currently no BChE selective inhibitor being employed clinically.

The study on AChE and BChE inhibitory activities of the isolated alkaloids showed that it's were influenced by the alkaloids skeleton especially by the ring substituents with high degree of methoxylation at ring A and the presence of tertiary amine. Five different types of alkaloids were isolated, namely, aporphine, *seco*phenanthroindolizidine, proaporphine, phenanthrene and benzylisoquinoline. Alkaloids atherosperminine **15** and 2-methoxyatherosperminine **72** which belong to the phenanthrene type, having acyclic tertiary amine, exhibited good BChE inhibitory activity with IC_{50} values of 19.34 and 3.95 μM respectively. Meanwhile alkaloids (-)-desmethylsecoantofine **130**, (+)-*N*-methylisococlaurine **14**, (+)-*N*-methyllaurotetanine **87** and (+)-reticuline **76** with cyclic tertiary amine exhibited moderate to weak BChE inhibitory activity as compared to alkaloids 2-methoxyatherosperminine **72** and atherosperminine **15**. In addition, between alkaloids atherosperminine **15** and 2-methoxyatherosperminine **72**, the latter having high degree of methoxylation at ring A, exhibited better BChE inhibitory activity. Thus, the finding suggest that acyclic tertiary amine and high degree of methoxylation at ring A could play an important role in BChE

inhibition. Moreover, moderate and low cholinesterase inhibitory activity of the aporphine alkaloids could be due to the lack of one aromatic ring than that found in phenanthrene alkaloids. Compounds lacking aromatic ring demonstrated a decrease in activity, indicating the significance of an aromatic planar moiety in interactions with enzyme-binding sites (Wang et al., 2010).

Alkaloids (-)-desmethylsecoantofine-*N*-oxide **131** and (-)-desmethylsecoantofine **130** are structurally related, with the significant difference being in the former's carbon framework which bears an additional *N*-oxide moiety. The weak cholinesterase inhibitory activities of (-)-desmethylsecoantofine-*N*-oxide **131** ($IC_{50\ AChE}$ = 153.47 μM and $IC_{50\ BChE}$ = 213.08 μM) and (-)-desmethylsecoantofine **130** ($IC_{50\ AChE}$ = 201.52 μM and $IC_{50\ BChE}$ = 166.69 μM) strongly suggested that the *N*-oxide moiety in (-)-desmethylsecoantofine-*N*-oxide **131** did not influence its inhibitory effect (Othman et al., 2016).

As for prodensiflorin A **126** (IC_{50} = 137.50 μM) and prodensiflorin B **127** (IC_{50} = 83.26 μM), their AChE inhibiting potentials were only evaluated as their amounts were insufficient for further analysis. A closer look at their structures revealed that they were proaporphine type alkaloids structurally related (+)-oridine **125**. Based on current and previous investigations (Othman et al., 2016), it may suggest that proaporphine type alkaloids are moderate to weak AChE and BChE inhibitors.

Table 4.2: Acetylcholinesterase (AChE) and butyrylcholinesterase (BChE) inhibitory activities of the isolated alkaloids

Compounds	% inhibition at 100 µg/mL		IC_{50}				Selectivity	
	AChE [a]	BChE [a]	AChE		BChE		AChE [b]	BChE [c]
			µg/mL [a]	µM	µg/mL [a]	µM		
(+)-Nornantenine **123**	50.38 ± 3.24	75.81 ± 2.81	66.83 ± 1.18	205.55	30.71 ± 1.93	94.45	0.46	2.18
(-)-Desmethylsecoantofine **130**	51.41 ± 1.21	59.41 ± 1.56	70.77 ± 3.87	201.52	58.54 ± 1.61	166.69	0.83	1.21
(+)-Oridine **125**	27.89 ± 0.64	52.09 ± 1.40	NT	NT	83.38 ± 3.68	288.34	-	-
(+)-Laurotetanine **86**	17.51 ± 0.68	22.58 ± 0.47	NT	NT	NT	NT	-	-
Atherosperminine **15**	2.06 ± 1.29	83.87 ± 0.46	NT	NT	6.29 ± 0.88	19.34	-	-
(+)-*N*-methylisococlaurine **14**	14.93 ± 0.53	37.33 ± 1.56	NT	NT	NT	NT	-	-
(+)-*N*-methyllaurotetanine **87**	38.79 ± 2.6	50.95 ± 1.41	NT	NT	74.65 ± 2.10	218.81	-	-
2-methoxyatherosperminine **72**	31.58 ± 2.87	95.18 ± 0.24	NT	NT	1.34 ± 0.05	3.95	-	-
(+)-Reticuline **76**	52.96 ± 5.71	84.07 ± 0.38	99.08 ± 0.34	301.01	21.41 ± 0.47	65.04	0.22	4.63
Prodensiflorin A **126**	68.10 ± 1.18	-	39.46 ± 1.73	137.50	-	NT	-	-
Prodensiflorin B **127**	79.61 ± 4.31	-	23.73 ± 1.16	83.26	-	NT	-	-
(-)-Desmethylsecoantofine-*N*-oxide **131**	63.07 ± 4.74	54.45 ± 2.01	56.35 ± 5.11	153.47	78.24 ± 0.57	213.08	1.39	0.72
Physostigmine **138** (standard) [d]	-	-	0.046 ± 0.01	0.16	0.16 ± 0.02	0.58	3.63	0.28
Galantamine **139** (standard) [d]	-	-	0.27 ± 0.07	0.94	8.12 ± 0.61	28.29	30.10	0.03

[a] Data presented as Mean ± SD (n = 3)
[b] Selectivity for AChE is defined as IC_{50} (BChE)/IC_{50} (AChE)
[c] Selectivity for BChE is defined as IC_{50} (AChE)/IC_{50} (BChE)
[d] Literature values from (Liew et al., 2015)

4.5.2 BChE Kinetic Study of 2-methoxyatherosperminine 72

Enzyme kinetic of the most active inhibitor; 2-methoxyatherosperminine **72** against BChE was carried out by Lineweaver-Burk (LB) analysis (Figure 4.2). Results suggested that 2-methoxyatherosperminine **72** is a mixed-mode inhibitor of BChE, where it can bind to the enzyme's active site or allosteric site. *Ki* value of BChE inhibition by 2-methoxyatherosperminine **72** was 6.72 μM, derived from the secondary replot of LB plot.

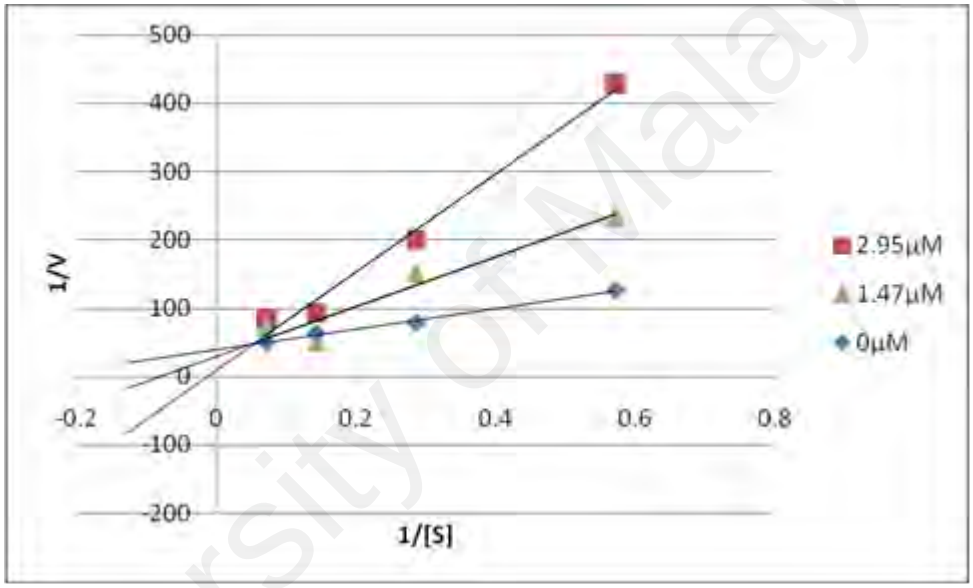

Figure 4.2: Lineweaver-Bulk (LB) plot of BChE activity over a range of substrate concentration for 2-methoxyatherosperminine **72**

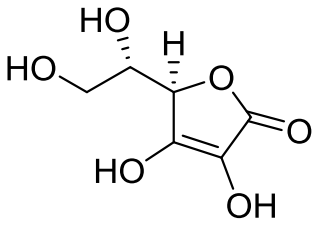

137

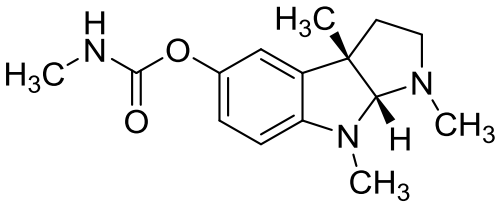

138

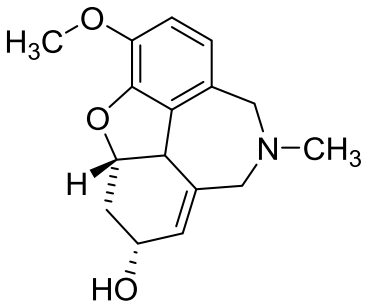

139

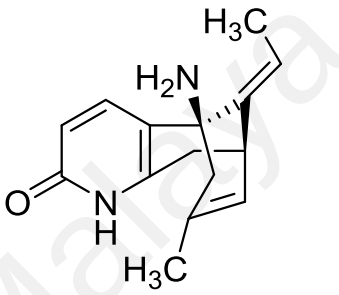

140

Figure 4.3: Structure of the standard used in the DPPH antioxidant (**137**) and cholinesterase inhibitory (**138-140)** activities

CHAPTER 5: CONCLUSION

Three plant species from the Lauraceae family, *Cryptocarya densiflora* Blume, *Cryptocarya infectoria* Miq. and *Cryptocarya griffithiana* Wight have been studied for their alkaloidal content and bioactivity studies. Phytochemical studies of these three plant species led to the identification of twenty alkaloids using several chromatographic techniques such as column chromatography (CC), thin layer chromatography (TLC) and preparative thin layer chromatography (PTLC). Their structural elucidation was performed through combination of spectroscopic methods, notably 1D NMR (^{1}H, ^{13}C and DEPT), 2D NMR (COSY, NOESY, HSQC and HMBC), MS, UV, IR as well as by comparison with the literature values. The alkaloids found by the author can be divided into seven main groups:

i) Aporphine: (+)-laurotetanine **86**, (+)-*N*-methyllaurotetanine **87** and (+)-nornantenine **123**

ii) Oxoapophine: dicentrinone **124** and liriodenine **136**

iii) Proaporphine: (+)-oridine **125**, prodensiflorin A **126** and prodensiflorin B **127**

iv) Phenanthroindolizidine: (-)-antofine **6**, (-)-densiindolizidine **128** (-)-desmethylsecoantofine **130** and (-)-desmethylsecoantofine-*N*-oxide **131**

v) Phenanthrene: 2-hydroxyatherosperminine **13**, atherosperminine **15**, 2-methoxyatherosperminine **72** and argentinine **135**

vi) Benzylisoquinoline: (+)-*N*-methylisococlaurine **14** and (+)-reticuline **76**

vii) Pavine: (-)-isocaryachine **61** and crychine **134**

Among the twenty alkaloids which were isolated from this study, four new alkaloids were obtained from the leaves of *C. densiflora*, namely prodensiflorin A **126**, prodensiflorin B **127**, (-)-densiindolizidine **128** and (-)-desmethylsecoantofine-*N*-oxide **131**. In addition, (-)-desmethylsecoantofine **130** which isolated from the same species was afforded as a major compound. Furthermore, alkaloids (-)-desmethylsecoantofine-*N*-oxide **131** was the first reported *seco*-phenanthroindolizidine-*N*-oxide found in *Cryptocarya* plants while alkaloids (+)-oridine **125**, prodensiflorin A **126** and prodensiflorin B **127** are the first reported proaporphines having unsaturation in ring B. To the best of the knowledge of authors, all compounds were isolated for the first time from these three species.

The antioxidant activity was determined by DPPH free radical scavenging assay. The results revealed that alkaloid (-)-desmethylsecoantofine **130** were more effective free radical scavengers with an IC_{50} value of 62.40 µg/mL followed by (+)-*N*-methyllaurotetanine **87** with an IC_{50} value of 130.00 µg/mL. The cholinesterase activity had revealed that most of the tested alkaloids were found to exhibit moderate to weak activity against AChE and BChE. Despite this, potent inhibition activity was shown by phenanthrene type alkaloid, 2-methoxyatherosperminine **72** with an IC_{50} value of 3.95 µM against BChE. Furthermore, BChE kinetic study of 2-methoxyatherosperminine **72** exhibited mixed-mode type inhibiton with estimated *Ki* value of 6.72 µM. These are the first studies on the cholinesterase inhibiting potential of *Cryptocarya*.

From this study, it can be observed that *Cryptocarya* plants are rich producers of isoquinoline type alkaloids with various skeletal features. Thus, we can learn the variety of chemical nature in plants. Moreover, the discovery of antioxidant and anti-cholinesterase compounds of some of the isolated alkaloids are helpful in our strive to overcome the health problems encountered today such as cancer and Alzheimer diseases.

CHAPTER 6: EXPERIMENTAL

6.1 Plant Materials

The plant materials and botanical identification were carried out by the phytochemical group of the Department of Chemistry, Faculty of Science, University of Malaya. The voucher specimens were deposited at the Herbarium of the Department of Chemistry, Faculty of Science, University of Malaya, Kuala Lumpur, Malaysia. The plant species and their respective localities are shown in Table 6.1 below.

Table 6.1: Plant species and locality

Voucher specimen	**Species**	**Part of plant**	**Locality and date of collection**
KL 5211	*C. densiflora* Blume	Leaves	Tembat Ulu, Terengganu, Malaysia. 22nd April 2009
KL 5229	*C. infectoria* Miq.	Bark & Leaves	Reserved Forest Sg. Badak, Sintok, Kedah, Malaysia. 20th March 2000
KL 5469	*C. griffithiana* Wight	Bark	Reserved Forest Lenggor, Mersing, Johor, Malaysia. 13th May 1998

6.2 Solvent

All solvents were of AR grade. Those used for bulk extraction were distilled prior to use. The solvents used were hexane, dichloromethane, methanol, ammonia solution and hydrochloric acid.

6.3 Instrumentation

The 1D and 2D NMR spectra were acquired in deuterated chloroform, $CDCl_3$ (Merck, Germany) with tetramethylsilane as the internal standard, and deuterated pyridine, C_5D_5N (Merck, Germany) using Bruker AVN400 FT NMR and Bruker AVN600 FT NMR spectrometer systems. Data were analysed *via* TopSpin software package. Chemical shifts were reported in ppm and internally referenced to the residual non-deuterated solvent signals in $CDCl_3$ (^1H δ 7.26; ^{13}C δ 77.0) and pyridine-D_5 (^1H δ 7.22, 7.58, 8.74; ^{13}C δ 123.9, 135.9, 150.4).

LCMS-IT-TOF spectra were carried out on Agilent Technologies 6530 Accurate-Mass Q-TOF LC/MS, with ZORBAX Eclipse XDB-C18 Rapid Resolution HT 4.6 mm id. x 50 mm x 1.8 µm column. HPLC grade methanol, acetonitrile and deionized water were used as mobile phase solvents. All solvents and samples were filtered with 0.2 µm nylon membrane filter (WHATMAN) prior to LCMS analysis.

The ultraviolet spectra, were recorded on a Shimadzu UV-Visible recording Spectrophotometer using HPLC grade methanol as solvent with mirror UV cell.

The Fourier Transform Infrared (FT-IR) spectra were obtained through Perkin Elmer FT-IR Spectrometer Spectrum RX1 using spectroscopic grade chloroform as solvent.

The optical rotations were recorded on a JASCO (Japan) P1020 Automatic Polarimeter Machine equipped with a tungsten lamp and methanol as solvent.

6.4 Chromatography

Purification processes were performed using various chromatographic techniques such as thin layer chromatography, column chromatography and preparative thin layer chromatography over silica gel.

6.4.1 Thin Layer Chromatography (TLC)

Aluminium supported silica gel 60 F_{254} plates (Merck) was used to see the spots of the isolated compound. UV Light Model UVGL-58 Mineralight Lamp 230V~50/60 Hz (254 and 365 nm) was used to examine spots or bands on the TLC before spraying with the Dragendorff's reagents.

6.4.2 Column Chromatography (CC)

Silica gel 60 (63-200 µm-70-230 mesh ASTM) and silica gel 60 (40-63 µm-70-230 mesh ASTM) were used for column chromatography. A slurry of silica gel 60 (approximately 30:1 silica gel to sample ratio) in dichloromethane was poured into a glass column of appropriate size with gentle tapping to remove trapped air bubbles. The crude extract was initially dissolved in minimum amount of solvent and loaded on top the packed column. The extract was eluted with an appropriate solvent system at a certain flow rate. Fractions were collected in either test tubes or conical flasks and evaporated for the next step. Fractions with similar profile in TLC were pooled together to obtain the sub-fractions which were then subjected to further chromatographic analysis.

6.4.3 Preparative Thin Layer Chromatography (PTLC)

PTLC silica gel 60 F_{254} glass plates of size 20 cm x 20 cm (Merck 1.05715.0001) was used for the separation of compounds. UV Light Model UVGL-58 Mineralight Lamp 230V~50/60 Hz was used to examine bands on the PTLC plates.

6.5 Reagent for Detection of Spots

Reagents used for detection of alkaloid contents were Mayer's reagent and Dragendorff's reagent.

6.5.1 Mayer's Reagent (Potassium Mercuric Iodide)

A solution of mercury (II) chloride (1.4g) in distilled water (60 mL) was poured onto a solution of potassium iodide (5.0 g) in distilled water (10 mL). The mixture was then made up to 150 ml. A positive test result was indicated by the formation of white precipitate when the aqueous layer (acidified) is treated with 2 to 3 drops of Mayer's reagent.

6.5.2 Dragendorff's Reagent (Potassium Bismuth Iodide)

Bismuth (III) nitrate (0.85 g) in a mixture of glacial acetic acid (10 mL) and distilled water (40 mL) as solution A. Potassium iodide (8.0 g) in distilled water (200 mL) as solution B. Stock solution was prepared by mixing solution A and solution B in equal volumes. The stock solution (20 mL) was then diluted in a mixture of acetic acid (20 mL) and distilled water (60 mL) to prepare the spray reagent. A positive test result was indicated by the formation of orange precipitate or spots.

6.6 Extraction of Plant Materials

6.6.1 Extraction of Bark

The milled dried plant materials, *C. infectoria* (1.7 kg) and *C. griffithiana* (1.5 kg) were first defatted with hexane (15 L) by cold percolation at room temperature for 3 days. The hexane extracts were combined and the solvent evaporated. The dried plant material were then moistened with 25% NH_4OH (1 L) and left for 2 hours to aggregate the nitrogen containing compounds in the plant. It was then macerated with dichloromethane (CH_2Cl_2) (15 L) twice for a 3 day period. After filtration, the supernatant obtained was concentrated under reduced pressure using a rotary evaporator to a volume of 500 mL and tested for alkaloid content (using TLC and confirmed by spraying with Dragendorff's reagent). The

extracts were finally concentrated and dried to yield 11.50 and 9.30 g of bark extracts from the plants of *C. infectoria* and *C. griffithiana* respectively.

6.6.2 Extraction of Leaves

Extraction procedures for the leaves of *C. densiflora* (2.5 kg) and *C. infectoria* (1.8 kg) were almost the same as bark but with additional acid-base extraction for CH_2Cl_2 extract. First, the dried plant materials were soaked with hexane (20 L, 2x) for three days at room temperature. Then, the hexane crude was obtained by filtration followed by the drying using rotary evaporator. The residues were dried at room temperature and then moistened with 25% of NH_3 and left for 2 hours. They were then re-extracted with CH_2Cl_2 (15 L, 3x) for three days at room temperature to obtained CH_2Cl_2 extract.

Next, the CH_2Cl_2 extract was concentrated under reduced pressure to a volume of approximately 500 mL. The alkaloid content in the extract was tested using TLC and spraying the developed TLC plate with Dragendorff's reagent. The dichloromethane extract was then extracted with 5% of hydrochloric acid and monitored with the Mayer's reagent test. The hydrochloric acid solution obtained was basified with NH_3 solution to a pH of 11 followed by extraction with CH_2Cl_2 again. The CH_2Cl_2 extract then washed with distilled water and dried with anhydrous sodium sulphate and finally concentrated under reduced pressure to give the CH_2Cl_2 crude of *C. densiflora* (15.00 g) and *C. infectoria* (9.50 g).

The residues were soaked again with MeOH (17 L) for three-day period at room temperature to obtain MeOH crude. The hexane crude, CH_2Cl_2 crude and MeOH crude exrtracts were each obtained in the form of a sticky dark green residue.

The amount of the plant materials used for extraction and the yield for all the crudes are listed in Table 6.2.

Table 6.2: Amount of each plant material used for extraction and percentage yield of the crudes

Plant material	Part of plant	Amount (kg)	Yield of crude (g)	Percentage yield (%)
C. densiflora	Leaves	2.5	Hexane - 25.50 CH_2Cl_2 - 15.00	Hexane – 1.02 CH_2Cl_2 - 0.60
C. infectoria	Bark	1.7	Hexane - 8.78 CH_2Cl_2 - 11.50	Hexane - 0.52 CH_2Cl_2 - 0.68
	Leaves	1.8	Hexane - 20.45 CH_2Cl_2 - 9.50	Hexane - 1.14 CH_2Cl_2 - 0.53
C. griffithiana	Bark	1.5	Hexane - 3.42 CH_2Cl_2 - 9.30	Hexane - 0.23 CH_2Cl_2 - 0.62

6.7 Isolation and Purification

The CH_2Cl_2 crude extract was subjected to exhaustive column chromatography over silica gel and eluted with CH_2Cl_2 which was gradually enriched with MeOH. Solvent systems used for column chromatographic separation of CH_2Cl_2 crude of *C. densiflora*, *C. Infectoria* and *C. griffithiana* are shown in Table 6.3.

Table 6.3: Solvent system for the isolation and purification of the CH_2Cl_2 crude of bark and leaves of *C. densiflora*, *C. infectoria* and *C. griffithiana*.

Dichloromethane (CH_2Cl_2)	Methanol (MeOH)
100	0
99	1
98	2
97	3
96	4
95	5
94	6
90	10
83	17
75	25
50	50
0	100

Eluents were collected every 100 ml and each fraction was tested with TLC plate for the presence of alkaloids. The alkaloid spots were first detected by UV light (254 and 365 nm) and confirmed by spraying with Dragendorff's reagent. Fraction having spots with the same R_f values and stains were combined and treated as a group. The combined groups were purified again with CC or preparative TLC to get the alkaloids. The structures of the isolated compounds were elucidated with the aid of spectroscopic methods such as 1D NMR (^{1}H, ^{13}C and DEPT), 2D NMR (COSY, NOESY, HSQC and HMBC), UV, IR and LCMS-IT-TOF. The optical rotation for the optically active compounds were also determined.

The isolated alkaloids from *C. densiflora* (leaves), *C. infectoria* (leaves and bark) and *C. griffithiana* (bark) are listed in Table 6.4-6.7. The isolation and purification of the alkaloids from these species are shown in Scheme 6.1-6.4.

Table 6.4: Alkaloids isolated from the leaves of *C. densiflora* and respective solvent system used in chromatographic separation

Alkaloids	**Type of crude**	**Solvent system**	**Weight (mg)**
(+)-*N*-methyllaurotetanine **87**	CH_2Cl_2	100:0 (CH_2Cl_2:MeOH)	7.3
(+)-Laurotetanine **86**	CH_2Cl_2	100:0 (CH_2Cl_2:MeOH)	8.5
(+)-Nornantenine **123**	CH_2Cl_2	99:1 (CH_2Cl_2:MeOH)	12.0
(+)-Reticuline **76**	CH_2Cl_2	99:1 (CH_2Cl_2:MeOH)	8.2
(-)-Densiindolizidine **128**	CH_2Cl_2	99:1 (CH_2Cl_2:MeOH)	7.8
Prodensiflorin B **127**	CH_2Cl_2	99:1 (CH_2Cl_2:MeOH)	10.6
(-)-Desmethylsecoantofine **130**	CH_2Cl_2	98:2 (CH_2Cl_2:MeOH)	13.8
(-)-Antofine **6**	CH_2Cl_2	98:2 (CH_2Cl_2:MeOH)	9.2
Prodensiflorin A **126**	CH_2Cl_2	97:3 (CH_2Cl_2:MeOH)	7.5
(+)-Oridine **125**	CH_2Cl_2	97:3 (CH_2Cl_2:MeOH)	6.2
(-)-Desmethylsecoantofine-*N*-oxide **131**	CH_2Cl_2	97:3 (CH_2Cl_2:MeOH)	9.2
Crychine **134**	CH_2Cl_2	97:3 (CH_2Cl_2:MeOH)	7.2
(-)-Isocaryachine **61**	CH_2Cl_2	97:3 (CH_2Cl_2:MeOH)	8.4
Dicentrinone **124**	CH_2Cl_2	97:3 (CH_2Cl_2:MeOH)	5.6

Table 6.5: Alkaloids isolated from the bark of *C. infectoria* and respective solvent system used in chromatographic separation

Alkaloids	Type of crude	Solvent system	Weight (mg)
Atherosperminine **15**	CH_2Cl_2	98:2 (CH_2Cl_2:MeOH)	9.4
(+)-*N*-methylisococlaurine **14**	CH_2Cl_2	98:2 (CH_2Cl_2:MeOH)	12.0
(+)-*N*-methyllaurotetanine **87**	CH_2Cl_2	97:3 (CH_2Cl_2:MeOH)	12.0
(+)-Laurotetanine **86**	CH_2Cl_2	97:3 (CH_2Cl_2:MeOH)	5.7
(+)-Reticuline **76**	CH_2Cl_2	97:3 (CH_2Cl_2:MeOH)	8.8
Argentinine **135**	CH_2Cl_2	97:3 (CH_2Cl_2:MeOH)	6.8

Table 6.6: Alkaloids isolated from the leaves of *C. infectoria* and respective solvent system used in chromatographic separation

Alkaloids	Type of crude	Solvent system	Weight (mg)
Liriodenine **136**	CH_2Cl_2	98:2 (CH_2Cl_2:MeOH)	3.2
Argentinine **135**	CH_2Cl_2	97:3 (CH_2Cl_2:MeOH)	5.5

Table 6.7: Alkaloids isolated from the bark of *C. griffithiana* and respective solvent system used in chromatographic separation

Alkaloids	Type of crude	Solvent system	Weight (mg)
(+)-Nornantenine **123**	CH_2Cl_2	100:0 (CH_2Cl_2:MeOH)	6.7
(+)-*N*-methyllaurotetanine **87**	CH_2Cl_2	99:1 (CH_2Cl_2:MeOH)	9.7
2-Methoxyatherosperminine **72**	CH_2Cl_2	98:2 (CH_2Cl_2:MeOH)	6.5
2-Hydroxyatherosperminine **13**	CH_2Cl_2	98:2 (CH_2Cl_2:MeOH)	5.8
(+)-Reticuline **76**	CH_2Cl_2	97:3 (CH_2Cl_2:MeOH)	8.7
Argentinine **135**	CH_2Cl_2	97:3 (CH_2Cl_2:MeOH)	9.3

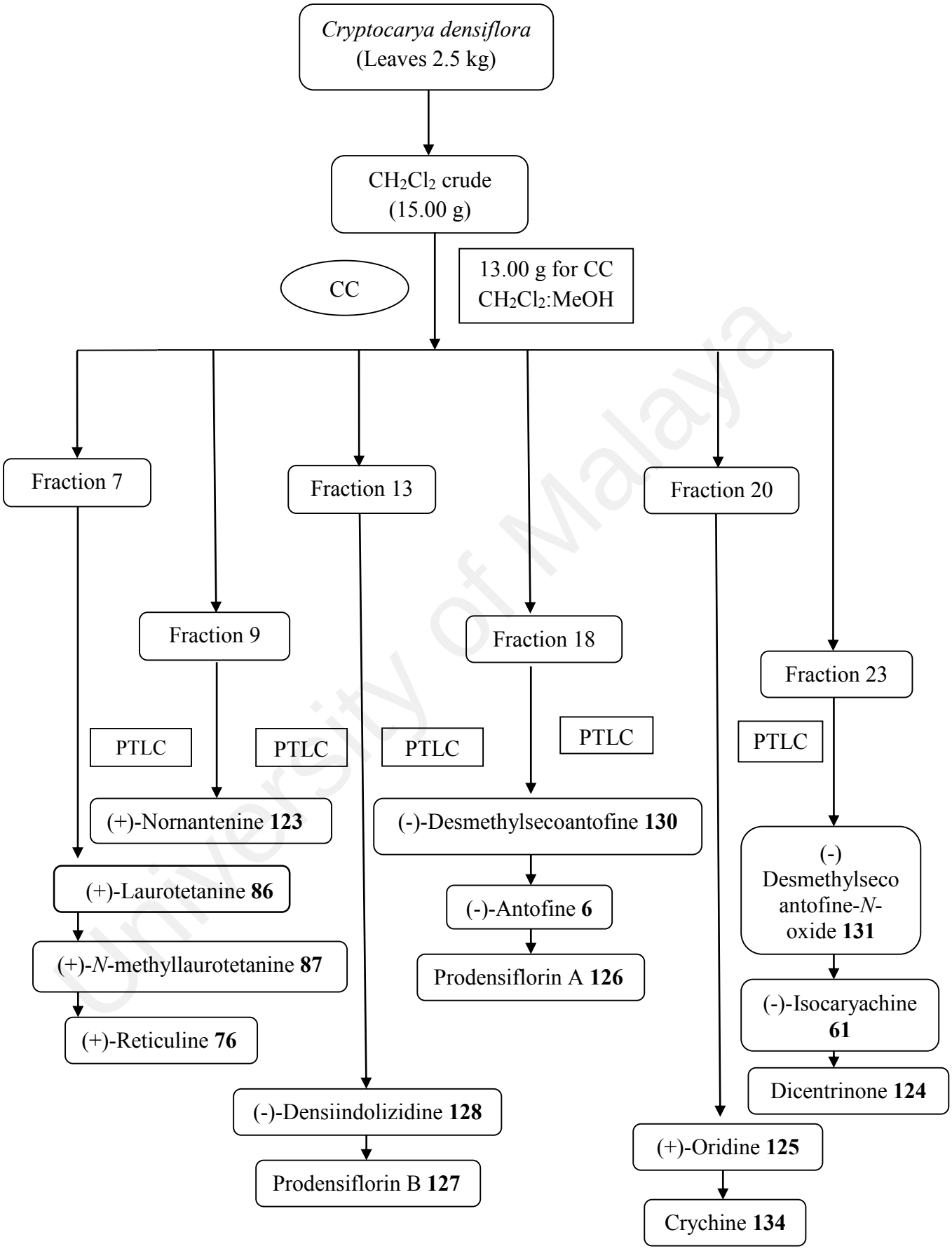

Scheme 6.1: Isolation and purification of the alkaloids from the CH_2Cl_2 crude extract of leaves of *C. densiflora*

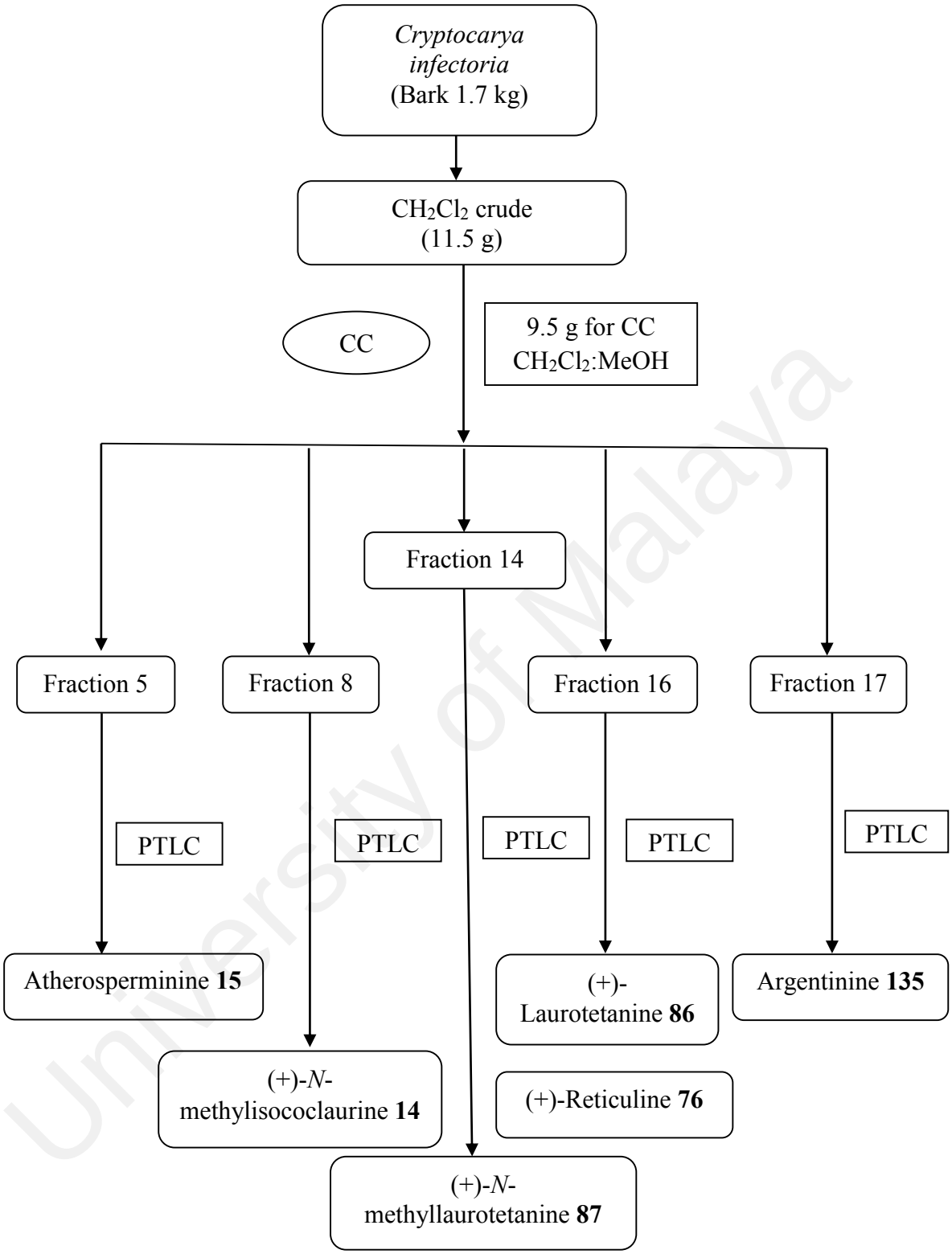

Scheme 6.2: Isolation and purification of the alkaloids from the CH_2Cl_2 crude extract of bark of *C. infectoria*

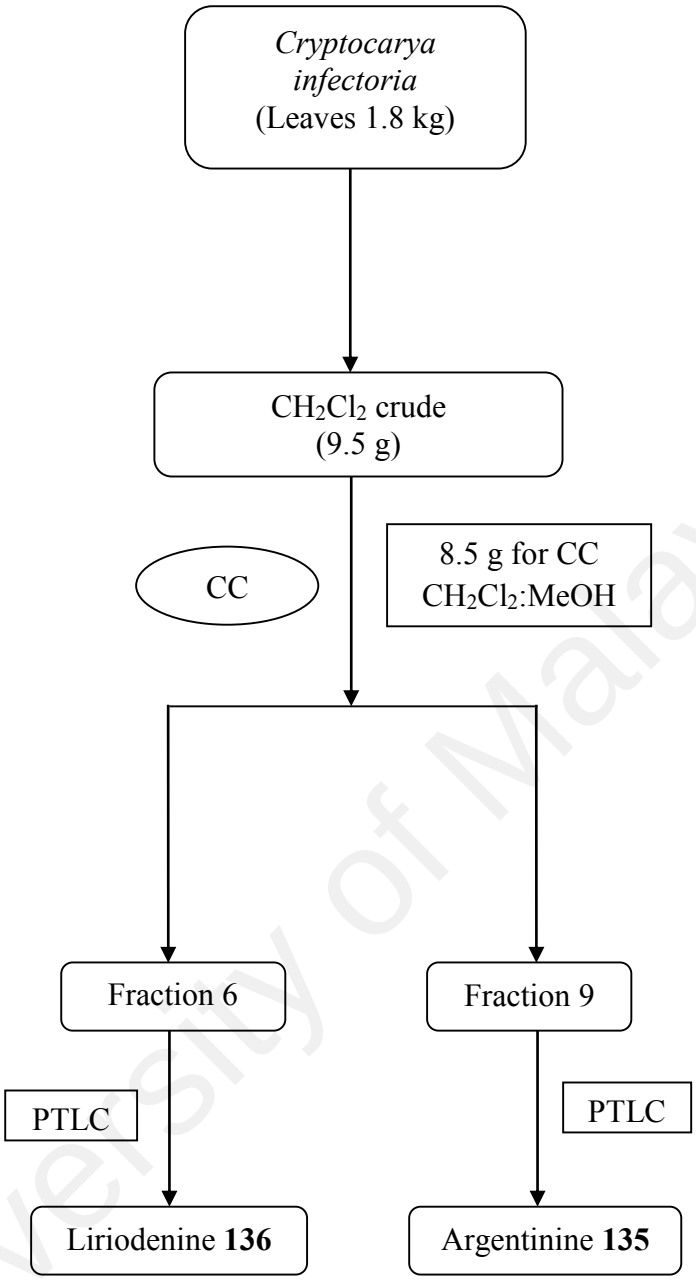

Scheme 6.3: Isolation and purification of the alkaloids from the CH_2Cl_2 crude extract of leaves of *C. infectoria*

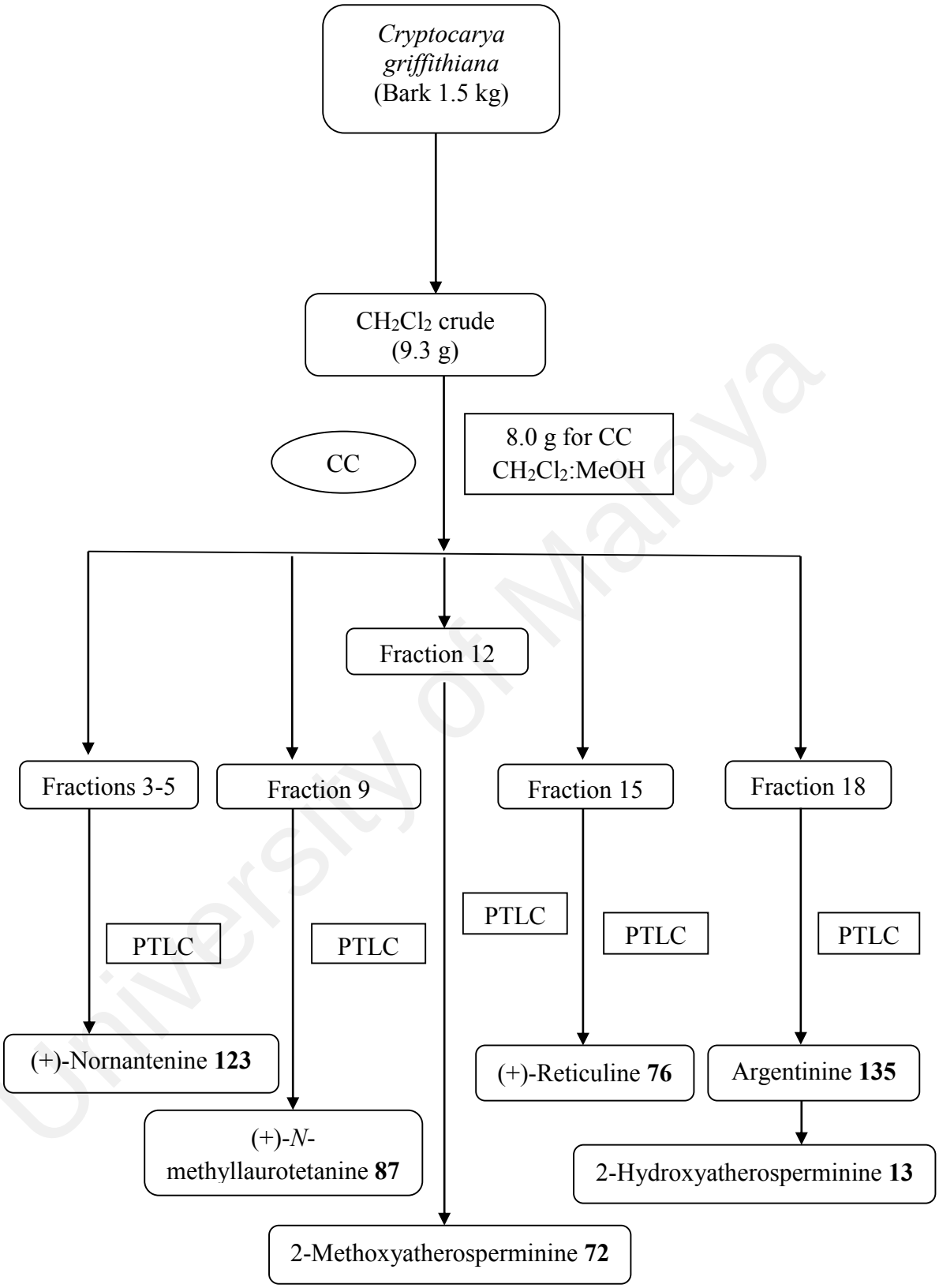

Scheme 6.4: Isolation and purification of the alkaloids from the CH_2Cl_2 crude extract of bark of *C. griffithiana*

6.8 Physical and Spectral Data of the Isolated Compounds

(-)-Antofine 6

Physical appearance	: Brownish amorphous
$[\alpha]_D^{25}$	: –15° (*c*=0.02, MeOH)
Molecular formula	: $C_{23}H_{25}NO_3$
Mass spectrum *m/z*	: 364.1927 ($[M+H]^+$)
UV λ_{max}, nm	: 257, 284, 310, 340
IR ν_{max}, cm^{-1}	: 1512, 1529
^1H NMR ($CDCl_3$) δ ppm	: See Table 3.9
^{13}C NMR ($CDCl_3$) δ ppm	: See Table 3.9

2-Hydroxyatherosperminine 13

Physical appearance	: Brownish amorphous
Molecular formula	: $C_{20}H_{23}NO_3$
Mass spectrum *m/z*	: 326.0934 ($[M+H]^+$)
UV λ_{max}, nm	: 274, 298
IR ν_{max}, cm^{-1}	: 3394
^1H NMR ($CDCl_3$) δ ppm	: See Table 3.21
^{13}C NMR ($CDCl_3$) δ ppm	: See Table 3.21

(+)-*N*-methylisococlaurine 14

Physical appearance	: Brownish amorphous
$[\alpha]_D^{25}$	: +67° (*c*=0.02 MeOH)
Molecular formula	: $C_{18}H_{21}NO_3$
Mass spectrum *m/z*	: 300.1573 ($[M+H]^+$)
UV λ_{max}, nm	: 228, 293
IR ν_{max}, cm^{-1}	: 2337, 3303
^1H NMR ($CDCl_3$) δ ppm	: See Table 3.18
^{13}C NMR ($CDCl_3$) δ ppm	: See Table 3.18

Atherosperminine 15

Physical appearance	: Brownish amorphous
Molecular formula	: $C_{20}H_{23}NO_2$
Mass spectrum *m/z*	: 310.1795 ($[M+H]^+$)
UV λ_{max}, nm	: 218, 220, 256, 308, 342
IR ν_{max}, cm^{-1}	: 1610
^1H NMR ($CDCl_3$) δ ppm	: See Table 3.17
^{13}C NMR ($CDCl_3$) δ ppm	: See Table 3.17

(-)-Isocaryachine 61

Physical appearance	: Brownish amorphous
$[\alpha]_D^{25}$	: –125 (*c*=0.02, MeOH)
Molecular formula	: $C_{19}H_{19}NO_4$
Mass spectrum *m/z*	: 326.1000 ($[M+H]^+$)
UV λ_{max}, nm	: 280, 283
IR ν_{max}, cm^{-1}	: 925, 1230, 3436
^1H NMR ($CDCl_3$) δ ppm	: See Table 3.15
^{13}C NMR ($CDCl_3$) δ ppm	: See Table 3.15

2-Methoxyatherosperminine 72

Physical appearance	: Dark brownish amorphous
Molecular formula	: $C_{21}H_{25}NO_3$
Mass spectrum *m/z*	: 340.1076 ($[M+H]^+$)
UV λ_{max}, nm	: 284, 293
IR ν_{max}, cm^{-1}	: 1650, 2951
^1H NMR ($CDCl_3$) δ ppm	: See Table 3.20
^{13}C NMR ($CDCl_3$) δ ppm	: See Table 3.20

(+)-Reticuline 76

Physical appearance	: Brownish amorphous
$[\alpha]_D^{25}$	: +55° (*c*=0.02, MeOH)
Molecular formula	: $C_{19}H_{23}NO_4$
Mass spectrum *m/z*	: 330.0860 ($[M+H]^+$)
UV λ_{max}, nm	: 231, 288
IR ν_{max}, cm^{-1}	: 1637, 3299
^1H NMR ($CDCl_3$) δ ppm	: See Table 3.13
^{13}C NMR ($CDCl_3$) δ ppm	: See Table 3.13

(+)-Laurotetanine 86

Physical appearance	: Dark brownish amorphous
$[\alpha]_D^{25}$	: +36° (*c*=0.098, MeOH)
Molecular formula	: $C_{19}H_{21}NO_4$
Mass spectrum *m/z*	: 328.1521 ($[M+H]^+$)
UV λ_{max}, nm	: 220, 281, 302, 312
IR ν_{max}, cm^{-1}	: 1654, 2098, 3430
^1H NMR ($CDCl_3$) δ ppm	: See Table 3.2
^{13}C NMR ($CDCl_3$) δ ppm	: See Table 3.2

(+)-*N*-methyllaurotetanine 87

Physical appearance	: Dark brownish amorphous
$[\alpha]_D^{25}$	: +70° (*c*=0.02, MeOH)
Molecular formula	: $C_{20}H_{23}NO_4$
Mass spectrum *m/z*	: 342.1683 ($[M+H]^+$)
UV λ_{max}, nm	: 227, 248, 303
IR ν_{max}, cm^{-1}	: 2998, 3465
^1H NMR ($CDCl_3$) δ ppm	: See Table 3.3
^{13}C NMR ($CDCl_3$) δ ppm	: See Table 3.3

(+)-Nornantenine 123

Physical appearance	: Brownish amorphous
$[\alpha]_D^{25}$	: +49° (*c*=0.12, MeOH)
Molecular formula	: $C_{19}H_{19}NO_4$
Mass spectrum *m/z*	: 326.1389 ($[M+H]^+$)
UV λ_{max}, nm	: 218, 282, 310
IR ν_{max}, cm^{-1}	: 984, 1273
^1H NMR ($CDCl_3$) δ ppm	: See Table 3.4
^{13}C NMR ($CDCl_3$) δ ppm	: See Table 3.4

Dicentrinone 124

Physical appearance	: Yellowish amorphous
Molecular formula	: $C_{19}H_{13}NO_5$
Mass spectrum *m/z*	: 336.0795 ($[M+H]^+$)
UV λ_{max}, nm	: 246, 273, 295, 410
IR ν_{max}, cm^{-1}	: 980, 1264, 1598, 1644
^1H NMR ($CDCl_3$) δ ppm	: See Table 3.5
^{13}C NMR ($CDCl_3$) δ ppm	: See Table 3.5

(+)-Oridine 125

Physical appearance	: Brownish amorphous
$[\alpha]_D^{25}$	: +30° (*c*=0.045, MeOH)
Molecular formula	: $C_{17}H_{23}NO_3$
Mass spectrum *m/z*	: 290.1762 ($[M+H]^+$)
UV λ_{max}, nm	: 217, 228, 286
IR ν_{max}, cm^{-1}	: 3156, 3408
^1H NMR ($CDCl_3$) δ ppm	: See Table 3.6
^{13}C NMR ($CDCl_3$) δ ppm	: See Table 3.6

Prodensiflorin A 126

Physical appearance : Brownish amorphous

Molecular formula : $C_{17}H_{21}NO_3$

Mass spectrum *m/z* : 288.1615 ($[M+H]^+$)

UV λ_{max}, nm : 230, 317, 369

IR ν_{max}, cm^{-1} : 1652, 2918, 3430

^1H NMR ($CDCl_3$) δ ppm : See Table 3.7

^{13}C NMR ($CDCl_3$) δ ppm : See Table 3.7

Prodensiflorin B 127

Physical appearance : Dark brownish amorphous

Molecular formula : $C_{17}H_{19}NO_3$

Mass spectrum *m/z* : 286.1503 ($[M+H]^+$)

UV λ_{max}, nm : 236, 320, 382

IR ν_{max}, cm^{-1} : 1595, 3379, 2924

^1H NMR ($CDCl_3$) δ ppm : See Table 3.8

^{13}C NMR ($CDCl_3$) δ ppm : See Table 3.8

(-)-Densiindolizidine 128

Physical appearance : Dark brownish amorphous

$[\alpha]_D^{25}$: -115^o (*c*=1.1, MeOH)

Molecular formula : $C_{22}H_{23}NO_3$

Mass spectrum *m/z* : 350.1759 ($[M+H]^+$)

UV λ_{max}, nm : 252, 260, 280, 342, 351

IR ν_{max}, cm^{-1} : 1519, 1596, 3340

^1H NMR ($CDCl_3$) δ ppm : See Table 3.10

^{13}C NMR ($CDCl_3$) δ ppm : See Table 3.10

(-)-Desmethylsecoantofine 130

Physical appearance	: Dark brownish amorphous
$[\alpha]_D^{25}$	: –20° (*c*=0.02, MeOH)
Molecular formula	: $C_{22}H_{25}NO_3$
Mass spectrum *m/z*	: 352.1981 ($[M+H]^+$)
UV λ_{max}, nm	: 225, 260, 281
IR ν_{max}, cm^{-1}	: 1516, 1642, 3448
^1H NMR (C_5D_5N) δ ppm	: See Table 3.11
^{13}C NMR (C_5D_5N) δ ppm	: See Table 3.11

(-)-Desmethylsecoantofine-*N*-oxide 131

Physical appearance	: Dark brownish amorphous
$[\alpha]_D^{25}$	: –30° (*c*=0.5, MeOH)
Molecular formula	: $C_{22}H_{25}NO_4$
Mass spectrum *m/z*	: 368.1855 ($[M+H]^+$)
UV λ_{max}, nm	: 205, 231, 259, 282
IR ν_{max}, cm^{-1}	: 1260, 1738, 2925
^1H NMR (C_5D_5N) δ ppm	: See Table 3.12
^{13}C NMR (C_5D_5N) δ ppm	: See Table 3.12

Crychine 134

Physical appearance	: Brownish amorphous
Molecular formula	: $C_{19}H_{17}NO_4$
Mass spectrum *m/z*	: 324.1216 ($[M+H]^+$)
UV λ_{max}, nm	: 238, 290 and 294
IR ν_{max}, cm^{-1}	: 936, 1040
^1H NMR ($CDCl_3$) δ ppm	: See Table 3.14
^{13}C NMR ($CDCl_3$) δ ppm	: See Table 3.14

Argentinine 135

Physical appearance	: Brownish amorphous
Molecular formula	: $C_{19}H_{21}NO_2$
Mass spectrum *m/z*	: 296.1627 ($[M+H]^+$)
UV λ_{max}, nm	: 218, 223, 258, 304, 338
IR ν_{max}, cm^{-1}	: 1600, 3392
^1H NMR ($CDCl_3$) δ ppm	: See Table 3.16
^{13}C NMR ($CDCl_3$) δ ppm	: See Table 3.16

Liriodenine 136

Physical appearance	: Yellowish amorphous
Molecular formula	: $C_{17}H_9NO_3$
Mass spectrum *m/z*	: 276.0651 ($[M+H]^+$)
UV λ_{max}, nm	: 238, 295, 308, 405
IR ν_{max}, cm^{-1}	: 982, 1264, 1561, 1649
^1H NMR ($CDCl_3$) δ ppm	: See Table 3.19
^{13}C NMR ($CDCl_3$) δ ppm	: See Table 3.19

REFERENCES

Abe, F., Hirokawa, M., Yamauchi, T., Honda, K., Hayashi, N., Ishii, M., Imagawa, S., & Iwahana, M. (1998). Further investigation of phenanthroindolizidine alkaloids from *Tylophora tanakae*. *Chemical and Pharmaceutical Bulletin, 46*(5), 767-769.

Adewusi, E. A., Moodley, N., & Steenkamp, V. (2010). Medicinal plants with cholinesterase inhibitory activity: A Review. *African Journal of Biotechnology, 9*(49), 8257-8276.

Aiello, A., Fattorusso, E., Menna, M., Taglialatela-Scafati, O., Fattorusso, E., & Taglialatela-Scafati, O. (2008). Modern alkaloids structure, isolation, synthesis and biology by Fattorusso E., Taglialatela-Scafati O. Weinheim: Wiley-VCH Verlag GmbH & Co. KgaA, 271-304.

Al-Amri, A., Smith, R., El-Haj, B., & Juma'a, M. (2004). The GC–MS detection and characterization of reticuline as a marker of *Opium* use. *Forensic Science International, 140*(2), 175-183.

Al-Ashaal, H. A., Aboutabl, M. E., Maklad, Y. A., & El-Beih, A. A. (2013). Tropane alkaloids of *Atropa belladonna* L.: *in vitro* production and pharmacological profile. *Egyptian Pharmaceutical Journal, 12*(2), 130-135.

Awang, K., Hadi, A. H. A., Saidi, N., Mukhtar, M. R., Morita, H., & Litaudon, M. (2008). New phenantrene alkaloids from *Cryptocarya crassinervia*. *Fitoterapia, 79*(4), 308-310.

Baarschers, W., Arndt, R., Pachler, K., Weisbach, J., & Douglas, B. (1964). 921. Nuclear magnetic resonance study of aporphine alkaloids. *Journal of the Chemical Society* (Resumed), 4778-4782.

Bartley, J. P., Baker, L. T., & Carvalho, C. F. (1994). Alkaloids of *Stephania bancroftii*. *Phytochemistry, 36*(5), 1327-1331.

Barton, D., Kirby, G., Steglich, W., Thomas, G., Battersby, A., Dobson, T., & Ramuz, H. (1965). 444. Investigations on the biosynthesis of morphine alkaloids. *Journal of the Chemical Society* (Resumed), 2423-2438.

Baumgartner, B., Erdelmeier, C. A., Wright, A. D., Rali, T., & Sticher, O. (1990). An antimicrobial alkaloid from *Ficus septica*. *Phytochemistry, 29*(10), 3327-3330.

Bhakuni, D., Satish, S., & Dhar, M. (1970). The alkaloids of *Croton sparsiflorus*. *Phytochemistry, 9*(12), 2573-2580.

Bhakuni, D., Tewari, S., & Dhar, M. (1972). Aporphine alkaloids of *Annona squamosa*. *Phytochemistry, 11*(5), 1819-1822.

Bick, I. R. C., & Sinchai, W. (1981). Chapter 3 Phenanthroindolizidine and phenanthroquinolizidine alkaloids. *The Alkaloids: Chemistry and Physiology, 19*, 193-228.

Bick, I. R. C., Preston, N. W., & Potier, P. (1972). Alcaloides de *Cryptocarya odorata* (Panch. et Seb.) Guillaum. (Lauracees). *Bulletin de la Société Chimique de France, 12*, 4596-4597.

Bick, I. R. C., Sévenet, T., Sinchai, W., Skelton, B. W., & White, A. H. (1981). Alkaloids of *Cryptocarya longifolia*: X-ray crystal structure of thalifoline and longifolonine. *Australian Journal of Chemistry, 34*(1), 195-207.

Blanchfield, J. T., Sands, D. P., Kennard, C. H., Byriel, K. A., & Kitching, W. (2003). Characterisation of alkaloids from some Australian *Stephania* (Menispermaceae) species. *Phytochemistry, 63*(6), 711-720.

Blaschke, G. (1968). Die Biosynthese des aporphin-alkaloids bulbocapnin aus reticulin I. Mitt.: *Untersuchungen zur Biosynthese von Alkaloiden. Archiv der Pharmazie, 301*(6), 432-439.

Borthakur, N., Mahanta, P. K., & Rastogi, R. C. (1981). Alkaloids and olefinic acids from *Cryptocarya amygdalina*. *Phytochemistry, 20*(3), 501-504.

Broadbent, T. A., & Paul, E. G. (1983). Carbon-13 nuclear magnetic resonance in alkaloid chemistry. *Chemischer Informationsdienst, 14*(40).

Brown, R. (1810). *Prodromus Florae Novae Hollandiae et Insulae Van-Diemen*. Londini: Typis R. Taylor et socii.

Castedo, L., & Tojo, G. (1990). Chapter 3 Phenanthrene alkaloids. *The Alkaloids: Chemistry and Pharmacology, 39*, 99-138.

Castedo, L., Granja, J. A., de Lera, A. R., & Villaverde, M. C. (1991). Alkaloids from *Guatteria goudotiana*. *Phytochemistry, 30*(8), 2781-2783.

Castro, C. O., Lopez, V. J., & Vegara, G. A. (1985). Aporphine alkaloids from *Phoebe pittieri*. *Phytochemistry, 24*(1), 203-204.

Cava, M., & Venkateswarlu, A. (1971). Dehydroocopodine, dicentrinone, and other alkaloids from *Ocotea macropoda* and *Hernandia jamaicensis*. *Tetrahedron, 27*(13), 2639-2643.

Cavé, A., Leboeuf, M., Moskowitz, H., Ranaivo, A., Bick, I. R. C., Sinchai, W., Nieto, M., Sévenet, T., & Cabalion, P. (1989). Alkaloids of *Cryptocarya phyllostemon*. *Australian Journal of Chemistry, 42*(12), 2243-2263.

Chang, F. R., Chen, C. Y., Hsieh, T. J., Cho, C. P., & Wu, Y. C. (2000). Chemical constituents from *Annona glabra* III. *Journal of the Chinese Chemical Society, 47*(4B), 913-920.

Chang, Y.-C., Chang, F.-R., Khalil, A. T., Hsieh, P.-W., & Wu, Y.-C. (2003). Cytotoxic benzophenanthridine and benzylisoquinoline alkaloids from *Argemone mexicana*. *Zeitschrift für Naturforschung C, 58*(7-8), 521-526.

Cheng, X.-F., Meng, Z.-M., & Chen, Z.-L. (1998). A pyridine-type alkaloid from *Mallotus apelta*. *Phytochemistry, 49*(7), 2193-2194.

Chia, Y.-C., Chen, K.-S., Chang, Y.-L., Teng, C.-M., & Wu, Y.-C. (1999). Antiplatelet actions of aporphinoids from Formosan plants. *Bioorganic & Medicinal Chemistry Letters, 9*(23), 3295-3300.

Chou, T.-H., Chen, J.-J., Lee, S.-J., Chiang, M. Y., Yang, C.-W., & Chen, I.-S. (2010). Cytotoxic flavonoids from the leaves of *Cryptocarya chinensis*. *Journal of Natural Products, 73*(9), 1470-1475.

Choudhary, M. I. (1999). Recent studies on bioactive natural products. *Pure and Applied Chemistry, 71*(6), 1079-1081.

Cooke, R., & Haynes, H. (1954). The Alkaloids of *Cryptocarya angulata* CT White and *C. triplinervis*. *Australian Journal of Chemistry, 7*(1), 99-103.

Cordell, G. A. (1981). *Introduction to Alkaloids: A Biogenetic Approach*. New York: Wiley-Interscience.

Cordell, G. A. (2000). *The Alkaloids: Chemistry and Biology* (Vol. 53). New York: Academic Press.

Corner, E. J. H. (1988). Wayside trees of Malaya in two volumes. *Wayside trees of Malaya in two volumes, 1*(3), 371-381.

Costa, E. V., Dutra, L. M., Nepel, A., & Barison, A. (2013). Isoquinoline alkaloids from the leaves of *Xylopia laevigata* (Annonaceae). *Biochemical Systematics and Ecology, 51*, 331-334.

Costa, E. V., Sampaio, M. F. C., Salvador, M. J., Nepel, A., & Barison, A. (2015). Chemical constituents from the stem bark of *Annona pickelii* (Annonaceae). *Química Nova*, *38*(6), 769-776.

Cox, P. A. (2008). Etnnopharmacology and the search for new drugs. *Bioactive compounds from plants*. New York: Wiley-Interscience.

Custodio, D. L., & da Veiga Junior, V. F. (2014). Lauraceae alkaloids. *RSC Advances*, *4*(42), 21864-21890.

Damu, A. G., Kuo, P.-C., Shi, L.-S., Li, C.-Y., Kuoh, C.-S., Wu, P.-L., & Wu, T.-S. (2005). Phenanthroindolizidine alkaloids from the stems of *Ficus septica*. *Journal of Natural Products, 68*(7), 1071-1075.

Dassonneville, L., Lansiaux, A., Wattelet, A., Wattez, N., Mahieu, C., Van Miert, S., Pieters, L., Bailly, C. (2000). Cytotoxicity and cell cycle effects of the plant alkaloids cryptolepine and neocryptolepine: relation to drug-induced apoptosis. *European Journal of Pharmacology, 409*(1), 9-18.

De Kok, R. (2016). A revision of *Cryptocarya* R. Br.(Lauraceae) of Peninsular Malaysia. *Kew Bulletin, 71*(1), 1-26.

De la Lande, I. (1948). The alkaloids of *Cryptocarya pleurosperma*. *Australian Journal of Experimental Biology & Medical Science, 26*(2), 181-187.

Dembitsky, V. M., Gloriozova, T. A., Poroikov, V. V. (2015). Naturally occurring plant isoquinoline *N*-oxide alkaloids: Their pharmacological and SAR activities. *Phytomedicine, 22*(1), 183-202.

de Moraes, P. L., Nehme, C. J., Alves, M. C., Derbyshire, M. T. V., & Cavalheiro, A. J. (2007). Chemical composition of flavonoids and styrylpyrones and the genetic variability of isozymes in natural populations of *Cryptocarya mandioccana* Meisner (Lauraceae). *Biochemical Systematics and Ecology, 35*(4), 233-244.

Deulofeu, V., Comin, J., & Vernengo, J. (1968). Chapter 6 The benzylisoquinoline alkaloids. *The Alkaloids: Chemistry and Physiology*, *10*, 401-461.

Dolejš, L. (1974). Mass spectra of proaporphine alkaloids. Collection of Czechoslovak *Chemical Communications, 39*(2), 571-579.

Drewes, S. E., Horn, M. H., & Mavi, S. (1997). *Cryptocarya liebertiana* and *Ocotea bullata*—their phytochemical relationship. *Phytochemistry, 44*(3), 437-440.

Dumontet, V., Hung, N. V., Adeline, M.-T., Riche, C., Chiaroni, A., Sévenet, T., & Guéritte, F. (2004). Cytotoxic flavonoids and α-pyrones from *Cryptocarya obovata*. *Journal of Natural Products, 67*(5), 858-862.

Elansary, H. (2014). Natural antioxidants and their role against human cancer. *Journal of Plant Biochemistry and Physiology, 2*(2), 1-2.

Erasto, P., Omolo, J., & Hamilton, C. (2013). Antimycobacterial quinoline alkaloid from the root wood of *Teclea amaniensis* Engl. *Scientific Journal of Microbiology, 2*(12), 214-219.

Ewing, J., Hughes, G., Ritchie, E., & Taylor, W. (1953). The alkaloids of *Cryptocarya bowiei* (Hook.) Druce. *Australian Journal of Chemistry, 6*(1), 78-85.

Fabricant, D. S., & Farnsworth, N. R. (2001). The value of plants used in traditional medicine for drug discovery. *Environmental Health Perspectives, 109*(Suppl 1), 69-75.

Felpin, F.-X., & Lebreton, J. (2004). History, chemistry and biology of alkaloids from *Lobelia inflata*. *Tetrahedron, 60*(45), 10127-10153.

Fienena, R. F., Rasoanaivo, L. H., Wadouachi, A., Rajemiarimiraho, M., Koleana, J., Ramahambimanana & Raharisololalao, A. (2016). Isoquinoline alkaloids from stem bark of *Colubrina decipiens* (Baill.) Capuron. *International Journal of Chemical Studies, 4*(4), 106-117.

Flor, S. C., Doorenbos, N., Svoboda, G., Knapp, J., & Schiff, P. (1974). Chemical constituents of *Legnephora moorei* Miers (Menispermaceae). *Journal of Pharmaceutical Sciences, 63*(4), 618-619.

Funayama, S., & Cordell, G. A. (2014). *Alkaloids: A Treasury of Poisons and Medicines*. UK: Academic Press.

García, V. P., Valdés, F., Martín, R., Luis, J., Afonso, A., & Ayala, J. (2006). Biosynthesis of antitumoral and bactericidal sanguinarine. *Journal of Biomedicine and Biotechnology, 2006*, 1-6.

Geissman, T. A. (1970). *Biosynthesis specialist periodical report* (Vol. 1). London: The Chemical Society.

Gellert, E., & Pelletier, S. (1987). *Alkaloids: Chemical and Biological Perspectives*. New York: Academic Press.

Giglioli-Guivarc'h, N. (2013). Advances in botanical research. *New light on alkaloid biosynthesis and future prospects* (Vol. 68). UK: Academic Press.

Gözler, B. (1987). Chapter 7 Pavine and isopavine alkaloids. *The Alkaloids: Chemistry and Pharmacology, 31*, 317-389.

Gözler, B., Lantz, M. S., & Shamma, M. (1983). The pavine and isopavine alkaloids. *Journal of Natural Products, 46*(3), 293-309.

Greig, N. H., Utsuki, T., Ingram, D. K., Wang, Y., Pepeu, G., Scali, C., Yu, Q. S., Mamczarz, J., Holloway, H. W., Giordano, T., Chen, D., Furukawa, K., Sambamurti, K., Brossi, A., & Lahiri, D. K. (2005). *Selective butyrylcholinesterase inhibition elevates brain acetylcholine, augments learning and lowers Alzheimer β-amyloid peptide in rodent. Proceedings of the National Academy of Sciences of the United States of America, 102*(47), 17213-17218.

Guinaudeau, H., Leboeuf, M., & Cavé, A. (1988). Aporphinoid alkaloids, IV. *Journal of Natural Products, 51*(3), 389-474.

Guinaudeau, H., Lebœuf, M., & Cavé, A. (1994). Aporphinoid alkaloids, V. *Journal of Natural Products, 57*(8), 1033-1135.

Harrigan, G. G., Gunatilaka, A. L., Kingston, D. G., Chan, G. W., & Johnson, R. K. (1994). Isolation of bioactive and other oxoaporphine alkaloids from two annonaceous plants, *Xylopia aethiopica* and *Miliusa* cf. *banacea*. *Journal of Natural Products, 57*(1), 68-73.

Hawkins, K. M., & Smolke, C. D. (2008). Production of benzylisoquinoline alkaloids in *Saccharomyces cerevisiae*. *Nature Chemical Biology, 4*(9), 564-573.

Houghton, P. J., Ren, Y., & Howes, M.-J. (2006). Acetylcholinesterase inhibitors from plants and fungi. *Natural Product Reports, 23*(2), 181-199.

Huang, H.-W., Chung, Y.-A., Chang, H.-S., Tang, J.-Y., Chen, I.-S., & Chang, H.-W. (2014). Antiproliferative effects of methanolic extracts of *Cryptocarya concinna* Hance roots on oral cancer Ca9-22 and CAL 27 cell lines involving apoptosis, ROS induction, and mitochondrial depolarization. *The Scientific World Journal*, *2014*.

Hunter, T. J., & O'Doherty, G. A. (2001). An enantioselective synthesis of *Cryptocarya* diacetate. *Organic Letters, 3*(17), 2777-2780.

Huxtable, R. J., & Schwarz, S. K. (2001). The isolation of morphine—first principles in science and ethics. *Molecular Interventions, 1*(4), 189-191.

Ienco, E. C., LoGerfo, A., Carlesi, C., Orsucci, D., Ricci, G., Mancuso, M., & Siciliano, G. (2011). Oxidative stress treatment for clinical trials in neurodegenerative diseases. *Journal of Alzheimer's Disease, 24*(supplement2), 111-126.

Inada, A., Nishino, H., Kuchide, M., Takayasu, J., Mukainaka, T., Nobukuni, Y., Okuda, M., & Tokuda, H. (2001). Cancer chemopreventive activity of odorine and odorinol from *Aglaia odorata*. *Biological and Pharmaceutical Bulletin, 24*(11), 1282-1285.

Iwu, M. M., Duncan, A. R., & Okunji, C. O. (1999). New antimicrobials of plant origin. *Perspectives on new crops and new uses*. Alexandria: ASHS Press.

Jackman, L. M., Trewella, J. C., Moniot, J. L., Shamma, M., Stephens, R. L., Wenkert, E., Leboeuf, M., & Cavé, A. (1979). The carbon-13 NMR spectra of aporphine alkaloids. *Journal of Natural Products, 42*(5), 437-449.

Janssen, R. H., Lousberg, R. J. C., Wijkens, P., Kruk, C., & Theuns, H. G. (1989). Assignment of ^{1}H and ^{13}C NMR resonances of some isoquinoline alkaloids. *Phytochemistry, 28*(10), 2833-2839.

Jantan, I. (2004). Medicinal plant research in Malaysia: scientific interests and advances. *Malaysian Journal of Health Science*, *2*(2), 27-46.

Ji, L.-L., Zhang, M., Sheng, Y.-C., & Wang, Z.-T. (2005). Pyrrolizidine alkaloid clivorine induces apoptosis in human normal liver L-02 cells and reduces the expression of p53 protein. *Toxicology in vitro, 19*(1), 41-46.

Johns, S., Lamberton, J., & Sioumis, A. (1967). Laurotetanine and *N*-methyllaurotetanine from *Palmeria fengeriana* Perk.(family Monimiacea). *Australian Journal of Chemistry, 20*(8), 1787-1788.

Johns, S., Lamberton, J., & Tweeddale, H. (1969). Identification of (–)-armepavine as the major leaf alkaloid of *Cryptocarya archboldiana* (Lauraceae). *Australian Journal of Chemistry, 22*(6), 1313-1313.

Juliawaty, L. D., Kitajima, M., Takayama, H., Achmad, S. A., & Aimi, N. (2000a). A 6-substituted-5, 6-dihydro-2-pyrone from *Cryptocarya strictifolia*. *Phytochemistry, 54*(8), 989-993.

Juliawaty, L. D., Kitajima, M., Takayama, H., Achmad, S. A., & Aimi, N. (2000b). A new type of stilbene-related secondary metabolite, idenburgene, from *Cryptocarya idenburgensis*. *Chemical and Pharmaceutical Bulletin, 48*(11), 1726-1728.

Thakur, B. K., Anthwal, A., Rawat, D. S., Rawat, B., Rashmi., & Rawat, M. S. M. (2012). A review on genus Alseodaphne: *Phytochemistry and Pharmacology. Mini-Reviews in Organic Chemistry, 9*(4), 433-445.

Kabera, J. N., Semana, E., Mussa, A. R., & He, X. (2014). Plant secondary metabolites: biosynthesis, classification, function and pharmacological properties. *Journal of Pharmacy and Pharmacology, 2*, 377-392.

Kaur, R., & Arora, S. (2015). Alkaloids important therapeutic secondary metabolites of plant origin. *Journal of Critical Reviews, 2*(3), 1-8.

Keng, H. (1978). *Orders and families of Malayan seed plants: synopsis of orders and families of Malayan gymnosperms, dicotyledons, and monocotyledons*. Singapore: Singapore Univ. Press.

Khamis, S., & Nizam, M. (2013). *Distribution of Litsea complex (lauraceae) and their association with soil properties in different forest types of Peninsular Malaysia*. Paper presented at The 2013 UKM FST Postgraduate Colloquium: *Proceedings of the Universiti Kebangsaan Malaysia, Faculty of Science and Technology 2013 Postgraduate Colloquium.*

Khaw, K. Y., Choi, S. B., Tan, S. C., Wahab, H. A., Chan, K. L., & Murugaiyah, V. (2014). Prenylated xanthones from mangosteen as promising cholinesterase inhibitors and their molecular docking studies. *Phytomedicine, 21*(11), 1303-1309.

Kini, S., & Ramana, M. (2004). A new convenient synthesis of phenanthrene alkaloids from 1-arylmethyl-1, 2, 3, 4-tetrahydroisoquinolines. *Tetrahedron Letters, 45*(21), 4171-4173.

Knekt, P., Jarvinen, R., Reunanen, A., & Maatela, J. (1996). *Flavonoid intake and coronary mortality in Finland: a cohort study*. *BMJ, 312*(7029), 478-481.

Kochummen, K. M. (1997). *Tree flora of Pasoh Forest*. Malaysia: Forest Research Institute.

Kostermans, A. J. G. H. (1939). Enumeratio lauracearum Madagascariensium et ex Insulis Mascarenis. *Notulae Systematicae. Herbier du Muséum de Paris 8*, 67–128.

Kuo, R.-Y., Chen, C.-Y., Lin, A.-S., Chang, F.-R., & Wu, Y.-C. (2004). A new phenanthrene alkaloid, romucosine I, form *Rollinia mucosa* Baill. *Zeitschrift für Naturforschung B, 59*(3), 334-336.

Lam, B., Hollingdrake, E., Kennedy, J. L., Black, S. E., & Masellis, M. (2009). Cholinesterase inhibitors in Alzheimer's disease and Lewy body spectrum disorders: the emerging pharmacogenetic story. *Human Genomics, 4*(2), 1-16.

Lam, K. S. (2007). New aspects of natural products in drug discovery. *Trends in Microbiology, 15*(6), 279-289.

Lamberton, J., & Vashist, V. (1972). Alkaloids of *Litsea leefeana* and *Cryptocarya foveolata* (Lauraceae). *Australian Journal of Chemistry, 25*(12), 2737-2738.

Lebœuf, M., Ranaivo, A., Cavé, A., & Moskowitz, H. (1989). La velucryptine, nouvel alcaloïde isoquinoléique isolé de *Cryptocarya velutinosa*. *Journal of Natural Products, 52*(3), 516-521.

Lee, S.-S., Chen, C.-H., & Liu, Y.-C. (1993). Additional alkaloids from *Cryptocarya chinensis*. *Journal of Natural Products, 56*(2), 227-232.

Lee, S.-S., Lin, Y.-J., Chen, C.-K., Liu, K. C., & Chen, C.-H. (1993). Quaternary alkaloids from *Litsea cubeba* and *Cryptocarya konishii*. *Journal of Natural Products, 56*(11), 1971-1976.

Lee, S.-S., Liu, Y.-C., & Chen, C.-H. (1989). Carbon-13 nuclear magnetic resonance assignments and spectral characteristics for some pavine alkaloids. *The Kaohsiung Journal of Medical Sciences, 5*(11), 637-641.

Lee, S.-S., Liu, Y.-C., & Chen, C.-H. (1990). Neocaryachine, a new pavine alkaloid from *Cryptocarya chinensis*, and NMR spectral properties of related alkaloids. *Journal of Natural Products, 53*(5), 1267-1271.

Lee, Y.-Z., Huang, C.-W., Yang, C.-W., Hsu, H.-Y., Kang, I.-J., Chao, Y.-S., Chen, I.-S., Chang, H.-Y., Lee, S.-J. (2011). Isolation and biological activities of phenanthroindolizidine and septicine alkaloids from the Formosan *Tylophora ovata*. *Planta medica, 77*(17), 1932-1938.

Leitão, G. G., Soares, S. S., Brito, M., Delle Monache, F., & de Barros, T. (2000). Kaempferol glycosides from *Siparuna apiosyce*. *Phytochemistry, 55*(6), 679-682.

Lemmens, R. H. M. J., Soerianegara, I., & Wong, W. C. (1995). Plant resources of South-East Asia No. *5*(2). *Timber trees: minor commercial timbers*. Leiden: Backhuys Publishers.

Li, Z., Jin, Z., & Huang, R. (2001). Isolation, total synthesis and biological activity of phenanthroindolizidine and phenanthroquinolizidine alkaloids. *Synthesis, 2001*(16), 2365-2378.

Liew, S. Y., Khaw, K. Y., Murugaiyah, V., Looi, C. Y., Wong, Y. L., Mustafa, M. R., Litaudon, M., Awang, K. (2015). Natural indole butyrylcholinesterase inhibitors from *Nauclea officinalis*. *Phytomedicine, 22*(1), 45-48.

Likhitwitayawuid, K., Angerhofer, C. K., Chai, H., Pezzuto, J. M., Cordell, G. A., & Ruangrungsi, N. (1993). Cytotoxic and antimalarial alkaloids from the tubers of *Stephania pierrei*. *Journal of Natural Products, 56*(9), 1468-1478.

Lin, F.-W., Wang, J.-J., & Wu, T.-S. (2002). New pavine *N*-oxide alkaloids from the stem bark of *Cryptocarya chinensis* Hemsl. *Chemical and Pharmaceutical Bulletin, 50*(2), 157-159.

Lin, F.-W., Wu, P.-L., & Wu, T.-S. (2001). Alkaloids from the leaves of *Cryptocarya chinensis* Hemsl. *Chemical and Pharmaceutical Bulletin, 49*(10), 1292-1294.

Linnanen, T., Brisander, M., Mohell, N., & Johansson, A. M. (2001). Serotonergic and dopaminergic activities of rigidified (R)-aporphine derivatives. *Bioorganic & Medicinal Chemistry Letters, 11*(3), 367-370.

Liu, W., Wang, Y., He, D.-d., Li, S.-p., Zhu, Y.-d., Jiang, B., Cheng, X. -m., Wang, Z.-t., Wang, C.-h. (2015). Antitussive, expectorant, and bronchodilating effects of quinazoline alkaloids (±)-vasicine, deoxyvasicine, and (±)-vasicinone from aerial parts of *Peganum harmala* L. *Phytomedicine, 22*(12), 1088-1095.

López-Martín, J., Anam, E. M., Boira, H., Sanz, M. J., & Blázquez, M. A. (2002). Chromone and phenanthrene alkaloids from *Dennettia tripetala*. *Chemical and Pharmaceutical Bulletin, 50*(12), 1613-1615.

Lu, J.-J., Bao, J.-L., Chen, X.-P., Huang, M., & Wang, Y.-T. (2012). Alkaloids isolated from natural herbs as the anticancer agents. *Evidence Based Complementary and Alternative Medicine*, *2012,* 1-12.

Lu, S.-T. (1967). Studies on the alkaloids of formosan lauraceous plants. XII. Alkaloids of *Cryptocarya konishii* Hayata and *Machilus acuminatissima* (Hay.) Kanehira. *Yakugaku zasshi: Journal of the Pharmaceutical Society of Japan, 87*(10), 1278-1281.

Ma, L., Wen, S., Zhan, Y., He, Y., Liu, X., & Jiang, J. (2008). Anticancer effects of the Chinese medicine matrine on murine hepatocellular carcinoma cells. *Planta Medica, 74*(3), 245-251.

Mahiou, V., Roblot, F., Fournet, A., & Hocquemiller, R. (2000). Bisbenzylisoquinoline alkaloids from *Guatteria boliviana* (Annonaceae). *Phytochemistry, 54*(7), 709-716.

Mander, L., & Liu, H.-W. (2010). *Comprehensive Natural Products II Chemistry and Biology* (Vol. 1). Italy: Elsevier Science.

Mandhare, A. A., Dhulap, S. A., Dhulap, A. S., & Biradar, S. C. (2015). Review on the anticancer and in-silico binding studies of phenanthroindolizidine alkaloids. *Chemical Informatics*, *1*(1:5), 1-15.

Mann, J. (2000). *Murder, magic, and medicine*. U. S. A.: Oxford University Press.

Manske, R. H. F. (1981). *The Alkaloids: Chemistry and Physiology* (A. Press Ed. Vol. XIX). U. S. A.: Academic Press.

Manske, R. H. F., & Holmes, H. L. (1981). Chapter 3: Phenanthroindolizidine and Phenanthroquinolizidine Alkaloids. *The Alkaloids: Chemistry and Physiology* (Vol. 19): U. S. A.: Academic Press.

Marsaioli, A. J., Magalhães, A. F., Rúveda, E. A., & de AM Reis, F. (1980). ^{13}C NMR analysis of some oxoaporphine alkaloids. *Phytochemistry, 19*(5), 995-997.

McCarthy, C. E., Candelario, D. M., & Liu, M. T. (2014). Anxiety-inducing dietary supplements: a review of herbs and other supplements with anxiogenic properties. *Pharmacology & Pharmacy, 5*(10), 966-981.

Menezes, L. R. A., Costa, C. O. D., Rodrigues, A. C. B. d. C., Santo, F. R. d. E., Nepel, A., Dutra, L. M., Silva, F. M. A., Soares, M. B. P., Barison, A., Costa, E. V., & Bezerra, D. P. (2016). Cytotoxic alkaloids from the stem of *Xylopia laevigata*. *Molecules, 21*, 1-10.

Montenegro, H., Gutierrez, M., Romero, L. I., Ortega-Barría, E., Capson, T. L., & Rios, L. C. (2003). Aporphine alkaloids from *Guatteria spp*. with leishmanicidal activity. *Planta Medica, 69*(7), 677-678.

Mukherjee, P. K., Kumar, V., Mal, M., & Houghton, P. J. (2007). Acetylcholinesterase inhibitors from plants. *Phytomedicine, 14*(4), 289-300.

Mukhtar, M. R., Aziz, A. N., Thomas, N. F., Hadi, A. H. A., Litaudon, M., & Awang, K. (2009). Grandine A, a new proaporphine alkaloid from the bark of *Phoebe grandis*. *Molecules, 14*(3), 1227-1233.

Mukhtar, M. R., Hadi, A. H. A., Rondeau, D., Richomme, P., Litaudon, M., Rais Mustafa, M., & Awang, K. (2008). New proaporphines from the bark of *Phoebe scortechinii*. *Natural Product Research, 22*(11), 921-926.

Mulabagal, V., & Tsay, H.-S. (2004). Plant cell cultures-an alternative and efficient source for the production of biologically important secondary metabolites. *International Journal of Applied Science and Engineering Research, 2*(1), 29-48.

Munoz, V., Sauvain, M., Mollinedo, P., Callapa, J., Rojas, I., Gimenez, A., Valentin, A., & Mallie, M. (1999). Antimalarial activity and cytotoxicity of (-)-roemrefidine isolated from the stem bark of *Sparattanthelium amazonum*. *Planta Medica, 65*(5), 448-449.

Murray, A. P., Faraoni, M. B., Castro, M. J., Alza, N. P., & Cavallaro, V. (2013). Natural AChE inhibitors from plants and their contribution to Alzheimer's disease therapy. *Current Neuropharmacology, 11*(4), 388-413.

Nasrullah, A. A., Zahari, A., Mohamad, J., & Awang, K. (2013). Antiplasmodial alkaloids from the bark of *Cryptocarya nigra* (Lauraceae). *Molecules, 18*(7), 8009-8017.

Ng, F. S. P. (1989). *Tree Flora of Malaya a Manual for Foresters*, (Vol. 4). Kuala Lumpur, Malaysia: Longman.

Norscia, I., & Borgognini-Tarli, S. M. (2006). Ethnobotanical reputation of plant species from two forests of Madagascar: A preliminary investigation. South African *Journal of Botany, 72*(4), 656-660.

Ohashi, M., Wilson, J., Budzikiewicz, H., Shamma, M., Slusarchyk, W. A., & Djerassi, C. (1963). Mass spectrometry in structural and stereochemical problems. XXXI. 1 aporphines and related alkaloids 2. *Journal of the American Chemical Society, 85*(18), 2807-2810.

Othman, W. N. N. W., Liew, S. Y., Khaw, K. Y., Murugaiyah, V., Litaudon, M., & Awang, K. (2016). Cholinesterase inhibitory activity of isoquinoline alkaloids from three *Cryptocarya* species (Lauraceae). *Bioorganic & Medicinal Chemistry, 24*(18), 4464-4469.

Patwardhan, B. (2009). *Drug discovery and development*: *traditional medicine and ethnopharmacology perspectives*. New Delhi: New India Publishing Agency.

Patwardhan, B., Vaidya, A. D., & Chorghade, M. (2004). Ayurveda and natural products drug discovery. *Current Science Bangalore, 86*(6), 789-799.

Pelletier, S. W. (1970). *Chemistry of the alkaloids*. UK: Van Nostrand Reinhold Company.

Perry, L. M., & Metzger, J. (1980). *Medicinal plants of east and southeast Asia: attributed properties and uses*. London: MIT Press.

Pimenta, L., & Mendonça, D. (2012). Aporphine alkaloids and feruloylamides from the bark of *Xylopia benthamii* RE Fries (Annonaceae). *Natural Product Research, 26*(20), 1948-1950.

Plemenkov, V. (2001). *Introduction to the chemistry of natural compounds*. Rusia: MPIK.

Poljsak, B., Šuput, D., & Milisav, I. (2013). Achieving the balance between ROS and antioxidants: when to use the synthetic antioxidants. *Oxidative Medicine and Cellular Longevity*, *2013*, 1-11.

Pyo, M. K., Yun-Choi, H. S., & Hong, Y.-J. (2003). Antiplatelet activities of aporphine alkaloids isolated from leaves of *Magnolia obovata*. *Planta Medica, 69*(3), 267-269.

Rabbani, G., Butler, T., Knight, J., Sanyal, S., & Alam, K. (1987). Randomized controlled trial of berberine sulfate therapy for diarrhea due to enterotoxigenic *Escherichia coli* and *Vibrio cholerae*. *Journal of Infectious Diseases, 155*(5), 979-984.

Rao, S. R., & Ravishankar, G. (2002). Plant cell cultures: chemical factories of secondary metabolites. *Biotechnology Advances, 20*(2), 101-153.

Ratnagiriswaran, A., & Venkatachalam, K. (1935). The chemical examination of *Tylophora asthmatica* and isolation of the alkaloids tylophorine and tylophorinine. *Indian Journal of Medical Research, 22*(3), 433-441.

Ríos, J. L., Máñez, S., Giner, R. M., & Recio, M. C. (1999). Biological aspects of aporphinoid alkaloids. *The Alkaloids: Chemistry and Biology, 53*, 57-117.

Saidi, N. (2011). *Aphorpines and benzylisoquinoline alkaloids from bark of Cryptocarya crassinervia*. Paper presented at the *Proceedings of The Annual International Conference, Syiah Kuala University-Life Sciences & Engineering Chapter*.

Saidi, N., Hadi, A. H. A., Awang, K., & Mukhtar, M. R. (2010). Aporphine alkaloids from bark of *Cryptocarya ferrea*. *Indonesian Journal of Chemistry, 9*(3), 461-465.

Saidi, N., Morita, H., Litaudon, M., Mukhtar, M. R., Awang, K., & Hadi, A. H. A. (2011). Benzylisoquinoline alkaloids from bark of *Cryptocarya rugulosa*. *Indonesian Journal of Chemistry, 11*(1), 59-66.

Sari, A., Gray, A., & Sariyar, G. (2004). A new dehydroaporphine alkaloid from *Papaver fugax*. *Natural Product Research, 18*(3), 265-268.

Sarma, A. D., Mallick, A. R., & Ghosh, A. (2010). Free radicals and their role in different clinical conditions: an overview. *International Journal of Pharma Sciences and Research, 1*(3), 185-192.

Seigler, D. S. (2012). *Plant secondary metabolism*. New York: Springer Science & Business Media.

Shamma, M. (1972). *The isoquinoline alkaloids chemistry and pharmacology* (Vol. 25): New York: Academic Press.

Shamma, M. (1972a). Chapter 14 The phenanthrene alkaloids: *The Isoquinoline Alkaloids Chemistry and Pharmacology* (Vol. 25). New York: Academic Press.

Shamma, M., & Castenson, R. (1973). Chapter 6 The oxoaporphine alkaloids. *The Alkaloids: Chemistry and Physiology, 14*, 225-264.

Shamma, M., Yao, S., Pai, B., & Charubala, R. (1971). The ultraviolet spectra of phenolic aporphines in basic solution. *The Journal of Organic Chemistry, 36*(21), 3253-3254.

Shimada, K., Fujikawa, K., Yahara, K., & Nakamura, T. (1992). Antioxidative properties of xanthan on the autoxidation of soybean oil in cyclodextrin emulsion. *Journal of Agricultural and Food Chemistry, 40*(6), 945-948.

Soni, A., & Sosa, S. (2013). Phytochemical analysis and free radical scavenging potential of herbal and medicinal plant extracts. *Journal of Pharmacognosy and Phytochemistry, 2*(4), 22-29.

Stadler, R., Kutchan, T. M., & Zenk, M. H. (1989). (*S*)-Norcoclaurine is the central intermediate in benzylisoquinoline alkaloid biosynthesis. *Phytochemistry, 28*(4), 1083-1086.

Stærk, D., Christensen, J., Lemmich, E., Duus, J. Ø., Olsen, C. E., & Jaroszewski, J. W. (2000). Cytotoxic activity of some phenanthroindolizidine *N*-oxide alkaloids from *Cynanchum vincetoxicum*. *Journal of Natural Products, 63*(11), 1584-1586.

Stærk, D., Lykkeberg, A. K., Christensen, J., Budnik, B. A., Abe, F., & Jaroszewski, J. W. (2002). *In vitro* cytotoxic activity of phenanthroindolizidine alkaloids from *Cynanchum vincetoxicum* and *Tylophora tanakae* against drug-sensitive and multidrug-resistant cancer cells. *Journal of Natural Products, 65*(9), 1299-1302.

Stevigny, C., Bailly, C., & Quetin-Leclercq, J. (2005). Cytotoxic and antitumor potentialities of aporphinoid alkaloids. *Current Medicinal Chemistry Anti Cancer Agents, 5*(2), 173-182.

Stuart, K., & Cava, M. (1968). Proaporphine alkaloids. *Chemical Reviews, 68*(3), 321-339.

Subbulakshmi, G., Thalavaipandian, A., Bagyalakshmi, R., & Rajendran, A. (2012). Bioactive endophytic fungal isolates of *Biota orientalis* (L) Endl., *Pinus excelsa* Wall. and *Thuja occidentalis* L. *International Journal of Advanced Life Sciences, 4*, 9-15.

Sulaiman, S. N., Mukhtar, M. R., Hadi, A. H. A., Awang, K., Hazni, H., Zahari, A., Litaudon, M., Zaima, K., & Morita, H. (2011). Lancifoliaine, a new bisbenzylisoquinoline from the bark of *Litsea lancifolia*. *Molecules, 16*(4), 3119-3127.

Tadeusz, A. (2007). Alkaloids secrets of life. *Alkaloid Chemistry, Biological Ecological, Applications and Ecological Role. Primera Edición*. Netherlands: Elsevier.

Tewari, S., Bhakuni, D., & Dhar, M. (1972). The aporphine alkaloids of *Litsea glutenosa*. *Phytochemistry, 11*(3), 1149-1152.

Tomita, M., Kikuchi, T., Fujitani, K., Kato, A., Furukawa, H., Aoyagi, Y., Kitano, M., & Ibuka, T. (1966). Mass spectrometry of bisbenzylisoquinoline alkaloids. *Tetrahedron Letters, 7*(8), 857-864.

Toribio, A., Bonfils, A., Delannay, E., Prost, E., Harakat, D., Henon, E., Richard, B., Litaudon, M., Nuzillard, J.-M., & Renault, J.-H. (2006). Novel *seco*-dibenzopyrrocoline alkaloid from *Cryptocarya oubatchensis*. *Organic Letters, 8*(17), 3825-3828.

Trease, G., & Evans, M. (2001). Pharmacopoeial and related drugs of biological origin. *A Textbook of Pharmacognosy, 15th ed*. London: WB Saunders.

Tso, T., & Jeffrey, R. (1953). Paper chromatography of alkaloids and their transformation products in Maryland tobacco. *Archives of Biochemistry and Biophysics, 43*(2), 269-285.

Uprety, H., Bhakuni, D., & Dhar, M. (1972). Aporphine alkaloids *of Litsea sebifera*, *L. wightiana* and *Actinodaphne obovata*. *Phytochemistry, 11*(10), 3057-3059.

Urzúa, A., & Cassels, B. K. (1982). Additional alkaloids from *Laurelia philippiana* and *L. novae*-zelandiae. *Phytochemistry, 21*(3), 773-776.

Valko, M., Leibfritz, D., Moncol, J., Cronin, M. T., Mazur, M., & Telser, J. (2007). Free radicals and antioxidants in normal physiological functions and human disease. *The International Journal of Biochemistry & Cell Biology, 39*(1), 44-84.

van der Werff, H., & Richter, v. d. H. (1996). Toward an improved classification of Lauraceae. *Annals of the Missouri Botanical Garden*. U. S. A.: Missouri Botanical Garden Press.

Veznik, F., Sedmera, P., Preininger, V., Simanek, V., & Slavik, J. (1981). Isooridine, a new alkaloid from *Papaver oreophilum*. *Phytochemistry, 20*, 347-348.

Wang, B., Mai, Y.-C., Li, Y., Hou, J.-Q., Huang, S.-L., Ou, T.-M., Tan, J.-H., An, L.-K., Li, D., Gu, L.-Q., & Huang, Z.-S. (2010). Synthesis and evaluation of novel rutaecarpine derivatives and related alkaloids derivatives as selective acetylcholinesterase inhibitors. *European Journal of Medicinal Chemistry, 45*(4), 1415-1423.

Wang, Z., & Liang, G. (2009). Zhong Yao Hua Xue. Shanghai: Shanghai Scientific & Technical Publishers.

Wijeratne, E. K., Hatanaka, Y., Kikuchi, T., Tezuka, Y., & Gunatilaka, A. L. (1996). A dioxoaporphine and other alkaloids of two Annonaceous plants of Sri Lanka. *Phytochemistry, 42*(6), 1703-1706.

Wink, M. (1998a). *Chemical ecology of alkaloids alkaloids*. New York: Springer.

Wink, M. (1998b). *A short history of alkaloids Alkaloids*. New York: Springer.

Wu, H., Ding, L., Shen, J., Zhu, H., & Zhang, X. (2009). A new proaporphine alkaloid from Meconopsishorridula. *Fitoterapia, 80*(4), 252-254.

Wu, T.-S., & Lin, F.-W. (2001). Alkaloids of the wood of *Cryptocarya chinensis*. *Journal of Natural Products, 64*(11), 1404-1407.

Wu, T.-S., Su, C.-R., & Lee, K.-H. (2012). Cytotoxic and anti-HIV phenanthroindolizidine alkaloids from *Cryptocarya chinensis*. *Natural Product Communications, 7*(6), 725-727.

Wu, Y.-C., Chang, F.-R., Chao, Y.-C., & Teng, C.-M. (1998). Antiplatelet and vasorelaxing actions of aporphinoids from *Cassytha filiformis*. *Phytotherapy Research, 12*(S1), S39-S41.

Wu, Y.-C., Chang, G.-Y., Chang-Yih, D., & Shang-Kwei, W. (1993). Cytotoxic alkaloids of *Annona montana*. *Phytochemistry, 33*(2), 497-500.

Yang, T. H., Chen, C. M., & Kuan, S. S. (1971). Studies on the alkaloids of *Anona glabra* L.(I). The isolation of (−)-*N*-methylactinodaphnine. *Journal of the Chinese Chemical Society, 18*(3), 133-136.

Yinggang, L., Bogang, L., & Guolin, Z. (2000). Alkaloids from *Desmos yunnanensis*. *Natural Product Research and Development*; 2000-06.

Zahari, A., Cheah, F. K., Mohamad, J., Sulaiman, S. N., Litaudon, M., Leong, K. H., & Awang, K. (2014). Antiplasmodial and antioxidant isoquinoline alkaloids from *Dehaasia longipedicellata*. *Planta medica, 80*(7), 599-603.

Zhang, M., Liang, G., Yu, J., & Pan, W. (2010). Aporphine alkaloids from the roots of *Stephania viridiflavens*. *Natural Product Research, 24*(13), 1243-1247.

Zhen, Y., Huang, X., Yu, D., & Yu, S. (2001). Antitumor alkaloids isolated from *Tylophora ovata*. *Acta Botanica Sinica, 44*(3), 349-353.

LIST OF PUBLICATION

1) **Othman, W. N. N. W.**, Liew, S. Y., Khaw, K. Y., Murugaiyah, V., Litaudon, M., & Awang, K. (2016). Cholinesterase inhibitory activity of isoquinoline alkaloids from three *Cryptocarya* species (Lauraceae). *Bioorganic & Medicinal Chemistry, 24*(18), 4464-4469.

2) **Othman, W. N. N. W.**, Sivasothy, Y., Liew, S. Y., Mohamad, J., Nafiah, M. A., Ahmad, K., Litaudon, M., Awang, K. (2017). Alkaloids from *Cryptocarya densiflora* Blume (Lauraceae) and their cholinesterase inhibitory activity. *Phytochemistry Letter*s, *21*, 230-236.

Bioorganic & Medicinal Chemistry 24 (2016) 4464–4469

Contents lists available at ScienceDirect

Bioorganic & Medicinal Chemistry

journal homepage: www.elsevier.com/locate/bmc

Cholinesterase inhibitory activity of isoquinoline alkaloids from three *Cryptocarya* species (Lauraceae)

Wan Nurul Nazneem Wan Othman [a], Sook Yee Liew [a,b], Kooi Yeong Khaw [c,†], Vikneswaran Murugaiyah [c], Marc Litaudon [d], Khalijah Awang [a,b,*]

[a] Department of Chemistry, Faculty of Science, University of Malaya, 50603 Kuala Lumpur, Malaysia
[b] Centre for Natural Products and Drug Discovery (CENAR), University of Malaya, 50603 Kuala Lumpur, Malaysia
[c] Discipline of Pharmacology, School of Pharmaceutical Sciences, Universiti Sains Malaysia, 11800 Penang, Malaysia
[d] Institut de Chimie des Substances Naturelles, CNRS-ICSN UPR2301, University Paris-Saclay, 91198 Gif-sur-Yvette Cedex, France

ARTICLE INFO

Article history:
Received 25 May 2016
Revised 20 July 2016
Accepted 20 July 2016
Available online 21 July 2016

Keywords:
Cryptocarya
2-Methoxyatherosperminine
Phenanthrene
Butyrylcholinesterase
Enzyme kinetic
Molecular docking

ABSTRACT

Alzheimer's disease is the most common form of dementia among older adults. Acetylcholinesterase and butyrylcholinesterase are two enzymes involved in the breaking down of the neurotransmitter acetylcholine. Inhibitors for these enzymes have potential to prolong the availability of acetylcholine. Hence, the search for such inhibitors especially from natural products is needed in developing potential drugs for Alzheimer's disease. The present study investigates the cholinesterase inhibitory activity of compounds isolated from three *Cryptocarya* species towards acetylcholinesterase (AChE) and butyrylcholinesterase (BChE). Nine alkaloids were isolated; (+)-nornantenine **1**, (−)-desmethylsecoantofine **2**, (+)-oridine **3**, (+)-laurotetanine **4** from the leaves of *Cryptocarya densiflora* Bl., atherosperminine **5**, (+)-*N*-methylisococlaurine **6**, (+)-*N*-methyllaurotetanine **7** from the bark of *Cryptocarya infectoria* Miq., 2-methoxyatherosperminine **8** and (+)-reticuline **9** from the bark of *Cryptocarya griffithiana* Wight. In general, most of the alkaloids showed higher inhibition towards BChE as compared to AChE. The phenanthrene type alkaloid; 2-methoxyatherosperminine **8**, exhibited the most potent inhibition against BChE with IC_{50} value of 3.95 μM. Analysis of the Lineweaver–Burk (LB) plot of BChE activity over a range of substrate concentration suggested that 2-methoxyatherosperminine **8** exhibited mixed-mode inhibition with an inhibition constant (*Ki*) of 6.72 μM. Molecular docking studies revealed that 2-methoxyatherosperminine **8** docked well at the choline binding site and catalytic triad of *h*BChE (butyrylcholinesterase from *Homo sapiens*); hydrogen bonding with Tyr 128 and His 438 residues respectively.

1. Introduction

The genus *Cryptocarya* of the family Lauraceae comprises of more than 350 species[1] of which 19 species are found in Malaysia.[2] This species is a medium sized tree that grows up to 20 m tall. *Cryptocarya* species are known to produce many types of interesting bioactive phytochemicals, in particular the alkaloids.[3–5] Some of these alkaloids have been found to exhibit interesting pharmacological properties.[6] However, these compounds were most extensively studied for their cytotoxicity. Some *Cryptocarya* species are used in traditional medicines for the treatment of skin illness and diarrhoea.[7,8]

Alzheimer's disease (AD), a common neurodegenerative disease, is characterized by low levels of the neurotransmitter, acetylcholine (ACh) in the brain region involved with cognition. AD is one of the most common forms of dementia affecting many elderly people. Clinical treatment of this disease among other include enhancement of cholinergic function by prolonging the availability of ACh released into the neuronal synaptic cleft. This is achieved by the use of cholinesterase inhibitors, which inhibit the enzyme responsible for breaking down ACh. There are two types of cholinesterase, namely acetylcholinesterase (AChE) and butyrylcholinesterase (BChE). A potential source of AChE and BChE inhibitors is certainly provided by the abundance of plants in nature.[9] To date, several potent AChE and BChE plant-derived inhibitors have been isolated such as physostigmine, galantamine, and

Abbreviations: AChE, acetylcholinesterase; BChE, butyrylcholinesterase; ACh, acetylcholine; AD, Alzheimer's disease.

* Corresponding author. Tel.: +60 3 7967 4064; fax: +60 3 7967 4193.
E-mail address: khalijah@um.edu.my (K. Awang).
† Present address: University of Queensland, Brisbane, QLD 4072, Australia.

http://dx.doi.org/10.1016/j.bmc.2016.07.043
0968-0896/

Phytochemistry Letters 21 (2017) 230–236

Contents lists available at ScienceDirect

Phytochemistry Letters

journal homepage: www.elsevier.com/locate/phytol

Short communication

Alkaloids from *Cryptocarya densiflora* Blume (Lauraceae) and their cholinesterase inhibitory activity

Wan Nurul Nazneem Wan Othman[a], Yasodha Sivasothy[a], Sook Yee Liew[a,b], Jamaludin Mohamad[c], Mohd Azlan Nafiah[d], Kartini Ahmad[d], Marc Litaudon[e], Khalijah Awang[a,b,*]

[a] Department of Chemistry, Faculty of Science, University of Malaya, 50603, Kuala Lumpur, Malaysia
[b] Centre for Natural Products and Drug Discovery (CENAR), University of Malaya, 50603, Kuala Lumpur, Malaysia
[c] Institute of Biological Sciences, Faculty of Science, University of Malaya, 50603, Kuala Lumpur, Malaysia
[d] Department of Chemistry, Faculty of Science and Mathematics, Universiti Pendidikan Sultan Idris, 35900, Tanjong Malim, Perak, Malaysia
[e] Institut de Chimie des Substances Naturelles, CNRS-ICSN UPR2301, University Paris-Saclay, 91198 Gif-sur-Yvette Cedex, France

ARTICLE INFO

Keywords:
Cryptocarya densiflora Blume
(−)-Desmethylsecoantofine *N*-oxide
Prodensiflorin A
Prodensiflorin B
Cholinesterase inhibitory activities
DPPH free radical scavenging activity

ABSTRACT

(−)-Desmethylsecoantofine *N*-oxide (**1**), a new *seco*-phenanthroindolizidine alkaloid along with prodensiflorins A and B (**2-3**), two new proaporphine alkaloids, were isolated from the leaves of *Cryptocarya densiflora* Blume. Their structures were established on the basis of 1D and 2D NMR techniques and LCMS-IT-TOF analysis. (+)-*N*-methyllaurotetanine (**4**), (+)-laurotetanine (**5**), (+)-nornantenine (**6**), crychine (**7**), (−)-isocaryachine (**8**), (+)-reticuline (**9**), (−)-desmethylsecoantofine (**10**), (+)-oridine (**11**), dicentrinone (**12**) and (−)-antofine (**13**) were also isolated with compounds **4**, **7–9** and **12–13** being characterized for the first time in this plant. Compounds **1-3** were moderate to weak AChE and BChE inhibitors while compound **10** was a DPPH free radical scavenger.

1. Introduction

Cryptocarya densiflora Blume (Lauraceae) is a medium sized tree, up to 20 m in height and 135 cm in girth. The bark is smooth and grayish in colour with large scattered lenticels. The inner bark is reddish brown and granular while the sapwood is pale yellow. The leaf blades are leathery and elliptic to oblong. The flowers are pale yellow, while the fruits are globose and green upon ripening. This species is distributed throughout hills and mountain forests up to 1500 m in Malaysia and Indonesia (Ng, 1989). Little is known about the chemical constituents of this species apart from a paper which reports on two new anti-tumor furanosesquiterpenes from the bark more than two decades ago (Achmad et al., 1992).

In 2016, our group investigated the alkaloidal content of the leaves of this species and their cholinesterase inhibitory activities for the first time. Four alkaloids were identified; (+)-laurotetanine, (+)-nornantenine, (−)-desmethylsecoantofine and (+)-oridine, and they were found to be weak AChE and BChE inhibitors (Othman et al., 2016a). In the current work however, we decided to increase the amount of plant material and reinvestigate its chemical constituents which in turn led to the characterization of three new (**1–3**) and ten known (**4–13**) alkaloids (Fig. 1). Selected compounds were evaluated for their acetylcholinesterase (AChE) and butyrylcholinesterase (BChE) inhibitory and DPPH free radical scavenging activities. The cholinesterase activity was inspired by the fact that many alkaloids have been reported to exert potent inhibitory effect on cholinesterase such as physostigmine and galantamine.

2. Results and discussion

Compound **1** was assigned a molecular formula $C_{22}H_{25}NO_4$ as deduced from its ^{13}C NMR spectrum (Table 1) and positive LCMS-IT-TOF {$[M+H]^+$ *m/z* 368.1855 (calcd. for $C_{22}H_{26}NO_4$, 368.1856)}, consistent with eleven degrees of unsaturation. The ^1H NMR and ^{13}C NMR spectra (Table 1) of compound **1** were almost superimposable with those of compound **10** (Table 1), thus implying that compound **1** was also a *seco*-phenanthroindolizidine type alkaloid which was structurally related to compound **10**. There was however a significant difference between the indolizidine moiety of compound **1** with that of compound **10**. Unlike that of the latter, the above mentioned substructure in compound **1** was an indolizidine *N*-oxide moiety. This was evident from the downfield shift in the resonances of C-9, C-11 and C-13a upon

* Corresponding author at: Department of Chemistry, Faculty of Science, University of Malaya, 50603, Kuala Lumpur, Malaysia.
E-mail address: khalijah@um.edu.my (K. Awang).

http://dx.doi.org/10.1016/j.phytol.2017.07.002
Received 7 December 2016; Received in revised form 24 June 2017; Accepted 7 July 2017